NUREG/CR-0342
ORNL/NUREG-51

ORTCAL—A Code for THTF Heater Rod Thermocouple Calibration

L. J. Ott
R. A. Hedrick

Prepared for the U.S. Nuclear Regulatory Commission
Office of Nuclear Regulatory Research
Under Interagency Agreements DOE 40-551-75 and 40-552-75

OAK RIDGE NATIONAL LABORATORY
OPERATED BY UNION CARBIDE CORPORATION · FOR THE DEPARTMENT OF ENERGY

Printed in the United States of America. Available from
National Technical Information Service
U.S. Department of Commerce
5285 Port Royal Road, Springfield, Virginia 22161

NUREG/CR-0342
ORNL/NUREG-51
Dist. Category R2

Contract No. W-7405-eng-26

Engineering Technology Division

ORTCAL — A CODE FOR THTF HEATER ROD THERMOCOUPLE CALIBRATION

L. J. Ott R. A. Hedrick

Manuscript Completed — January 15, 1979
Date Published — February 1979

Prepared for the
U.S. Nuclear Regulatory Commission
Office of Nuclear Regulatory Research
Under Interagency Agreements DOE 40-551-75 and 40-552-75

NRC FIN No. B0125

Prepared by the
OAK RIDGE NATIONAL LABORATORY
Oak Ridge, Tennessee 37830
operated by
UNION CARBIDE CORPORATION
for the
DEPARTMENT OF ENERGY

Contents

LIST OF TABLES

LIST OF FIGURES

ORTCAL — A CODE FOR THTF HEATER ROD THERMOCOUPLE CALIBRATION

L. J. Ott R. A. Hedrick

ABSTRACT

This report develops and presents an experimental thermocouple calibration procedure and a four-part calibration program, ORTCAL (ORNL Thermocouple Calibration), which supplies heater rod performance information to the inverse heat conduction code ORINC. Case studies are presented to illustrate the effect of noncalibration of fuel pin simulators on the inverse calculations.

1. INTRODUCTION

1.1 Background[1]

The ORNL Pressurized-Water Reactor Blowdown Heat Transfer (PWR-BDHT) Program is an experimental separate-effects study of the relations among the principal variables that can alter the rate of blowdown, the presence of flow reversal and rereversal, time delay to critical heat flux (CHF), the rate at which dryout progresses, and similar time- and space-related functions that are important to loss-of-coolant accident (LOCA) analysis.

Overall program objectives are (1) to concurrently determine, for a wide range of parameters, pre-CHF heat fluxes, ΔT (surface driving potential), heat transfer coefficients, and local fluid properties; time to CHF; and post-CHF heat fluxes, ΔT, heat transfer coefficients, and local fluid properties; and (2) to test the ability of existing codes such as RELAP to predict the behavior of the single- and multirod loops under blowdown conditions.

The parameters to be studied include (1) single- and double-ended coolant line breaks of varying area ratio; (2) depressurization rates; (3) different combinations of system power and pressure to obtain different values of departure from nuclear boiling ratio (DNBR); (4) a range of power cutoff delays; and (5) a range of power decay rates.

Secondary objectives are (1) to obtain CHF data under steady-state conditions over a range of coolant pressures, inlet and exit subcooling, and inlet flow rate appropriate to PWR interests; (2) to evaluate the thermal-hydraulic behavior of the test loops during simulated operational upsets that include variations in local power, system pressure, or coolant flow using a typical anticipated transient without scram (ATWS[2]) as a guide; and (3) to determine the effect of different spacer grids and power distribution profiles on both transient and steady-state CHF.

1.2 Test Facilities[1]

Primary test results are obtained from the Thermal-Hydraulic Test Facility (THTF), a large nonnuclear experimental loop with a test section that contains a 7 × 7 array of 365.76-cm (12-ft) stepped, chopped-cosine heater rods with outside diameters of 1.0719 cm (0.422 in.).

A schematic of the THTF is shown in Fig. 1.1. Fluid discharged from the pump flows through two control valves, where excess pump head is dissipated and flow adjusted to the desired level by diverting a portion through the bypass line. Heat generated in the fluid by the pump is removed in the small Graham "Heliflow" heat exchanger in the bypass line. The primary flow then passes through inlet instrumented spool pieces 1 and 2, where flow conditions are monitored by a combination of a drag disk, gamma densitometer, turbine meter, and temperature and pressure sensors in each spool piece. Flow enters the test section at the top of the rectangular shroud box, flows down its length, and enters the bottom of the rod bundle. The fluid exits the bundle through outlet spool pieces 1 and 2, which are identical to those on the inlet. The energy added by the test section heater rods is removed by Graham "Heliflow" heat exchangers A, B, and C. Finally, the fluid returns to the pump suction past the line from the pressurizer, which provides the primary pressure control for the loop and at the same time serves as a surge tank.

Supporting experiments are carried out in the Forced Convection Test Facility (FCTF). The primary purpose of the FCTF is to qualify prototype heaters for use in the THTF and to obtain blowdown heat transfer and steady-state CHF results for single rods in an annular geometry. In its

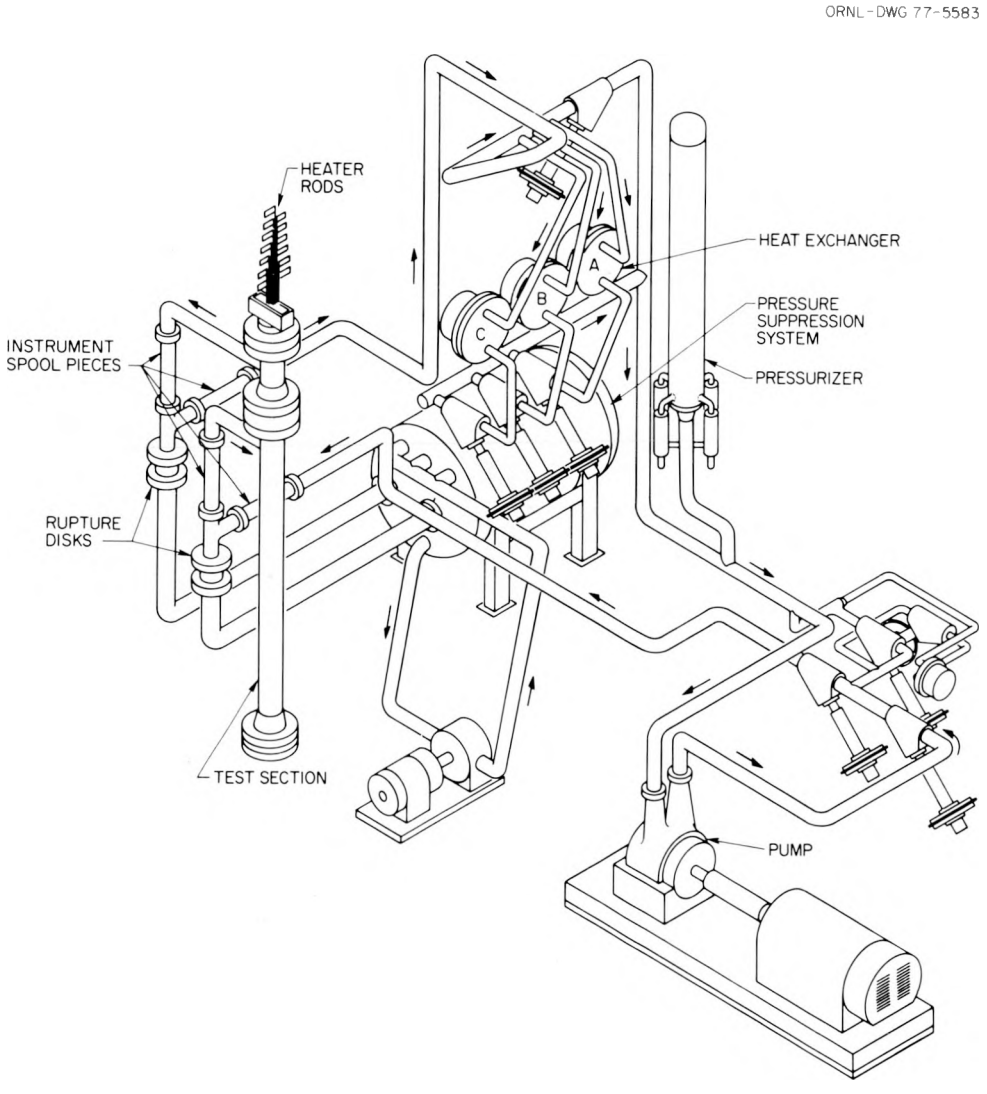

Fig. 1.1. Thermal-Hydraulic Test Facility.

present configuration, the FCTF is capable of conducting only single-ended break tests.

1.3 Heater Rod Description[1]

The indirect electric heater rods used in THTF bundle 1 are 1.0719 cm in diameter (0.422 in.) with a stepped, chopped-cosine power profile length of 365.76 cm (12 ft) (see Fig. 1.2). The overall rod length is 548.64 to 640.08 cm (18 to 21 ft), depending on its location in the bundle. The rod

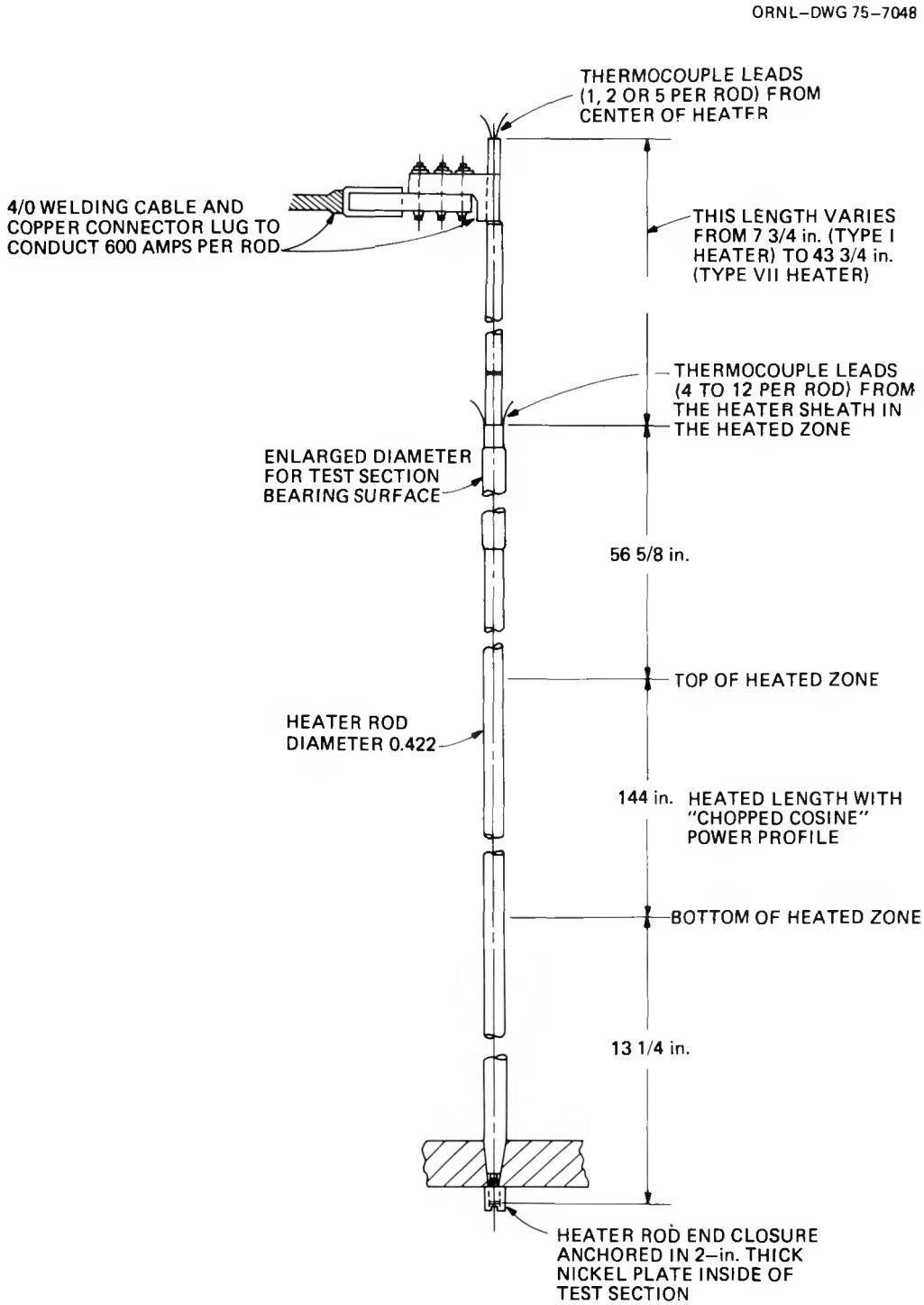

Fig. 1.2. Indirect heater rod assembly (1 in. = 2.54 cm).

is double-ended, with the sheath and ground-lead extension welded together at the lower end and the power lead insulated from the sheath at the upper end.

The heater rods have a dual-sheath design (see rod cross section in Fig. 1.3). The outer sheath is 0.0254-cm-thick (0.010-in.) stainless steel; the inner sheath is 0.0762-cm-thick (0.030-in.) stainless steel and is grooved to accept the 0.0508-cm (0.020-in.) Chromel vs Alumel thermocouples. The next inner layer is boron nitride (BN), which electrically insulates the heating element from the stainless steel sheaths. The heater element consists of a series of oversleeves swaged over a central base tube to provide the heat-generation zones. The central "hot zone," which consists of only the base Inconel 600 heater tube, has the highest electrical resistance and the maximum heat-generation rate. Successive oversleeves of Inconel 600 or Cupronickel are swaged over the heater element with each succeeding oversleeve extending to the end. As oversleeves are added between the central zone and the ends, the resistance and heat-generation rates of that particular zone decrease so that

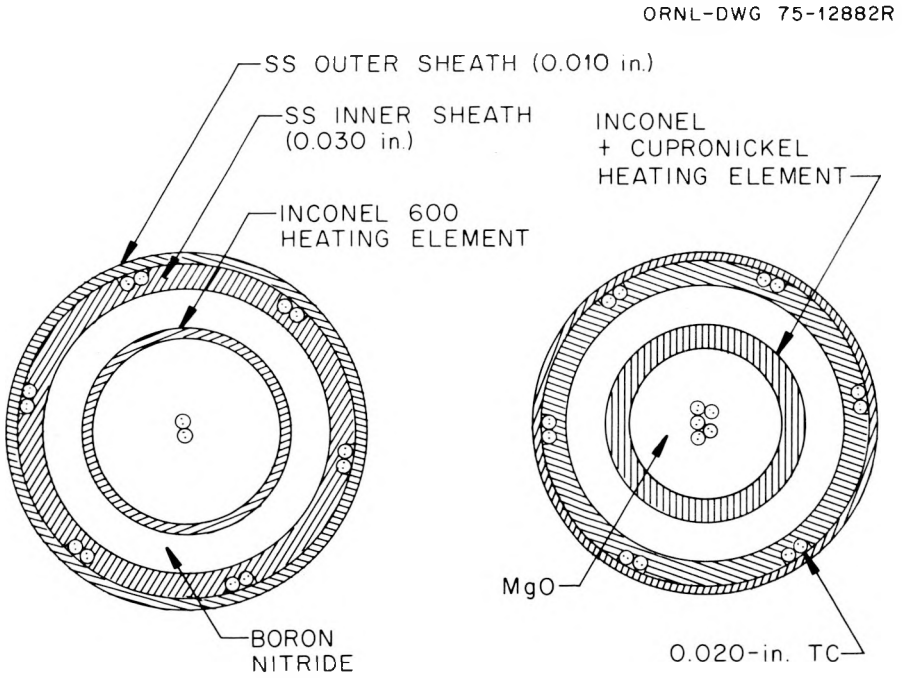

Fig. 1.3. Heater rod cross section (1 in. = 2.54 cm).

the step changes approximate the desired chopped-cosine power profile shown in Fig. 1.4. The lengths of the steps for different power levels were chosen to match the integrated chopped-cosine power profile (Fig. 1.5). Nominal heated zone lengths, power ratios, and local powers for

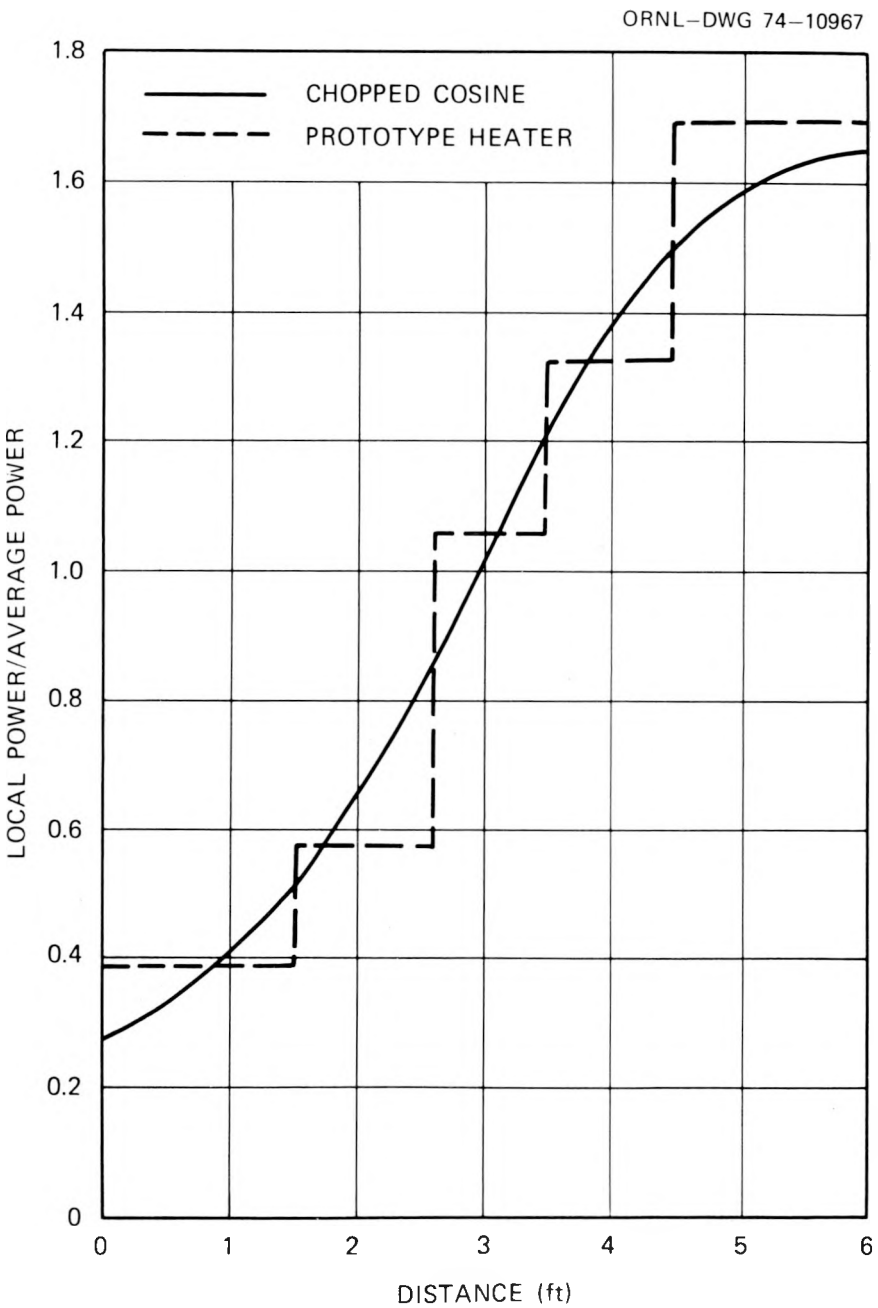

Fig. 1.4. Power profile of prototype heater (1 ft = 30.48 cm).

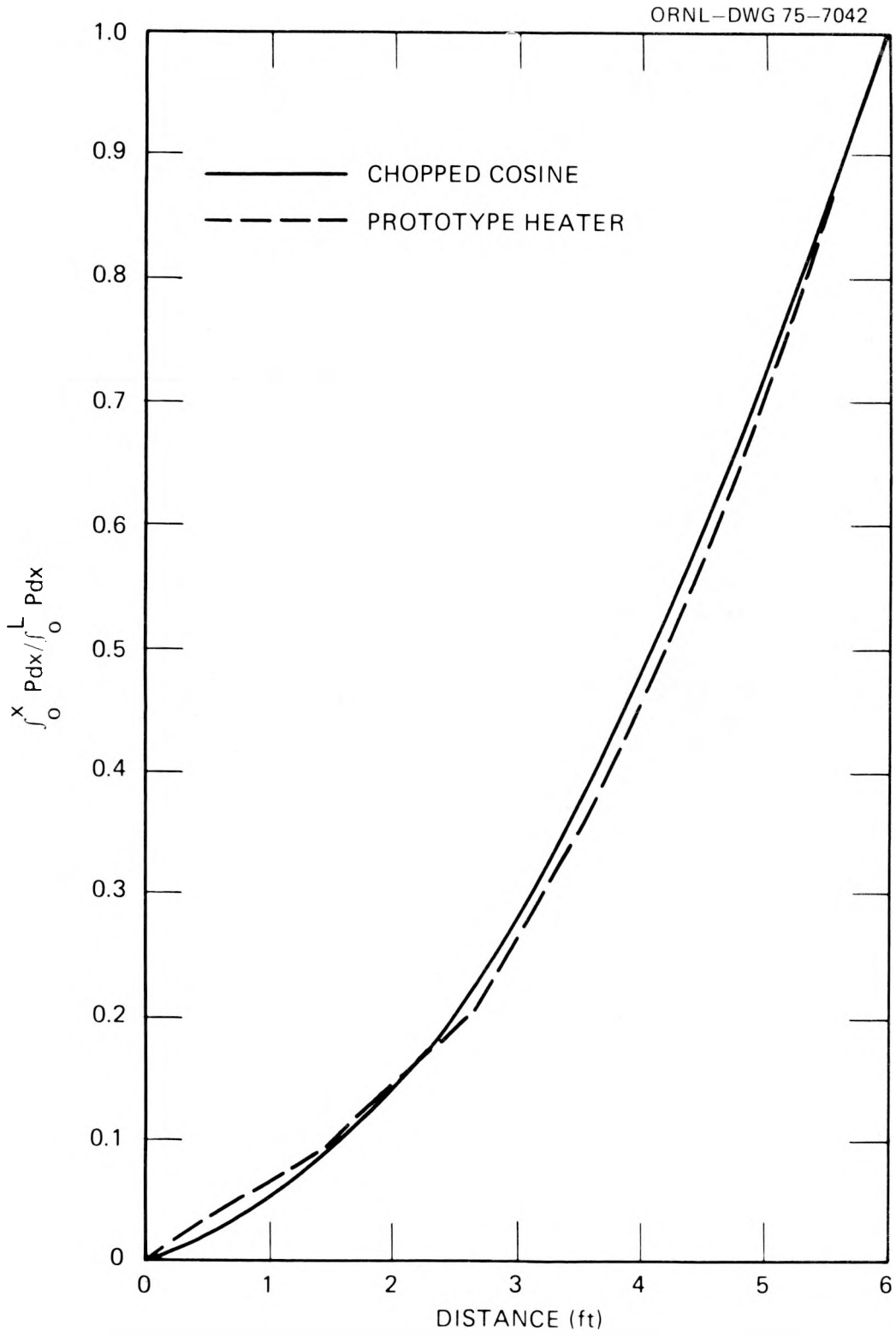

Fig. 1.5. Integrated power profile of stepped, chopped-cosine heater rod compared to the integrated power profile of a smooth chopped-cosine curve (1 ft = 30.48 cm).

THTF heaters are given in Table 1.1. The core of the heater element is filled with magnesium oxide (MgO), which serves as both a filler and an insulator between the heating element and the central rod thermocouple sheaths.

Table 1.1. Nominal power profile for the THTF indirect heater with average power of 12 kW/ft[a]

Length of heated zone from beginning (in.)	Local/average power ratio	Local power rate (kW/ft)
0–18	0.422	5.06
18–31.5	0.597	7.16
31.5–42	1.065	12.78
42–54	1.285	15.42
54–90	1.67	20.0
90–102	1.285	15.42
102–112.5	1.065	12.78
112.5–126	0.597	7.16
126–144	0.422	5.06

[a]1 in. = 2.54 cm; 1 kW/ft = 3.28084 kW/m.

The sheath thermocouples are located in axial grooves (two per groove) machined in the inner sheath. After the tips of the thermocouple sheath are spot-welded at the proper location, a stainless steel filler rod is added to the remainder of the groove (Fig. 1.6). The heater is then slipped into the 0.0254-cm-thick outer sheath and the whole assembly swaged to a 1.0719-cm OD.

BDHT heater 150-5 (originally S/N-5) was cross sectioned and micro-photographed[3] by the Y-12 Development Division Metallurgical Department. A typical cross-sectional view (Fig. 1.7) shows the peripheral location of sheath thermocouples and heater components. An enlarged view of the inner sheath groove area (Fig. 1.8) reveals that the groove has been milled to a depth of 0.0394 cm (0.0155 in.), which is less than the original 0.0508-cm OD of the thermocouple. As a result, during swaging operations the thermocouple is crushed to a somewhat elliptical shape and the

ORNL-DWG 77-12756

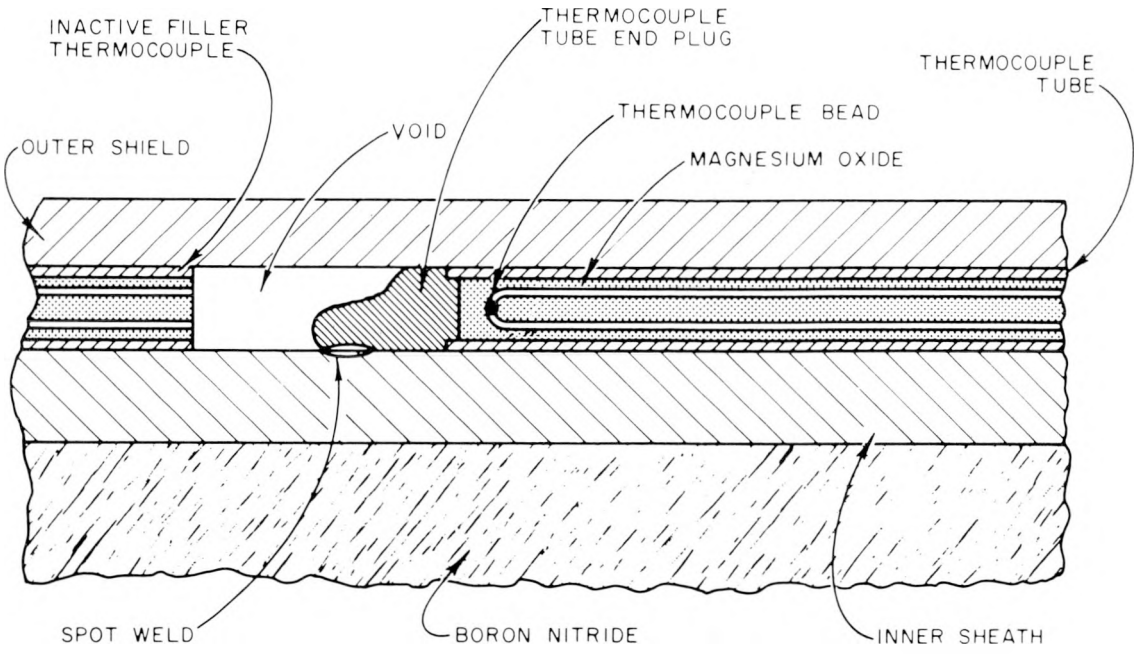

Fig. 1.6. Typical thermocouple junction configuration.

edge of the milled groove is pulled away from the outer sheath (Fig. 1.8). A review of all photographs of cross sections at thermocouple bead junctions in heater 150-5 results in the composite drawing shown in Fig. 1.9.

The heater rod is reduced to its final diameter by swaging, often creating an imperfect fit between the inner and outer sheaths at the thermocouple locations and resulting in a gap between the thermocouple junction and the outer sheath (Figs. 1.7 and 1.8). The thermocouple is welded to the inner sheath; thus, the gap between the junction and outer sheath grows with increasing fluid temperature and closes with increasing heater power. With successive blowdown transients, the residual gap increases, apparently due to plastic deformation of the outer sheath.

1.4 Heater Rod Bundle[1]

Bundle 1 consists of 49 rods in a 7 × 7 array spaced on 1.43-cm (0.563-in.) centers which are contained in a 10.16-cm-square (4-in.) shroud box. Low-pressure-drop grid spacers (Fig. 1.10) are provided at

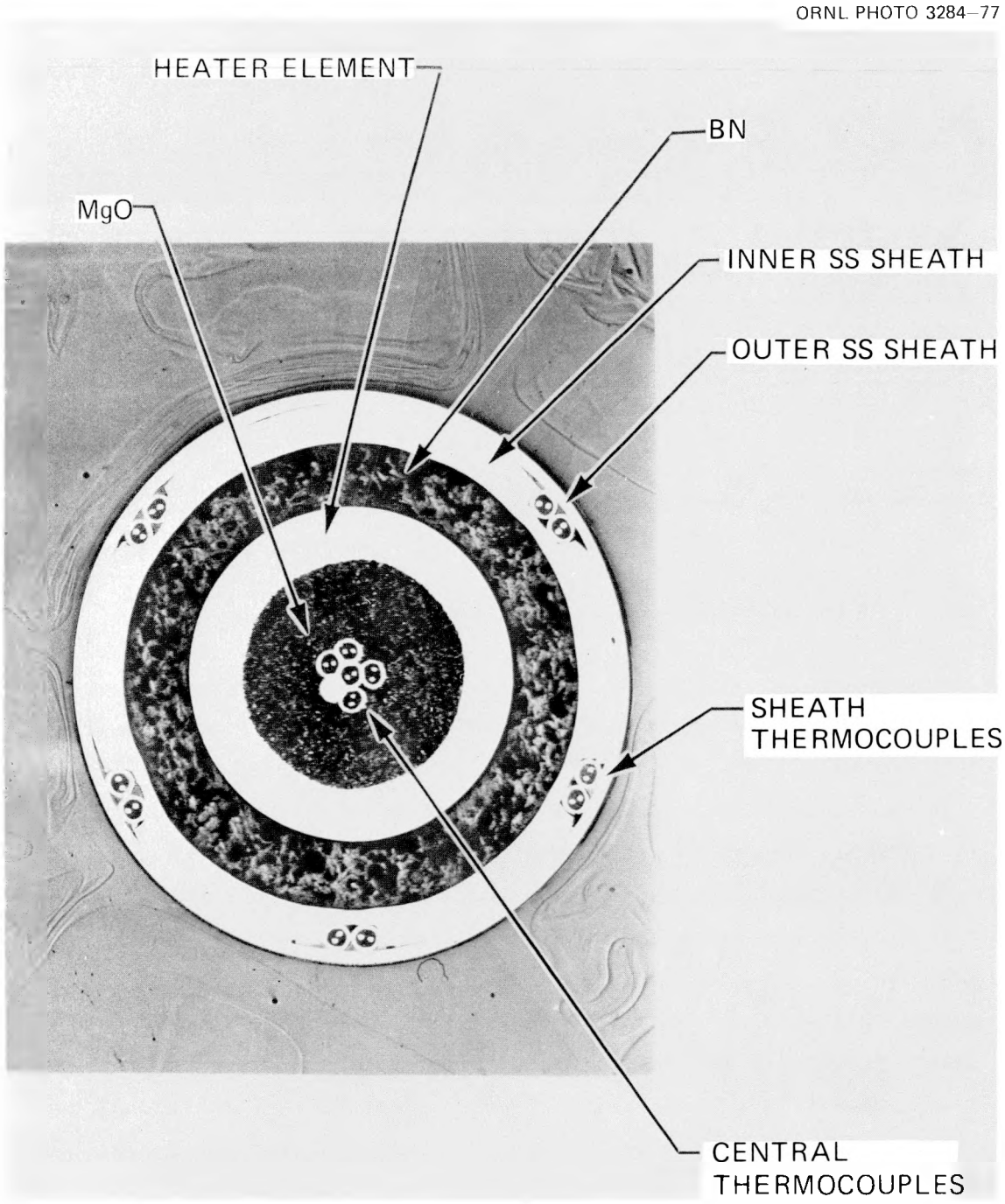

Fig. 1.7. Cross section of BDHT heater 150-5.

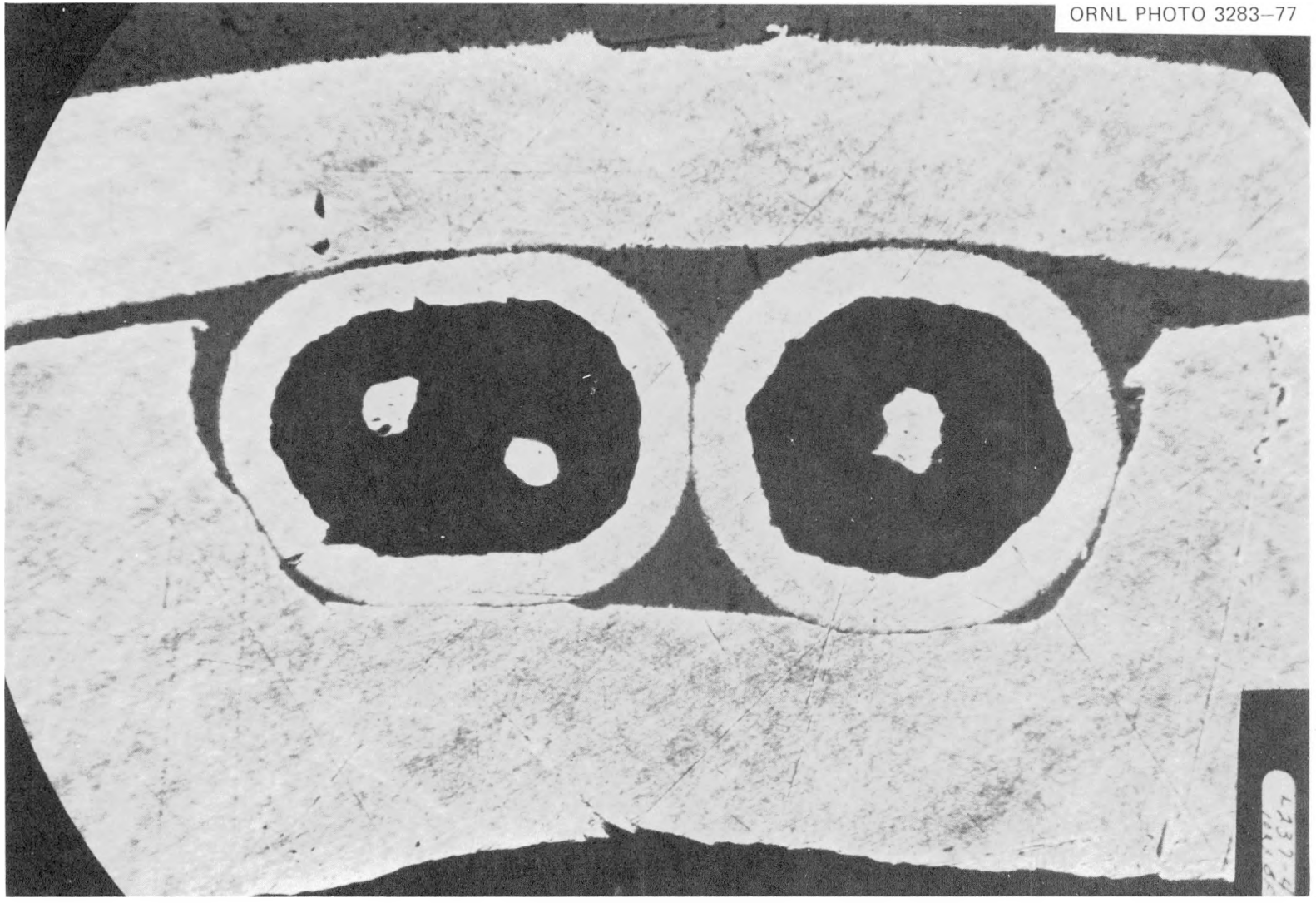

Fig. 1.8. Cross section of sheath thermocouples in BDHT heater 150-5.

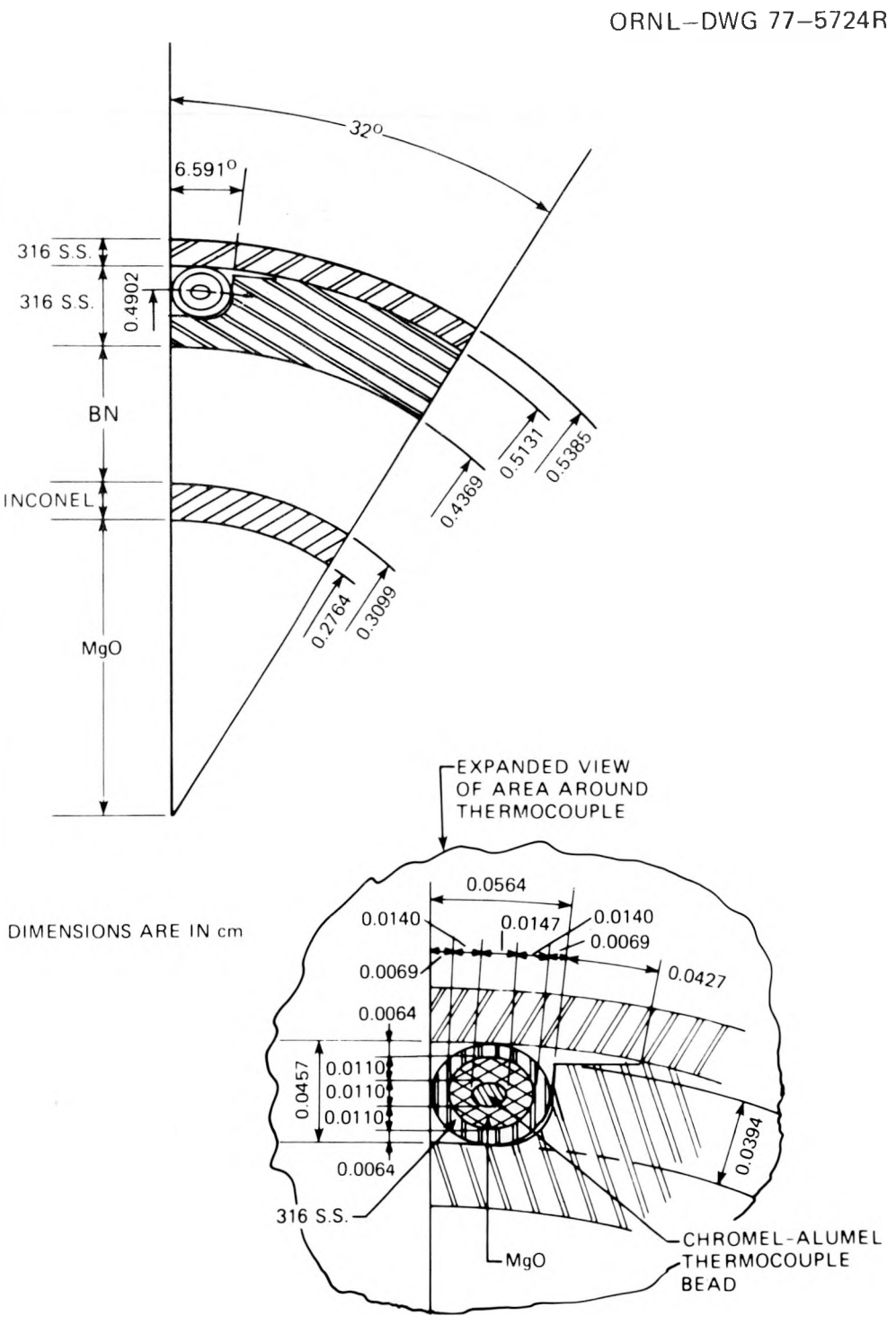

Fig. 1.9. Segment of heater showing mean dimensions in the thermocouple area (1 in. = 2.54 cm).

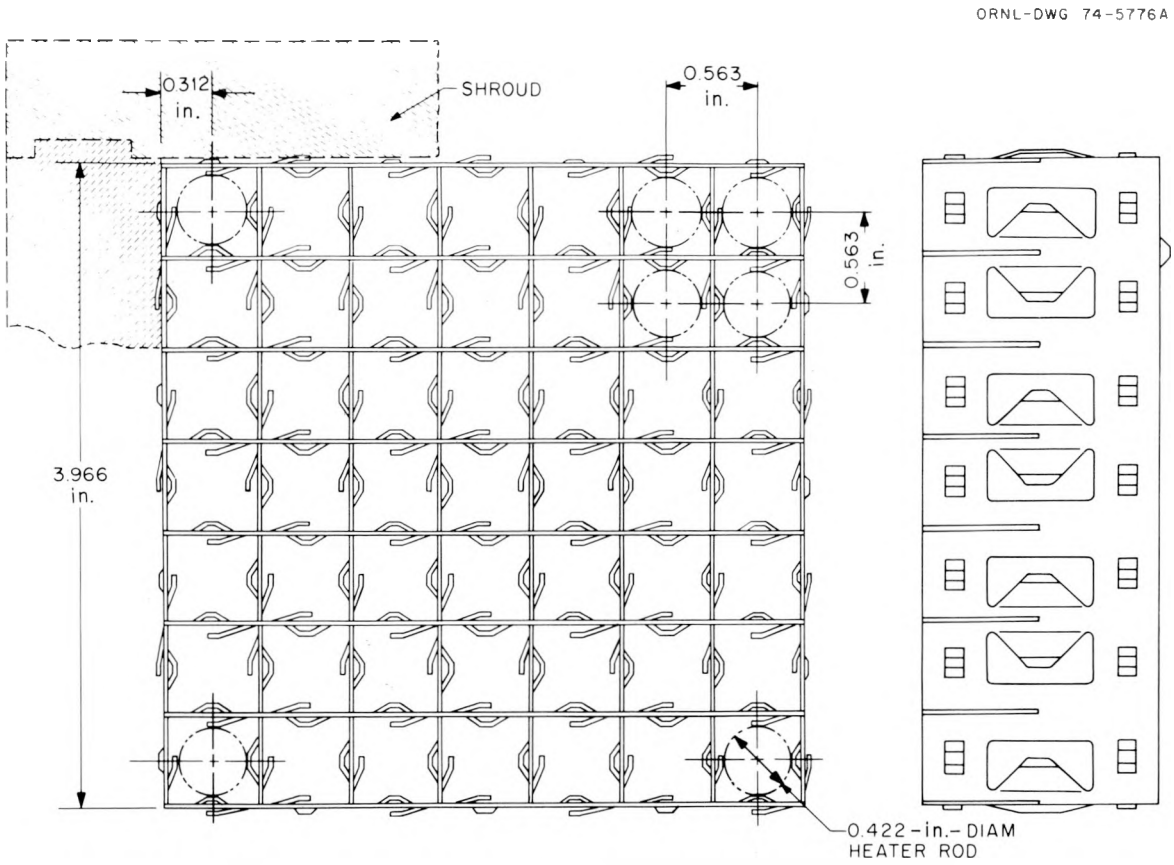

Fig. 1.10. Low-pressure-drop spacer grid assembly (1 in. = 2.54 cm).

approximately 30.48-cm (12-in.) intervals along the box which supports the spacer grids and forms the bundle flow channel. A cross-sectional view of the test section with the shroud box and bundle assembly in place is shown in Fig. 1.11.

The nominal locations of thermocouples, together with locations of power steps and spacer grids, are summarized in Table 1.2. After THTF bundle 1 was assembled, all thermocouples were tested for open circuits; 337 of 348 sheath thermocouples and 75 of 106 center thermocouples were in good condition. The distribution of these thermocouples in bundle 1 is presented in Fig. 1.12; a schematic illustration showing the locations of thermocouples at different levels is given in Fig. 1.13.

Of the available "good" sheath thermocouples, 50 are monitored by a multichannel temperature monitor (metrascope) with the thermal responses visually displayed. The cross-hatched rods in Fig. 1.14 are monitored

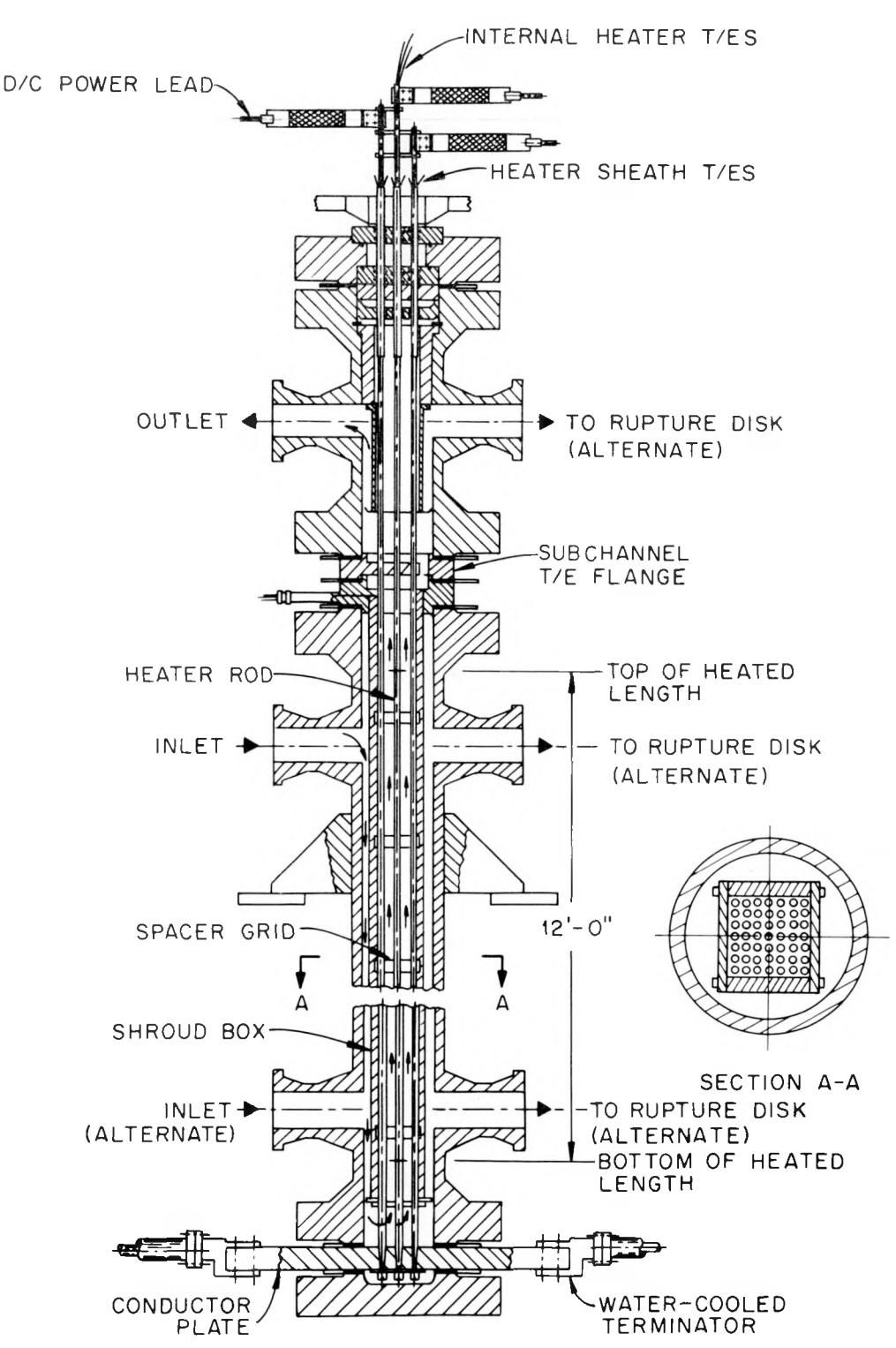

Fig. 1.11. Test section using indirect heater rod in 49-rod bundle (1 ft = 0.3048 m).

Table 1.2. Nominal location of thermocouples in THTF bundle 1 relative to power zone steps and grid spacers (1 in. = 2.54 cm)

Distance (in.) from lower end of heated zone[a]	Grid spacer location	Nominal power		Thermocouple level
		kW/m	kW/ft	
−3/4 to +3/4	X			
1				A
11 1/2 to 12 5/8	X	14.12	4.30	
13 1/8				B
18				
19		19.95	6.08	C
23 to 24 1/2	X			
31 1/2				
34 7/8 to 36 3/8	X			
36 7/8		35.56	10.84	D
42				
43				E
45 1/2 to 47	X	42.91	13.08	
54				
55				F
58 5/8 to 60 1/8	X			
70 1/2 to 72	X			
77		55.77	17.0	G
82 3/8 to 83 7/8	X			
89				H
90				
93				I
93 1/2 to 95	X	42.91	13.08	
101				J
102				
105 5/8				K
106 1/8 to 107 5/8	X	35.56	10.84	
111 1/2				L
112 1/2				
118 to 119 1/2	X			
125		19.95	6.08	M
126				
129 7/8 to 131 3/8	X			
141 1/4		14.12	4.30	N
141 3/4 to 143 1/4	X			
144				
145 1/4		1.21	0.37	O

[a] Distances in most cases are nominal and ±1/4 in.

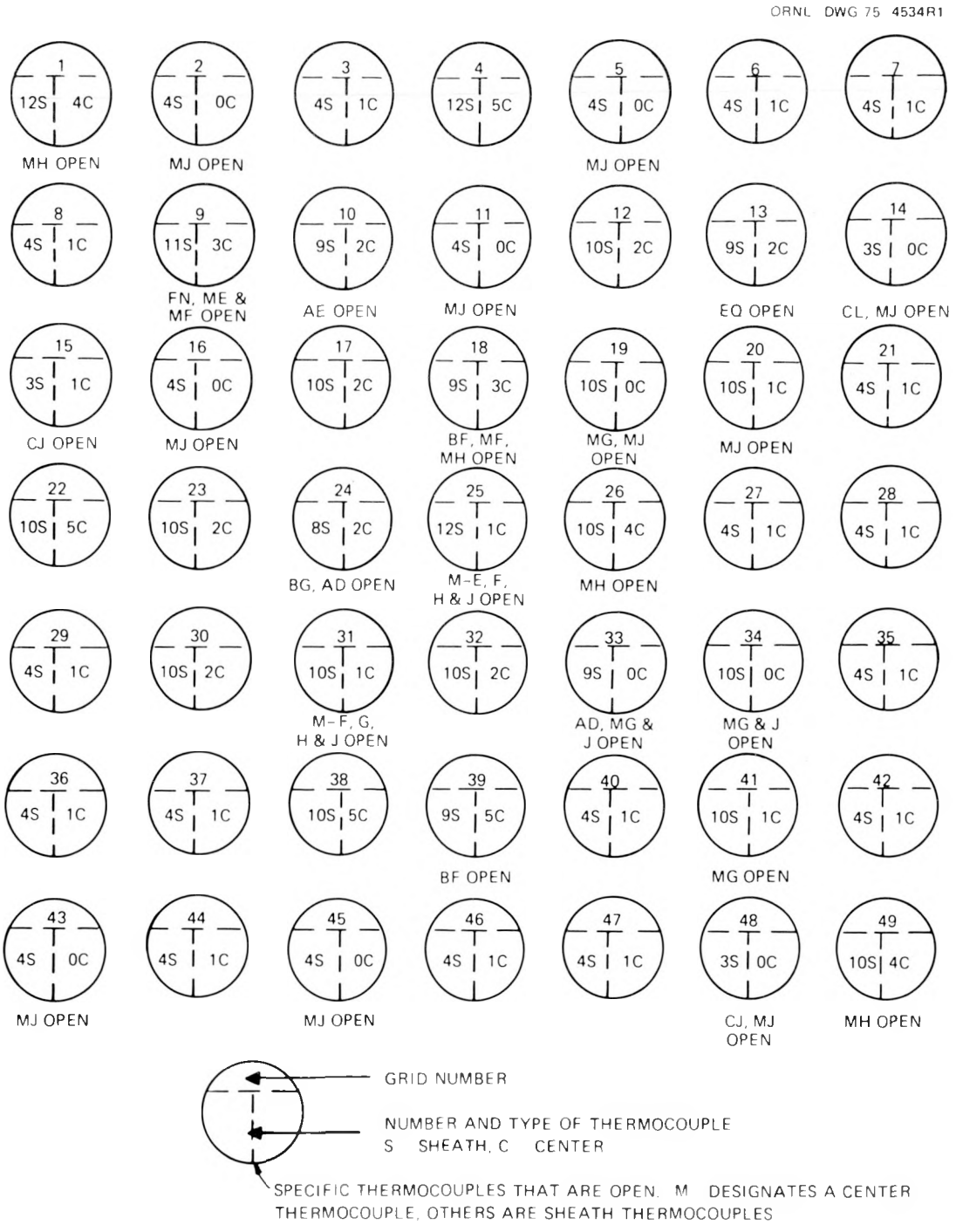

Fig. 1.12. Distribution of thermocouples in THTF test bundle 1 (May 24, 1976).

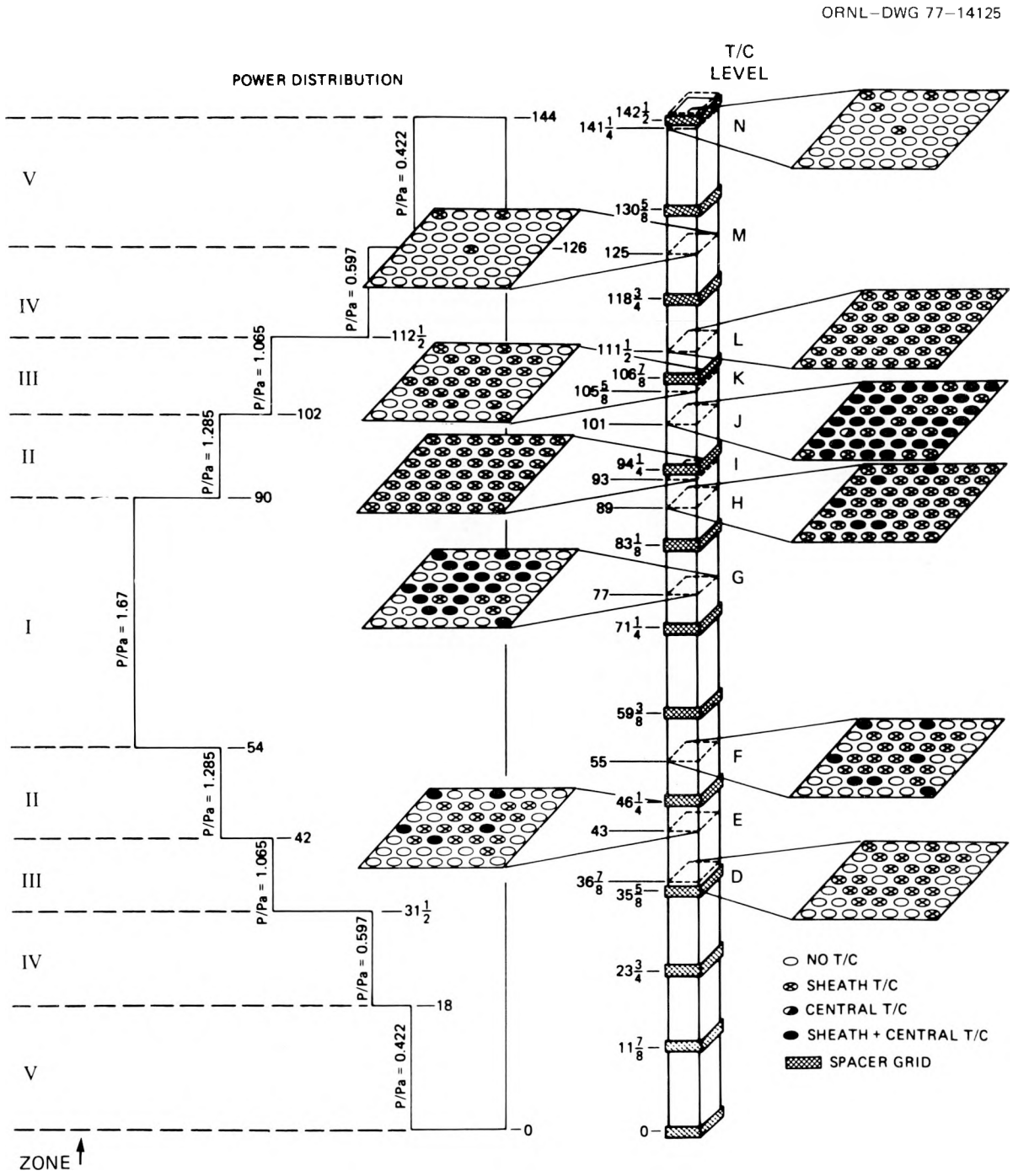

Fig. 1.13. Location of thermocouples in THTF bundle 1 (1 in. = 2.54 cm).

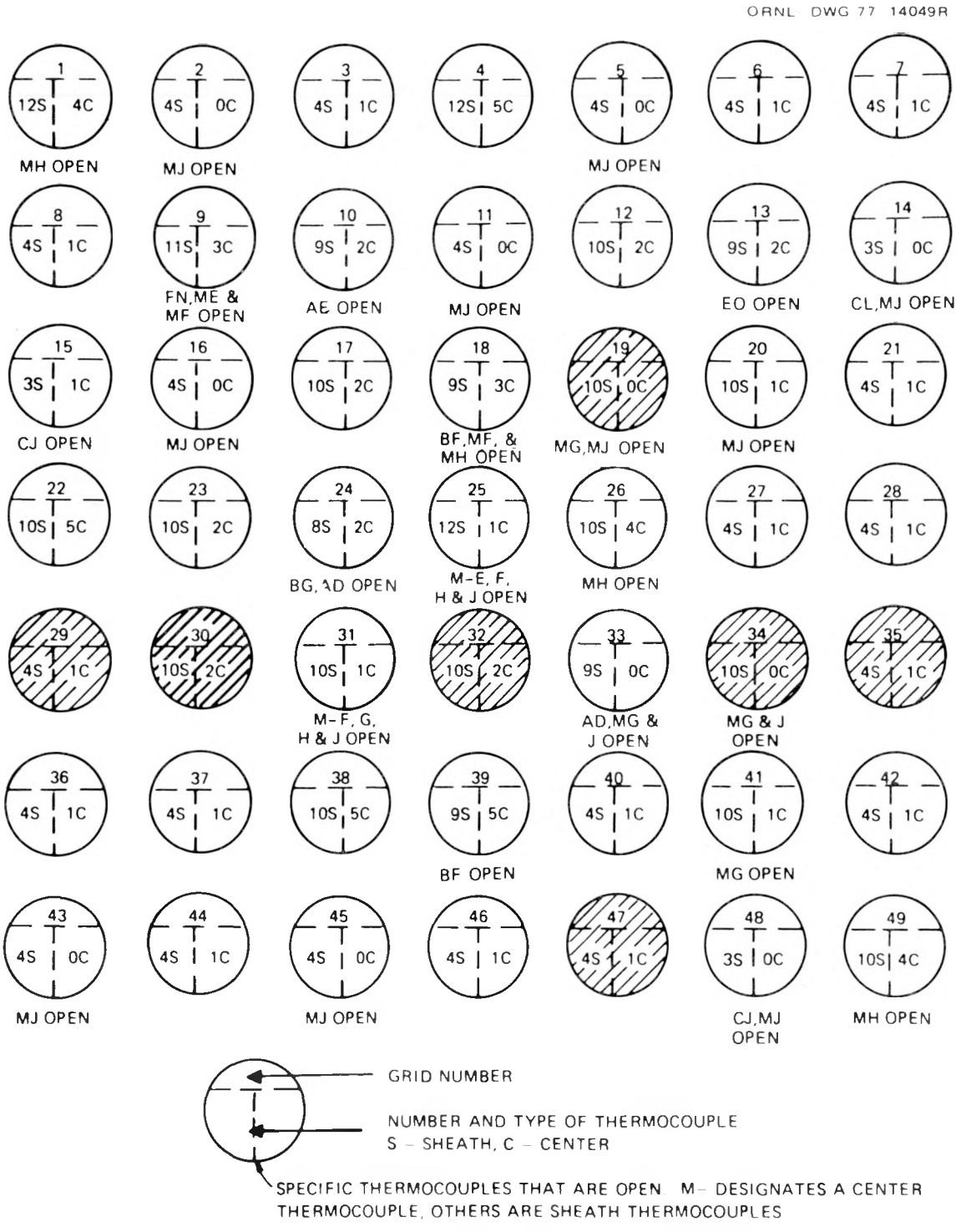

Fig. 1.14. THTF test bundle 1 rods monitored by metrascope (shown by cross hatching).

by the metrascope. Also, there are 19 thermocouples on level 0 for which the inverse model in ORINC[4] is not applicable. Therefore of the thermocouples scanned by the computer-controlled data acquisition system (CCDAS), inverse calculations can be made for 266 possible positions in bundle 1.

1.4.1 Radial dimensions[4]

For the inverse model and calculations and the calibration codes, the internal radial dimensions of the heater rod must be as accurate as possible. However, because of the rod manufacturing procedure, these dimensions are not readily available (i.e., as specifications or in any published form). The following description of the manufacturing procedure clarifies the reasons for this problem. The internal thermocouple cluster and a piano wire stiffener are inserted into the Inconel tube, and MgO cores are inserted over the thermocouple cluster. This assembly is then swaged to a given outer diameter, thus crushing and compacting the MgO. Successive sleeves of Inconel or Cupronickel are swaged over the base tube to a uniform outside diameter (further compacting the core and elongating the assembly). The finished heater assembly is placed inside the inner stainless steel sheath, and BN powder is poured into the annular region and compacted. After another swaging operation, the grooves are milled in the surface. The sheath thermocouples are subsequently tack-welded in the grooves and filler rods are added; this assembly is inserted in the outer sheath for the final swaging operation. Each swaging operation compacts (and elongates) the ceramic insulators and thins (and elongates) the metallic annular regions of the assembly.

The Y-12 Development Division Metallurgical Department measured the internal dimensions[5] of the cross sections of BDHT heater 150-5. The radial dimensions used by ORINC and the calibration codes for THTF bundle 1 are given in Table 1.3 (see Fig. 1.13 for zone designations).

1.4.2 Physical properties of components[4]

The inverse model and calibration codes require the following physical properties for each component in the heater rod: density ρ, thermal conductivity k, and specific heat C_p.

Table 1.3. Radial dimensions of THTF heater (1 in. = 2.54 cm)

Zone (refer to Fig. 1.13)	MgO outer diam [cm (in.)]	Base Inconel thickness [cm (in.)]	1st Inconel oversleeve thickness [cm (in.)]	2nd Inconel oversleeve thickness [cm (in.)]	1st Cu-Ni oversleeve thickness [cm (in.)]	2nd Cu-Ni oversleeve thickness [cm (in.)]	BN thickness [cm (in.)]	Inner SS sheath thickness [cm (in.)]	Outer SS sheath thickness [cm (in.)]
I	0.5527 (0.2176)	0.0335 (0.0132)					0.1270 (0.0500)	0.0762 (0.0300)	0.0254 (0.0100)
II	0.5319 (0.2094)	0.0340 (0.0134)	0.0099 (0.0039)				0.1270 (0.0500)	0.0762 (0.0300)	0.0254 (0.0100)
III	0.5126 (0.2018)	0.0348 (0.0137)	0.0099 (0.0039)	0.0089 (0.0035)			0.1270 (0.0500)	0.0762 (0.0300)	0.0254 (0.0100)
IV	0.4831 (0.1902)	0.0356 (0.0140)	0.0099 (0.0039)	0.0089 (0.0035)	0.0140 (0.0055)		0.1270 (0.0500)	0.0762 (0.0300)	0.0254 (0.0100)
V	0.4552 (0.1792)	0.0356 (0.0140)	0.0099 (0.0039)	0.0089 (0.0035)	0.0140 (0.0055)	0.0140 (0.0055)	0.1270 (0.0500)	0.0762 (0.0300)	0.0254 (0.0100)

Zone	MgO outer radius [cm (in.)]	Inconel outer radius [cm (in.)]	Cu-Ni outer radius [cm (in.)]	BN outer radius [cm (in.)]	Inner sheath outer radius [cm (in.)]	Outer sheath outer radius [cm (in.)]
I	0.2764 (0.1088)	0.3099 (0.1220)		0.4369 (0.1720)	0.5131 (0.2020)	0.5385 (0.2120)
II	0.2659 (0.1047)	0.3099 (0.1220)		0.4369 (0.1720)	0.5131 (0.2020)	0.5385 (0.2120)
III	0.2563 (0.1009)	0.3099 (0.1220)		0.4369 (0.1720)	0.5131 (0.2020)	0.5385 (0.2120)
IV	0.2416 (0.0951)	0.2959 (0.1165)	0.3099 (0.1220)	0.4369 (0.1720)	0.5131 (0.2020)	0.5385 (0.2120)
V	0.2276 (0.0896)	0.2819 (0.1110)	0.3099 (0.1220)	0.4369 (0.1720)	0.5131 (0.2020)	0.5385 (0.2120)

An extensive literature search[6-17] was conducted to collect the available physical property information for MgO, Inconel-600, Cupronickel, BN, and 316 stainless steel. Except for the thermal conductivities of MgO and BN, the optimum polynomial fit in terms of temperature was determined for the heat capacity and thermal conductivity of each component. These least-squares fits and graphical displays of the fits are presented in Appendix A.

The difficulty in presenting a single curve for the thermal conductivity of MgO is that it is an extreme function of the packed density (porosity) of the ceramic.[6] As stated in Section 1.4.1, the compaction of the MgO core varies according to the axial position in the rod and thus the effective MgO thermal conductivity must be determined in situ.

There are several obstacles to determining BN thermal conductivity: (1) thermal conductivity is a function of the packed density;[9] (2) most of the available data have been collected at temperatures in excess of 1089 K (1500°F), which is outside the range of our application;[6] and (3) the thermal conductivity is dependent on the direction of the molding (or applied) pressure (i.e., the ratio of the conductivity measured perpendicular to the molding pressure to that measured parallel to the molding pressure can be as much as 2).[11] Therefore, the effective BN thermal conductivity must also be determined in situ.

1.4.3 Calibration objectives

Because of rod-to-rod variance in manufacturing, the mechanical and thermal transients involved during a blowdown of the THTF, and changes in bundle response due to "aging," an extensive thermocouple calibration procedure was needed to supply heater rod performance information to the inverse heat conduction model.

The primary purpose of this report is to develop and present an experimental thermocouple calibration procedure and a four-part calibration program, ORTCAL (ORNL Thermocouple Calibration).

Part I of ORTCAL calculates basic gap information such as width and temperature drop and provides the "aging" history of each location. Part II uses temperatures indicated by the sheath and middle thermocouples to produce the effective thermal conductivity of the BN insulator.

Part III produces the effective thermal diffusivity of the MgO insulator, and Part IV uses regression analysis on the output from Part I to determine the expansion coefficients and proper bias points for the stainless steel annuli forming the gap. The mechanical model[4] chosen to utilize this information is one dimensional, which is consistent with the thermal model used in the inverse calculation.

The combined output from ORTCAL is a coefficient data tape which contains the regression and bias information for each thermocouple position in the THTF bundle. This information is then used by ORINC to simulate the thermomechanical response of the heater rod.

2. ROD CLASSIFICATION PROCEDURE

2.1 Preliminary Notes

2.1.1 Thermocouples

Before describing the experimental and analytical techniques required to determine the sheath gap behavior and the effective thermal conductivities of the insulators, it must be noted that these determinations are in addition to the normal measures taken by the Instrumentation and Controls Division personnel in the calibration of the loop (THTF or FCTF) instrumentation. In essence, these procedures assume that the thermocouples are calibrated, the junction reference boxes are at the correct temperatures, and the temperature indicated by the thermocouple is that of the thermocouple bead.

Considering the mass of thermocouple leads (454) exiting the top of THTF bundle 1, it is not inconceivable that some would be tagged incorrectly (i.e., the thermocouple tagged TE-349BG could be leaving rod 25 rather than rod 49). To verify the location of both sheath and center thermocouples, power was applied to one rod at a time for all 49 rods in the THTF.[18,19]

Given the fact that the rod locations of the thermocouples are known, the actual axial locations of the thermocouples in the rods must be determined in situ. The thermocouple locations given in Table 1.2 are nominal; even though the acceptable tolerances of ±0.635 cm (1/4 in.) are tight, it is possible to miss the desired positioning during the manufacturing process. Not only are the powered zone lengths (Table 1.2 or Fig. 1.13) different for each heater, the swaging operations must be allowed for; that is, the manufacturer must allow for the extrusion of the thermocouples and the constituents of the fuel pin simulator during the swaging operations. For example, the initial placement of TE-322ME might be 100 cm above the ground lead and thus end up at 109.8 cm (43 in.) above it after the final swaging operation. It is also possible to create "false" junctions in the thermocouples (especially during the swaging operations); that is, the thermal elements could touch (thus forming a junction) above the thermocouple bead and therefore respond differently

from the remaining thermocouples on that level. In light of these possibilities and the desire to locate level E, F, H, J, and M thermocouples within 2.54 cm of the powered zone breaks (Fig. 1.13 or Table 1.2), the analyst must know the axial position of the effective thermocouple junction. The pin radial dimensions change with axial position; but, more importantly, the axial power peaking factor is a function of the axial position. Therefore, in addition to x rays of the fuel pin simulators, hot and cold water fill tests (using the configuration shown in Fig. 2.1) are conducted with the bundle in place to determine the axial positions of the bundle thermocouples. In short, the fill tests are conducted at atmospheric pressure (the test section is vented at a spare upper plenum outlet), flow to the test section from the standpipe is adjusted to fill the assembly in approximately 10 min, and the test section level and thermocouples are monitored by the CCDAS for approximately 12 min (about the capacity of one tape).[20]

2.1.2 Power peaking factors

The local axial power peaking factor is defined by

$$PFA_i = P_i/P_a \ , \tag{2.1}$$

where P_i is the local linear power generation rate and P_a is the average linear power generation rate. This approach to the calculation of P_i is taken because the determination of P_a by Eq. (2.2) is simple and straightforward:

$$P_a = I_s \ (V_G/L_{active}) \ , \tag{2.2}$$

where I_s is the shunt amperage, V_G is the generator voltage, and L_{active} is the active heated length of the fuel pin simulator. However, values for PFA_i and L_{active} from Tables 1.1 and 1.2 and Fig. 1.13 cannot be used since they are design values and are nominal. The PFA_i must be determined individually for each zone of each fuel pin simulator since the electrical resistance R_i and length L_i of each zone varies from rod to rod. For instance, the peaking factor in the high-power zone (I in Fig. 1.13 or 2.2) varies from 1.648 to 1.709 in bundle 1 with a mean of

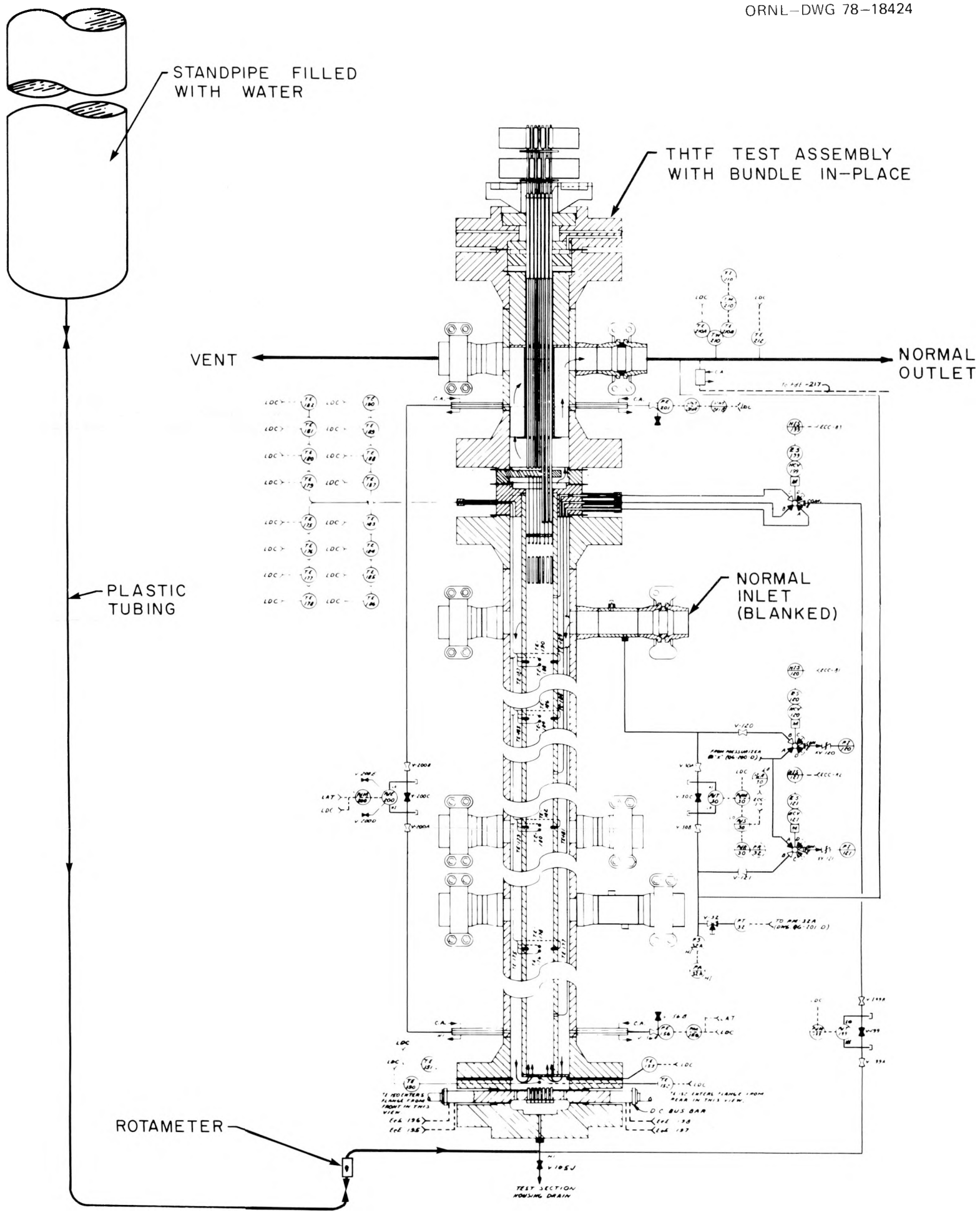

Fig. 2.1. Fill test configuration.

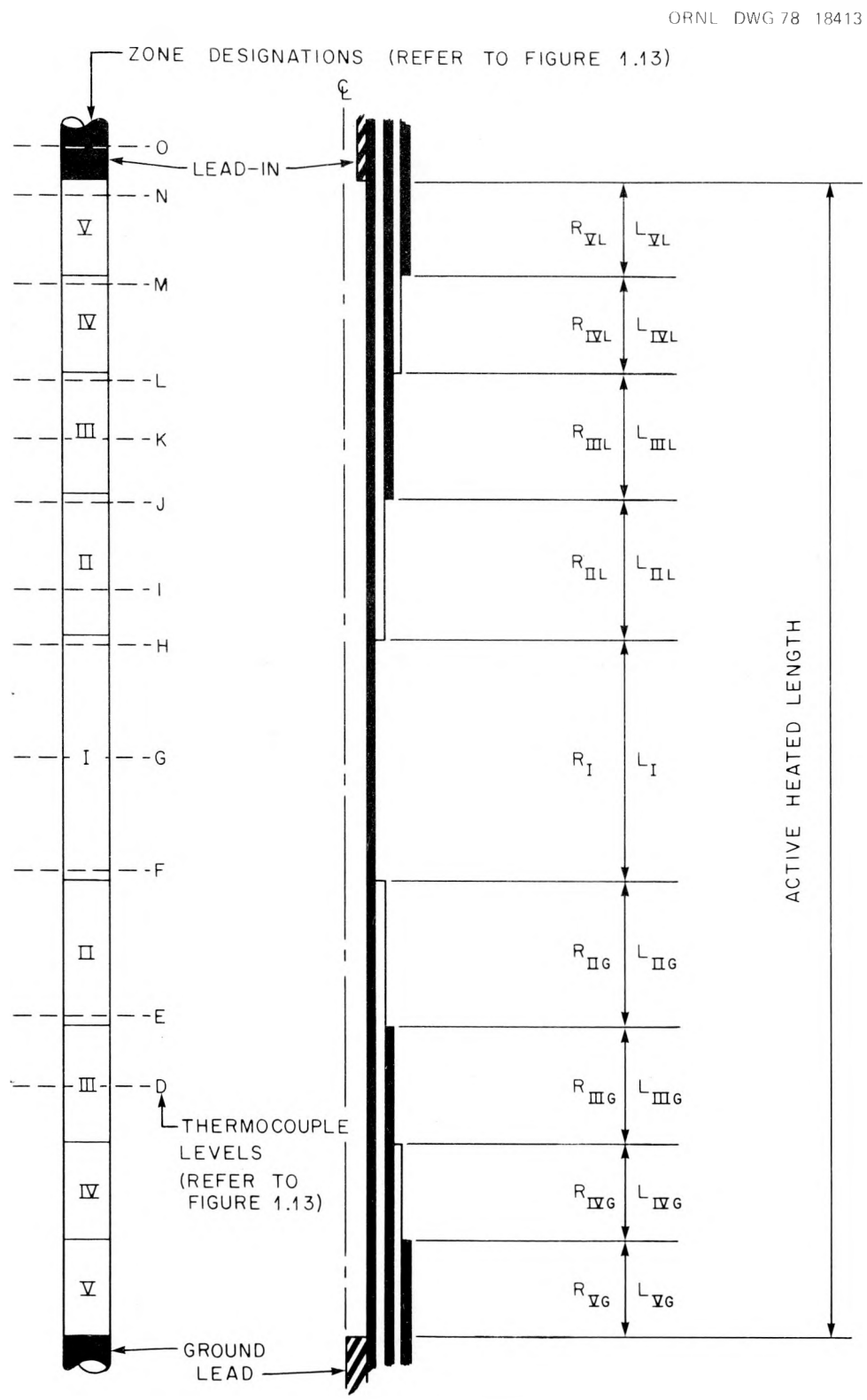

Fig. 2.2. Fuel pin simulator zone designations with thermocouple levels (bundle 1) and enlarged active component assembly.

1.679 and a standard deviation of 0.012. This is not as formidable a task as it would appear, since the data required to make the calculations (R_i, L_i pairs — see Fig. 2.2) were taken on the BDHT inspection reports for each swaged active-component assembly (ACA). Referring to Fig. 2.2, the overall resistance (R_0) for the ACA can be determined by

$$R_0 = \sum_{i=VG,VL} L_i R_i \ . \tag{2.3}$$

Also, the total active heated length is given by

$$L_{active} = \sum_{i=VG,VL} L_i \ , \tag{2.4}$$

and the average resistance per foot of active heated length is given by

$$\overline{R} = R_0/L_{active} \ . \tag{2.5}$$

Therefore, the local axial power peaking factor for each power step of the heater is calculated by

$$PFA_i = R_i/\overline{R} \ , \tag{2.6}$$

for i = VG,VL.

2.1.3 Experiments

Two types of techniques can be used to generate the data required to classify the heater rods. Data from steady-state experiments at different boundary conditions (i.e., varying power generation rate and rod surface temperature) can be reduced to yield the desired gap information and the effective thermal conductivity of the BN insulator. Power drop tests ("controlled" transients) can be performed to determine the effective thermal diffusivity of the MgO core. It is assumed that centerline thermocouples exist in tandem with sheath thermocouples — that is, the rod centerline temperature *must* be monitored at the same axial position as that of the sheath thermocouple if the heater is to be fully classified. Without the centerline thermocouple, *only* the gap information can

be extracted from calibration tests. The consequence of not knowing the in-situ thermal conductivity of BN and the thermal diffusivity of MgO and thus having to use literature relationships for these functions will be discussed in Chapter 3.

The heat sink temperature range over which the experimental calibration runs should be made is largely dependent on the facility. As an upper limit (this is a function of the core flow rate, core inlet temperature, and pressure) the entire rod (at least during initial calibration runs) should be maintained in the forced convection heat transfer regime. This conclusion is based on surface heat flux perturbation studies[21] for the BDHT heaters using HEATING5 (Ref. 22), primarily a two-dimensional (R—θ) study of the flux perturbation caused by thermocouples between the sheaths and the 0.038-cm (0.015-in.) heater eccentricity[23] (maximum allowable eccentricity in the manufacturing specifications for bundle 1 BDHT heaters). Figure 2.3, which contains the results of that study along with a schematic of the cross section of the pin modeled, shows a surface flux skew of ∿28%. If the rod were in forced convection, the variation in the surface temperature would be ∿11.7 K (21°F); however, if the rod were in nucleate boiling, the variation would be only ∿1.2 K (2.2°F). Given the standard deviation of the temperature measurement of 2.4 K (4.3°F), *it is not possible* to determine whether the heating element is eccentric in relation to the sheaths if the rod is in the nucleate boiling regime. Therefore, for initial calibration runs, the entire rod should be maintained in the forced convection heat transfer regime.

The lower limit of the heat sink temperature range also depends on the facility. The FCTF is more or less limited by the capability of the loop heat exchanger to remove the core and pump energy input into the primary fluid. Initial calibration runs in the FCTF start with a core primary inlet temperature of 422 K (300°F), which is maintained by the loop exchanger up to a core power input of ∿100 kW. Above this power level, controlling the primary core inlet temperature at 422 K by manipulating the secondary flow to the exchanger becomes exceedingly difficult, and the temperature is allowed to climb.

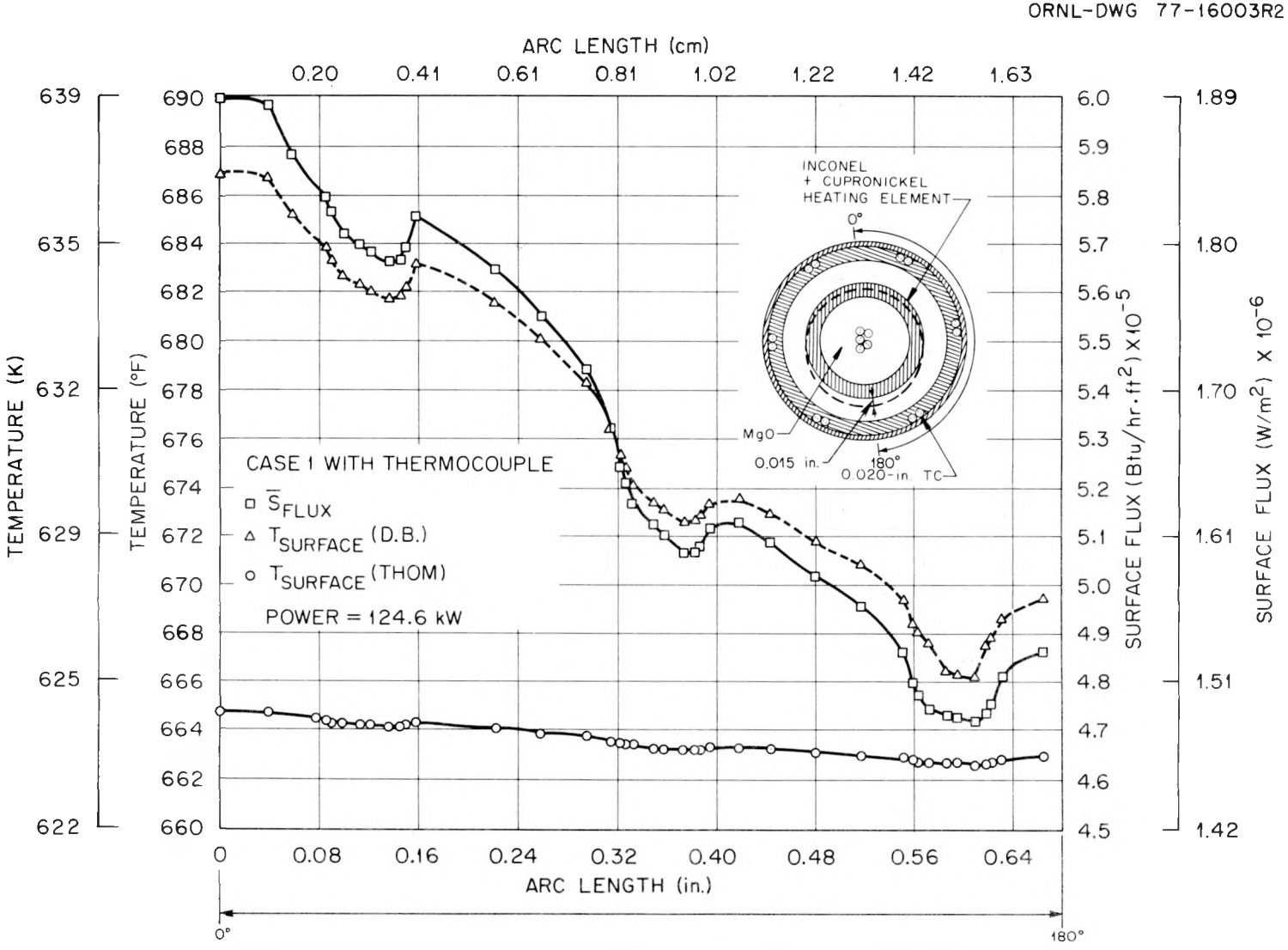

Fig. 2.3. Surface heat flux perturbation due to thermocouple presence and 0.015-in. heater eccentricity.

In the THTF, the lower limit of the heat sink temperature for calibration runs is set by the type (i.e., direct current) of power used by the core. In early 1976, during the first applications of power to bundle 1, temperatures indicated by the core Chromel/Alumel thermocouples were in error by about ±150% at 373 K. Studies[24,25] showed that these large errors could be attributed to an interaction of the temperature gradient and the magnetic field imposed on the thermocouples — the Ettingshausen-Nernst effect — which produces an electromotive force (emf) in a conductor, such as a thermocouple, placed in a magnetic field and a temperature gradient which are both transverse to the length of the conductor. These thermometry errors in the THTF core disappeared above ∿423 to 439 K (300—330°F), the Curie temperature of Alumel at which a material transforms from the ferromagnetic to the paramagnetic state; however, these thermometry errors do not occur when ac power (as in the FCTF) is used rather than dc power. With ac power, both the magnitude and direction of the magnetic field oscillate; therefore, the Ettingshausen-Nernst emf appears as an oscillating emf on the thermocouple output and is removed by the filters of the data acquisition system. In the THTF facility, the initial calibration points start at a core inlet temperature of ∿478 K (400°F), which is 39 to 55 K above the Curie temperature of Alumel.

As a final note, only calibration scans above the 30 kW/rod power level are used for the regression runs. In essence, at 10 kW/rod, the approximate temperature difference between the temperature indicated by the sheath thermocouple and that of the middle thermocouple is 13.9 K (25°F) for zones I and II in Fig. 2.2. This is of the same magnitude as the combined three standard deviations of the two temperature measurements, 14.3 K (25.7°F). Therefore, the 30-kW/rod power level was chosen as the minimum calibration scan to be included in the regressions. At a nominal 30 kW/rod, the approximate indicated temperature differences between sheath and middle thermocouples are 35 K (63°F) for zone II and 48 K (86.4°F) for zone I.

2.2 ORTCAL — Part I

2.2.1 Production and description of the "statistics" tape read by ORTCAL — Part I

During the approach to test power in the THTF, the operating checklist given in Appendix B is applicable (effective for tests after 166S for bundle 1); the checklist applies to the sequence, the type, and the number of computer scans to be taken. The operation log and/or T/C scan files are used for steady-state calibration points.

The steady-state files on the raw data tape are processed by a series of conversion codes and finally by a statistics code; the end product from data management is a statistics tape of the steady-state calibration points which consists of 1000-word block files (one file per calibration point). The first 500 words of each block contain the mean engineering-units responses of the instruments monitored by the CCDAS, and the second 500 words contain the standard deviations of those responses.

More flexibility is allowed in the FCTF operations. The calibration checklist for the FCTF is shown in Appendix B. However, the data processing is the same as for the THTF, and the end product is again a statistics tape which is read and processed by the FCTF version of ORTCAL — Part I.

The following discussion on Part I of ORTCAL pertains to the bundle 1 THTF configuration and the CCDAS; however, the code logic, structure, and purpose are independent of the loop configurations and are readily adaptable for instrumentation changes, loops, pin designs, etc.

2.2.2 Code logic and methods used

Given a statistics tape containing a number of steady-state calibration points, ORTCAL (Part I) reads one file at a time. The code computes the core coolant flow rate from a core heat balance and the local fluid conditions (i.e., bulk temperature, saturation temperature, and pressure) for each thermocouple level; subsequently, the heat transfer coefficient, heat transfer regime, pin radial gap, and pin temperature profile are determined for each bundle thermocouple position. All this information is accumulated on an updated ORTCAL thermocouple history tape (i.e., the

information from the tape is added to the information on an old ORTCAL thermocouple history tape). The information flow is shown in Fig. 2.4. The information contained on the history tapes is shown in Table 2.1, and examples of the abbreviated output (for thermocouple positions TE-318BG and TE-301DJ) are presented in Appendix C.

Given the precision of the flow measurements in the THTF,[26] it is fortunate that there are redundant measurements of the electric core coolant inlet–outlet temperatures. This redundancy allows the computation of the mean fluid core inlet temperature ($\bar{T}_{in}$) from up to 7 sensor responses and the mean fluid core outlet temperature ($\bar{T}_{out}$) from up to 35 sensor responses. The core plenum pressures (P_{in} and P_{out}) can be determined from PE-201 and PDE-200 (or PE-201 and PE-156, or PE-156 and PDE-200). Therefore, knowing that the fluid is subcooled and knowing the temperature and pressure at the core inlet and outlet, one can determine the fluid core inlet and outlet enthalpies (H_{in} and H_{out}) by a simple state search. The total power input to the core can be calculated from

$$TP_{core} = \sum_{i=1,49} I_{S_i} V_{G_i} . \tag{2.7}$$

Thus, the core flow rate is

$$F_{core} = TP_{core}/(H_{out} - H_{in}) . \tag{2.8}$$

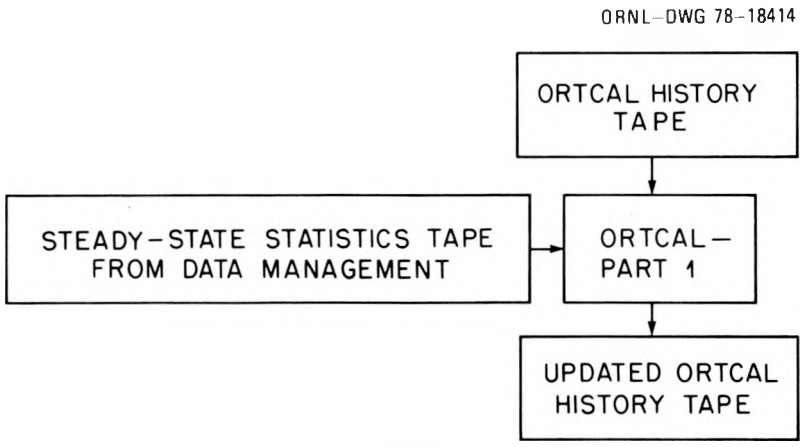

Fig. 2.4. Updated ORTCAL thermocouple history tape.

Table 2.1. Information contained on an ORTCAL thermocouple history tape[a]

Entry[b]	Description
IT(1)	Day of year
IT(2)	Number of hours since last day
IT(3)	Number of minutes since last hour
IT(4)	Number of quarter-seconds since last minute
F(1)*	Nominal power input to electrical pin (kW)
F(2)	Electrical current to pin (A)
F(3)	Generator voltage (V)
F(4)	Average power output (Btu/sec/ft)
F(5)*	Bundle inlet temperature (°F) [averaged from bottom flange TE(4) and TE-162, -24, -172]
F(6)*	Bundle outlet temperature (°F) [averaged from subchannel TE(32) and TE-222, -212, -40]
F(7)*	Upper plenum pressure from PE-201 (psia)
F(8)	Core inlet pressure from PE-156 (psia)
F(9)*	Calculated local bulk fluid pressure (psia)
F(10)*	Calculated local bulk fluid temperature (°F)
F(11)*	Calculated local saturation temperature (°F)
F(12)*	Core coolant flow rate (lb_m/sec) (calculated from heat balance on core)
F(13)*	Core coolant flow rate at inlet (gpm) [calculated from F(12) and fluid specific volume]
F(14)	Core coolant flow rate at inlet (gpm) (observed on either FE-19 or FE-166)
F(15)	Core coolant flow rate at outlet (gpm) [calculated from F(12) and fluid specific volume]
F(16)*	Sheath thermocouple response (°F)
F(17)*	Middle thermocouple response (°F) (if middle T/C is not on CCDAS during given run or does not exist, zero is entered)
F(18)	Calculated last node temperature in inner stainless steel sheath (°F)
F(19)	Calculated first node temperature in outer stainless steel sheath (°F)
F(20)*	Temperature difference across gap between sheaths (°F)
F(21)*	Surface heat transfer coefficient (Btu/hr·ft^2·°F)
F(22)*	Surface heat flux (Btu/hr·ft^2)
F(23)*	Mode of heat transfer at surface (i.e., forced convection or nucleate boiling)
F(24)*	Calculated gap between sheaths (mils of an inch)
F(25)—F(30)	Extra locations, loaded as zeroes

[a] Information available on the tape generated by ORTCAL.

[b] The entries are entered on the tape for each sheath thermocouple on the CCDAS during a given calibration run; the starred items are presented in the subsequent abbreviated paper output.

The local bulk fluid temperature is computed at each thermocouple level from

$$T_{local} = \bar{T}_{in} + \left[\frac{\sum_{i=1,49} \int_0^{\ell_{local}} PFA_i(\ell)\, P_{a_i}\, d\ell}{\sum_{i=1,49} \int_0^{\ell_{total}} PFA_i(\ell)\, P_{a_i}\, d\ell} \right] (\bar{T}_{out} - \bar{T}_{in}) , \qquad (2.9)$$

where ℓ is the heated length of the fuel pin simulator referenced to 0 at the ground end. The local fluid pressure is calculated by

$$P_{local} = P_{in} - \left(\frac{\ell_{EQ_{IN-LOCAL}}}{\ell_{EQ_{IN-OUT}}} \right) (P_{in} - P_{out}) , \qquad (2.10)$$

where $\ell_{EQ_{IN-LOCAL}}$ is the equivalent distance from PE-156 to the thermocouple level and $\ell_{EQ_{IN-OUT}}$ is the equivalent distance from PE-156 to PE-201.[27] The local saturation temperature is determined by interpolation from tables, given the local fluid pressure.

From the local fluid conditions (i.e., bulk temperature and pressure, saturation temperature, and mass flow) at each thermocouple level and the local power generation rate (i.e., $PFA_{local} \times P_a$) at each bundle thermocouple position, one can now determine the local heat transfer coefficient, heat transfer regime (either forced convection or subcooled nucleate boiling), pin radial gap, and pin temperature profile.

Consider the schematic of the fuel pin simulator in Fig. 2.5 with attention to the inset, in which the continuous homogeneous substrates (i.e., outer sheath, inner sheath, BN insulator, etc.) are handled better mathematically if the continuous domains are replaced by a pattern of discrete points (nodes) within the domains. The technique is consistent with the ORINC deviations;[4] briefly, the substrates are divided into a finite number of equal subvolumes and the centers of mass of the subvolumes are defined as the nodal points. The temperature of a subvolume is associated with its center of mass. A clearer understanding of the element notation can be gained by referring to Figs. 2.6 and 2.7.

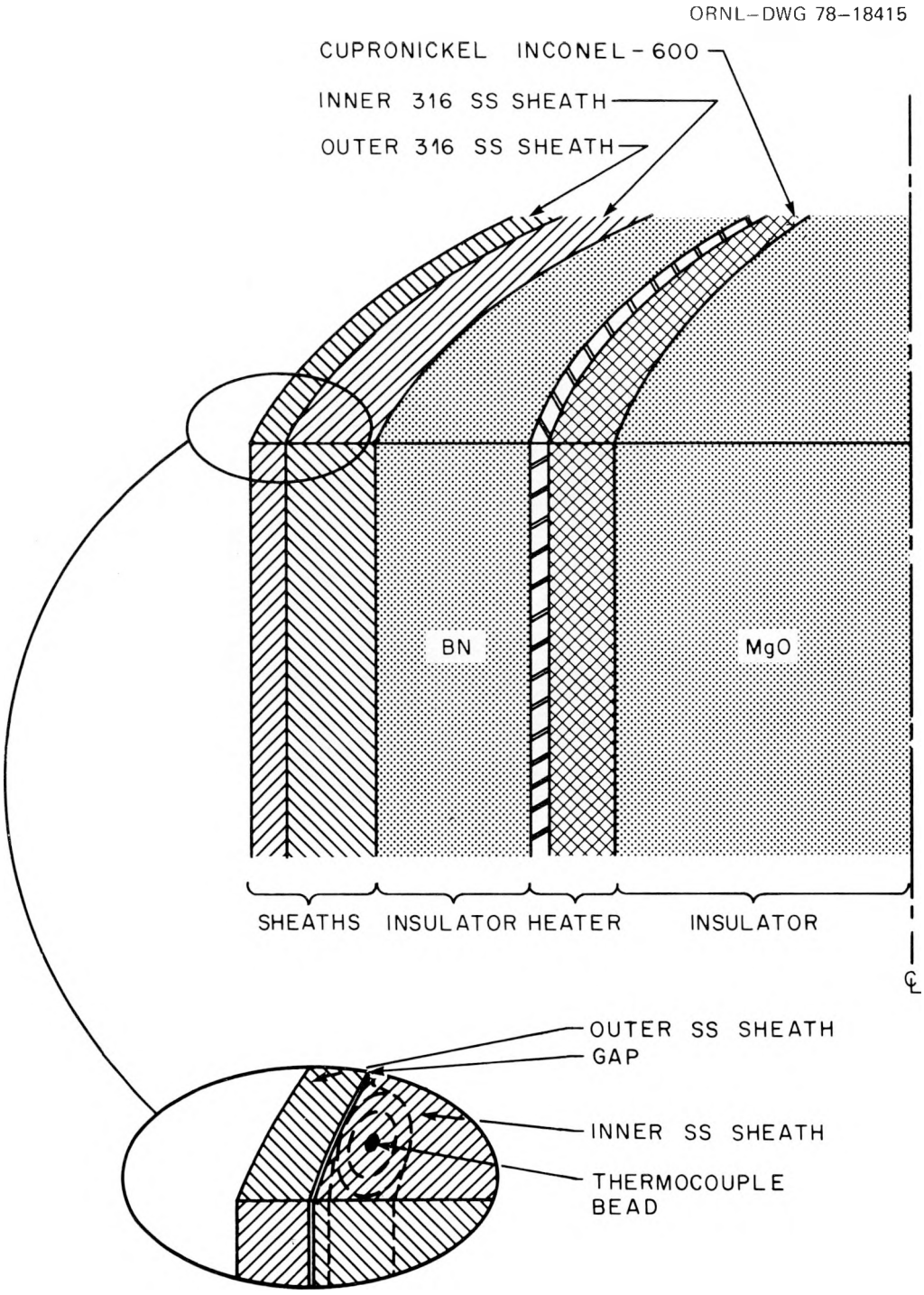

Fig. 2.5. Schematic of fuel pin simulator with inset showing thermocouple and groove superimposed on solid inner stainless steel sheath.

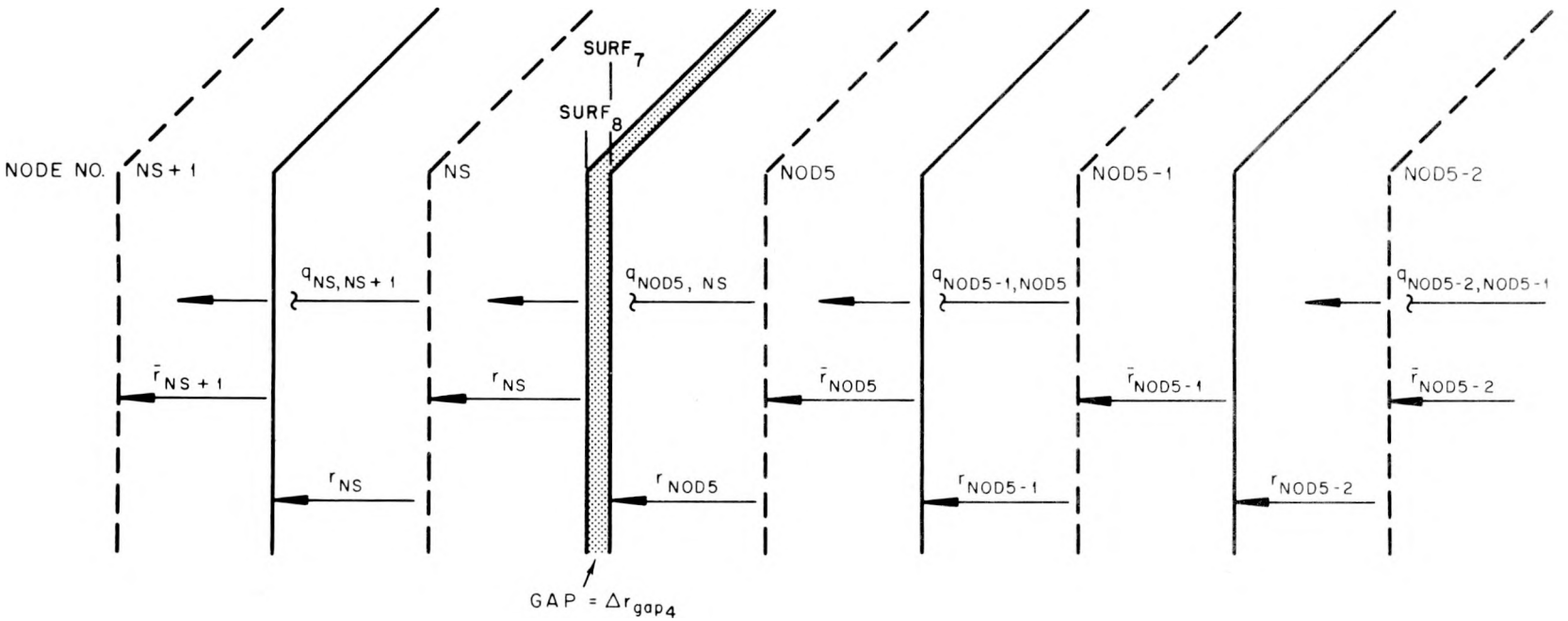

Fig. 2.6. Notation relative to the derivation of the heat transfer model at the interface of the inner and outer stainless steel sheaths.

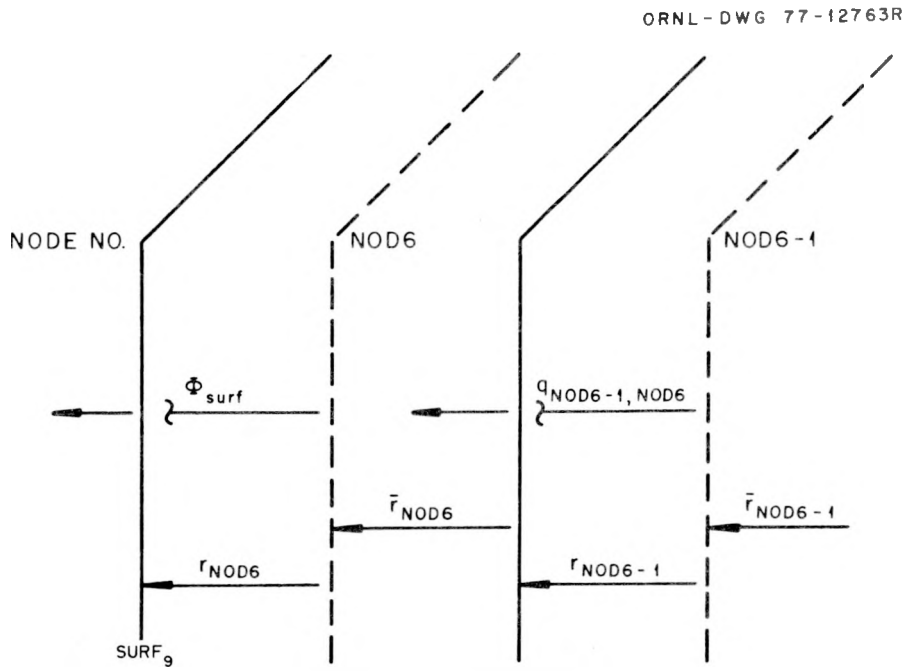

Fig. 2.7. Notation relative to the derivation of the heat transfer model at the heater surface.

The following mathematical derivations for the heat transfer models in the substrates and at the interfaces are based on the same assumptions as the ORINC models. All the ORTCAL mathematical models are one dimensional and no attempt is made to fine-structure the sheath thermocouple; it is treated as part of the solid inner stainless steel sheath (Fig. 2.5). Normally, during the discretizing of the inner sheath, an effort is made to subdivide the inner sheath such that the radial position of the last node ($\bar{r}_{NOD5}$, Fig. 2.6) is at approximately the same radial position as the thermocouple bead (Fig. 2.5).

The following assumptions are given:

1. steady-state conditions exist;
2. heat flow between nodes is constant for any r between nodes;
3. the thermal conductivity k_i is evaluated at the nodal temperature T_i;
4. a gap exists at the sheath-to-sheath interface and heat can be transferred by conduction, convection, and radiation across the gap;
5. the last node (NOD5, Fig. 2.6) temperature (T_{NOD5}) in the inner sheath is known;

6. the local fluid conditions (i.e., flow rate, bulk and saturation temperature, and pressure) are known;
7. the local power-generation rate is known.

The mathematical model for heat transfer between nodes i − 1 and i within a substrate (e.g., the outer sheath) is

$$q_{i-1,i} = -\left[\frac{2}{\frac{\ell n(r_{i-1}/\bar{r}_{i-1})}{k_{i-1}} + \frac{\ell n(\bar{r}_i/r_{i-1})}{k_i}}\right](T_i - T_{i-1})\pi\ell \ . \quad (2.11)$$

Similarly, at the surfaces in Figs. 2.6 and 2.7,

Surface 9

$$\phi_{surf_9} = q_{NOD6,fluid}/\pi\ell = -\left[\frac{2}{\frac{\ell n(r_{NOD6}/\bar{r}_{NOD6})}{k_{NOD6}}}\right](T_{surf_9} - T_{NOD6})$$

$$= -2r_{NOD6}\, h_f(T_{sink} - T_{surf_9}) = -\left[\frac{2}{\frac{1}{r_{NOD6}h_f} + \frac{\ell n(r_{NOD6}/\bar{r}_{NOD6})}{k_{NOD6}}}\right]$$

$$\times (T_{sink} - T_{NOD6}) \ , \quad (2.12)$$

Surfaces 7 and 8

$$q_{NOD5,NS} = -\left[\frac{2}{\frac{\ell n(r_{NOD5}/\bar{r}_{NOD5})}{k_{NOD5}}}\right](T_{surf_7} - T_{NOD5})\pi\ell$$

$$= -\left\{\frac{2}{\frac{1}{\frac{k_{gap_4}}{\ell n[(r_{NOD5} + \Delta r_{gap_4})/r_{NOD5}]} + r_{NOD5}h_{gap_4} + r_{NOD5}h_{r_4}}}\right\}(T_{surf_8} - T_{surf_7})\pi\ell$$

$$= -\left[\frac{2}{\frac{\ell n(\bar{r}_{NS}/r_{NOD5})}{k_{NS}}}\right](T_{NS} - T_{surf_8})\pi\ell \ , \quad (2.13)$$

where h_{gap_4} is the convective heat transfer coefficient and h_{r_4} is defined by

$$h_{r_4} = \sigma f \, (T^2_{surf_8} + T^2_{surf_7})(T_{surf_8} + T_{surf_7}) \, . \tag{2.14}$$

Note, at steady state,

$$\begin{aligned} QDPI = q_{i-1,i}/\pi\ell = \phi_{surf_9} &= q_{NOD5,NS}/\pi\ell \\ &= q_{NOD6,fluid}/\pi\ell \, . \end{aligned} \tag{2.15}$$

Subsequently, knowing T_{NOD5} and QDPI allows the calculation of the gap inside surface temperature (T_{surf_7}) from Eq. (2.13) by

$$T_{surf_7} = T_{NOD5} - QDPI \Bigg/ \left[\frac{2}{\frac{\ell n(r_{NOD5}/\bar{r}_{NOD5})}{k_{NOD5}}} \right] . \tag{2.16}$$

Also, if QDPI and T_{surf_9} are known, the outer stainless steel sheath nodal temperature (T_i) and the gap outside surface temperature (T_{surf_8}) can be determined by manipulating Eqs. (2.11) through (2.13):

$$T_{NOD6} = T_{surf_9} + QDPI \Bigg/ \left[\frac{2}{\frac{\ell n(r_{NOD6}/\bar{r}_{NOD6})}{k_{NOD6}}} \right] , \tag{2.17}$$

$$T_{i-1} = T_i + QDPI \Bigg/ \left[\frac{2}{\frac{\ell n(r_{i-1}/\bar{r}_{i-1})}{k_{i-1}} + \frac{\ell n(\bar{r}_i/r_{i-1})}{k_i}} \right] , \tag{2.18}$$

where $i - 1 = NOD6 - 1, NS$ and

$$T_{surf_8} = T_{NS} + QDPI \Bigg/ \left[\frac{2}{\frac{\ell n(\bar{r}_{NS}/r_{NOD5})}{k_{NS}}} \right] . \tag{2.19}$$

Since the k_i values are dependent on the nodal temperatures, an iterative procedure is required to determine the nodal temperatures.

Calculation of the nodal temperatures above requires the knowledge of T_{surf_9}. The T_{surf_9} value is determined by the following procedure:

1. The pin is assumed to be locally in forced convection in subcooled liquid, and the film heat transfer coefficient (h_f) is calculated from the Dittus and Boelter[28] correlation,

$$h_f = 0.023\ (k_f/D_h)(Pr_f)^{0.4}\ (Re_f)^{0.8}\ , \tag{2.20}$$

where the physical properties are evaluated at T_{bulk} (i.e., T_{local}). Thus, substitution of h_f into Eq. (2.12) yields

$$T_{surf_9} = T_{bulk} + QDPI/2r_{NOD6}h_f\ . \tag{2.21}$$

2. The pin is then assumed to be locally in subcooled nucleate boiling, and Thom's[29] correlation yields

$$T_{surf_9} = T_{SAT} + 4.32 \left(\frac{QDPI}{2r_{NOD6}}\right)^{1/2} \exp\ (-P_{local}/1260)\ . \tag{2.22}$$

3. A comparison of the T_{surf_9} values by Dittus-Boelter and Thom allows the determination of the heat transfer regime, heat transfer coefficient and $(T_{surf_9})_{actual}$ (i.e., determination of mode of heat transfer is based on minimum surface temperature).

The surface temperatures of the gap (Fig. 2.6, T_{surf_7} and T_{surf_8}) have been calculated from Eqs. (2.16) and (2.19). Therefore, referring to the following variant of Eq. (2.13),

$$\frac{k_{gap_4}}{\ell n\left[\dfrac{(r_{NOD5} + \Delta r_{gap_4})}{r_{NOD5}}\right]} + r_{NOD5}\ h_{gap_4} + r_{NOD5}\ h_{r_4} = \frac{QDPI/2}{(T_{surf_7} - T_{surf_8})}\ ; \tag{2.23}$$

T_{surf_7}, T_{surf_8}, r_{NOD5}, and QDPI are known, and h_{r_4} can be calculated from

Eq. (2.14). Thus, the remaining unknowns in Eq. (2.23) are h_{gap_4}, k_{gap_4}, and Δr_{gap_4}. Since the gaps measured[3,5] by the Y-12 Development Division Metallurgical Department were less than 0.0013 cm wide, the convective heat transfer effect in Eq. (2.23) can be neglected. Also, because of the BDHT heater design,[1] the gap between the sheaths is exposed to the atmosphere (outside the bundle); therefore, the gas in the gap must be air, which has a known thermal conductivity. Thus, k_{gap_4} is evaluated from k_{air} at $(T_{surf_7} + T_{surf_8})/2.0$. Solving Eq. (2.23) for Δr_{gap_4} yields

$$\Delta r_{gap_4} = r_{NOD5} \left\{ \exp\left[\frac{k_{gap}}{\frac{QDPI/2}{(T_{surf_7} - T_{surf_8})} - r_{NOD5}\, h_{r_4}} \right] - 1.0 \right\}. \qquad (2.24)$$

The "aging" of THTF bundle 1 is illustrated in Figs. 2.8 to 2.10 for thermocouple positions TE-318BG and TE-301DJ. These are graphs of the calculated gap thickness (Δr_{gap_4}) vs the number of times bundle 1 has been brought to power (with the curves drawn through approximately equivalent boundary conditions). White[30-32] noted an upward drift in the indicated sheath thermocouple temperatures in the FCTF during testing of bundle 1 production heaters and conjectured that the shift was caused by an "increase in the thermal resistance from the inner sheath to the outer sheath which probably grows due to the decrease in contact pressure as the outer sheath expands plastically during heatup." The data also indicated that the thermocouple responses stabilized (i.e., no further drift) as the rod "aged." Actually, the increase in the thermal resistance occurs due to an increase in the gap (Δr_{gap_4}) between the sheaths as shown in Figs. 2.8 and 2.9. Also in the "aged" THTF bundle 1, the gaps have stabilized at thermocouple positions TE-318BG and TE-301DJ (Figs. 2.8 and 2.9) and the thermocouple responses have stabilized.

Figures 2.8 and 2.9 show gap closure when the rod surface temperature is held constant and the rod power-generation rate is increased (i.e., the inner sheath thermally expands, thus closing the gap). Figure 2.10 shows the gap opening when the power-generation rate is held constant

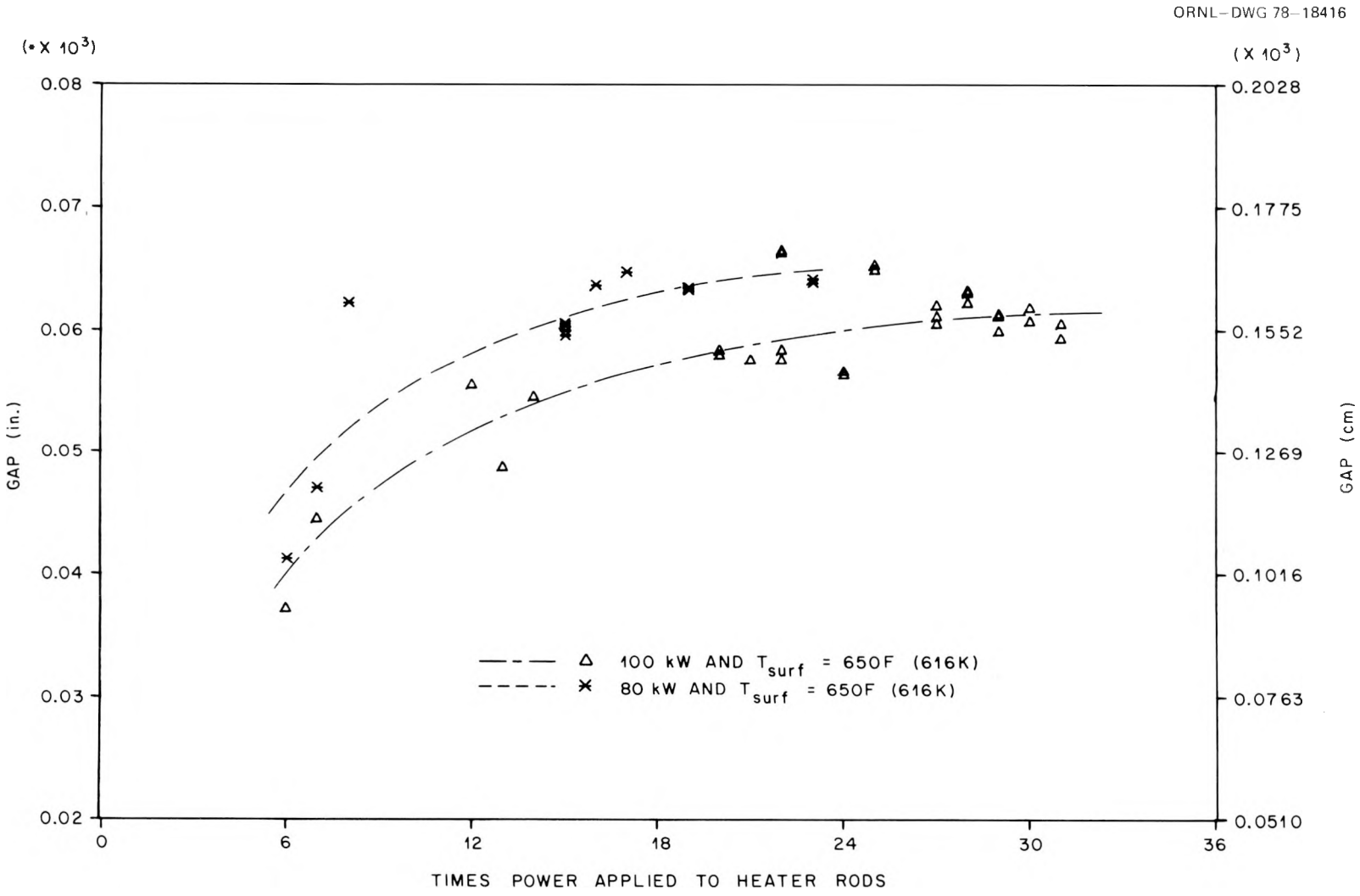

Fig. 2.8. Gap aging history at thermocouple position TE-318BG.

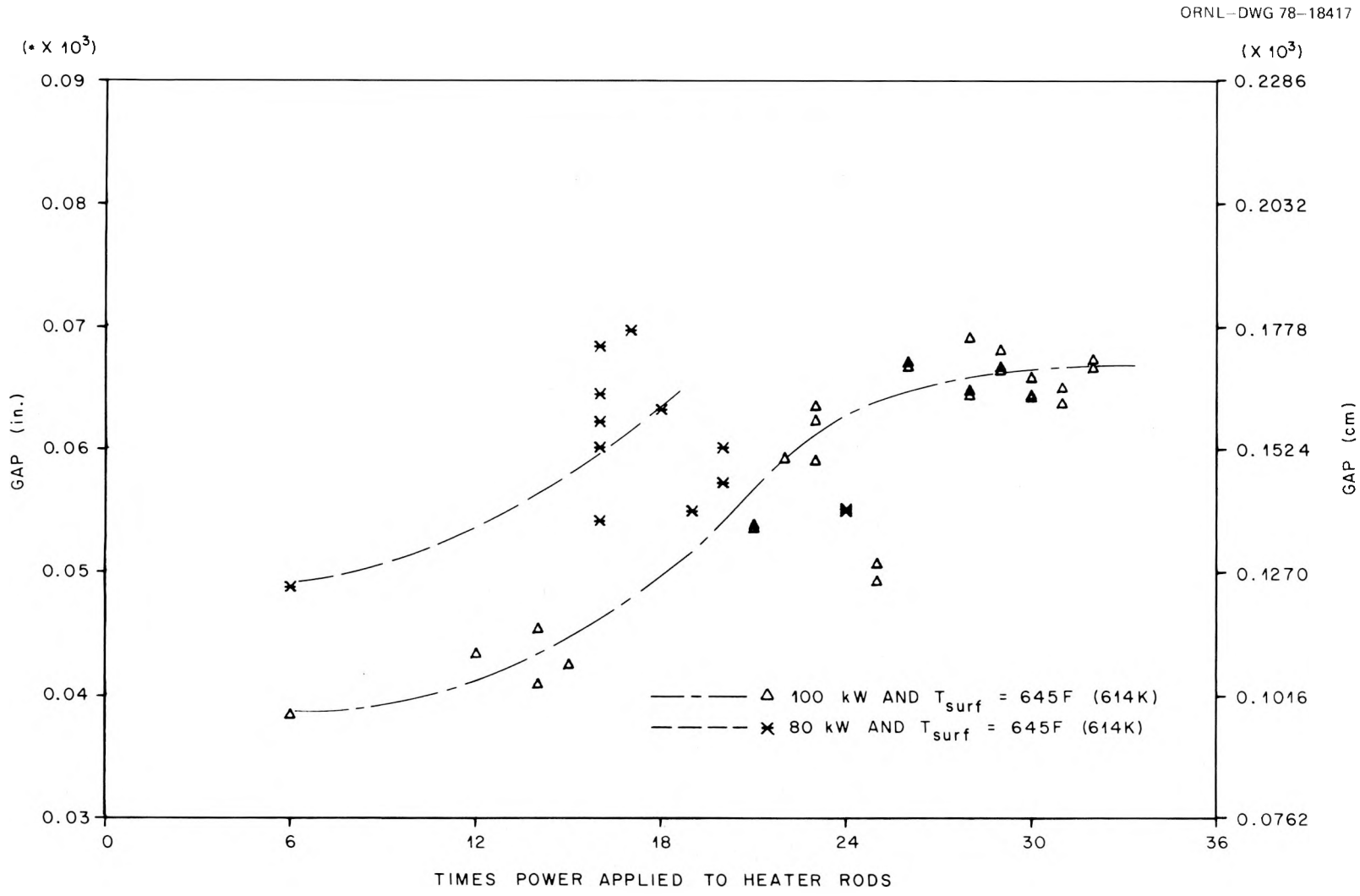

Fig. 2.9. Gap aging history at thermocouple position TE-301DJ (constant surface temperature).

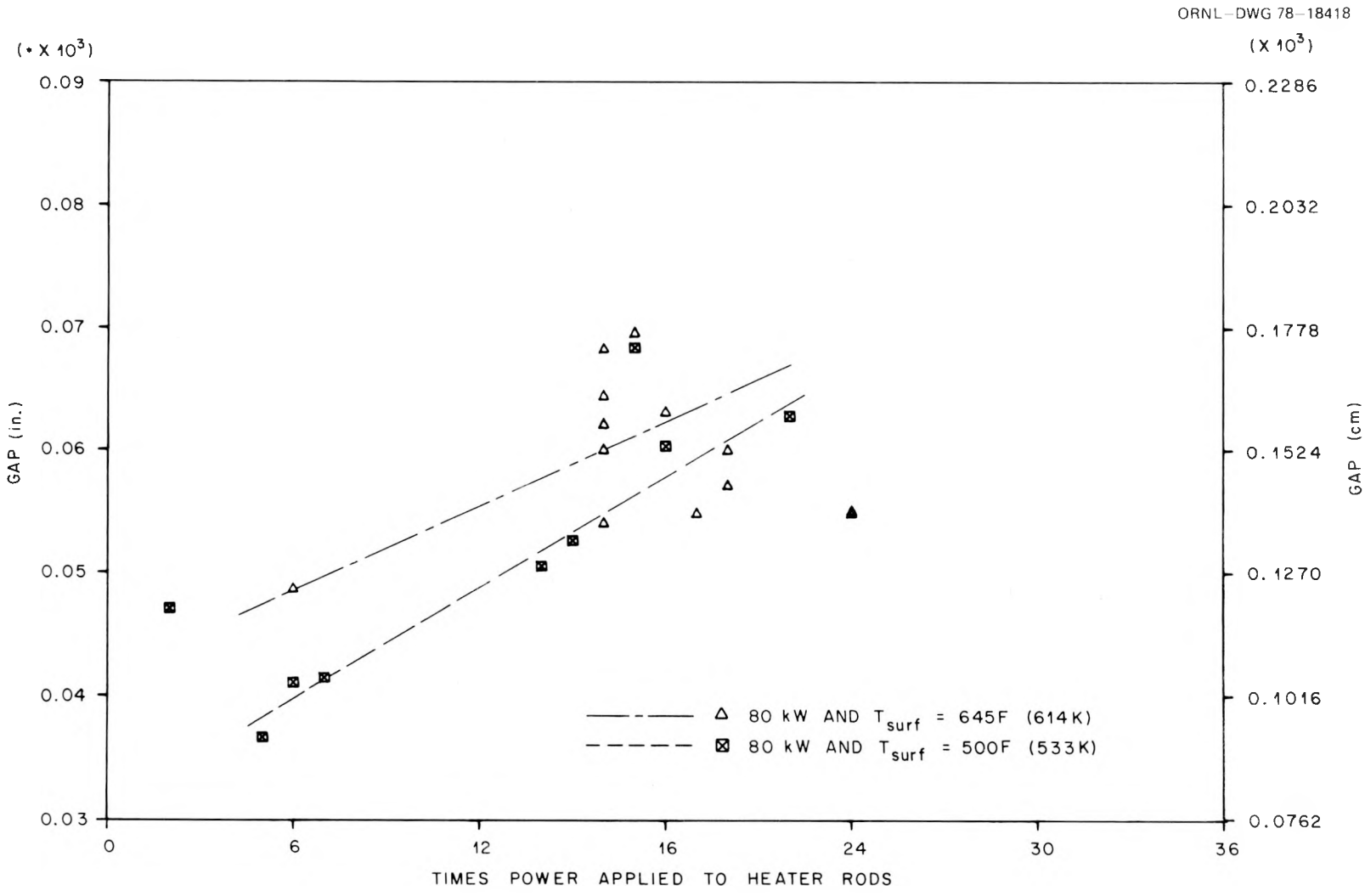

Fig. 2.10. Gap aging history at thermocouple position TE-301DJ (constant power-generation rate).

and the surface temperature increases (the outer sheath thermally expands away from the inner sheath).

2.3 ORTCAL — Part II

Part II of ORTCAL uses temperatures indicated by the sheath and middle thermocouples along with the power-generation rate [entries F(16), F(17), and F(4) in Table 2.1, respectively, from the thermocouple history tape] to produce the effective thermal conductivity of the BN insulator.

For a simulator with heater eccentricity equal to zero, the typical one-dimensional pin radial temperature profile at steady state is as shown in Fig. 2.11. The temperature gradient within the MgO is zero, since $\partial T/\partial r\big|_{r=0} = 0$ and $\dot{q}'''_{MgO} = 0$; therefore, if the pin centerline temperature is known (i.e., if the middle thermocouple exists, is good, and is monitored by the CCDAS), the inside surface temperature of the heater sublayer is known. Heat flow within the heater sublayer is proportional to r^2, which is expressed mathematically[4] as

$$q_{i-1,i} = -\frac{\bar{k}_{i-1,i}\, 4\pi \ell r^2_{i-1}}{(\bar{r}^2_i - \bar{r}^2_{i-1})} (T_i - T_{i-1}) , \tag{2.25}$$

to describe the heat flow between nodes i — 1 and i within the heater substrate. Heat flow within the BN and stainless steel sheath substrates is constant (an assumption) between nodes and is modeled mathematically by Eq. (2.11). Therefore, if the temperature dependencies of the substrate thermal conductivities and the power generation rate are known, the pin centerline temperature can be determined from the sheath thermocouple response or the sheath thermocouple temperature can be determined from the middle thermocouple response by using Eqs. (2.11) and (2.25).

The temperature dependencies of the thermal conductivities for 316 stainless steel, Cupronickel, and Inconel-600, presented in Appendix A, represent least-squares fits to literature data. It is assumed that the thermal conductivity of the BN can be approximated by a polynomial in terms of temperature, that is

$$k_{BN}(T) = C_1 + C_2 T + C_3 T^2 + C_4 T^3 , \tag{2.26}$$

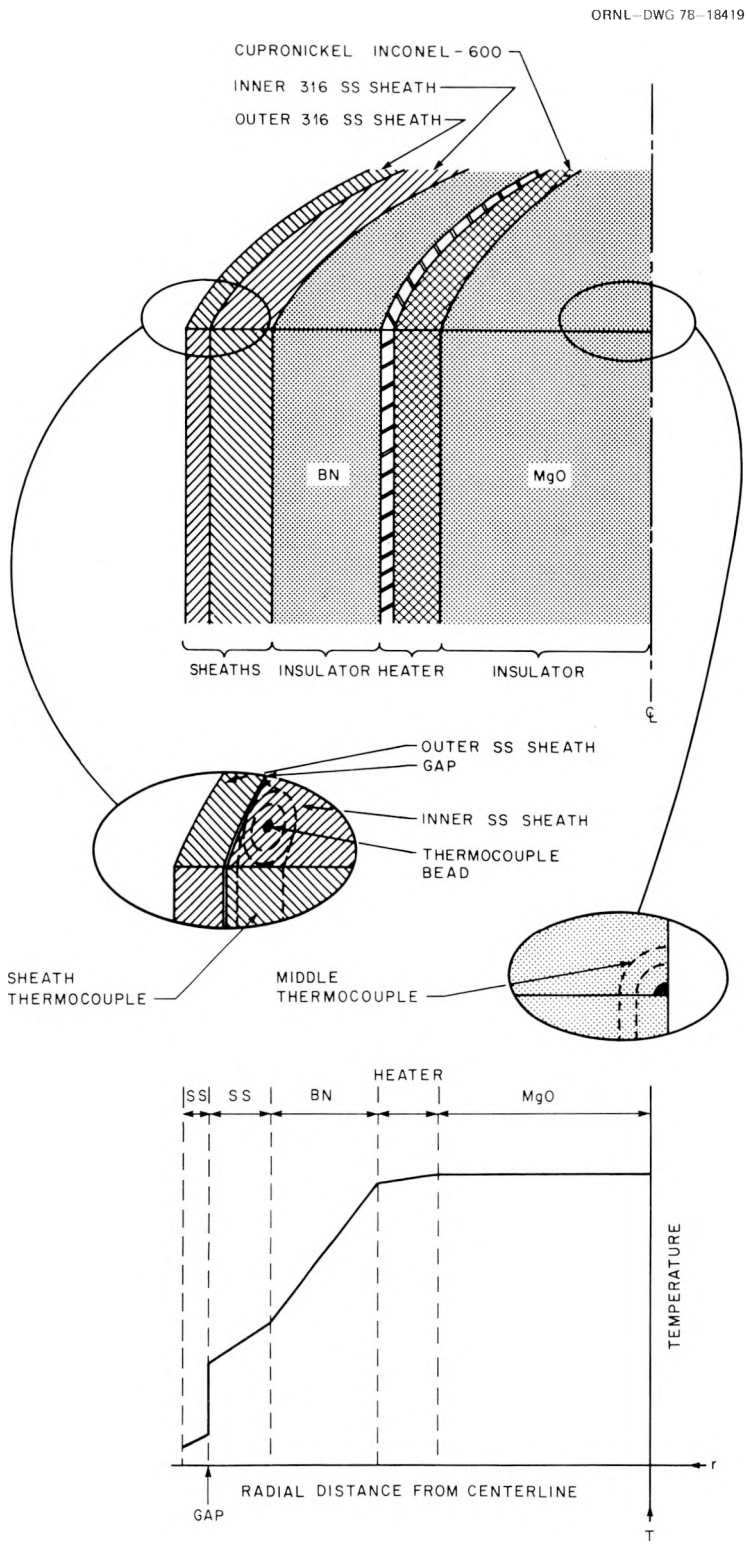

Fig. 2.11. Schematic of fuel pin simulator with sheath and middle thermocouples in insets with typical pin radial temperature profile at steady state.

where C_i are the polynomial coefficients. Thus, given a set of coefficients (C_i) for Eq. (2.26), the simulator centerline temperature (T_{center_j}) can be calculated for each steady-state observation (j) given the following boundary conditions (for each observation): (1) the sheath thermocouple response [entry F(16) in Table 2.1] and (2) the linear power-generation rate [entry F(4)].

The regression procedure for determining the temperature dependence of k_{BN} [Eq. (2.26)] involves the minimization of the sum-of-squares function

$$F(C_1, C_2, C_3, C_4) = \sum_{j=1}^{No.} (Y_{center_j} - T_{center_j})^2 \qquad (2.27)$$

with respect to the C_i parameters, where Y_{center_j} represents the observed middle thermocouple response [entry F(17) in Table 2.1, T_{center_j} is the calculated steady-state pin centerline temperature, and N is number of observations.

The technique employed for optimizing Eq. (2.27) is a numerical search using essentially a pattern search strategy. Pattern search is a direct search procedure which operates on an objective function [i.e., Eq. (2.27)] and proceeds to minimize the function. In general, this method involves the sequential examination of a finite set of trial values of the independent variables to determine whether the objective function can be improved and then changing the independent variables simultaneously in a pattern move based on information acquired in the exploratory search. Each pattern move is followed by a sequence of exploratory moves which revise the pattern. The search continues until the value of the objective function cannot be reduced. The initial work on pattern search was done by Hooke and Jeeves,[33] but the search technique used by ORTCAL (Part II) is based on an improved algorithm developed by Weisman, Wood, and Rivlin.[34]

Examples of the regression output are given in Appendix D for thermocouple positions TE-318BG (Table D.1) and TE-301DJ (Table D.2). The in-situ correlations from Tables D.1 and D.2 and literature values for the

thermal conductivity of BN are compared in Figs. 2.12 and 2.13. [Note: At the end of each table in Appendix D, there is a line stating the "total error" for that individual regression — this value is the minimum objective function, Eq. 2.27, value for the regression.] Also shown are the C_i parameters [i.e., the best-fit parameters for the temperature polynomial in Eq. (2.26)]. The variance of the fit is defined as

$$VAR = \sum_{j=1}^{No.} (Y_{center_j} - T_{center_j})^2/(N - 4) \ , \qquad (2.28)$$

where N = number of observations and N − 4 is the number of independent determinations of $(Y_{center_j} - T_{center_j})$; or, although there are N different values of $(Y_{center_j} - T_{center_j})$ that can be determined from the data, there are also four constraints [number of parameters (C_i)] to be determined. The standard deviation of the fit is

$$\delta_{SD} = \sqrt{VAR} \ . \qquad (2.29)$$

Therefore, given the fitted parameters from the regression and entries F(16) and F(4) for a steady-state observation, the calculated centerline temperature (T_{center_j}) would be expected to be within $\pm 3\delta_{SD}$ of entry F(17) at a 97% confidence level. For thermocouple position TE-318BG, three standard deviations equal ∿7.2 K (12.9°F), which is about half the combined three standard deviations of the two thermocouple (TE-318BG and TE-318MG) temperature measurements.

Thermocouple positions TE-318BG and TE-301DJ illustrate two of the "better" positions in THTF bundle 1 with regard to the k_{BN} regression. There is, of course, the undesirable side of the picture: position TE-322BF (Table D.3), which has a $3\delta_{SD}$ of 30.6 K (55.1°F). The "difference" column in Table D.3 shows that there has obviously been a gradual but steady change in the heater thermal performance over the life of the bundle at this position. The difference $(Y_{center_j} - T_{center_j})$ at a nominal 100 kW/rod was 14 K (25.1°F) during run 2.1 (bundle life ∿2 weeks), 3.9 K (7°F) during run 9.1 (a bundle life of ∿6 months, 2 weeks), and −14.4 K (−25.9°F) during run 23.3 (a bundle life of ∿20 months). White has often stated[30,35-38] that a measure of the thermal performance of a

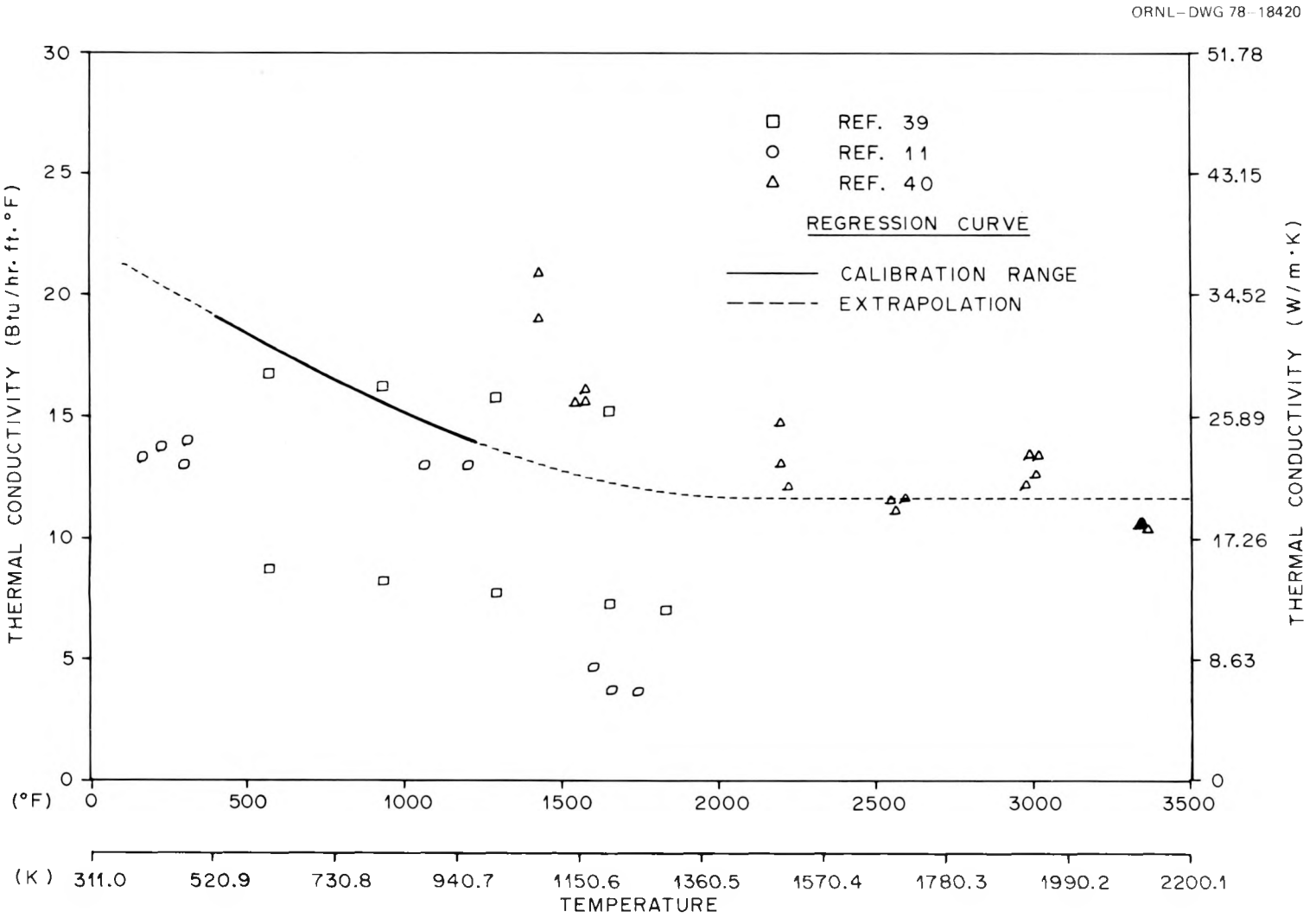

Fig. 2.12. Boron nitride thermal conductivity at 318BG (comparison of regression results with literature data).

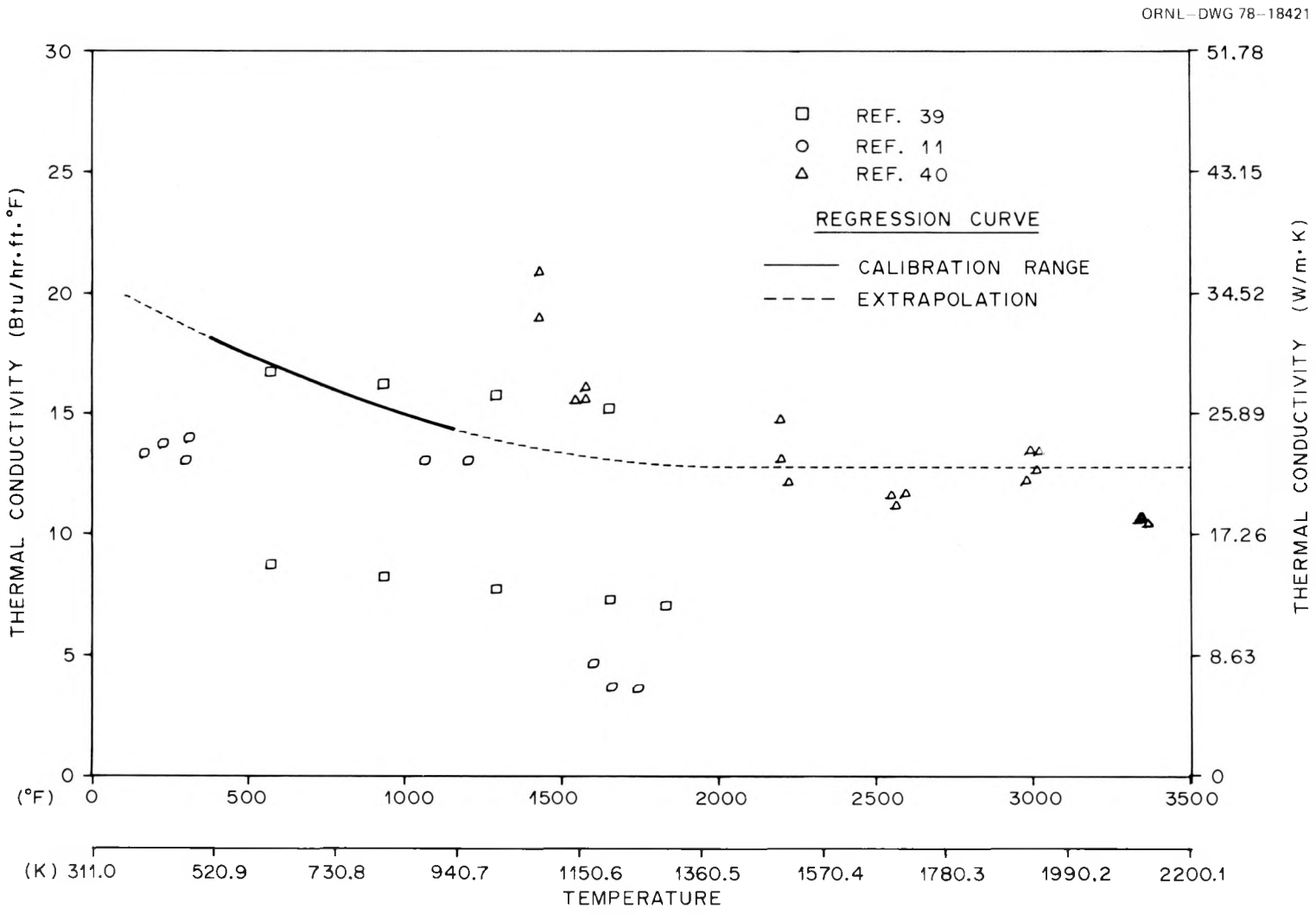

Fig. 2.13. Boron nitride thermal conductivity at 301DJ (comparison of regression results with literature data).

heater is the repeatability of the radial temperature difference between the center and sheath thermocouples. He has also stated that the radial ΔT must have diagnostic sensitivity to changes in the internal conditions of the heater. Plots similar to those of White for thermocouple positions 318BG, 301DJ, and 322BF are presented in Figs. 2.14 to 2.16, respectively. The radial temperature difference at positions 318BG and 301DJ remained relatively unchanged after 32 powered runs and $\sim$20 months; however, at position 322BF there was a drastic change between runs 2.1 and 23.3 [at 100 kW the ΔT changed 26.1 K (47°F)]. "Since radial ΔT's are insensitive to core flow rate, system pressure, heat transfer coefficient at the surface, and gap resistance between the heater sheaths, possible explanations for the changes are (1) a change in heater thermal properties; (2) a change in generated heat flux profile; (3) distortion of the heater; (4) degradation of the thermocouples;"[38] and (5) changes in the radial position of the heating element relative to the sheaths. Zero power temperature measurements and thermocouple electrical properties measurements discount point 4. The slope of the curves in Fig. 2.16 is approximately the same, thus detracting from point 2. The likely explanations are points 1, 3, and 5, with 5 being the most probable considering the manufacturing process (swaging) for these heaters. Regardless of the reason, analysis of the heat transfer from heater positions with this degree of uncertainty may prove very difficult, except for the determination of the time to CHF.

The primary purpose of ORTCAL (Part II) is to produce the effective thermal conductivity of the BN insulator. In essence, the ORTCAL package creates a coefficient data tape (CDT) which contains all the calibration and regression results for each thermocouple position in the THTF bundle. An example of the information contained on the CDT is shown in Table 2.2 for position TE-318BG. ORTCAL (Part II) supplies the information contained in the dashed block. The basic lines of information flow are illustrated in Fig. 2.17.

It is apparent after a review of Fig. 1.13 that all sheath thermocouples are not paired with middle thermocouples. These positions are

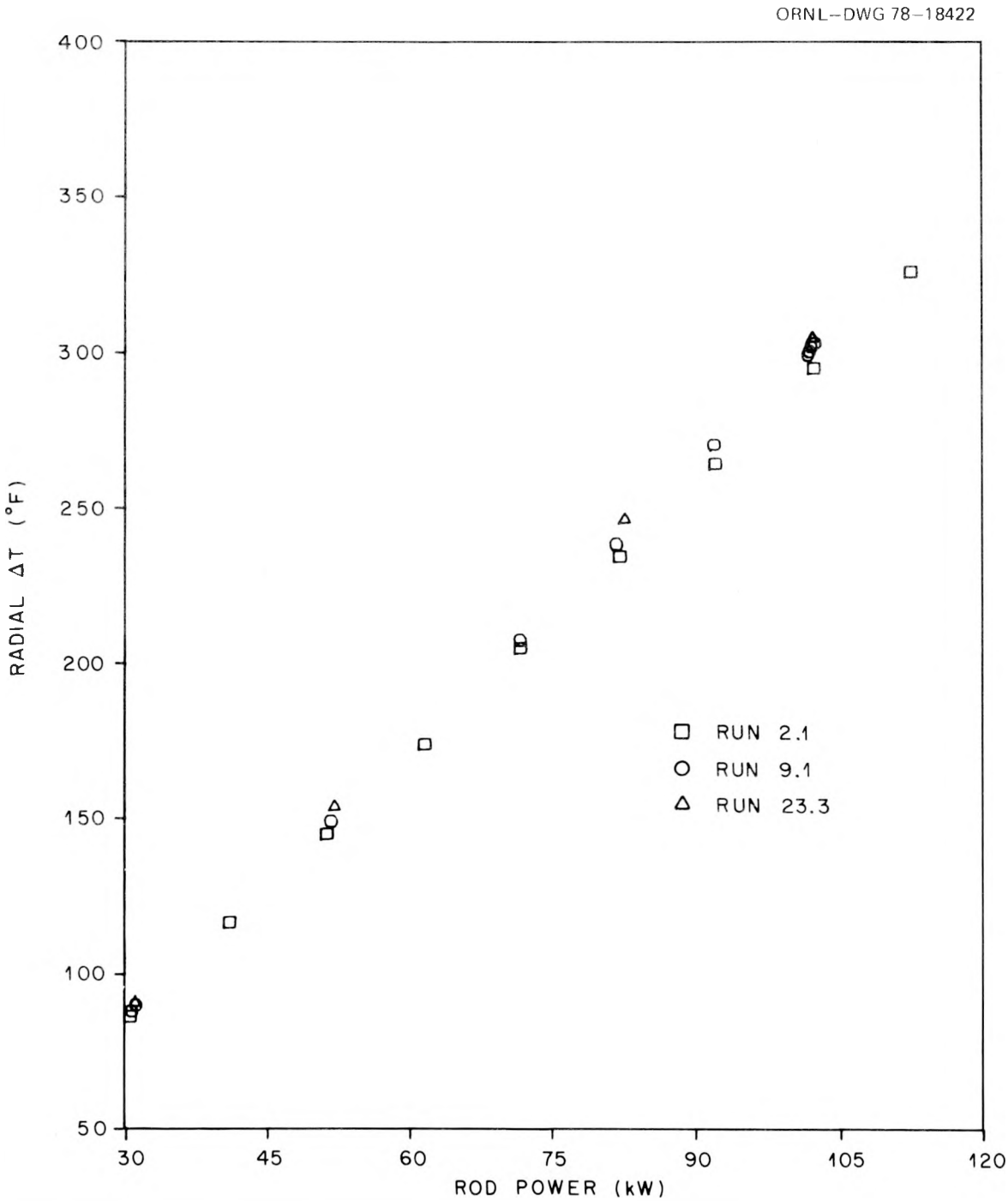

Fig. 2.14. Radial ΔT as a function of rod power (thermocouple position 318BG).

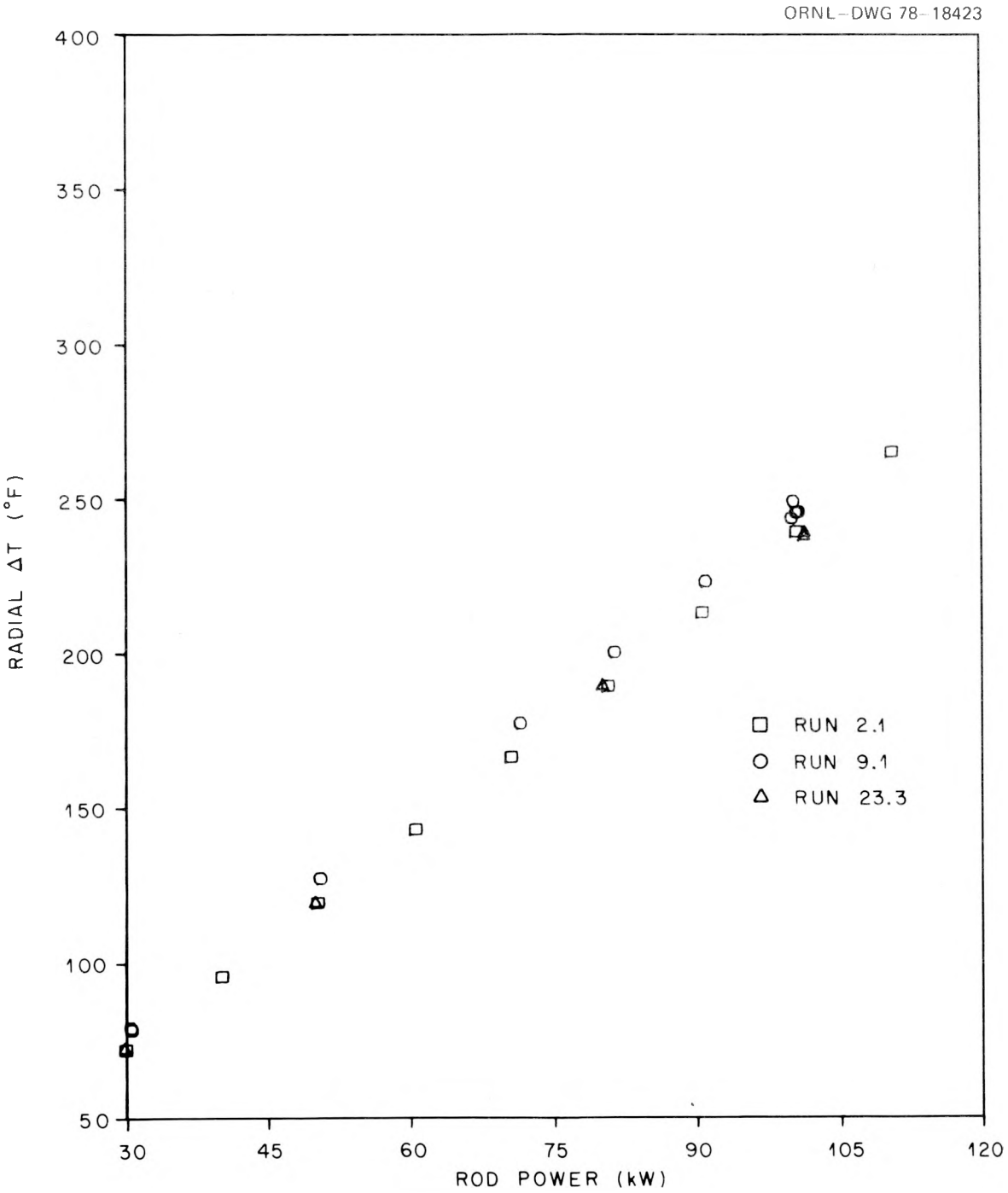

Fig. 2.15. Radial ΔT as a function of rod power (thermocouple position 301DJ).

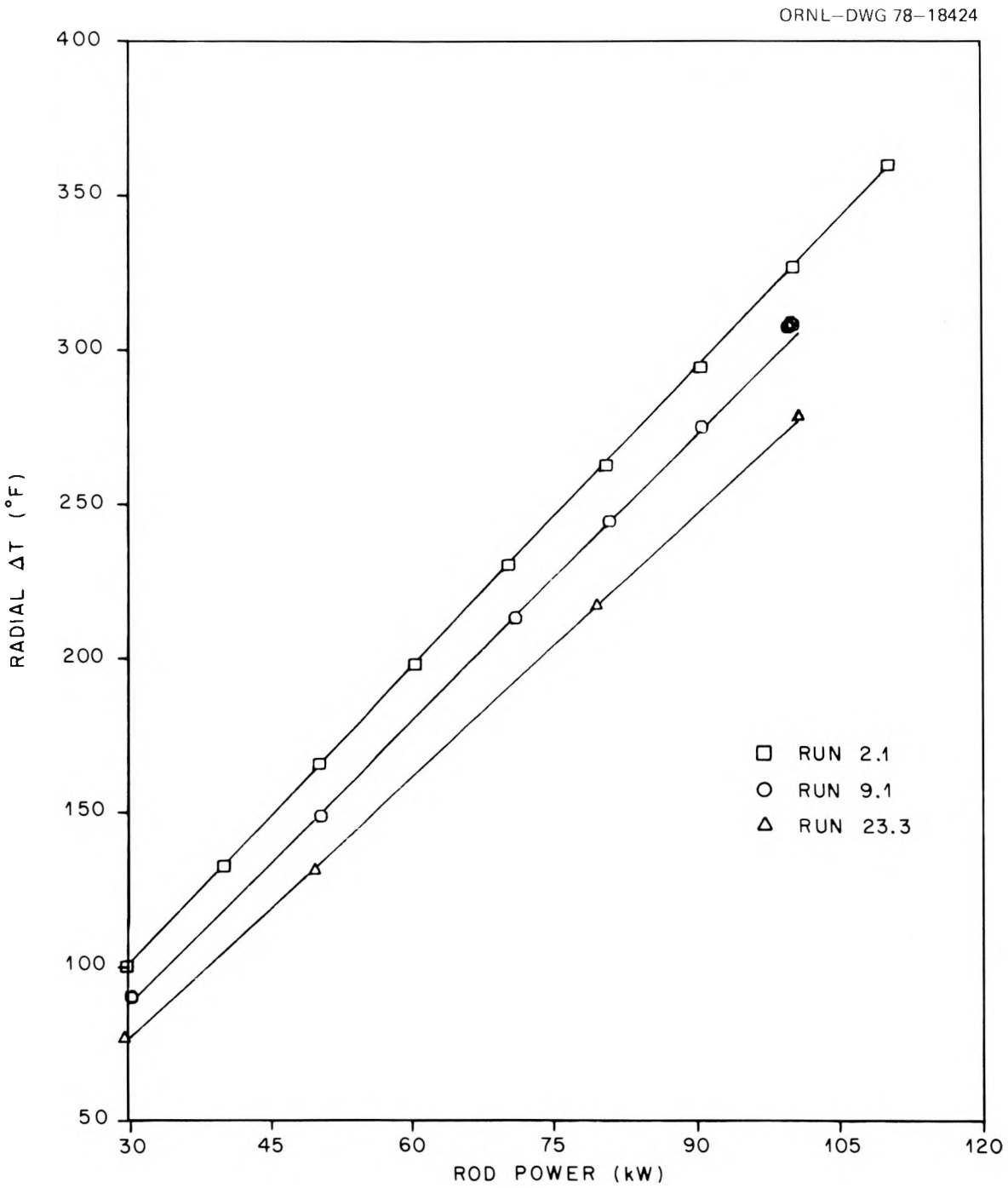

Fig. 2.16. Radial ΔT as a function of rod power (thermocouple position 322BF).

Table 2.2. Calibration results for position TE-318BG in THTF bundle 1

```
          **************************
        ******************************
      ***  THERMOCOUPLE NO. 318-BG  ***
        ******************************
          **************************

***** MIDDLE T/C --- 318-MG

***** DATE OF LAST MODIFICATION : MAY 1,1978

***** AXIAL POWER PEAKING FACTOR IS :   1.6659
      DETERMINED BY INDIV RESISTANCE CAL.

                    ØRTCAL – PART II

***** COEFFICIENTS FOR TEMPERATURE POLYNOMIAL FIT OF KBN
      DETERMINED FOR THE ABOVE SPECIFIC ITCS/ITCM PAIR
      C(1)=  0.21976151E 02
      C(2)= -0.74225366E-02
      C(3)= -0.73717558E-07
      C(4)=  0.59715699E-09

      VARIANCE OF FIT=  0.18624649E 02
      UNITS FOR KBN FIT :  BTU/(HR*FT**2/FT*F)

***** COEFFICIENTS FOR TEMPERATURE POLYNOMIAL FIT FOR KMGO
      DETERMINED FOR THE ABOVE SPECIFIC T/C PAIR
      C(1)=  0.72101288E 01
      C(2)= -0.10450333E-01
      C(3)=  0.79769443E-05
      C(4)= -0.29365270E-08
      C(5)=  0.45424298E-12

      VARIANCE OF FIT=  0.43312866E 03
      UNITS FOR KMGO FIT :  BTU/(HR*FT**2/FT*F)

      ACTUAL MGO POROSITY CALCULATED VIA MODIFIED
            RUSSELL EQUATION :   0.18648702E 00

***** COEFFICIENTS FOR THE THERMAL EXPANSION GAP MODEL FIT
      DETERMINED FOR THE ABOVE SHEATH T/C

      C(1)=  0.62502546E 01     SD=  0.12002551E 02
      C(2)=  0.60596764E-02     SD=  0.17433237E-01
      C(3)= -0.43716855E-05     SD=  0.87200751E-05

      VARIANCE OF FIT=  0.81365113E-04

      GAP CALCULATION AT THE BIAS POINT :          0.0547   (MILS)

      BIAS TEMP. INSIDE S.S.S. NODAL TEMP. :        815.4   DEG. F
      BIAS TEMP. OUTSIDE S.S.S. NODAL TEMP. :       700.8   DEG. F
      BIAS FLUX :   532344.1  BTU/HR/FT**2

      THE MAXIMUM TEMPERATURE FOR WHICH THE ABOVE
      REGRESSION FIT IS APPLICABLE IS   817.17 DEG. F
```

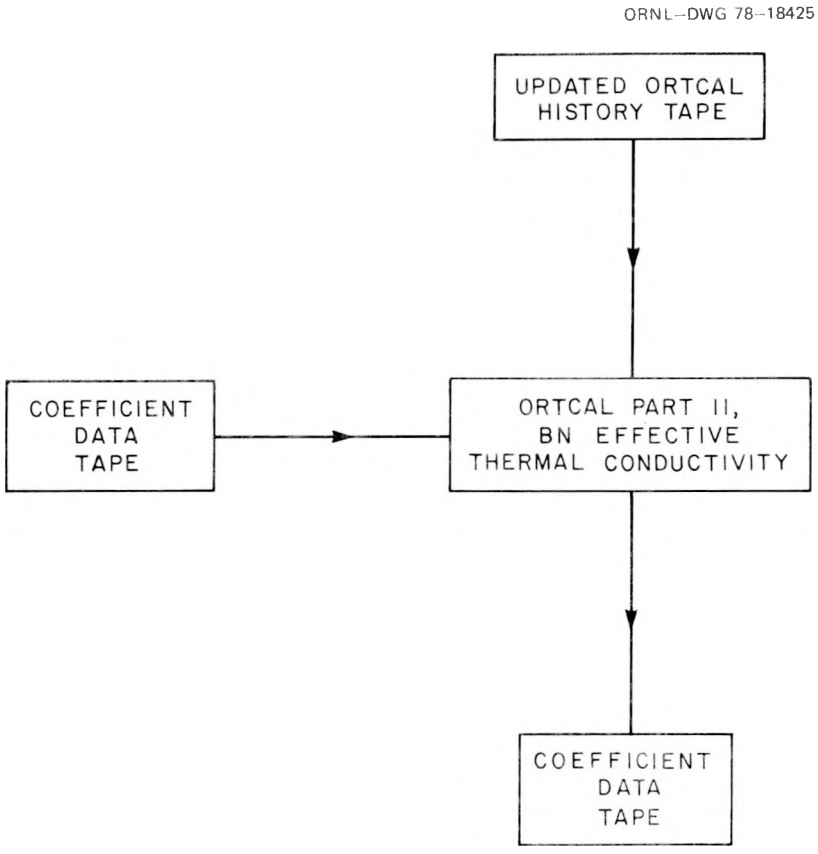

Fig. 2.17. Lines of information flow for ORTCAL — Part II.

classified by the following procedure:

1. For positions in the bundle where a middle thermocouple is paired with a sheath thermocouple, an individual regression is made and the regression coefficients and variance are loaded on the CDT only for that pair of thermocouples.

2. For levels with middle—sheath thermocouple pairs, a level regression is made; that is, the thermocouple pair responses are "lumped" together and an overall regression for the level is performed. The coefficients and variance resulting from this regression are loaded on the CDT for positions not covered by item 1.

3. For levels with no middle—sheath thermocouple pairs (levels D, I, K, L, M, and N in THTF bundle 1), a bundle regression is made. The coefficients and variance resulting from this regression are loaded on the CDT for positions not covered by item 1 or 2.

Figure 2.17 is actually a simplification of the network required to classify the thermal conductivity of the BN insulator. One computer program does the individual and level regressions and a second program handles the bundle regression; lines of information flow required to fully classify the BN thermal conductivity for the entire bundle are shown in Fig. 2.18. For comparison with the individual regressions in Figs. 2.12 and 2.13, a plot of the bundle regression is shown in Fig. 2.19.

2.4 ORTCAL — Part III

The thermal conductivity of MgO is a strong function of its packed density (or porosity) as shown in Fig. 2.20. Since the construction procedure for the THTF heaters involves a series of swaging operations with certain sections of the heater being swaged more than others, the estimated density of the MgO ceramic core ranges from 70 to 90% of the theoretical density.

Part III of ORTCAL uses the temperatures indicated by the sheath and the middle thermocouples along with the power-generation rate to produce the effective thermal diffusivity of the MgO core. [The regressions of ORTCAL — Part II (determination of the effective thermal conductivity of the BN insulator) must precede the regressions of ORTCAL — Part III.]

Power drop tests (i.e., controlled transients) are performed for use by Part III of ORTCAL. These tests involve simply "tripping" power to the bundle with the core mass flow rate and core inlet pressure and temperature remaining essentially constant throughout the test. The CCDAS is on fast scan during the test (duration $\sim$3 min); but most of the action is over within $\sim$10 sec after power is tripped.

An engineering units tape of the "trip" file is read by preprocessor programs, which determine trip point and mean steady-state instrument responses (prior to trip) and reorganize the information into the input format required by Part III.

It is assumed that the thermal conductivity of MgO can be approximated by a polynomial in terms of temperature, that is

$$k_{MgO}(T) = C_1 + C_2T + C_3T^2 + C_4T^3 + C_5T^4 \ , \qquad (2.30)$$

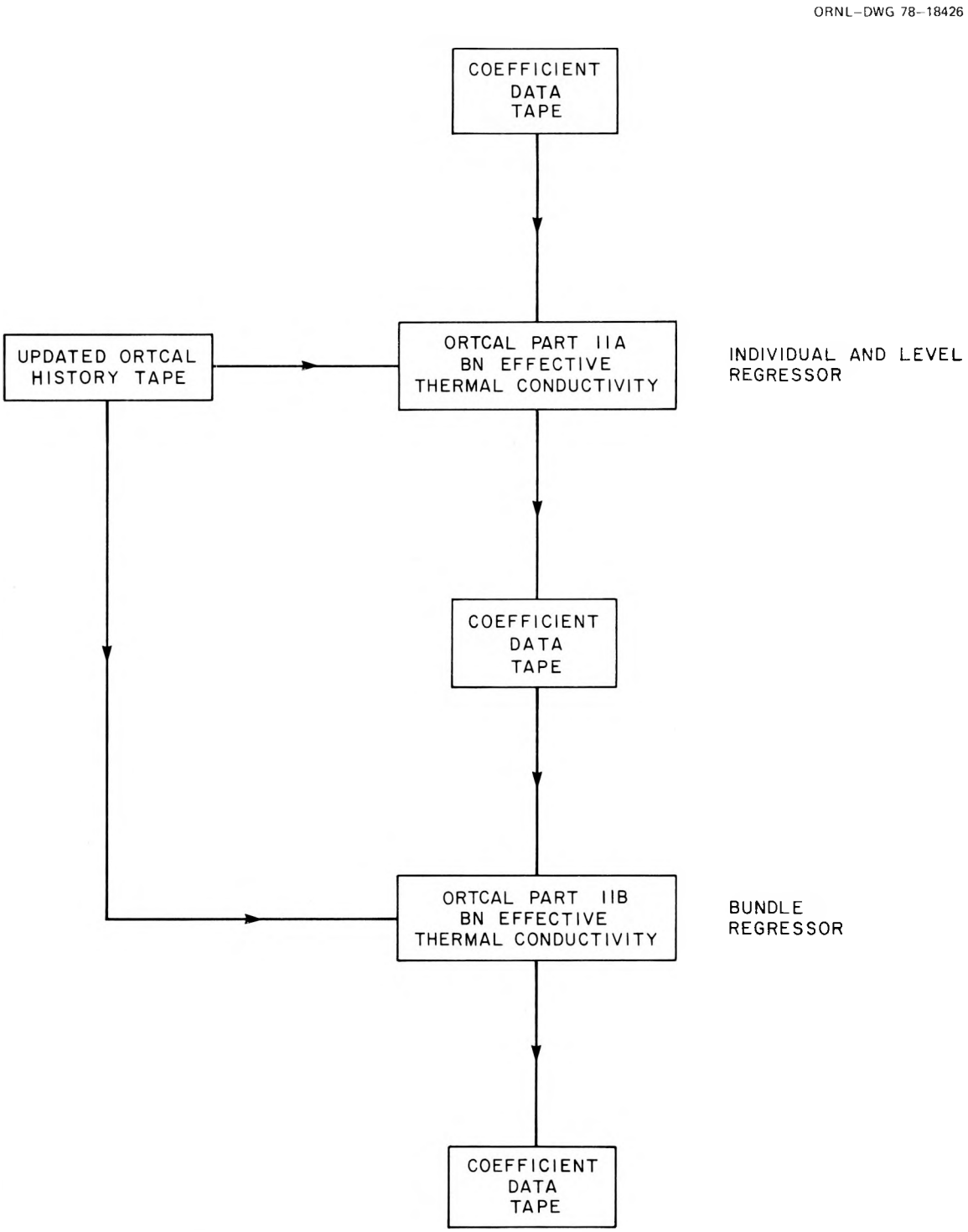

Fig. 2.18. Lines of information flow required for complete k_{BN} classification at all bundle thermocouple positions.

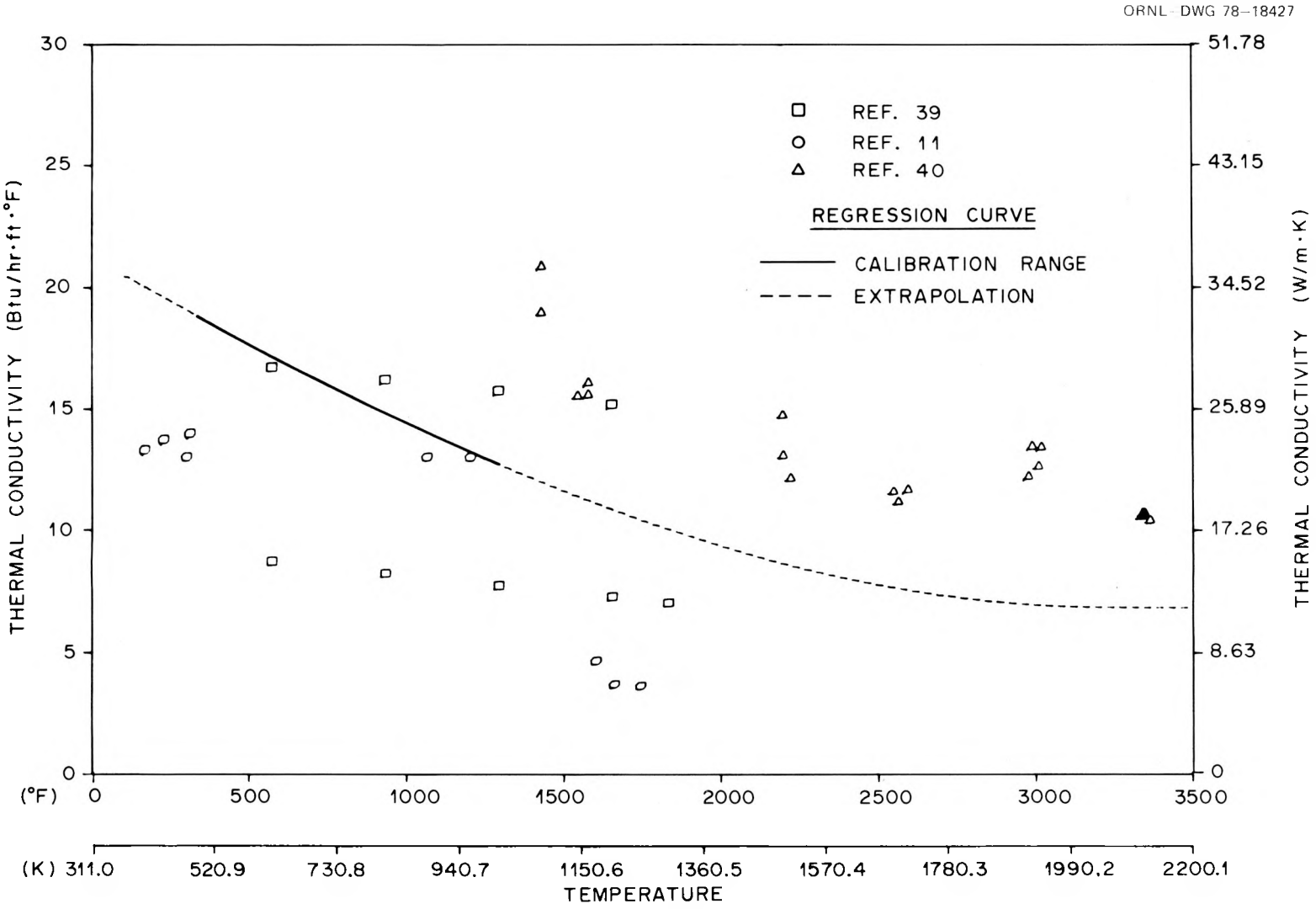

Fig. 2.19. Boron nitride thermal conductivity for bundle 1 (comparison of regression results with literature data).

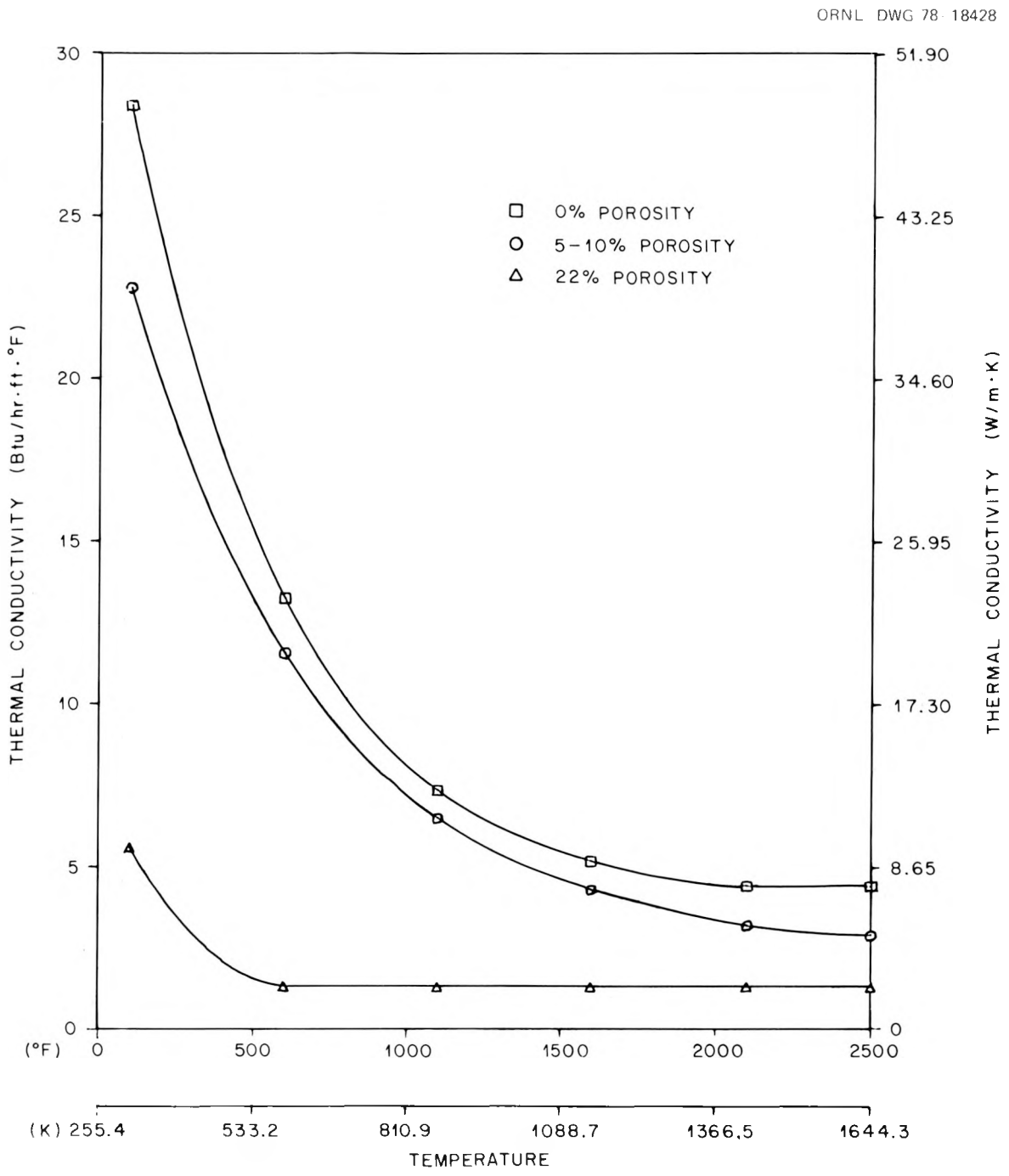

Fig. 2.20. MgO thermal conductivity as a function of temperature and porosity (literature data, Ref. 6).

where C_i are the polynomial coefficients. The MgO thermal diffusivity regression is based on minimization of the following sum-of-squares function,

$$F(C_1, C_2, C_3, C_4, C_5) = \sum_{j=1}^{N_\phi} \left[\sum_{i=1}^{\eta_I} (Y_{center_i} - T_{center_i})^2 \right]_j , \quad (2.31)$$

with respect to the C_i parameters. The term Y_{center_i} represents the observed middle thermocouple response, T_{center_i} is the calculated pin centerline temperature, η_I is the number of observations per power drop, and N_ϕ is the total number of power drops.

Part III essentially solves the forward conduction problem given a set of C_i coefficients and the following boundary conditions: (1) power-generation rate (as a function of time) and (2) sheath thermocouple response (as a function of time). The program runs the inverse package developed for ORINC[4] as a subroutine driven by a numerical pattern search (the same routine used by Part II) for the optimum polynomial coefficients.

Appendix E gives an example of ORTCAL — Part III regression output for thermocouple position TE-301DJ. Line plots which overlay the predicted (i.e., calculated) centerline temperatures and observed middle thermocouple responses for TE-301DJ for five power drops are also presented. The appendix also gives the overall regression results for position TE-301DJ, power trip 1.1 (from 50 kW/rod), power trip 1.2 (from 90 kW/rod), power trip 1.3 (from 122 kW/rod), power trip 1.4 (90 kW/rod), and power trip 8.1 (from 50 kW/rod).

A plot of the regression fits for TE-301DJ and TE-318BG vs literature data for the thermal conductivity of MgO is shown in Fig. 2.21. The "blocked" portion of Table 2.3 represents the contribution of Part III to the CDT file. A simplified flow chart of the information flow required for ORTCAL — Part III is presented in Fig. 2.22.

There are a limited number of locations in THTF bundle 1 that have sheath—middle thermocouple pairs monitored by the CCDAS (see Section 2.3). Therefore, the number of locations in bundle 1 for which the rigorous regressions of Part III can be applied is limited; however, the entire bundle (266 sheath thermocouple locations) must be classified. The

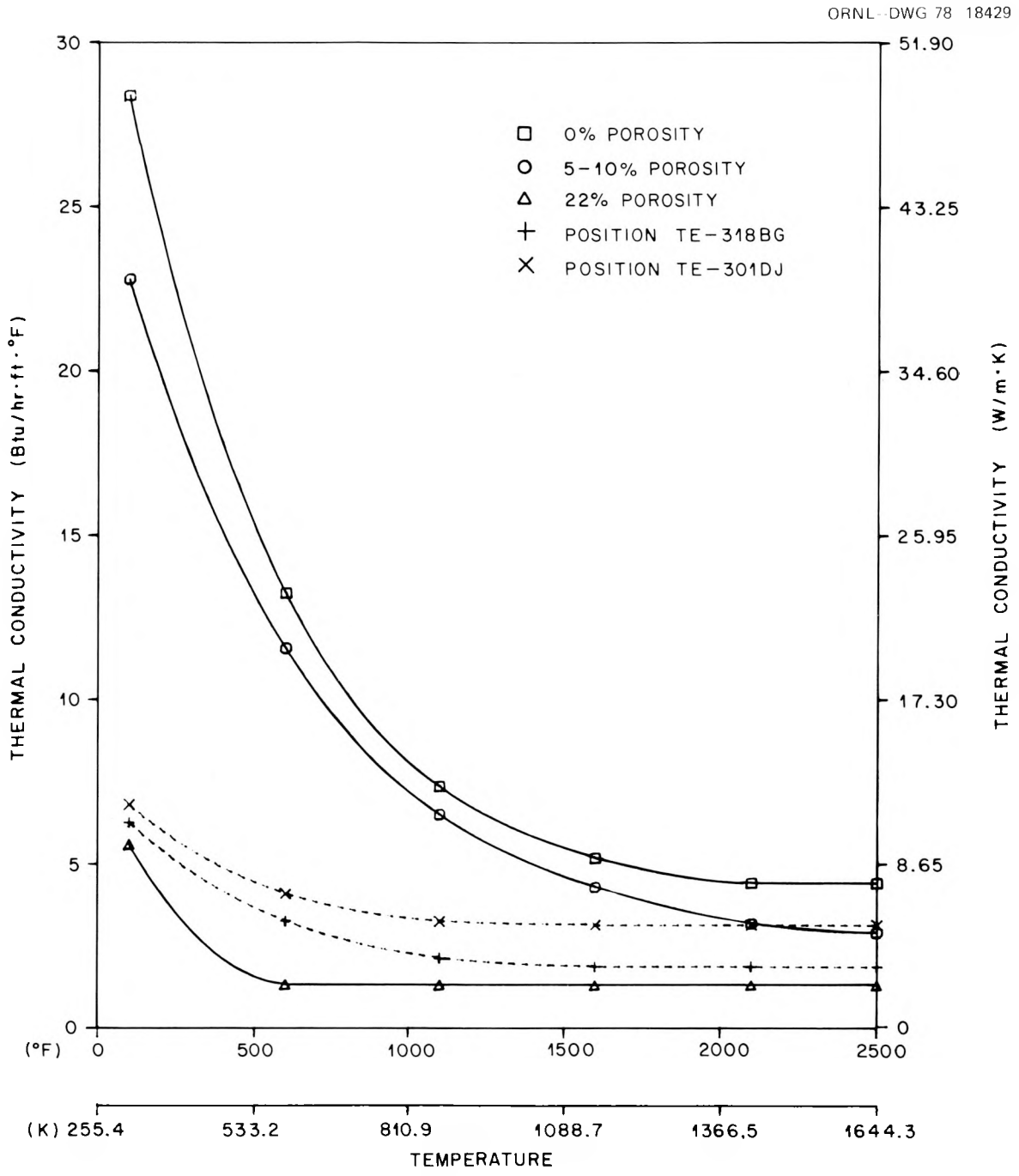

Fig. 2.21. MgO thermal conductivity as a function of temperature and porosity (comparison of regression results at 318BG and 301DJ with literature data, Ref. 6).

Table 2.3. Calibration results for position TE-301DJ in THTF bundle 1

```
          **************************
        ******************************
      ***  THERMOCOUPLE NO. 301-DJ  ***
        ******************************
          **************************


***** MIDDLE T/C --- 301-MJ

***** DATE OF LAST MODIFICATION : MAY 1,1978

***** AXIAL POWER PEAKING FACTOR IS :   1.3012
      DETERMINED BY INDIV RESISTANCE CAL.

***** COEFFICIENTS FOR TEMPERATURE POLYNOMIAL FIT OF KBN
      DETERMINED FOR THE ABOVE SPECIFIC ITCS/ITCM PAIR
      C(1)=  0.20594376E 02
      C(2)= -0.71305782E-02
      C(3)=  0.11995689E-05
      C(4)=  0.19595138E-09

      VARIANCE OF FIT=  0.15701573E 02
      UNITS FOR KBN FIT :  BTU/(HR*FT**2/FT*F)
```

ØRTCAL – PART III

```
***** COEFFIEIENTS FOR TEMPERATURE POLYNOMIAL FIT FOR KMGO
      DETERMINED FOR THE ABOVE SPECIFIC T/C PAIR
      C(1)=  0.77045898E 01
      C(2)= -0.99152625E-02
      C(3)=  0.79940228E-05
      C(4)= -0.28400076E-08
      C(5)=  0.37483889E-12

      VARIANCE OF FIT=  0.23226364E 02
      UNITS FOR KMGO FIT :  BTU/(HR*FT**2/FT*F)

      ACTUAL MGO POROSITY CALCULATED VIA MODIFIED
              RUSSELL EQUATION :   0.16666609E 00

***** COEFFICIENTS FOR THE THERMAL EXPANSION GAP MODEL FIT
      DETERMINED BY USING THE BIAS GAP VALUE AS A MEAN GAP

      C(1)=  0.0                SD=  0.0
      C(2)=  0.0                SD=  0.0
      C(3)=  0.0                SD=  0.0

      VARIANCE OF FIT=  0.0

      GAP CALCULATION AT THE BIAS POINT :          0.0547   (MILS)

      BIAS TEMP. INSIDE S.S.S. NODAL TEMP. :        780.7   DEG. F
      BIAS TEMP. OUTSIDE S.S.S. NODAL TEMP. :       691.2   DEG. F
      BIAS FLUX :   409356.5  BTU/HR/FT**2

      THE MAXIMUM TEMPERATURE FOR WHICH THE ABOVE
      REGRESSION FIT IS APPLICABLE IS     0.0  DEG. F
```

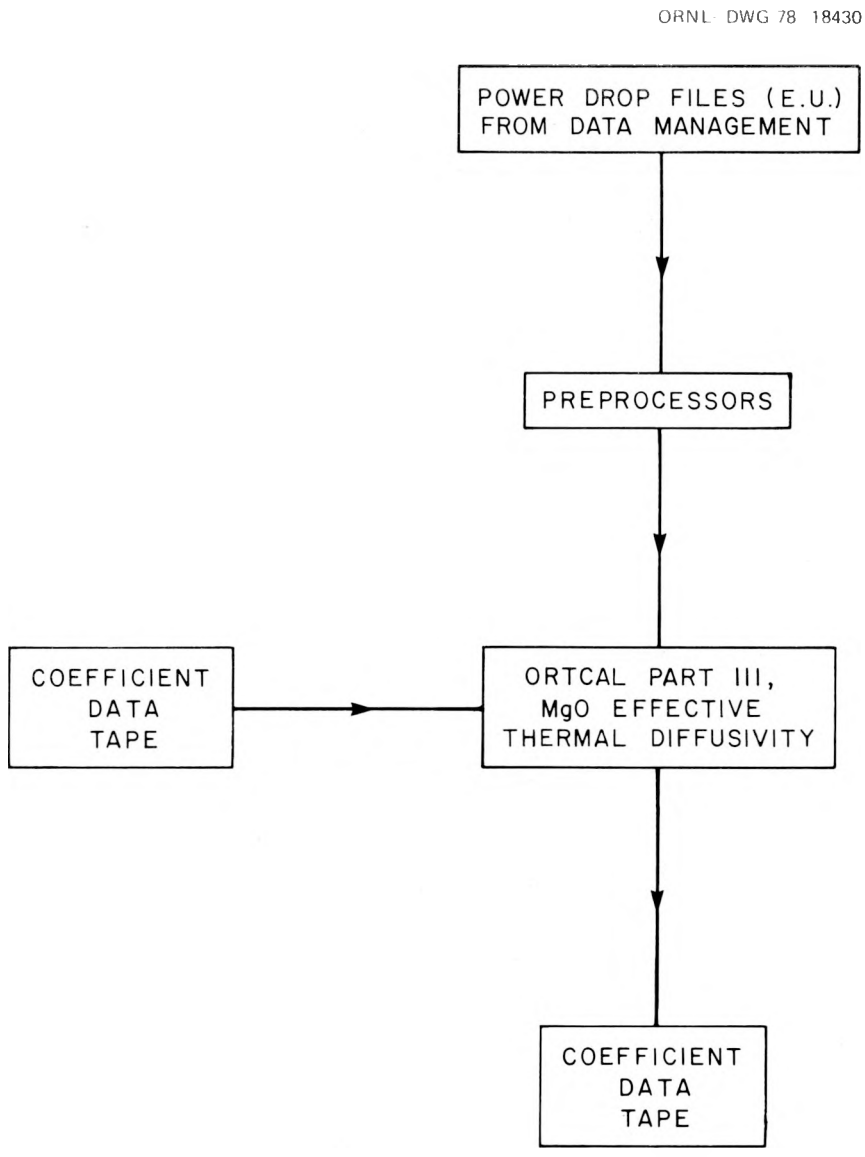

Fig. 2.22. Lines of information flow for ORTCAL — Part III.

following steps comprise the current approach to classifying bundle 1:

1. For positions in the bundle where there is a middle thermocouple paired with a sheath thermocouple, an individual regression is made and the regression coefficients and variance are loaded on the CDT only for that pair of thermocouples. The porosity of the MgO core is estimated from the regression fit and the modified Russell equation (Appendix G) and is entered on the CDT.

2. For levels with middle-sheath thermocouple pairs, a level regression is made; that is, the thermocouple pair responses are "lumped" together and an overall regression for the level is performed. The coefficients and variance resulting from this regression are loaded on the CDT for those positions that are not covered by item 1. The porosity of the MgO core for the levels is estimated from the regression fit and the modified Russell equation and the estimate is entered on the CDT.

3. Unlike the K_{BN} regressions, a bundle regression *cannot* be made for levels with no middle-sheath thermocouple pairs (levels D, I, K, L, M, and N in bundle 1). A bundle regression was appropriate for the k_{BN} because the radial dimensions of the BN (Table 1.3) are approximately constant throughout the rod and the expected compaction of the BN would be approximately the same. However, for the MgO core, the radial dimensions (Table 1.3) and degree of compaction vary in a rod depending on the power zone and the amount of swaging required. The thermal conductivity of MgO is estimated for levels D, I, K, L, M, and N by using the modified Russell equation, which contains the functional dependence of k_{MgO} for both temperature and porosity. All that is needed is an estimate of the porosity for the above levels. The porosity p of the core is assumed to be proportional to the cross-sectional area of the core or

$$p \propto R_{MgO}^2 \ . \tag{2.32}$$

Figure 2.23 contains a plot of the porosities estimated in items 1 and 2 for E, F, G, H, and J level thermocouples and a least-squares linear fit to the data yields the curve in Fig. 2.23. The estimated porosities for levels D, I, K, L, M, and N in bundle 1 are shown in Table 2.4.

2.5. ORTCAL — Part IV

Part IV of ORTCAL applies regression analysis to the output from Part I to determine the expansion coefficients and proper bias points for the stainless steel annuli forming the gap. The mechanical model chosen to utilize this information is one dimensional, which is consistent with the thermal model used in the inverse calculation. The linear

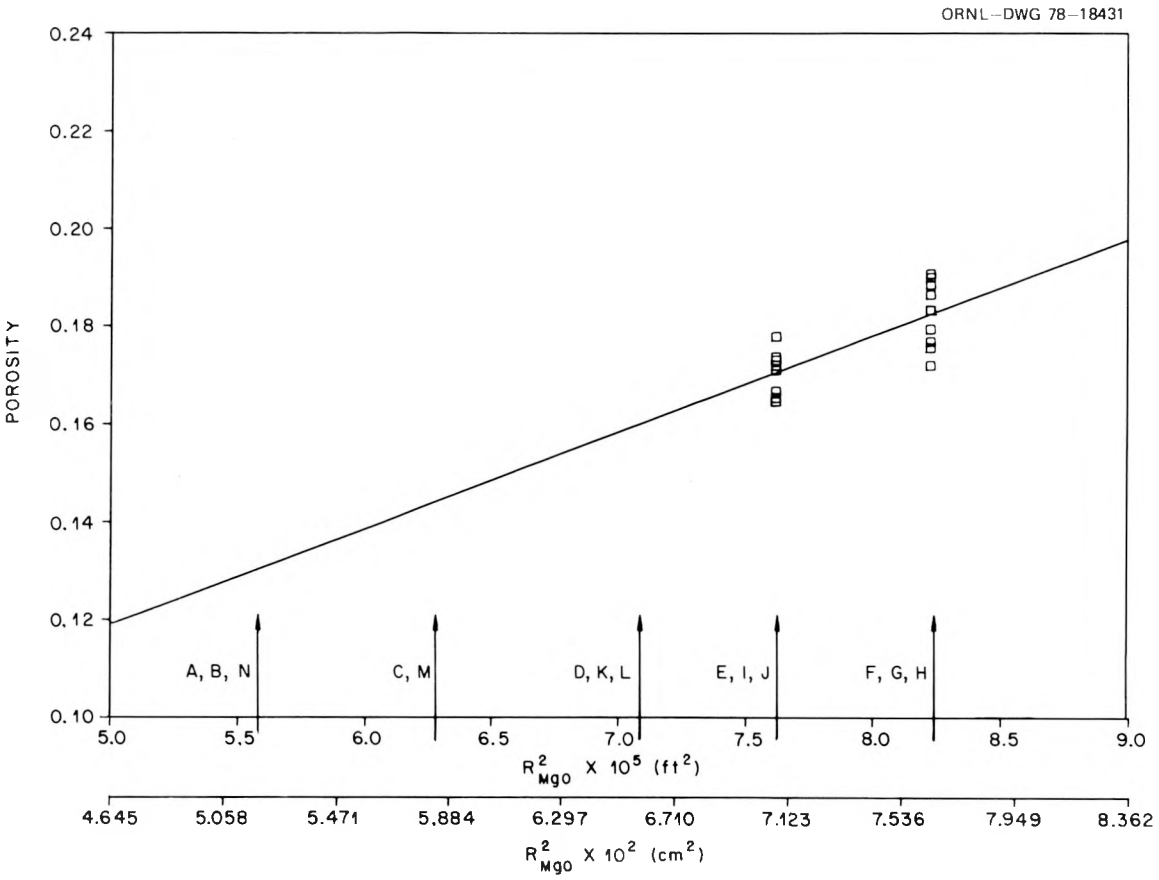

Fig. 2.23. Estimated MgO core porosity for THTF bundle 1.

Table 2.4. Bundle 1 estimated MgO core porosities

Level	Porosity
D	0.1598
I	0.1705
K	0.1598
L	0.1598
M	0.1442
N	0.1303

gap model used in ORINC is

$$\Delta gap = \Delta gap_0 + \Delta\bar{r}_{NS} - \Delta\bar{r}_{NOD5} , \tag{2.33}$$

where subscript 0 denotes the bias gap and subscripts NS and NOD5 refer to the first node in the outer sheath and the last node in the inner sheath, respectively (see Fig. 2.24). The values of $\Delta\bar{r}$ in Eq. (2.33) can be expanded by the following equation, which was derived[4] from the definition for the coefficient of linear expansion:

$$L - L_0 = L_0 \{\exp [C_1(T - T_0) + C_2(T^2 - T_0^2) + C_3(T^3 - T_0^3)] - 1.0\} . \tag{2.34}$$

Expanding $\Delta\bar{r}_{NS}$ and $\Delta\bar{r}_{NOD5}$ by using Eq. (2.34) and inserting the expansion in Eq. (2.33) yields

$$\begin{aligned}\Delta gap = \Delta gap_0 &+ \bar{r}_{NS} \{\exp[C_1(T_{NS} - T_{NS}|_0) + C_2 (T_{NS}^2 - T_{NS}|_0{}^2) \\ &+ C_3(T_{NS}^3 - T_{NS}|_0{}^3)] - 1.0\} - \bar{r}_{NOD5} \{\exp[C_1(T_{NOD5} - T_{NOD5}|_0) \\ &+ C_2(T_{NOD5}^2 - T_{NOD5}|_0{}^2) + C_3(T_{NOD5}^3 - T_{NOD5}|_0{}^3)] - 1.0\} .\end{aligned} \tag{2.35}$$

The term Δgap_0 is the bias gap and $T_{NS}|_0$ and $T_{NOD5}|_0$ are the bias nodal temperatures.

Part IV scans the history tape generated in Part I to find a specified thermocouple or thermocouple level and loads the observed gap [entry F(24) in Table 2.1] and nodal temperatures [entries F(18) and F(19)] for each steady-state point for all powered runs for that thermocouple or thermocouple level. The bias points (gap and nodal temperatures) for each powered run are also determined and loaded.

Since the gap behavior can be expressed in one concise mathematical formula [Eq. (2.35)], a nonlinear least-squares routine (rather than the pattern search technique used previously) is employed to determine the coefficients C_1, C_2, and C_3 in Eq. (2.35).

An example of the Part IV thermocouple level regression for the G level in bundle 1 at TE-318BG is given in Table F.1; the individual regression is presented in Table F.2 and a summary is shown in Table F.3.

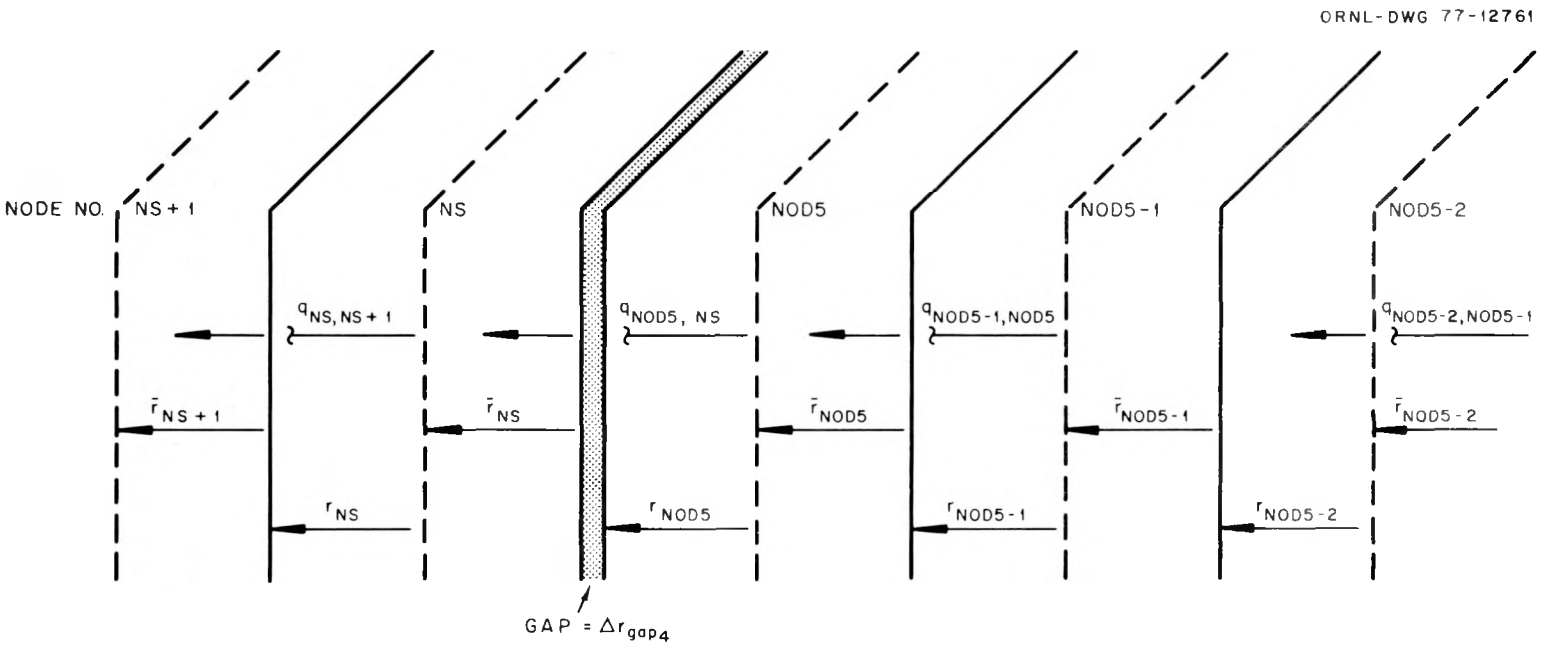

Fig. 2.24. Notation relative to the mathematical model of the thermo-mechanical behavior of the gap between the inner and outer stainless steel sheaths.

The contribution of Part IV to the CDT file is illustrated in the blocked portion of Table 2.5. A simplified flow chart of the information flow to and from Part IV is presented in Fig. 2.25.

Note that the coefficients, standard deviations of the coefficients, and variance of the fit are zeroed in Table 2.3. This indicates that the Part IV regression failed at this position and level. Failure modes for the gap coefficient regression are:

1. the nonlinear least-squares routine diverges in attempting to find a solution;
2. the nonlinear least-squares routine fails to converge (within specified error criterion) to a solution;
3. either or both of the level and individual regressions have negative first derivatives at any of the bias points.

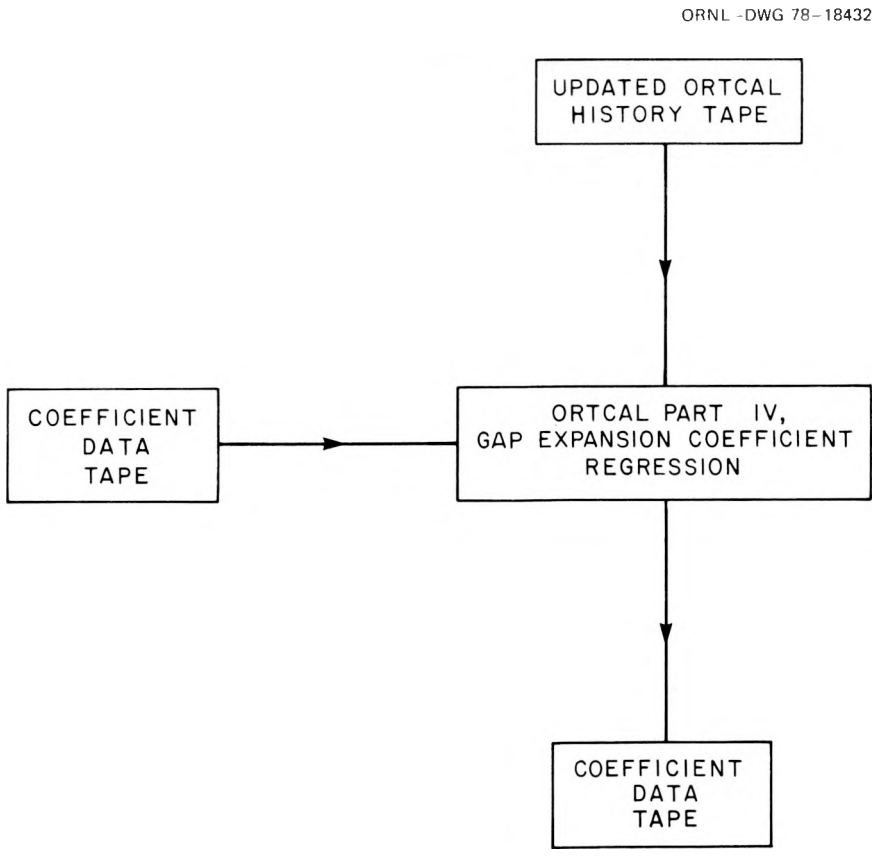

Fig. 2.25. Lines of information flow for ORTCAL — Part IV.

Table 2.5. The ORTCAL — Part IV contribution to the CDT file for position TE-318BG in THTF bundle 1

```
          *************************
        *********************************
      ***   THERMOCOUPLE NO. 318-BG   ***
        *********************************
          *************************


***** MIDDLE T/C --- 318-MG

***** DATE OF LAST MODIFICATION : MAY 1,1978

***** AXIAL POWER PEAKING FACTOR IS :   1.6659
      DETERMINED BY INDIV RESISTANCE CAL.

***** COEFFICIENTS FOR TEMPERATURE POLYNOMIAL FIT OF KBN
      DETERMINED FOR THE ABOVE SPECIFIC ITCS/ITCM PAIR
      C(1)=  0.21976151E 02
      C(2)= -0.74225366E-02
      C(3)= -0.73717558E-07
      C(4)=  0.59715699E-09

      VARIANCE OF FIT=  0.18624649E 02
      UNITS FOR KBN FIT :  BTU/(HR*FT**2/FT*F)

***** COEFFICIENTS FOR TEMPERATURE POLYNOMIAL FIT FOR KMGO
      DETERMINED FOR THE ABOVE SPECIFIC T/C PAIR
      C(1)=  0.72101288E 01
      C(2)= -0.10450333E-01
      C(3)=  0.79769443E-05
      C(4)= -0.29365270E-08
      C(5)=  0.45424298E-12

      VARIANCE OF FIT=  0.43312866E 03
      UNITS FOR KMGO FIT :  BTU/(HR*FT**2/FT*F)

      ACTUAL MGO POROSITY CALCULATED VIA MODIFIED
              RUSSELL EQUATION :   0.18648702E 00
```

ØRTCAL — PART IV

```
***** COEFFICIENTS FOR THE THERMAL EXPANSION GAP MODEL FIT
      DETERMINED FOR THE ABOVE SHEATH T/C

      C(1)=  0.62502546E 01     SD=  0.12002551E 02
      C(2)=  0.60596764E-02     SD=  0.17433237E-01
      C(3)= -0.43716855E-05     SD=  0.87200751E-05

      VARIANCE OF FIT=  0.91365113E-04

      GAP CALCULATION AT THE BIAS POINT :          0.0547   (MILS)

      BIAS TEMP. INSIDE S.S.S. NODAL TEMP. :        815.4   DEG. F
      BIAS TEMP. OUTSIDE S.S.S. NODAL TEMP. :       700.8   DEG. F
      BIAS FLUX :   532344.1  BTU/HR/FT**2


      THE MAXIMUM TEMPERATURE FOR WHICH THE ABOVE
      REGRESSION FIT IS APPLICABLE IS   817.17 DEG. F
```

The primary failure mechanism for the Part IV regressions is item 3, which implies that the simple one-dimensional linear thermal expansion model described by Eq. (2.33) is not capable of describing the dynamic gap behavior at those locations where regression failure occurs. A negative first derivative of Eq. (2.35) implies that the thermal expansion coefficient of stainless steel decreases with increasing temperature, but available physical property data[6] refute this behavior. The linear thermal expansion model accounts only for the radial expansion or contraction of the gap and does not allow for other mechanisms of stress relief. For instance, it is conjectured that there are severe torsional stresses imparted to the stainless steel sheaths by the swaging process during construction of the heaters and that these stresses would be worse at levels H and J. (The heaters are swaged in the direction of A to O level, and levels H and J are located in close proximity to power level breaks with significant radial dimensional differences prior to swaging.) The expected relief of these torsional stresses would be azimuthal rotation of the sheaths relative to each other and the heating element; thus, the gap could not be described by Eq. (2.33).

Part IV regressions are summarized in Table F.4 for THTF bundle 1 through run 24.1. Of the available 269 bundle thermocouple positions, approximately 65% (175) can be calibrated by use of Eq. (2.33). Of the 94 regression failures, 75 (80%) are due to the mode 3 failure mechanism and 73 of the failures occur on H and J level.

If the regressions fail for any of the above reasons, the bias gap is used as a mean gap (i.e., constant gap throughout the transient) in the inverse calculations.

3. CONSEQUENCES OF NONCALIBRATION OF FUEL PIN SIMULATORS

The effect of not classifying fuel pin simulators can best be illustrated by a series of examples that consist of ORINC runs on THTF test 105, where the points of interest in the rod calibration (i.e., BN thermal conductivity, MgO thermal diffusivity, and gap between the sheaths) were varied to qualitatively assess their effect on the inverse calculations. (For a description of the phenomenological sequences in the THTF during test 105, see Refs. 26 and 41.) These properties were not varied in such a manner that the quantitative sensitivity of the calculated surface temperature and flux (with respect to the properties) could be determined (this analysis is currently being done). At present, the only alternative to the approach described in Chapter 2 is to use temperature fits to the literature data for the BN and MgO thermal conductivities and to assume that there is no gap between the sheaths. Therefore, ORINC case studies were made using the following combinations:

1. Case 1. ORTCAL regressions for BN thermal conductivity and MgO thermal diffusivity and the sheath-gap model;
2. Case 2. ORTCAL regression for k_{BN} and α_{MgO} and all gaps zeroed;
3. Case 3. Least-squares fits to literature data for k_{BN} and α_{MgO} and ORTCAL regressions for the sheath-gap model;
4. Case 4. Least-squares fits to literature data for k_{BN} and α_{MgO} and all gaps zeroed.

Case 1 will be used as the base case; case 4 is the current state-of-the-art practice.

Typical rod surface temperature plots (case 1) for thermocouple levels E and G are presented in Figs. 3.1 and 3.2, respectively. Similar plots for the surface heat flux are shown in Figs. 3.3 and 3.4. The corresponding set of plots for case 2 is presented in Figs. 3.5 to 3.8.

A comparison of Figs. 3.3 and 3.4 and Figs. 3.7 and 3.8 reveals little difference in the computed surface heat fluxes. This is expected, since the inverse solutions of the transient conduction equation for cases 1 and 2 will yield identical results for the computed temperature profile from node 1 to node NOD5 (Figs. 3.9 and 3.10) and for the heat

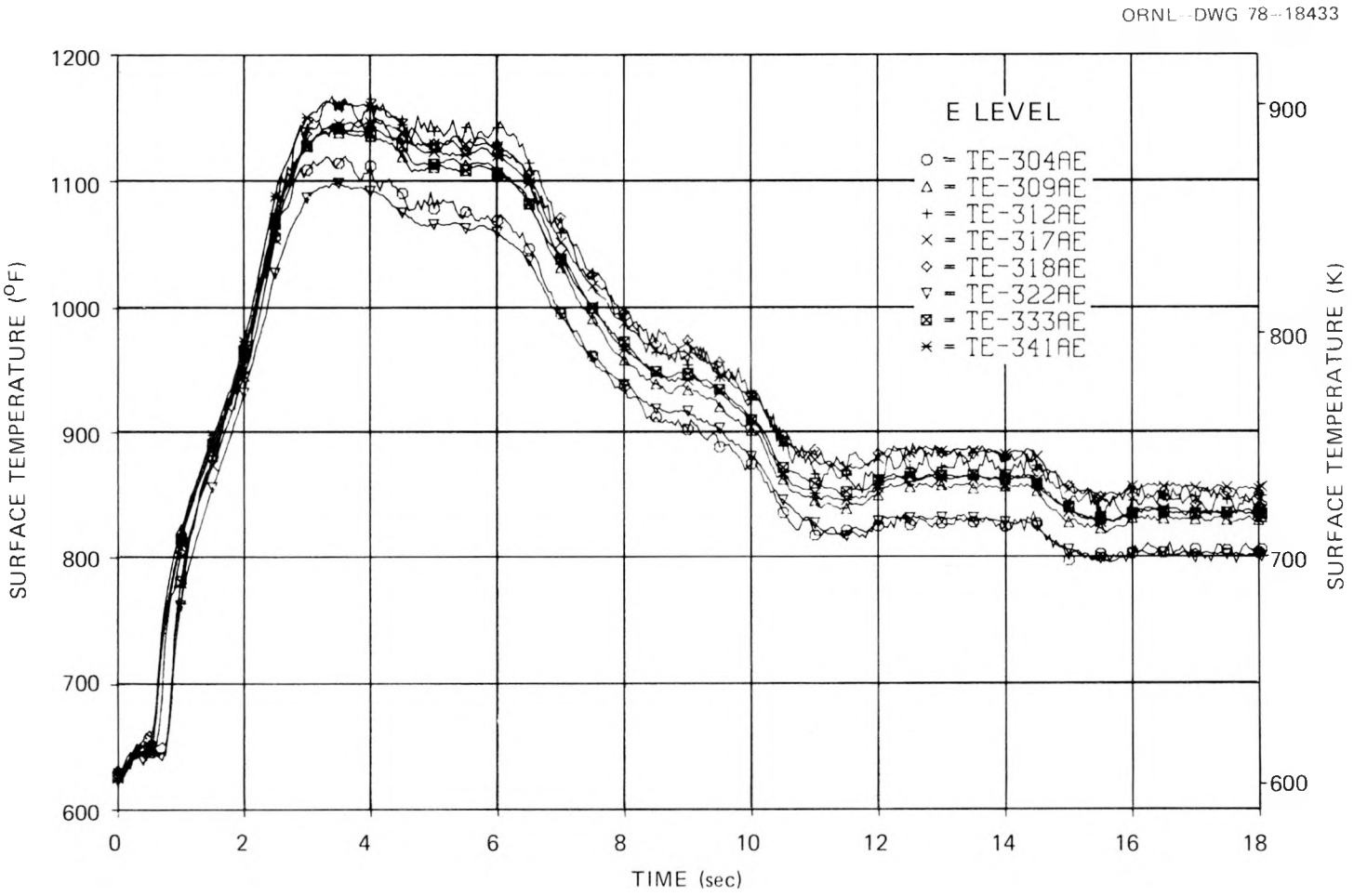

Fig. 3.1. ORINC rod surface temperatures, level E, THTF test 105, case 1.

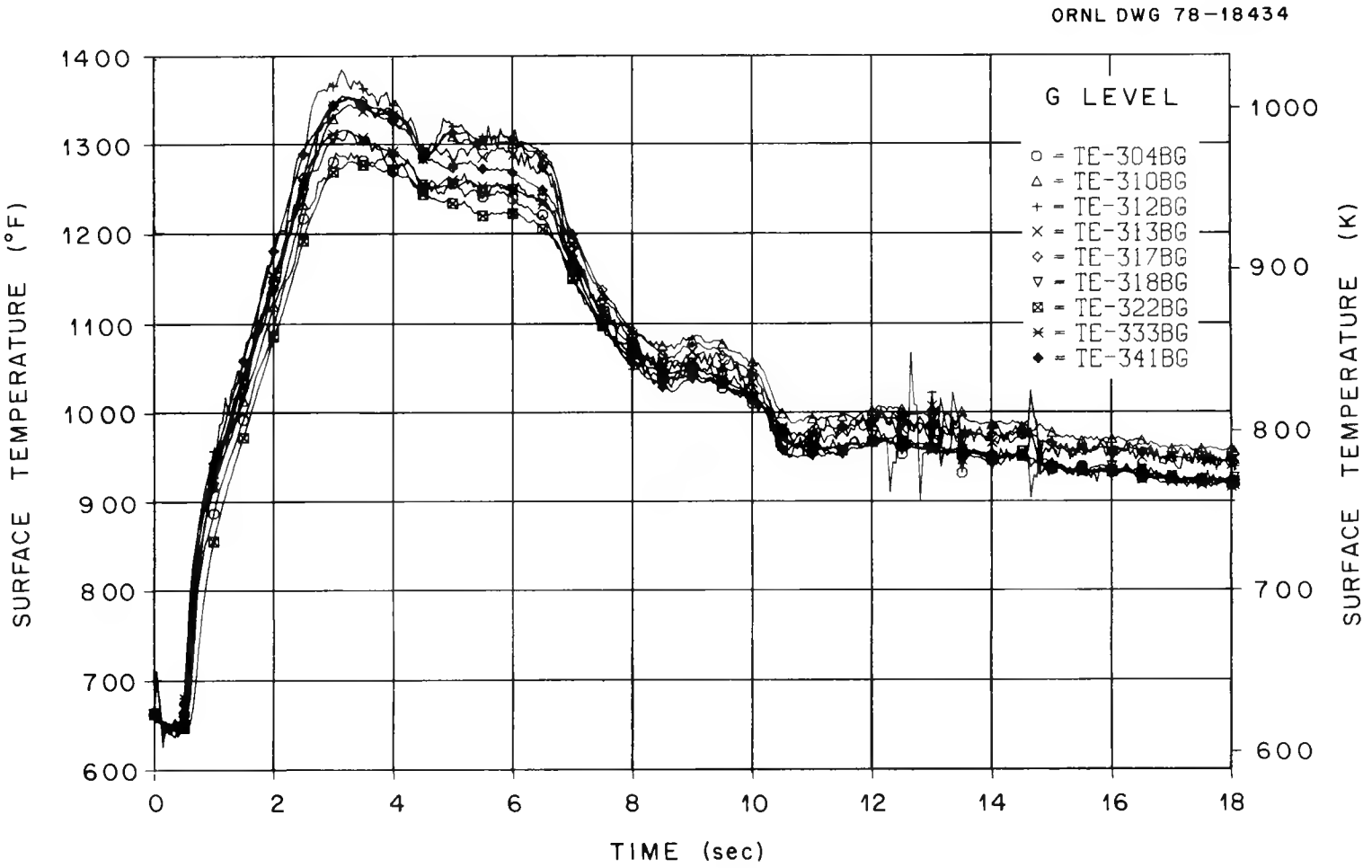

Fig. 3.2. ORINC rod surface temperatures, level G, THTF test 105, case 1.

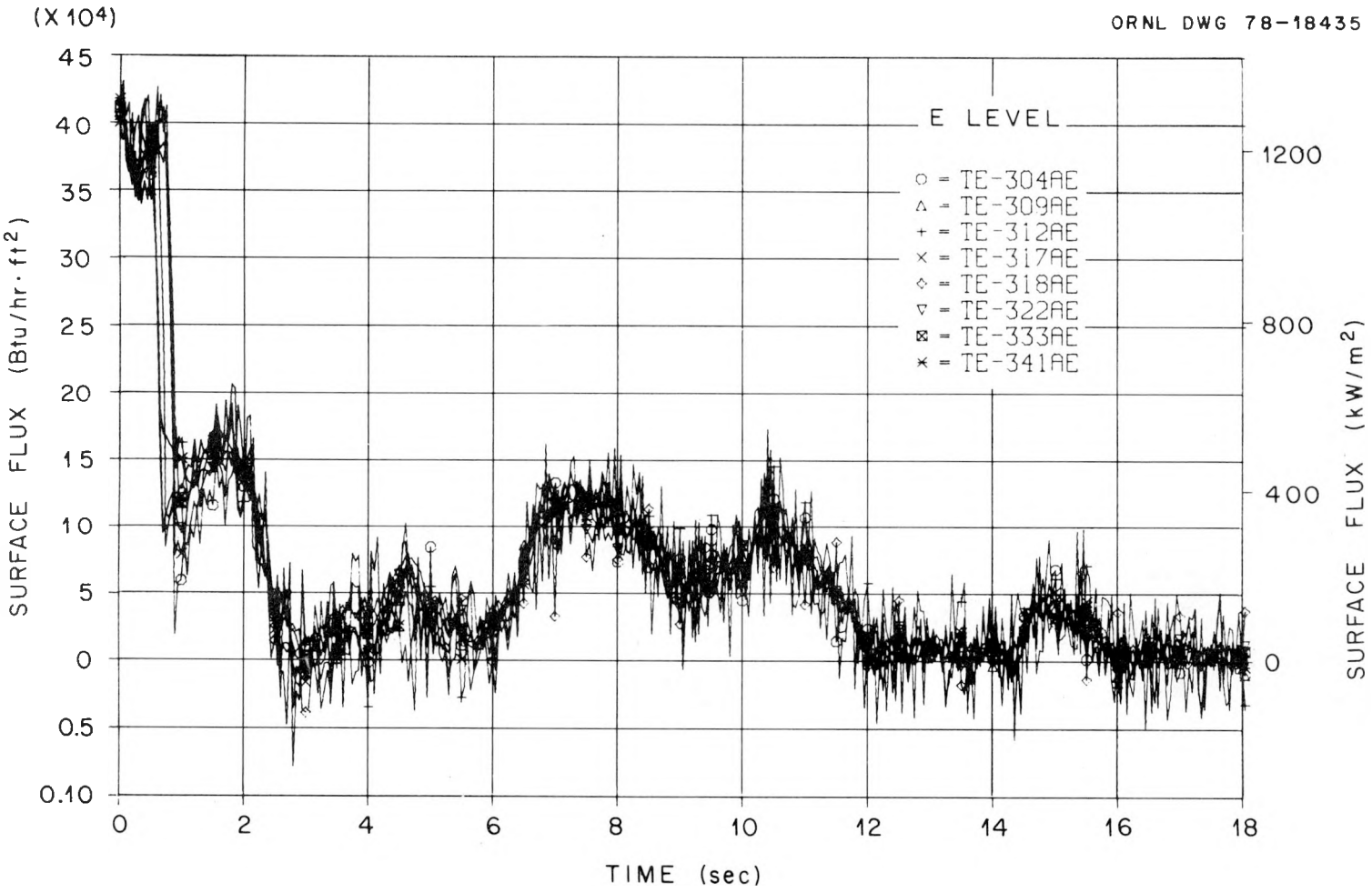

Fig. 3.3. ORINC rod surface heat fluxes, level E, THTF test 105, case 1.

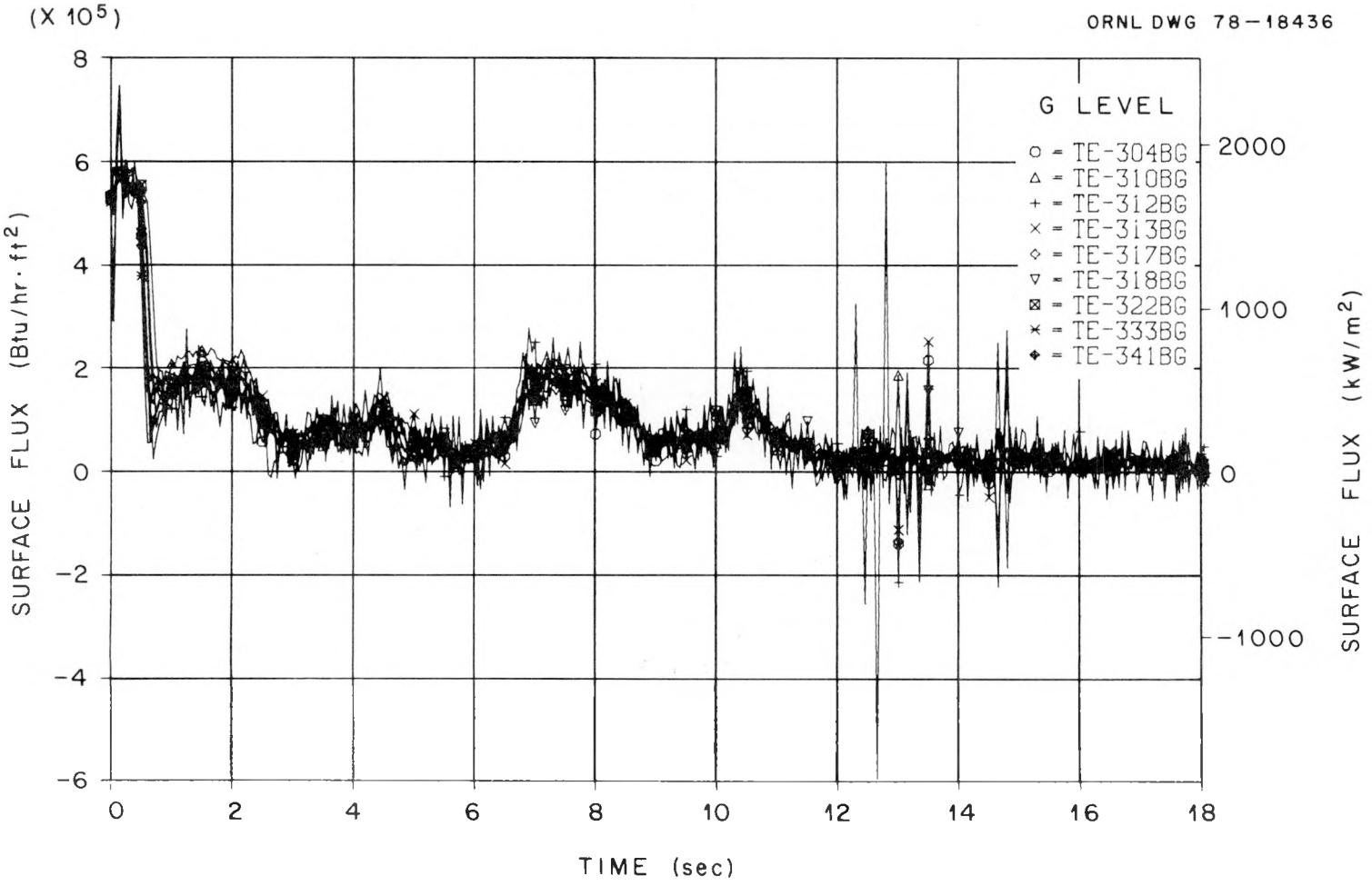

Fig. 3.4. ORINC rod surface heat fluxes, level G, THTF test 105, case 1.

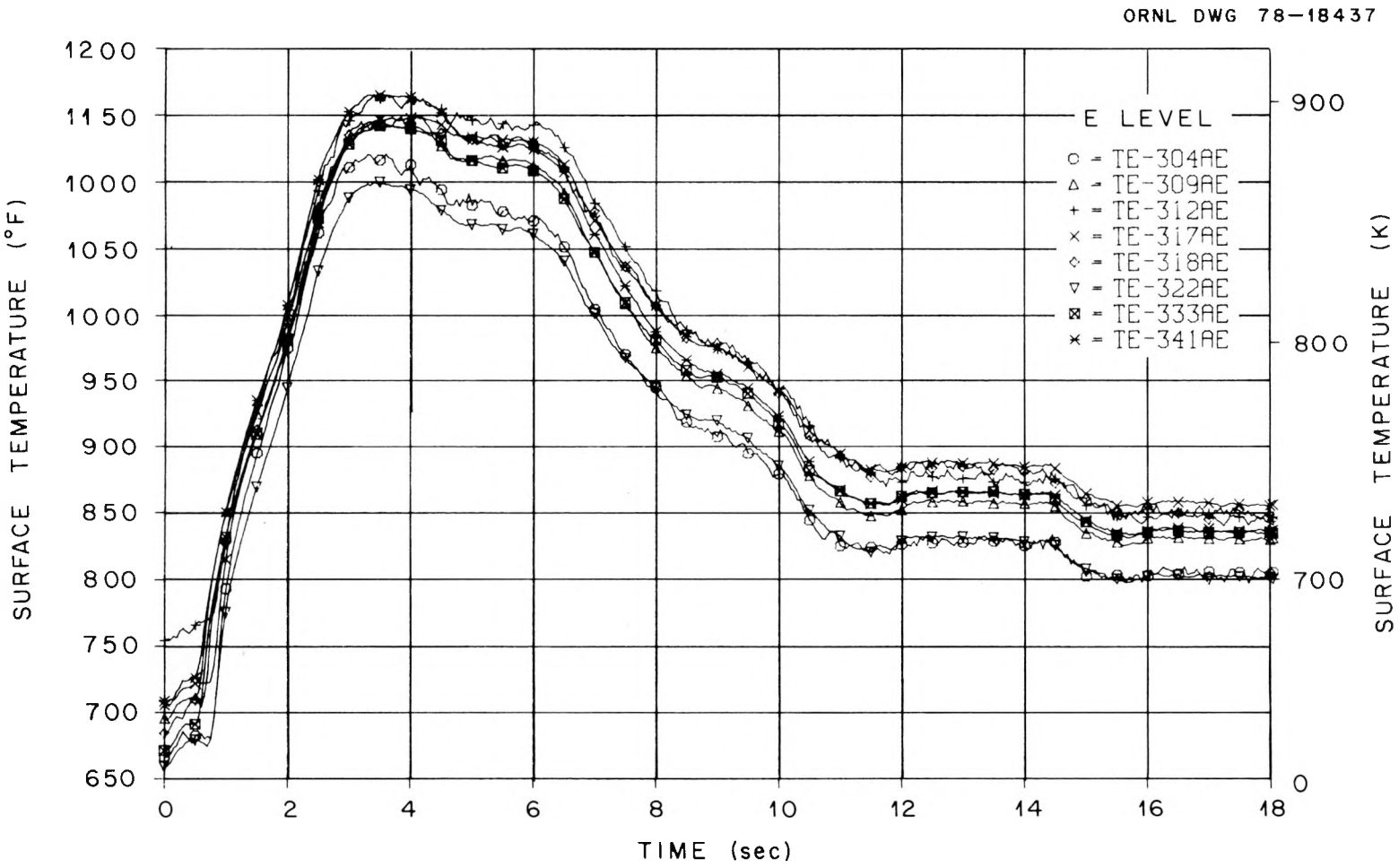

Fig. 3.5. ORINC rod surface temperatures, level E, THTF test 105, case 2.

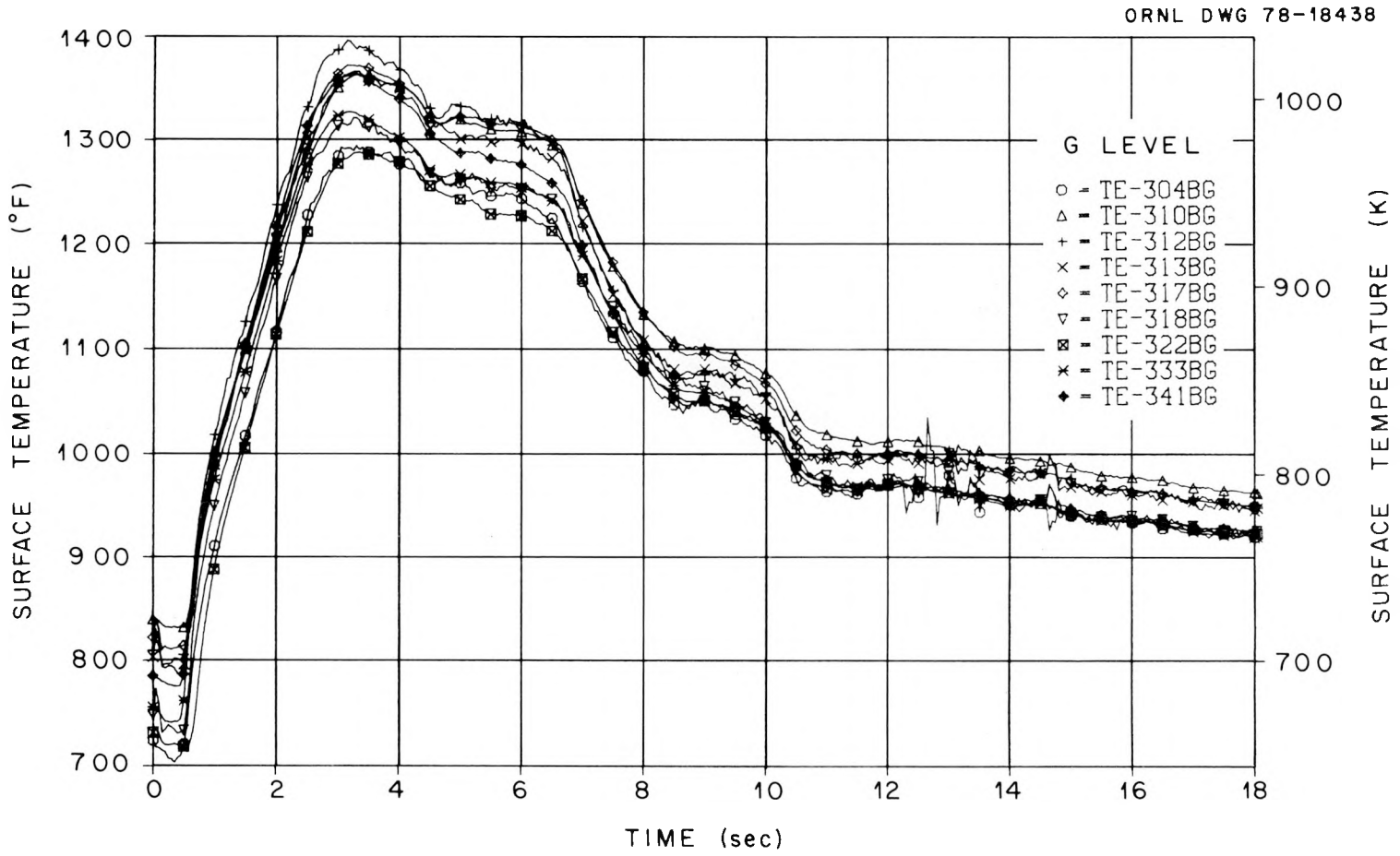

Fig. 3.6. ORINC rod surface temperatures, level G, THTF test 105, case 2.

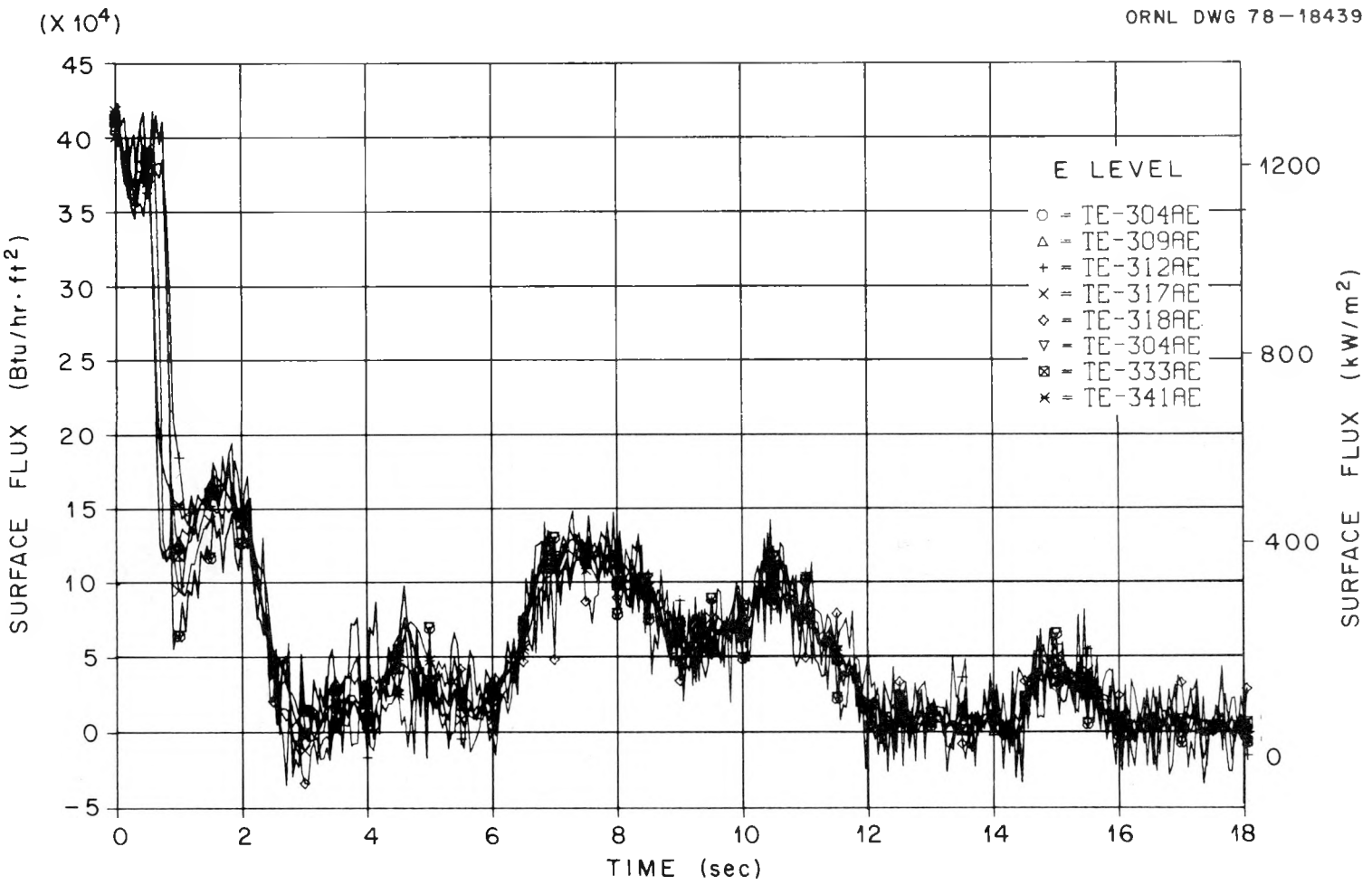

Fig. 3.7. ORINC rod surface heat fluxes, level E, THTF test 105, case 2.

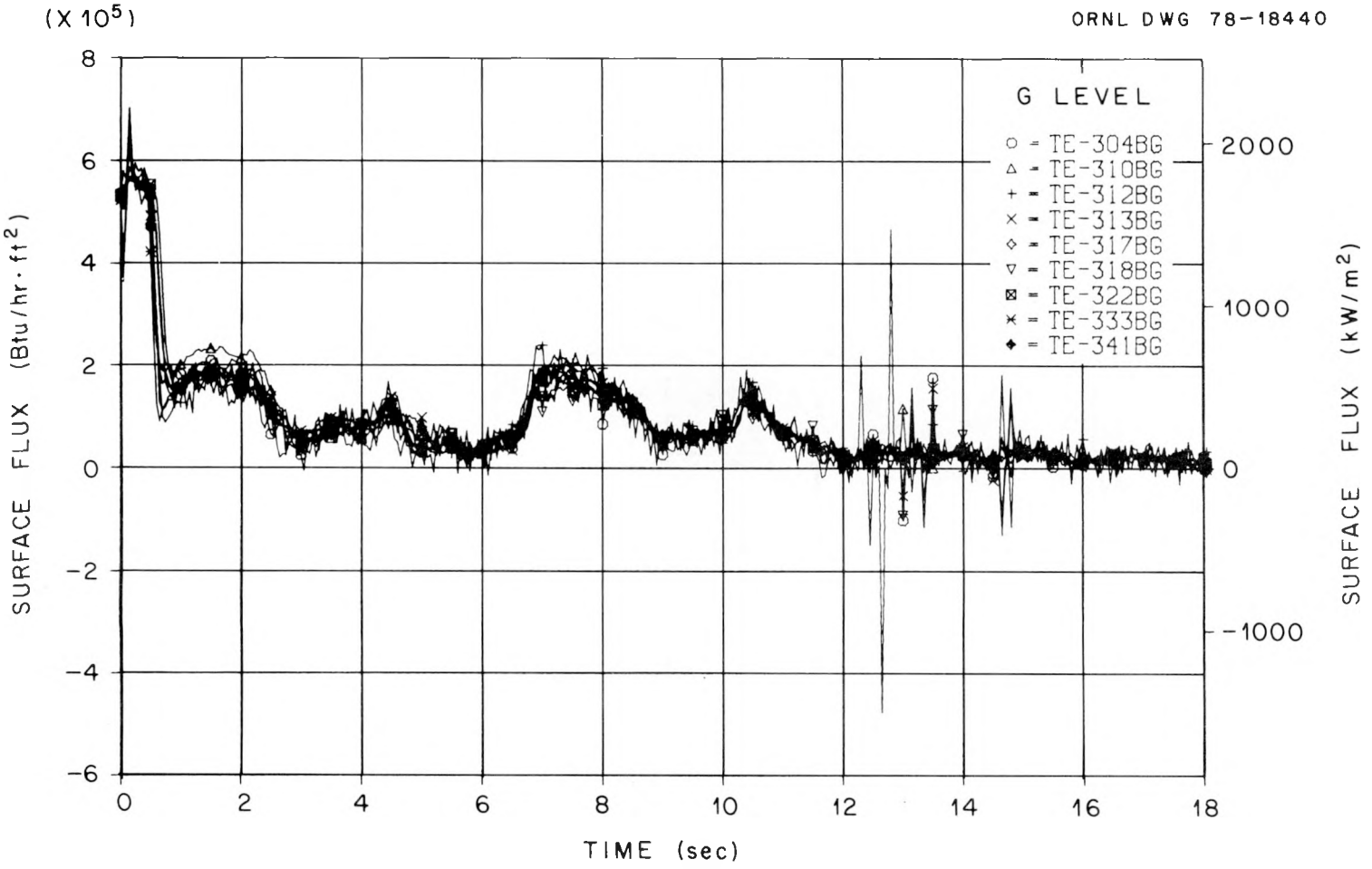

Fig. 3.8. ORINC rod surface heat fluxes, level G, THTF test 105, case 2.

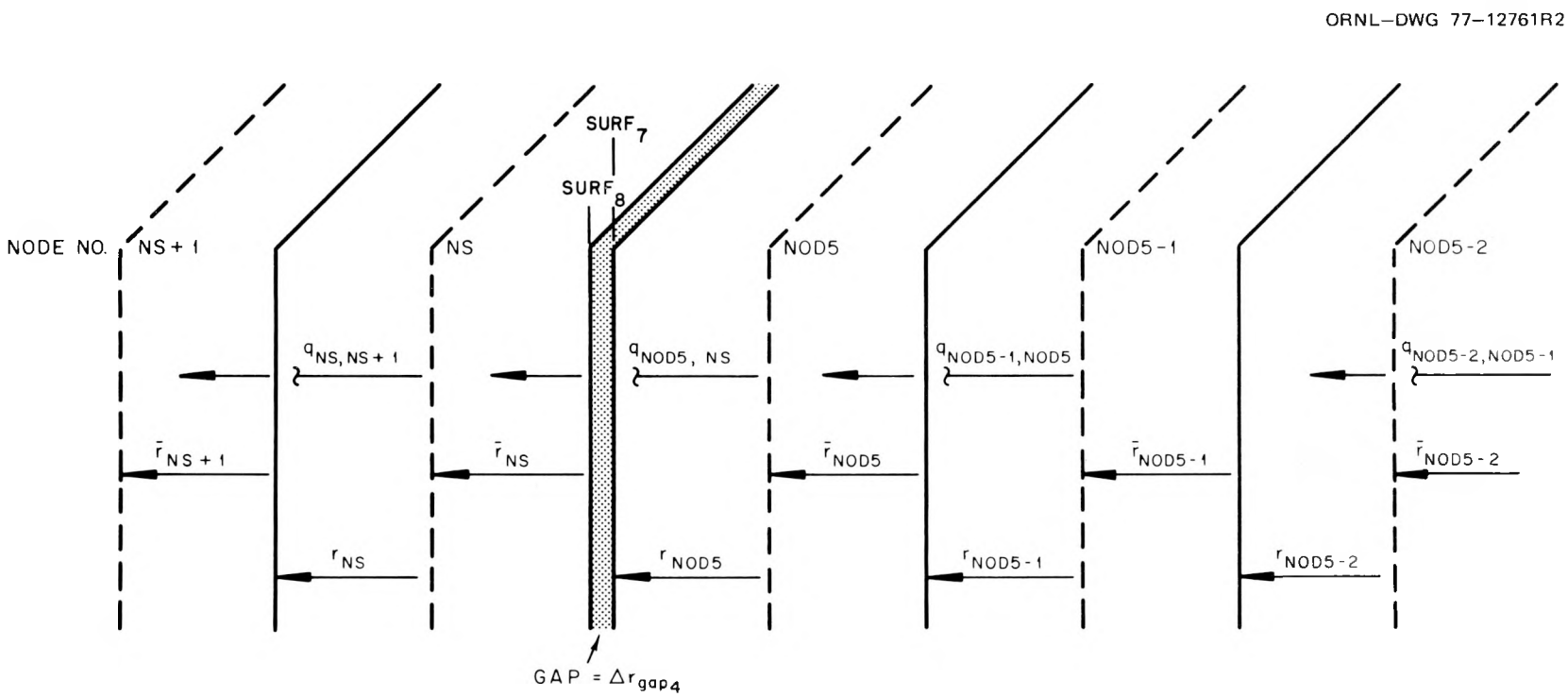

Fig. 3.9. Element notation at the inner stainless steel sheath to the outer stainless steel sheath interface.

ORNL-DWG 77-12763R

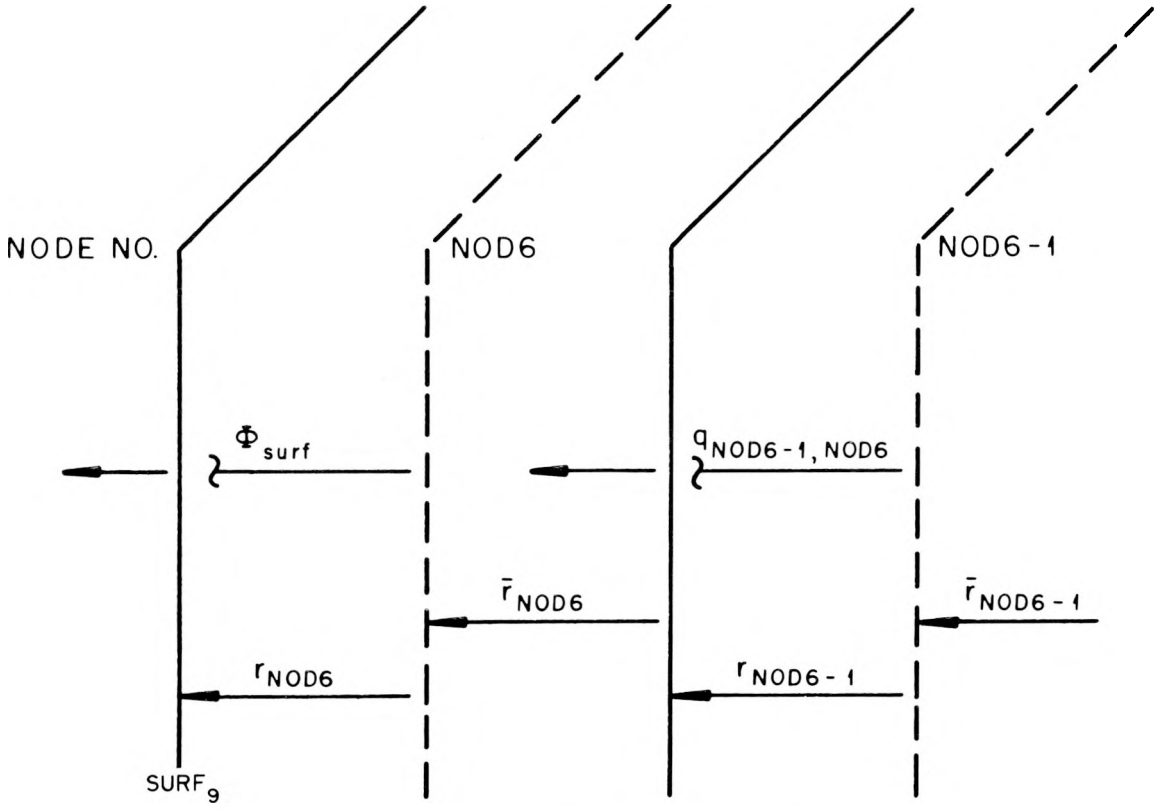

Fig. 3.10. Element notation at the heater surface.

flow from node NOD5 to node NS. Thus, since $q_{NOD5,NS}$ is the same for both cases, the temperature for node NS in the outer stainless steel sheath must be higher for case 2 because the thermal resistance of the gap has been removed. Not only will the temperatures in the outer sheath (nodes NS to NOD6) be higher, the computed surface heat flux (ϕ_{surf}) will also be slightly different because of the temperature dependence of the specific heat and the thermal conductivity of stainless steel.

The noteworthy difference between cases 1 and 2 is obvious when Figs. 3.1 and 3.2 and 3.5 and 3.6 are compared; there is a significant discrepancy in the surface temperature plots in the pre- and post-CHF regions prior to bundle power trip. The rod surface conditions for two time periods (0 and 2 sec) from Figs. 3.1 and 3.5 are compared in Table 3.1. For case 1 at steady state on level E, the rod surface temperatures

Table 3.1. Comparison of case 1 and case 2 surface conditions for level E at 0 and 2 sec[a]

Thermocouple	Heat transfer mode	Surface flux @ t = 0 [W/m^2 ($Btu/hr\ ft^2$)]	Surface temperature @ t = 0 [K (°F)]	Surface heat transfer coefficient @ t = 0 [$W/m^2\ K$ ($Btu/hr\ °F\ ft^2$)]	Surface flux @ t = 2 [W/m^2 ($Btu/hr\ ft^2$)]	Surface temperature @ t = 2 [K (°F)]
			Case 1			
304AE	Forced conv.	$1.299(10)^6$ [$4.1188(10)^5$]	604.8 [628.9]	$3.75(10)^4$ [6607]	$4.077(10)^5$ [$1.2926(10)^5$]	789.8 [962.0]
309AE	Forced conv.	$1.287(10)^6$ [$4.0809(10)^5$]	604.3 [628.1]	$3.76(10)^4$ [6625]	$4.550(10)^5$ [$1.4426(10)^5$]	794.0 [969.4]
312AE	Forced conv.	$1.268(10)^6$ [$4.0210(10)^5$]	604.5 [628.4]	$3.69(10)^4$ [6503]	$3.710(10)^5$ [$1.1763(10)^5$]	791.6 [965.3]
317AE	Forced conv.	$1.263(10)^6$ [$4.0052(10)^5$]	603.1 [625.8]	$3.83(10)^4$ [6753]	$4.593(10)^5$ [$1.4565(10)^5$]	781.0 [946.1]
318AE	Forced conv.	$1.310(10)^6$ [$4.1551(10)^5$]	605.9 [630.9]	$3.66(10)^4$ [6458]	$4.431(10)^5$ [$1.4049(10)^5$]	788.0 [958.7]
322AE	Forced conv.	$1.277(10)^6$ [$4.0478(10)^5$]	601.7 [623.5]	$4.04(10)^4$ [7112]	$4.183(10)^5$ [$1.3264(10)^5$]	773.2 [932.1]
333AE	Forced conv.	$1.296(10)^6$ [$4.1084(10)^5$]	603.5 [626.6]	$3.88(10)^4$ [6839]	$4.350(10)^5$ [$1.3794(10)^5$]	793.6 [968.9]
341AE	Forced conv.	$1.317(10)^6$ [$4.1769(10)^5$]	605.1 [629.4]	$3.77(10)^4$ [6640]	$4.629(10)^5$ [$1.4677(10)^5$]	796.4 [973.8]
			Case 2			
304AE	Nucleate boiling	$1.299(10)^6$ [$4.1188(10)^5$]	625.6 [666.4]	$1.98(10)^5$ [34830]	$4.003(10)^5$ [$1.2692(10)^5$]	797.1 [975.2]
309AE	Nucleate boiling	$1.287(10)^6$ [$4.0809(10)^5$]	641.9 [695.7]	$5.64(10)^4$ [9932]	$4.573(10)^5$ [$1.4501(10)^5$]	809.3 [997.1]
312AE	Nucleate boiling	$1.268(10)^6$ [$4.0210(10)^5$]	674.4 [754.3]	$2.29(10)^4$ [4035]	$3.931(10)^5$ [$1.2463(10)^5$]	814.9 [1007.1]
317AE	Nucleate boiling	$1.263(10)^6$ [$4.0052(10)^5$]	647.5 [705.8]	$4.44(10)^4$ [7825]	$4.582(10)^5$ [$1.4530(10)^5$]	800.8 [981.8]
318AE	Nucleate boiling	$1.310(10)^6$ [$4.1551(10)^5$]	635.7 [684.7]	$7.84(10)^4$ [13815]	$4.665(10)^5$ [$1.4792(10)^5$]	800.7 [981.6]
322AE	Nucleate boiling	$1.277(10)^6$ [$4.0478(10)^5$]	621.8 [659.5]	$4.66(10)^5$ [82044]	$4.266(10)^5$ [$1.3527(10)^5$]	780.1 [944.4]
333AE	Nucleate boiling	$1.296(10)^6$ [$4.1084(10)^5$]	628.3 [671.3]	$1.39(10)^5$ [24541]	$4.417(10)^5$ [$1.4006(10)^5$]	801.2 [982.5]
341AE	Nucleate boiling	$1.317(10)^6$ [$4.1769(10)^5$]	649.0 [708.5]	$4.40(10)^4$ [7745]	$4.652(10)^5$ [$1.4751(10)^5$]	815.3 [1007.8]

[a]At t = 0, bulk avg. temp. = 570.1 K (566.5°F); saturation temp. = 619.0 K (654.6°F); local fluid pressure = 15709.2 kPa (2280 psia).

range from 601.7 to 605.9 K with a predicted heat transfer mode of forced convection; however, for case 2 (zero gaps), the heat transfer mode changed to nucleate boiling and the rod surface temperature range became 621.8 to 674.4 K. There are similar results for 2 sec into the transient, with a rod surface temperature range of 773.2 to 796.4 K for case 1 and a rod surface temperature range of 780.1 to 815.3 K for case 2. The calculated surface temperatures for case 2 are higher than those for case 1, and the range is much broader. The question of which case is more accurate must be answered because, as noted earlier, the calculated surface

fluxes do not vary significantly between the cases but the driving potential (i.e, $T_{surface} - T_{sink}$) is drastically different. As a result, the computed surface heat transfer coefficient would be greatly affected.

A study of the steady-state conditions (at t = 0 sec) for cases 1 and 2 at level E gives a reasonable answer to the above question. Case 1 predicts forced convection at level E. Using the local fluid conditions in Table 3.1, the Dittus-Boelter correlation yields a film coefficient of 3.6×10^4 W/m^2-K. The mean of the coefficients determined by ORINC for level E in case 1 is 3.77×10^4 W/m^2-K (17 observations with a standard deviation about the mean of 0.05×10^4 W/m^2-K). At steady-state, the mean surface heat flux for level E is 1.290×10^6 W/m^2 (17 observations with a standard deviation about the mean of 0.020×10^6 W/m^2). If the surface temperature for level E is calculated by

$$T_{surf} = T_{bulk} + \frac{\bar{\phi} \pm 3\delta_{\bar{\phi}}}{h_{D-B}} , \tag{3.1}$$

the expected surface temperature range for level E would be 604.2 to 607.5 K, essentially the range determined for case 1. In case 2, for the nucleate boiling regime to be chosen by ORINC, the pin model had to transfer heat to a sink temperature equal to the saturation temperature (619.0 K at 15709.2 kPa). If Thom's correlation is used for the subcooled nucleate boiling regime, the expected surface temperature range for level E can be determined by

$$T_{surf} = T_{sat} + 0.0406\ (\bar{\phi} \pm 3\delta_{\bar{\phi}})^{1/2}\ e^{-P/8687} . \tag{3.2}$$

The expected range for level E would be 626.4 to 626.7 K if the local fluid pressure in Table 3.1 is used; however, the computed surface temperature range is 621.8 to 674.4 K. If there are pressure fluctuations radially at level E, the local pressures required to produce the computed rod surface temperatures in Table 3.1 for case 2 must be determined. Assuming Thom's correlation is applicable and using the rod surface heat fluxes (at t = 0) in Table 3.1, the local pressures shown in Table 3.2 and Fig. 3.11 would be required. From Fig. 3.11, it should be readily apparent that the existence of such radial pressure differences at one

Table 3.2. Local fluid pressure required to achieve surface temperatures for case 2 during nucleate boiling

Thermocouple No.	Surface temperature [K (°F)]	Required local fluid pressure [MPa (psia)]
304AE	625.6 (666.4)	16.23 (2354)
309AE	641.9 (695.7)	20.10 (2916)
312AE	674.4 (754.3)	*a*
317AE	647.5 (705.8)	*a*
318AE	635.7 (684.7)	18.57 (2694)
322AE	621.8 (659.5)	15.41 (2235)
333AE	628.3 (671.3)	16.84 (2442)
341AE	649.0 (708.5)	22.00 (3190)

*a*Greater than critical pressure.

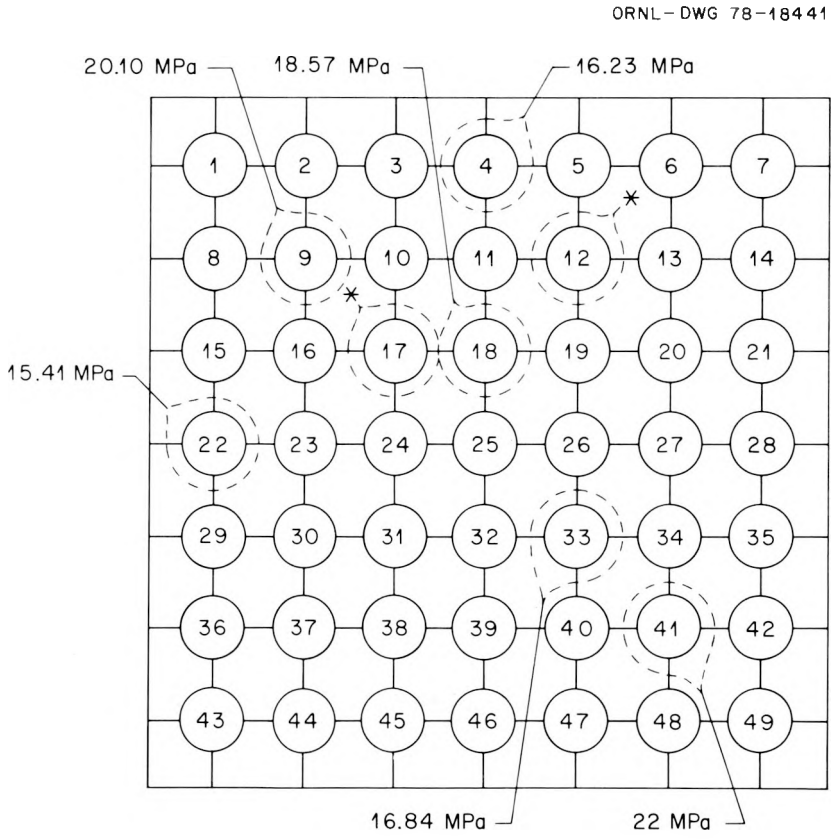

Fig. 3.11. Distribution of pressure superimposed on cross section of bundle 1 core.

axial level in the core is physically impossible. Thus, it could be concluded that case 1 describes the surface conditions at level E best and that case 2 (with the zero gap assumption) grossly miscalculates the surface temperatures.

Case 3 of the ORINC studies was an attempt to determine *only* the effect on the inverse calculations of using literature data for the insulator thermal conductivities; thus, both cases 1 and 3 use the ORTCAL dynamic gap model and gap regressions. The only differences between cases 1 and 3 are the regression fits for k_{BN} and α_{MgO} (i.e., ORTCAL regressions on THTF data in case 1 and least-squares fits to literature data in case 3). Fits to the literature data yield *higher* thermal conductivities values for both BN and MgO than those predicted by the ORTCAL regressions. The ORINC results at thermocouple position 318BG for THTF test 105 will be reviewed for cases 1 and 3.

A case result will be defined to be correct if the calculated pin internal thermal response from ORINC matches or closely approximates the actual internal response from a pin centerline thermocouple. The centerline thermocouple provides the means for independently verifying the model results.

The ORINC-calculated surface heat fluxes for cases 1, 3, and 4 are overlaid in Fig. 3.12 for 18 sec of the transient, and the corresponding surface temperatures are presented in Fig. 3.13. There appear to be minimal (if any) differences between cases 1 and 3; however, there is a very deceiving compression effect from the Y-axis scale factor (this will be reviewed later). Figure 3.14 is an overlay of the calculated pin centerline temperature response for cases 1, 3, and 4 with the response from thermocouple TE-318MG (the centerline thermocouple relative to TE-318BG). Note that case 1 very closely approximates the response of 318MG; however, case 3 not only initializes incorrectly at steady state but responds too fast, peaks too high, and rolls off too fast.

The incorrect setup in steady state for case 3 (the centerline temperature is $\sim$18 K low) is caused solely by the BN thermal conductivity. As stated earlier, a fit to literature data for the thermal conductivity of BN yields higher values than those predicted by the ORTCAL regressions; therefore, for the same power-generation rate, less thermal gradient is

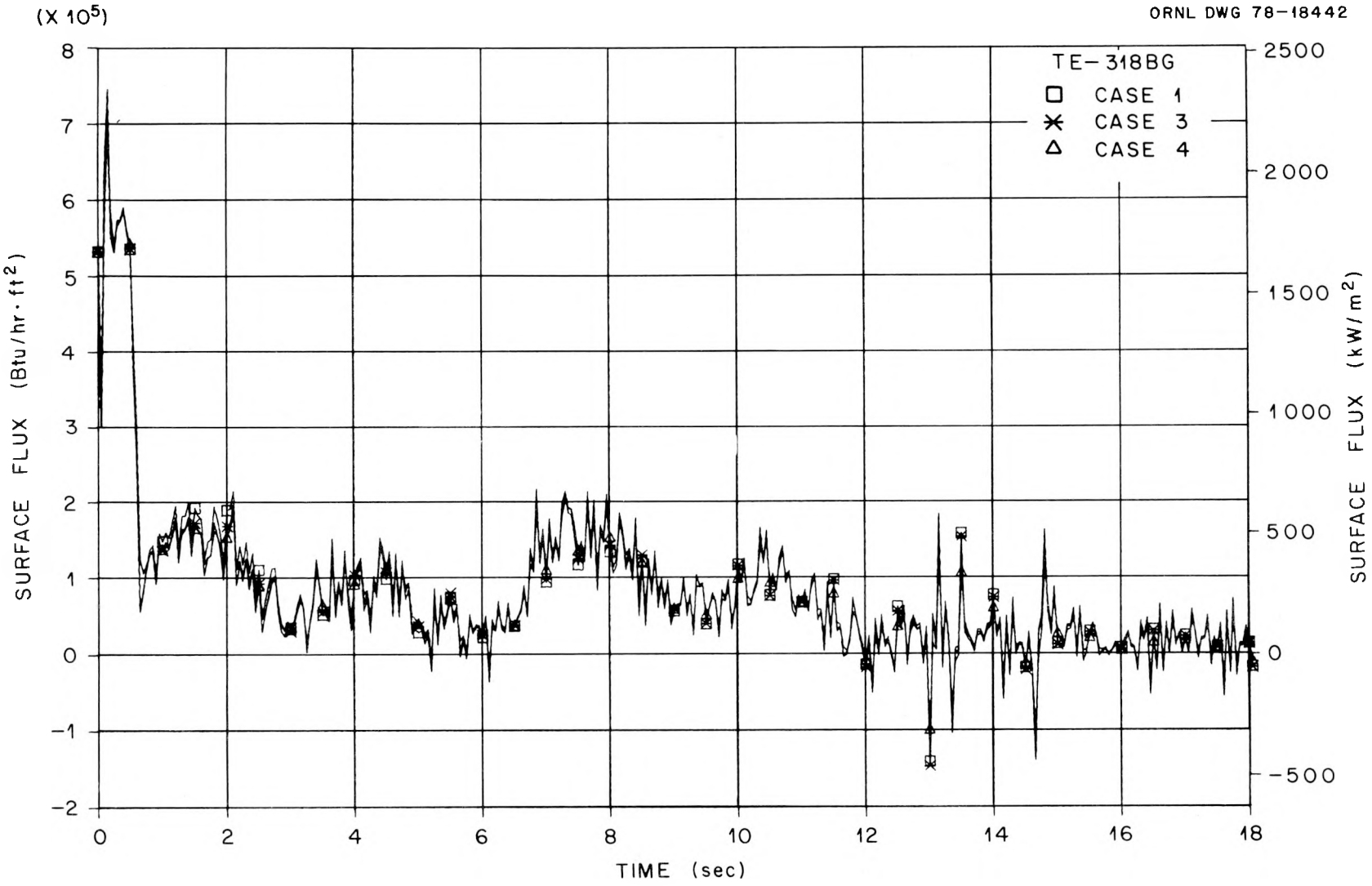

Fig. 3.12. ORINC rod surface heat flux, TE-318BG, THTF test 105, 0–18 sec.

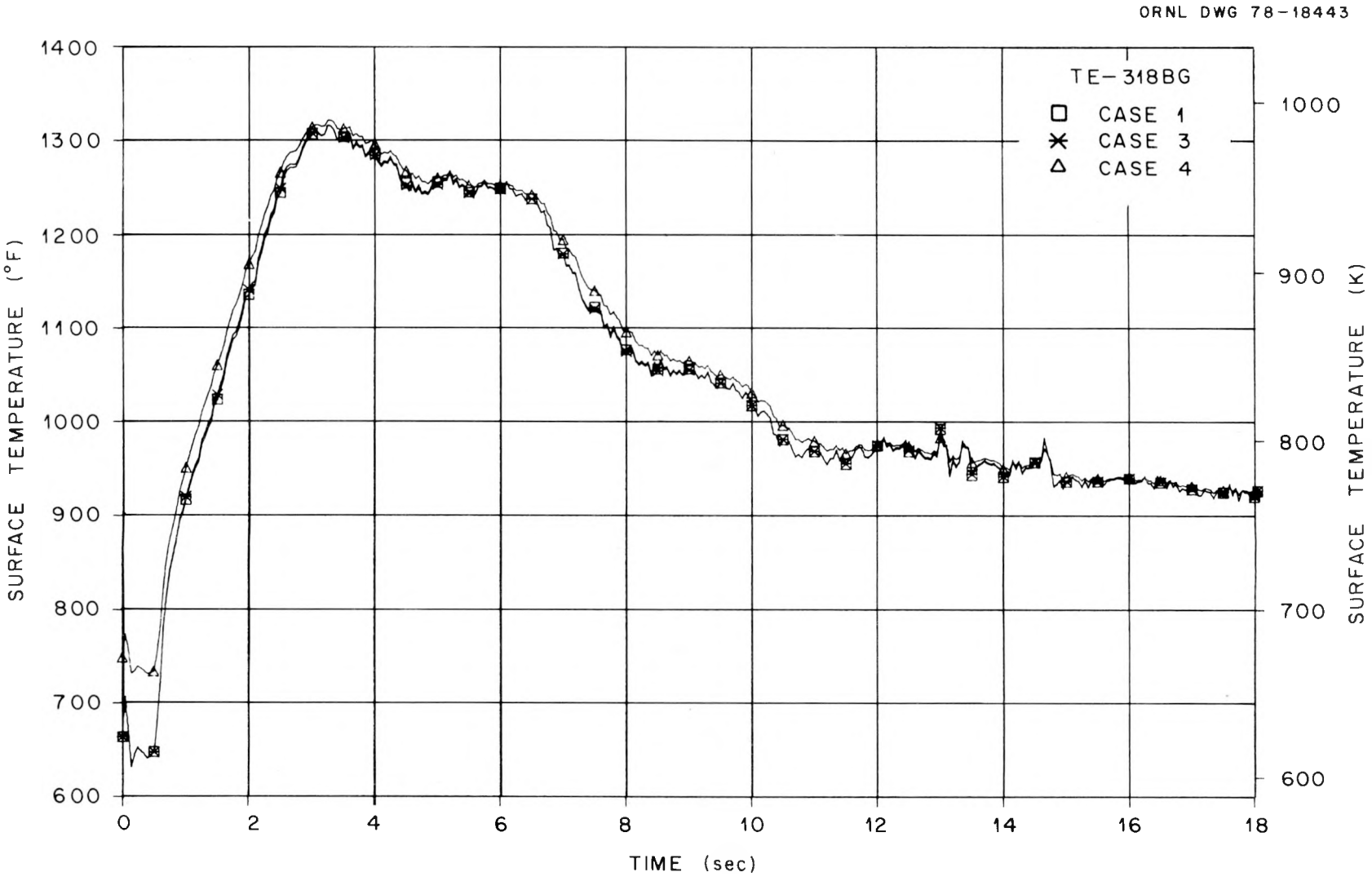

Fig. 3.13. ORINC rod surface temperature, TE-318BG, THTF test 105, 0–18 sec.

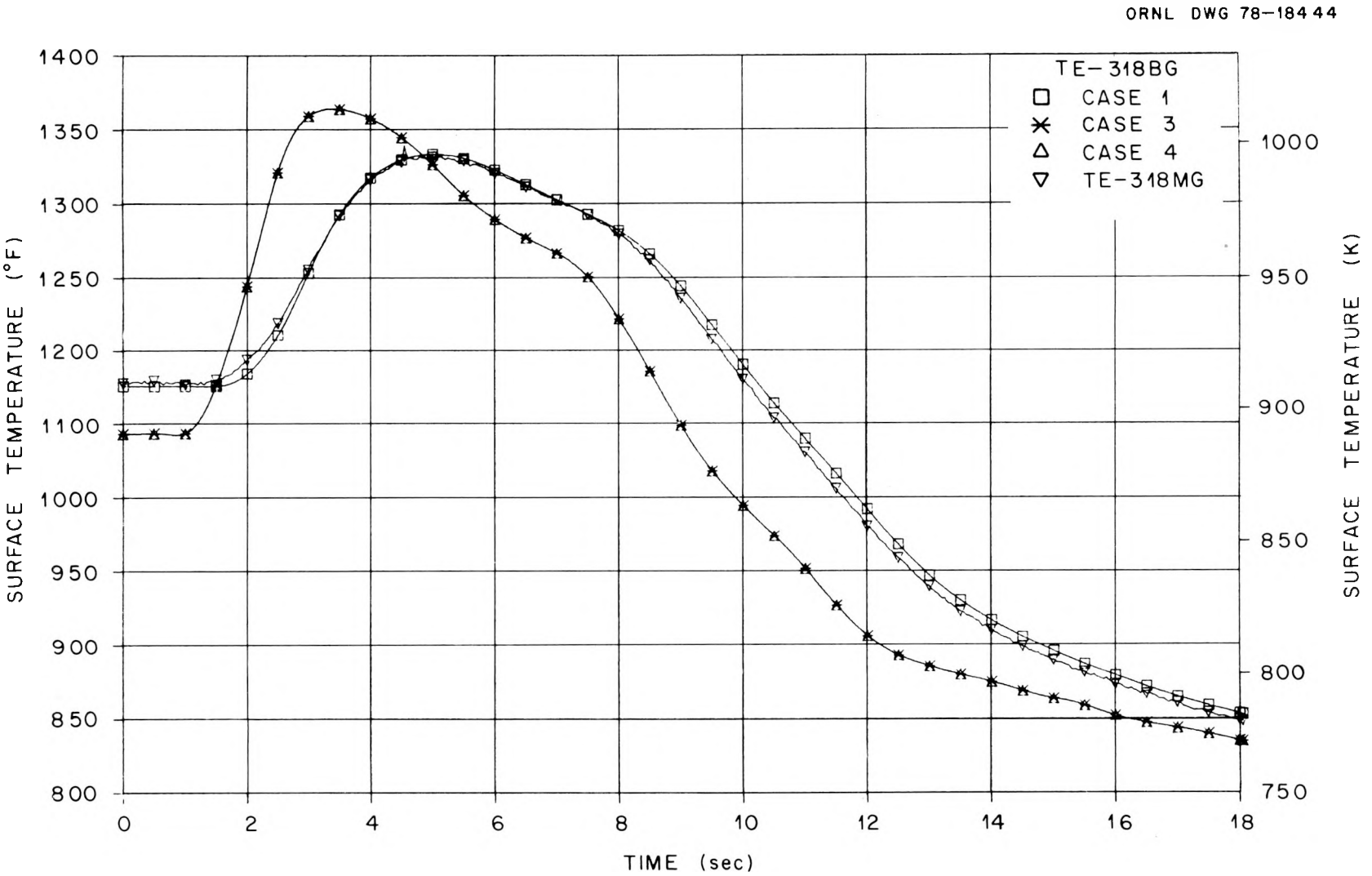

Fig. 3.14. Rod centerline temperature, TE-318BG, THTF test 105, 0–18 sec.

required in case 3 to move the heat through the BN and thus the centerline temperature is lower. As a result of the lower temperature profile, the total heat content of the pin is less at steady state. A comparison of the overall heat balance for cases 1 and 3 shows that the total heat removed per unit length of pin, as defined by

$$2\pi r_{surf} \int_0^{t_{end}} \phi_{surf} \, dt \ ,$$

is 1.8% less for case 3 (43.843 W-hr/m for case 1). The total energy input to the pin is the same for both cases (39.944 W-hr/m), but the change in internal energy for case 3 is ∿20.3% less than that for case 1 (3.957 W-hr/m for case 1). Since the final temperature profile for cases 1 and 3 is essentially the same (i.e., the final heat content of the pin would be the same), the error is in the steady-state initialization.

Do not assume that the 1.8% error in

$$2\pi r_{surf} \int_0^{t_{end}} \phi_{surf} \, dt$$

is distributed evenly over the time interval ($0—t_{end}$) because it is not. As noted earlier, Fig. 3.12 is misleading due to the Y-axis scaling.

The time range (0—18 sec) can be broken down into time intervals over which the value of the surface heat flux does not vary orders of magnitude; Figs. 3.15 to 3.18 show breakdowns of the 0—18-sec time range into intervals of 0—0.5, 0.5—2.0, 2.0—8.0, and 5.0—18.0 sec, respectively. The corresponding surface temperature plots are presented in Figs. 3.19 to 3.22. Over the time intervals of 0—0.65 and 3.3—18.0 sec, the calculated surface heat flux and surface temperature for cases 1 and 3 are basically the same. One of the primary forcing functions for the inverse calculations ($\dot{q}'''$) drops to 0.0 at ∿6.0 sec and drops to ∿1/10 of the steady-state value at ∿3.3 sec. Also, the pin at this position (318BG) is in nucleate boiling in steady state and remains so until CHF at ∿0.5 sec and thus there is little change in the internal response until ∿0.65 sec. Over the 0.65- to 3.0-sec interval, the calculated flux for case 3 ranges

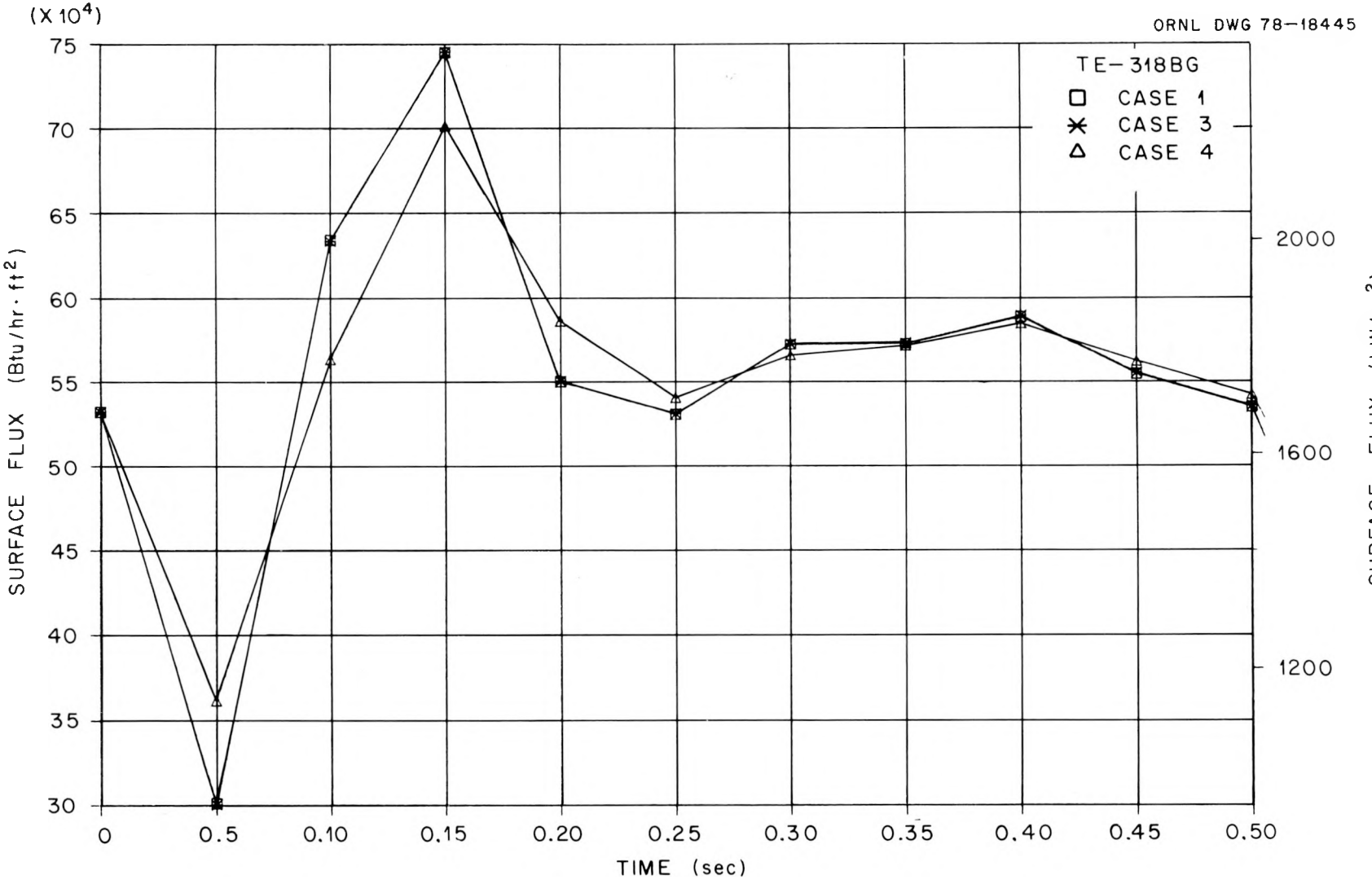

Fig. 3.15. ORINC rod surface heat flux, TE-318BG, THTF test 105, 0–0.5 sec.

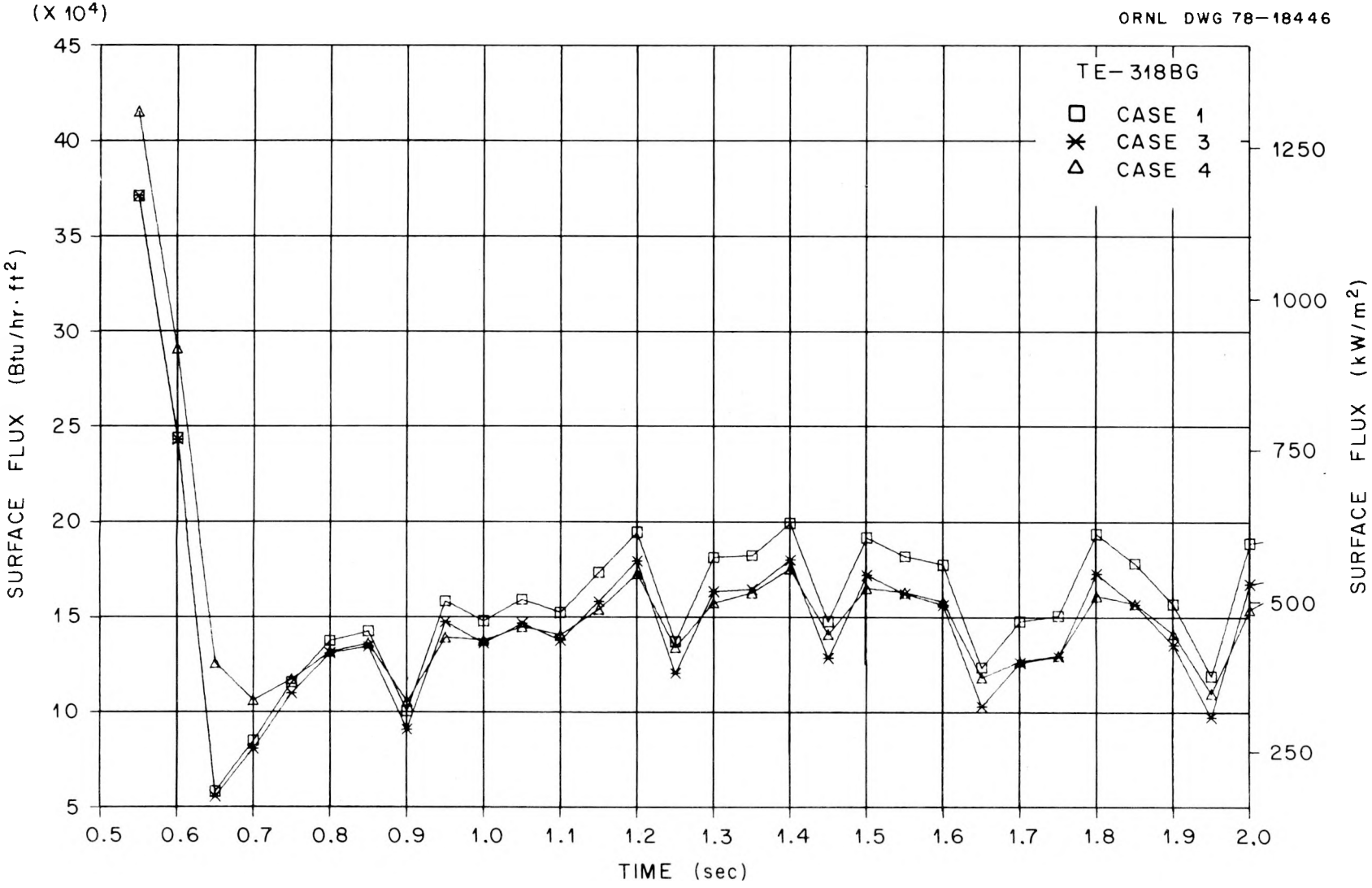

Fig. 3.16. ORINC rod surface heat flux, TE-318BG, THTF test 105, 0.5–2 sec.

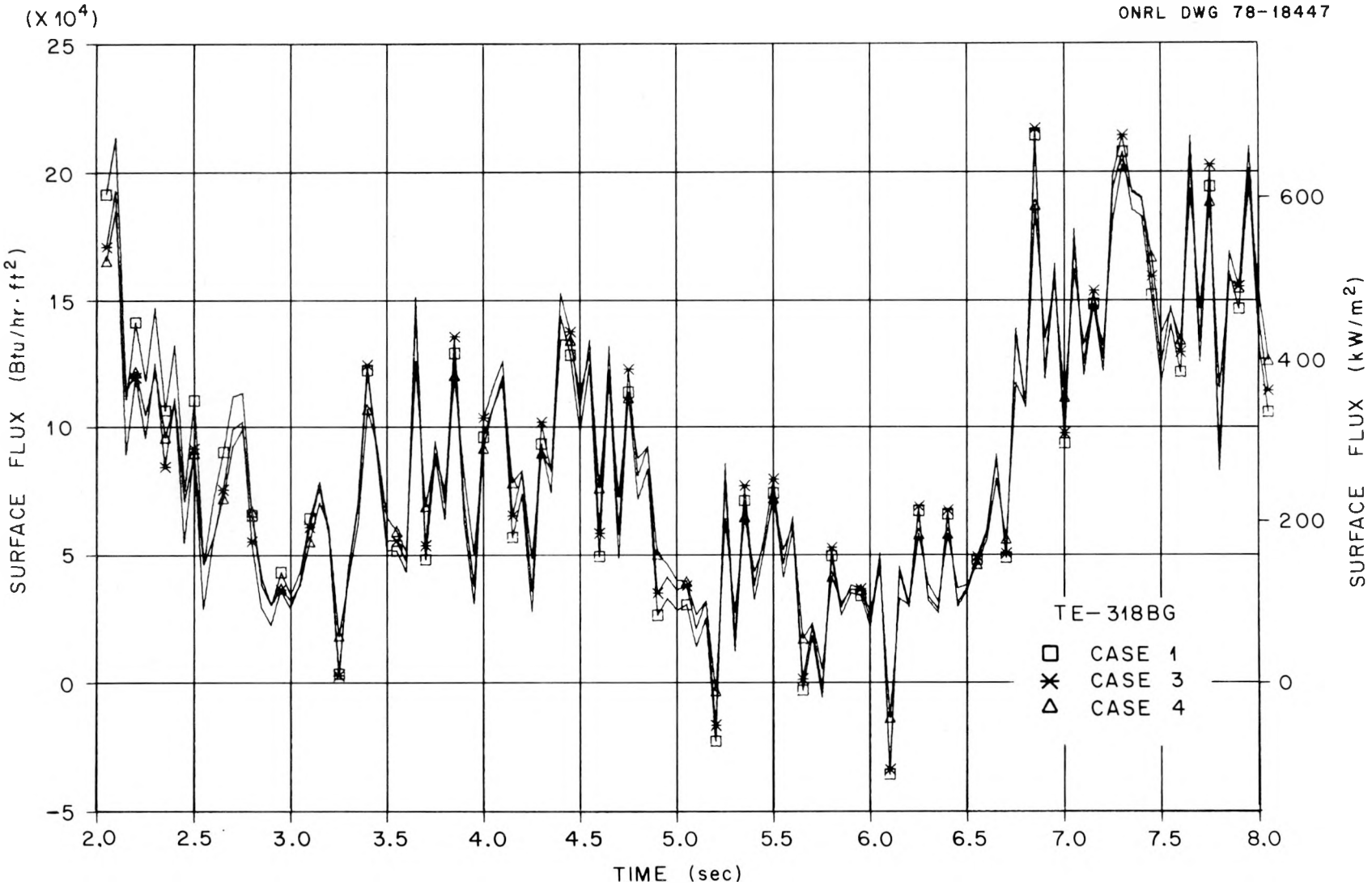

Fig. 3.17. ORINC rod surface heat flux, TE-318BG, THTF test 105, 2.0–8 sec.

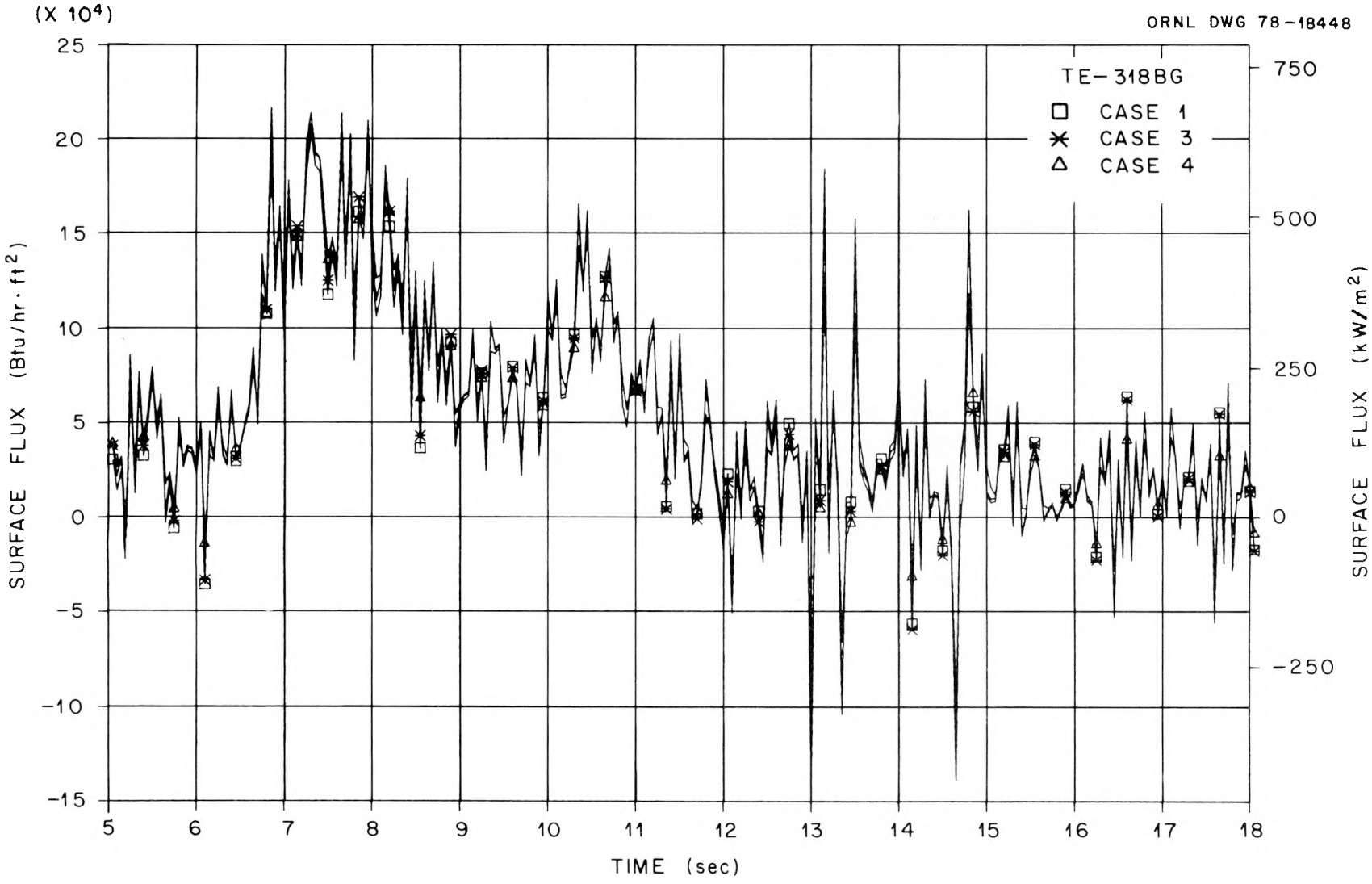

Fig. 3.18. ORINC rod surface heat flux, TE-318BG, THTF test 105, 5.0–18 sec.

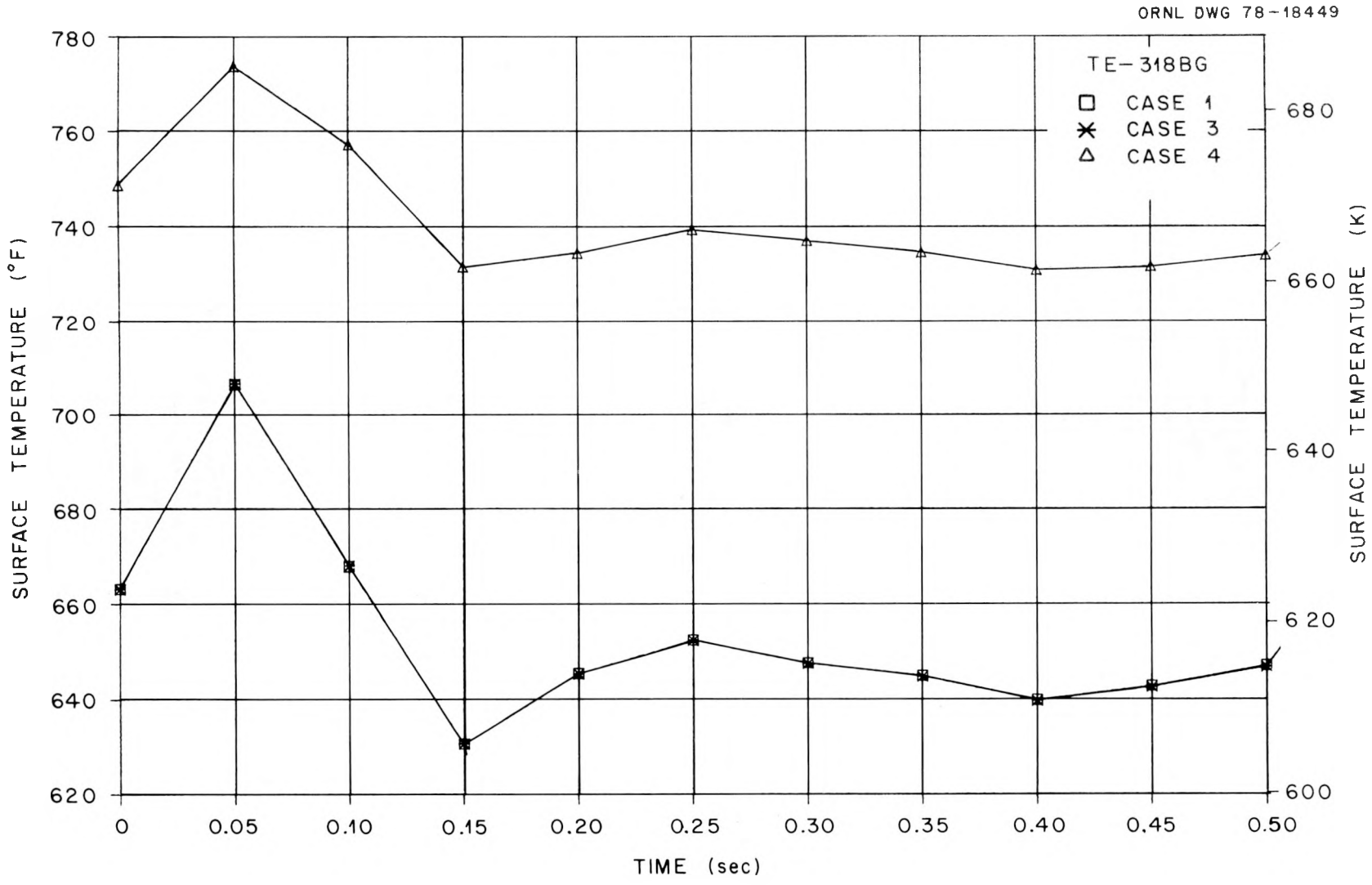

Fig. 3.19. ORINC rod surface temperature, TE-318BG, THTF test 105, 0–0.5 sec.

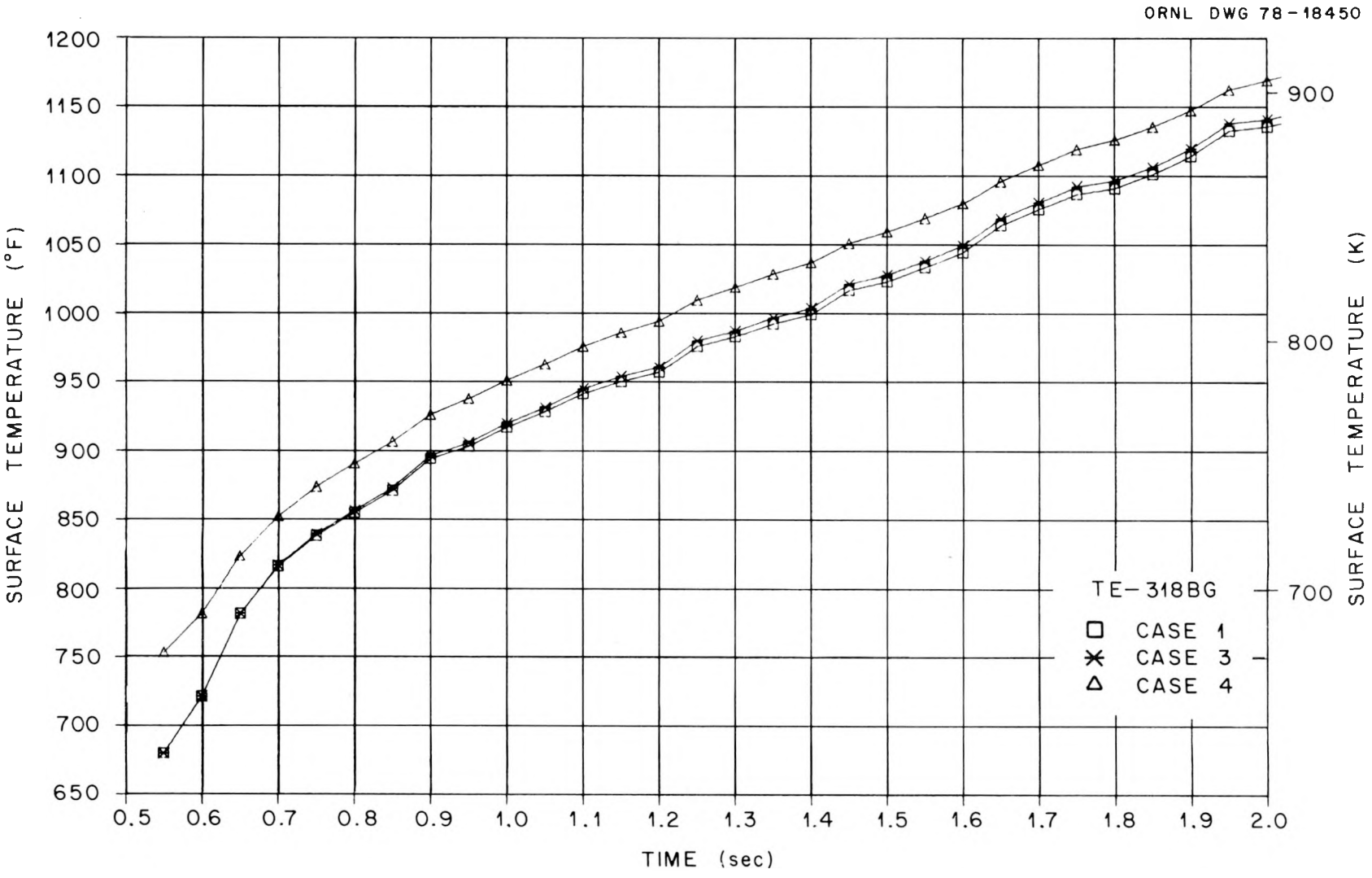

Fig. 3.20. ORINC rod surface temperature, TE-318BG, THTF test 105, 0.5–2 sec.

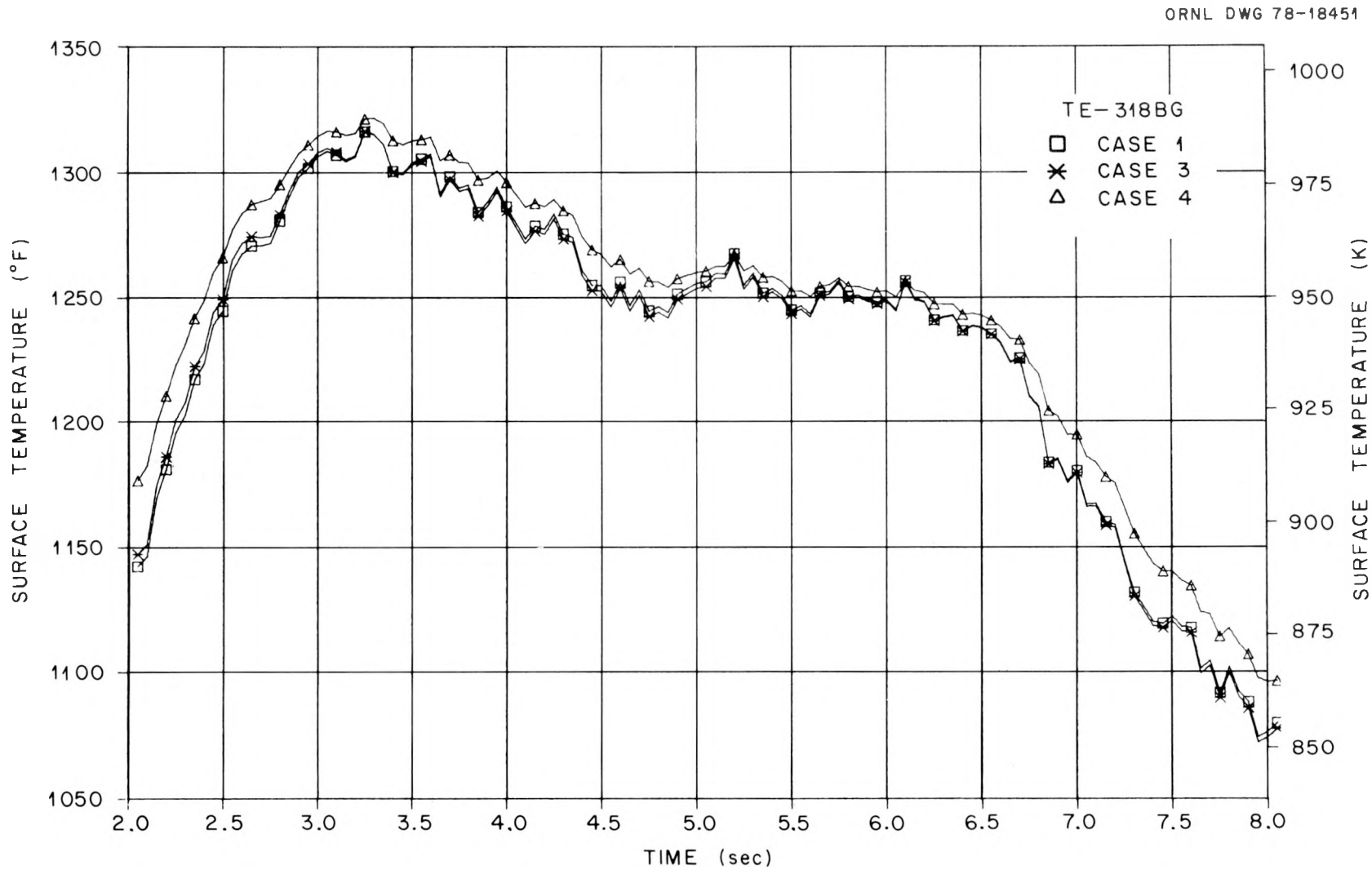

Fig. 3.21. ORINC rod surface temperature, TE-318BG, THTF test 105, 2.0–8 sec.

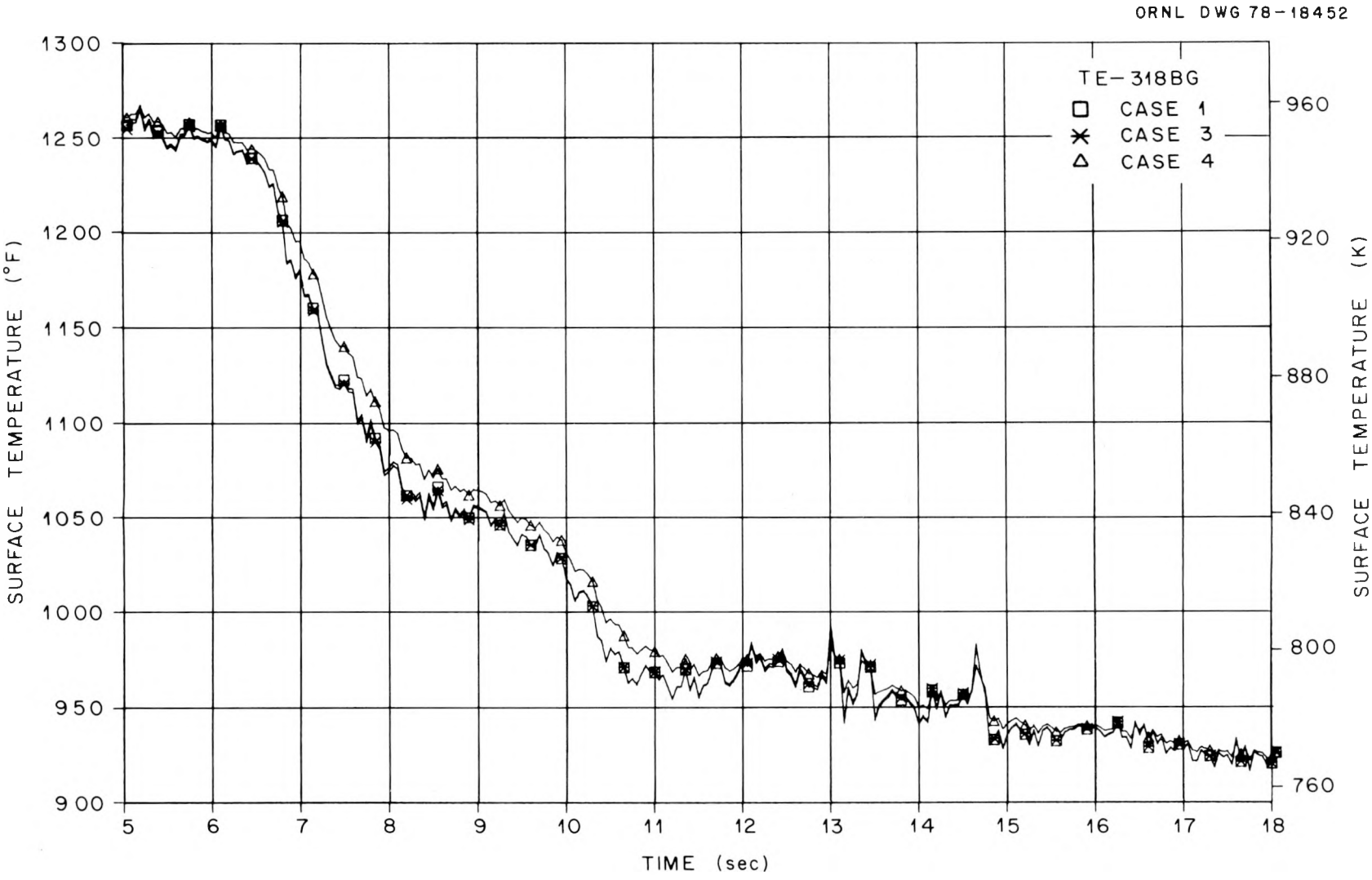

Fig. 3.22. ORINC rod surface temperature, TE-318BG, THTF test 105, 5.0–18 sec.

from 0.0 to 40.0% lower than for case 1. Figure 3.23 gives a plot of the surface heat flux ratio (case 3/case 1) for the 0.50- to 3.40-sec time interval. The general conclusion is that the inverse computed surface heat flux can be off by as much as 40% in comparing cases 3 and 1.

The general observation that the interior of the pin responds too fast in case 3 is obvious in Fig. 3.14. A better "feel" for what is occurring within the pin can be gained by referring to the sequence of radial temperature plots for 0–4.75 sec. Figures 3.24 through 3.28 give responses for case 1 and case 3. There is little perceivable difference between the cases through 0.75 sec (Fig. 3.24); however, the differences are very apparent from 1.00 to 4.75 sec. In Fig. 3.25, the active component (Inconel-600) temperature (at r = 0.3 cm) is higher in case 1, eventually peaking at 2.15 sec at 1061 K in case 1 and 1036 K in case 3, but the MgO temperatures (at r $\leqslant$ 0.2764 cm) are higher in case 3. Since the thermal diffusivity of the MgO is higher in case 3,

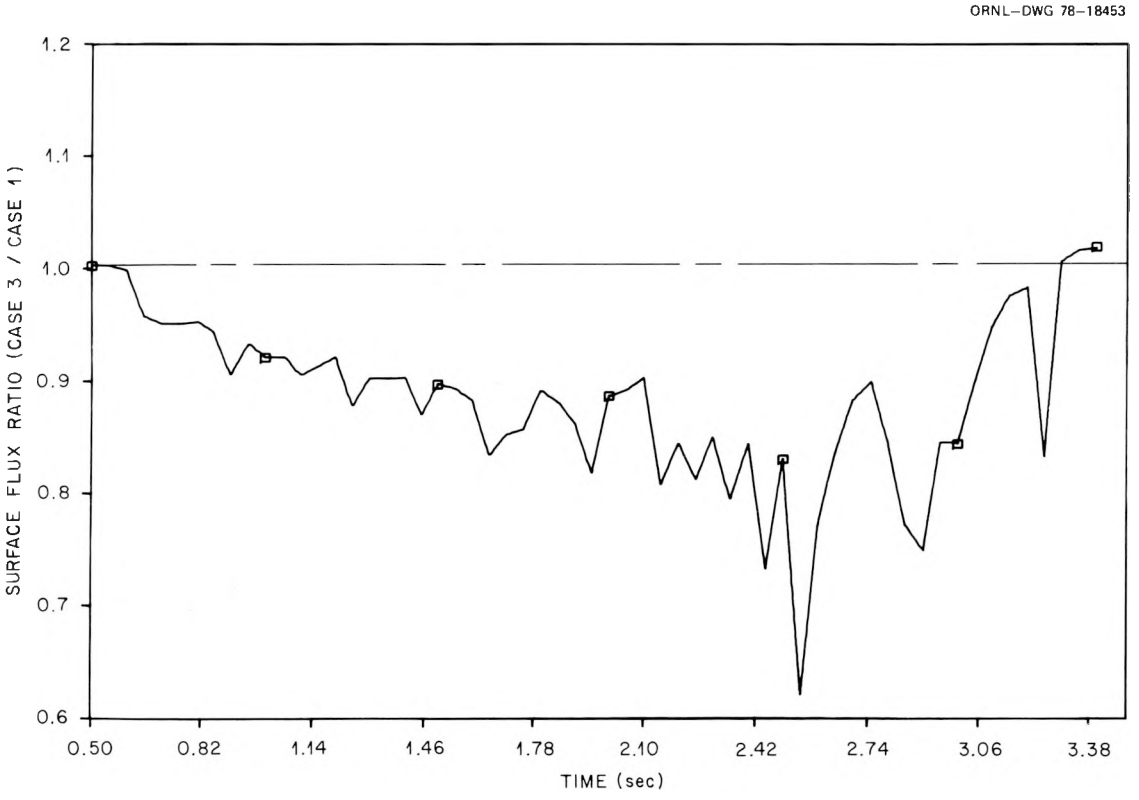

Fig. 3.23. Comparison of surface heat fluxes, cases 1 and 3.

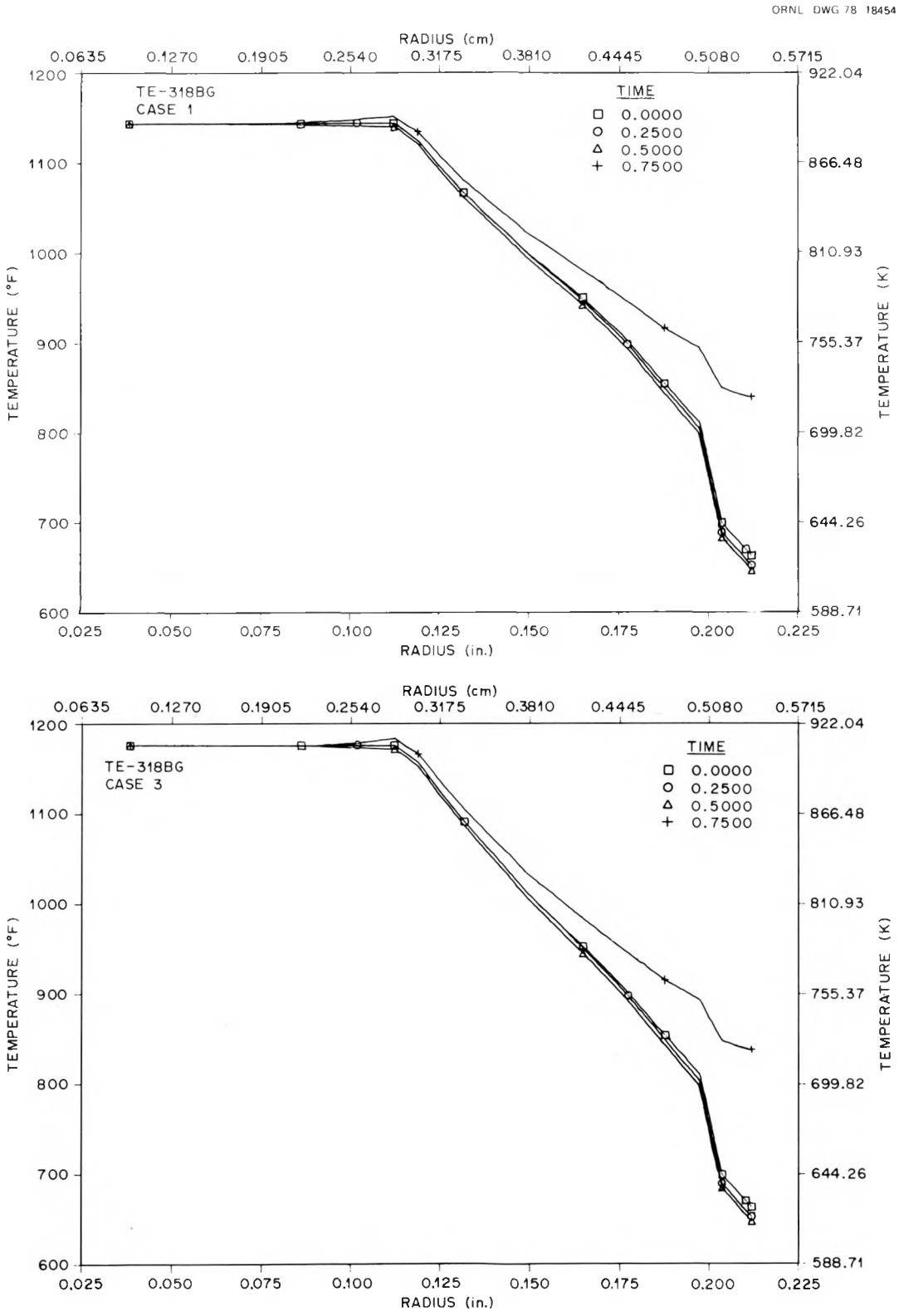

Fig. 3.24. Calculated pin internal thermal response, 0–0.75 sec.

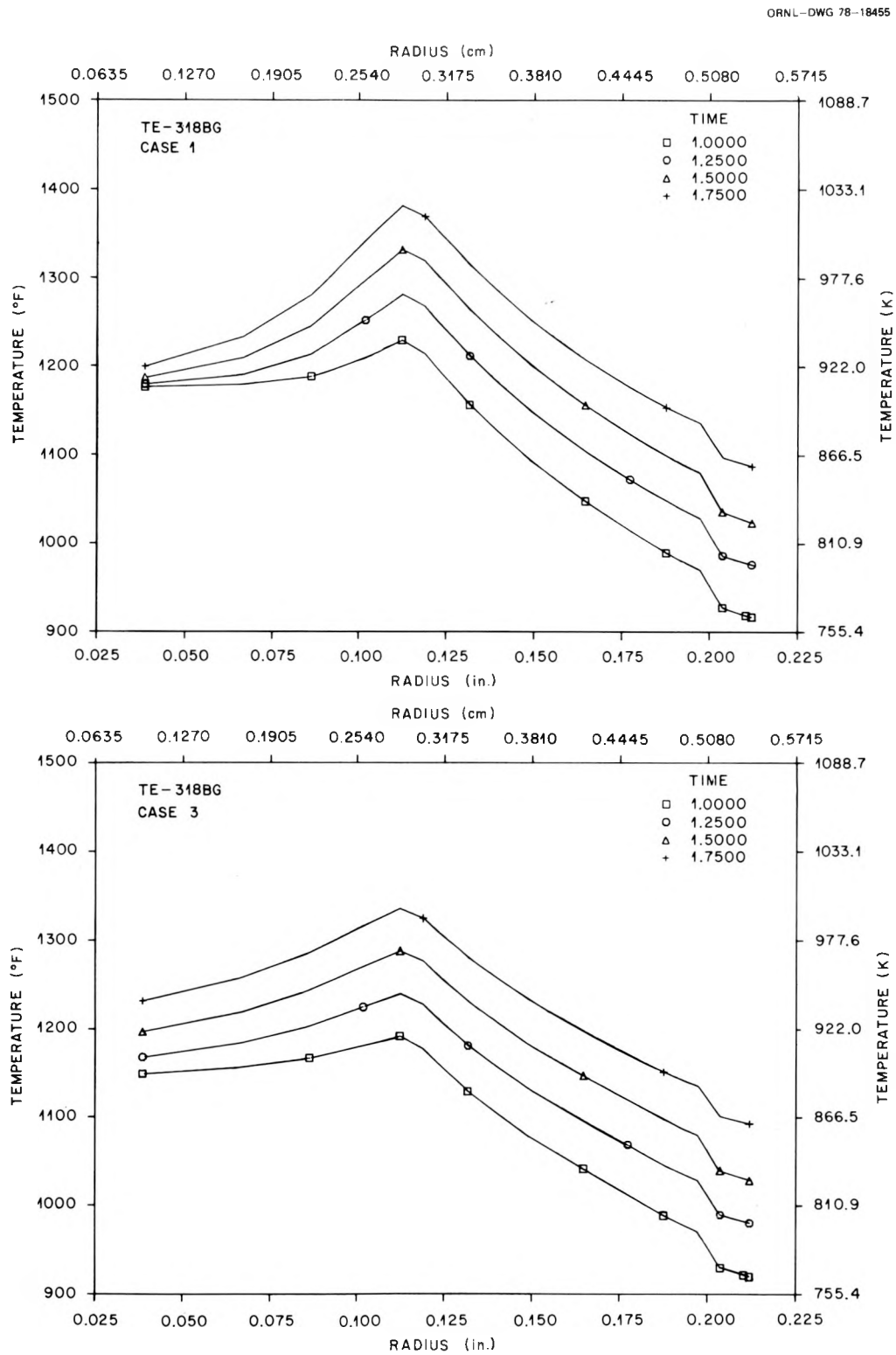

Fig. 3.25. Calculated pin internal thermal response, 1.0–1.75 sec.

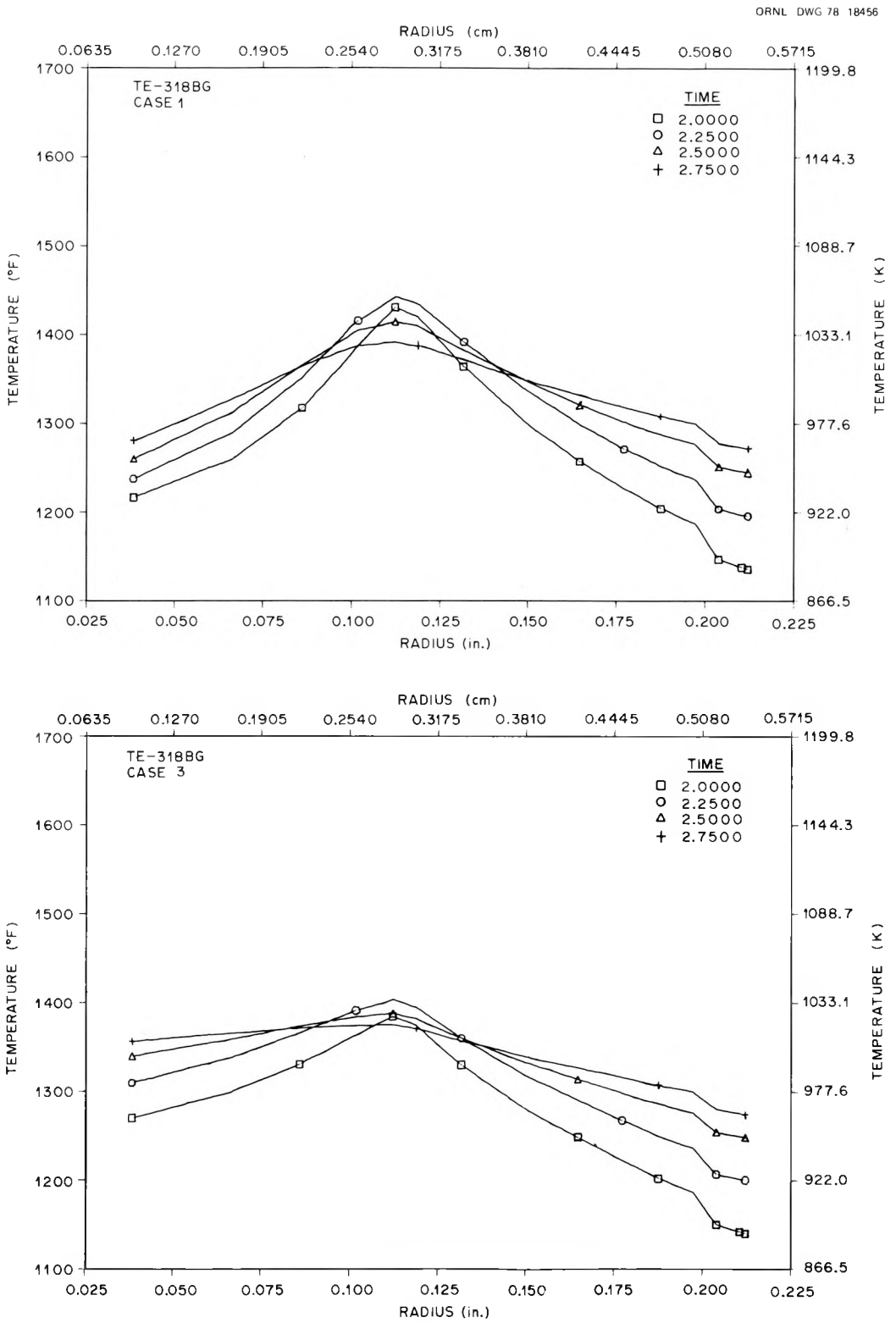

Fig. 3.26. Calculated pin internal thermal response, 2.0–2.75 sec.

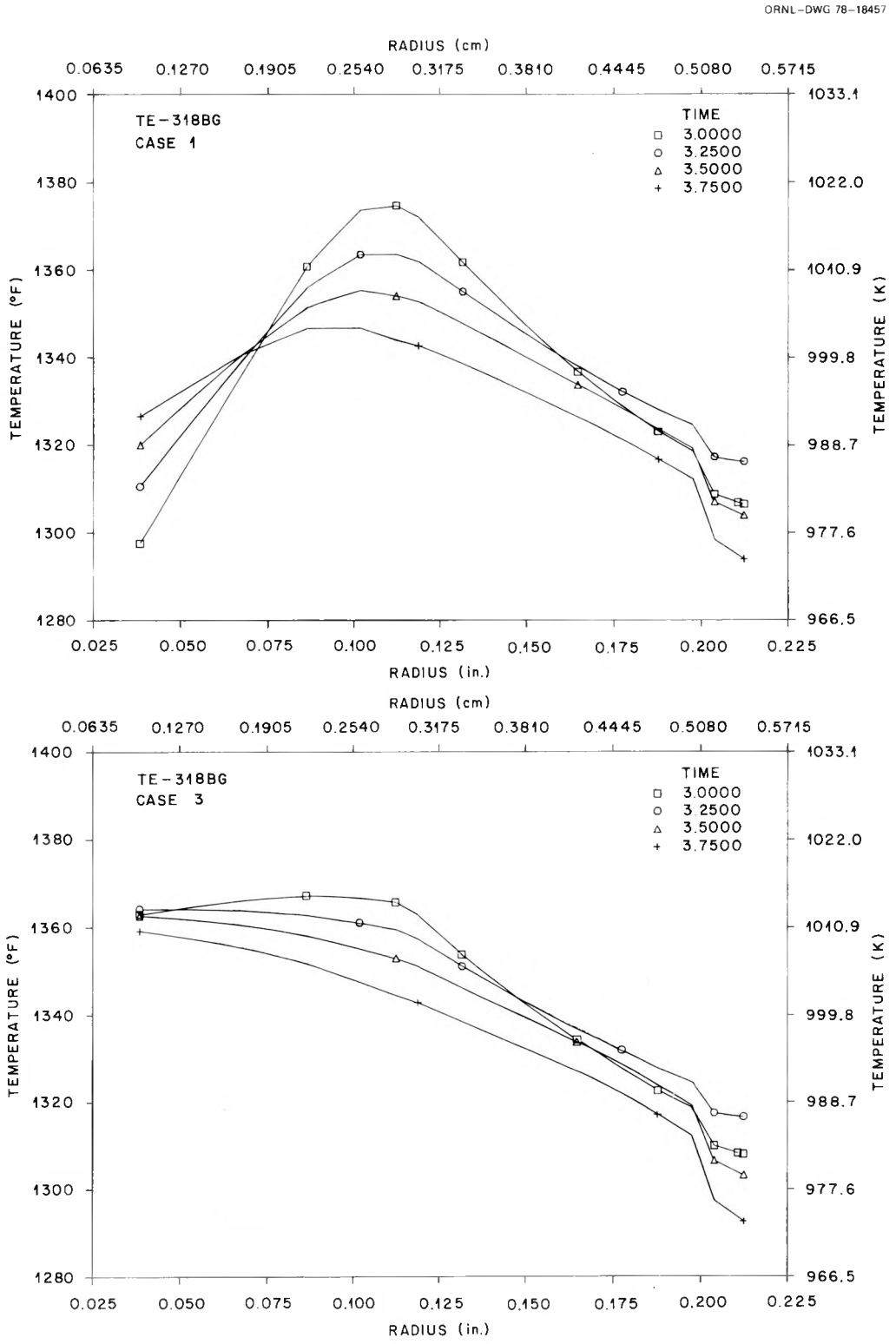

Fig. 3.27. Calculated pin internal thermal response, 3.0–3.75 sec.

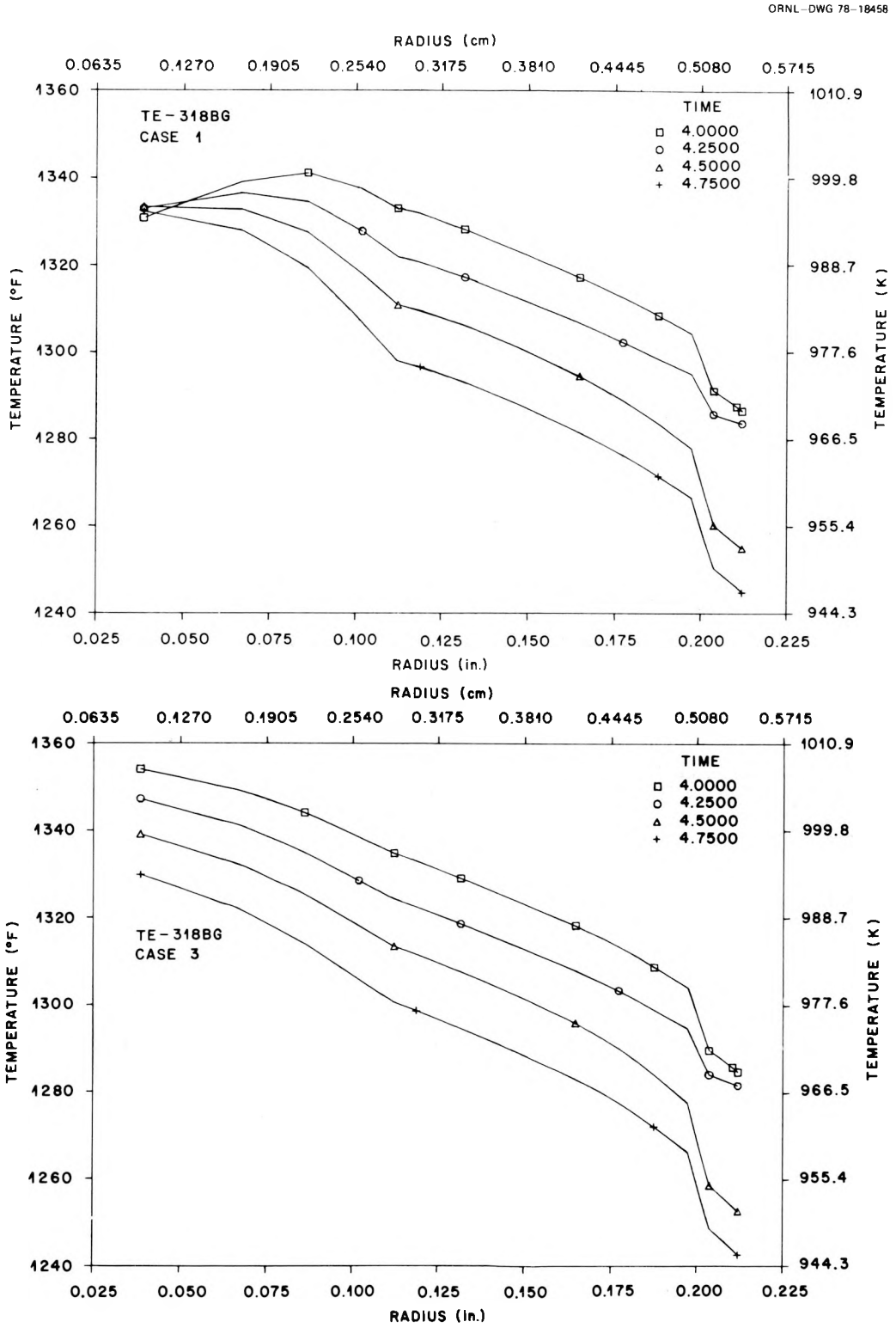

Fig. 3.28. Calculated pin internal thermal response, 4.0–4.75 sec.

the thermal resistance is less and thus more heat goes into the core of the simulator. Therefore, the centerline temperature in case 3 will respond faster and peak higher. The centerline temperature peaks at 1013 K at 3.20 sec and at 996 K at 4.45 sec for cases 3 and 1, respectively. The primary reason that the case 3 surface heat flux is less than that of case 1 in the 0.65- to 3.40-sec time interval is that more heat is being driven into the interior of the simulator rather than to the surface. Note that the temperature profile in case 3 "rolls over" between 3.00 and 3.25 sec, which is $\sim$1.25 sec before that of case 1.

Where neglect of the gap between the sheaths (as in case 2) affects the driving potential at the surface of the pin, the use of literature data for k_{BN} and α_{MgO} alters the spatial and temporal history of the heat flow within the pin and, as a result, the computed surface heat flux.

Case 4 will not be discussed to any extent other than to say that it represents the superposition of the errors in cases 2 and 3 and the state-of-the-art thermal analysis of fuel pin simulators prior to ORTCAL and ORINC.

4. CONCLUSIONS

An experimental thermocouple calibration procedure and a four-part calibration program, ORTCAL (ORNL Thermocouple Calibration), have been developed to supply heater rod performance information to the inverse heat conduction model and program ORINC.

Case studies have shown that failure to fully classify fuel pin simulators (i.e., with regard to component physical properties, gaps, etc.) can result in severe errors (during inverse calculations) in the computed driving potential at the surface of the pin (ΔT), the spatial and temporal history of the heat flow within the pin, and the computed surface heat flux.

REFERENCES

1. *Project Description ORNL-PWR Blowdown Heat Transfer Separate-Effects Program — Thermal Hydraulic Test Facility (THTF)*, ORNL/NUREG/TM-2 (February 1976).
2. *Anticipated Transients Without Scram for Water-Cooled Power Reactors*, WASH-1270 (September 1973).
3. R. L. Ludwig, *Metallographic Evaluation of Position of Outer Thermocouples in BDHT Heater 150-5*, Y-12 Development Division Metallurgical Department (September 1975).
4. L. J. Ott and R. A. Hedrick, *ORINC — A One-Dimensional Implicit Approach to the Inverse Heat Conduction Problem*, ORNL/NUREG-23 (November 1977).
5. R. L. Ludwig, personal communication, 1975.
6. Y. S. Touloukian, *Thermophysical Properties of High Temperature Solid Materials*, The Macmillan Company, New York, 1967.
7. E. W. Washburn, *International Critical Tables of Numerical Data, Physics, Chemistry, and Technology*, McGraw-Hill, New York.
8. R. E. Kirk and D. F. Othmer, *Encyclopedia of Chemical Technology*, The Interscience Encyclopedia, Inc., New York, 1952.
9. G. R. Finlay and G. H. Fetterley, "Boron Nitride — An Unusual Refractory," *Amer. Ceram. Soc., Bull. 31*, 141–43 (1952).
10. P. Popper, *Special Ceramics*, Heywood and Company Ltd., London, 1960.
11. J. E. Campbell and E. M. Sherwood, *High-Temperature Materials and Technology*, Wiley, New York.
12. J. Wolf, *Aerospace Structural Metals Handbook*, Mechanical Properties Data Center, Traverse City, Mich., 1973.
13. R. C. Weast, *Handbook of Chemistry and Physics*, The Chemical Rubber Company, Cleveland, Ohio, 1967.
14. S. Malang, *HETRAP: A Heat Transfer Analysis Program*, ORNL/TM-4555 (September 1974).
15. *International Nickel Co. Technical Bulletin T-7* (1956).
16. *ASTM Special Technical Publication No. 227* (1958).
17. *Alloy Digest, Cupro-Nickel, 30%–70%*, Engineering Alloys Digest, Inc., Upper Montclair, N.J., 1963.
18. J. D. White, *Recommended Procedures and Tests to Determine the Status of THTF Bundle No. 1*, BDHT-1879.
19. J. D. White, *Status of THTF Bundle*, BDHT-1883 (Nov. 4, 1976).
20. D. J. Fraysier, personal conversation, Mar. 16, 1978.
21. K. W. Childs and L. J. Ott, *Surface Heat Flux Perturbations in BDHT Heaters* (to be published).

22. W. D. Turner, D. C. Elrod, and I. I. Siman-Tov, *HEATING5 — An IBM 360 Heat Conduction Program*, ORNL/CSD/TM-15 (March 1977).

23. *Quarterly Progress Report on Blowdown Heat Transfer Separate-Effects Program for July–September 1977*, ORNL/NUREG/TM-149 (March 1978).

24. R. K. Adams, R. L. Anderson, and M. J. Roberts, *THTF Thermocouple Anomalous Readings*, BDHT-1819 (May 13, 1976).

25. T. G. Kollie et al., "Large Thermocouple Thermometry Errors Caused by Magnetic Fields," *Rev. Sci. Instrum.* 48(5), 501–511 (May 1977).

26. R. A. Hedrick et al., *PWR Blowdown Heat Transfer Separate-Effects Program Data Evaluation Report — System Response for Thermal-Hydraulic Test Facility Test Series 100*, ORNL/NUREG-19 (November 1977).

27. K. G. Turnage, personal communication.

28. M. Jakob, *Heat Transfer*, Vol. 1, Wiley, New York, 1957.

29. J. R. S. Thom et al., "Boiling in Subcooled Water During Flow up Heated Tubes or Annuli," *Proc. Inst. Mech. Engr.* 180, Part 3C, 226–46 (1966).

30. *Quarterly Progress Report on Blowdown Heat Transfer Program for July–September 1975*, ORNL/TM-5117 (November 1975).

31. *Quarterly Progress Report on Reactor Safety Programs Sponsored by the NRC Division of Reactor Safety Research for January–March 1975*, ORNL/TM-4914, Vol. 1 (July 1975).

32. *Quarterly Progress Report on Reactor Safety Programs Sponsored by the NRC Division of Reactor Safety Research for October–December 1974*, ORNL/TM-4808, Vol. 1 (April 1975).

33. R. Hooke and F. A. Jeeves, *J. Assoc. Comput. Mach.* 8, 119 (1961).

34. J. Weisman, C. F. Wood, and L. Rivlin, "Optimal Design of Chemical Process Systems," *Chem. Eng. Prog.* 61, 50–63 (1965).

35. *Quarterly Progress Report on Blowdown Heat Transfer Separate-Effects Program for April–June 1976*, ORNL/NUREG/TM-46 (January 1977).

36. *Quarterly Progress Report on Blowdown Heat Transfer Separate-Effects Program for July–September 1976*, ORNL/NUREG/TM-61 (February 1977).

37. *Quarterly Progress Report on Blowdown Heat Transfer Separate-Effects Program for January–March 1977*, ORNL/NUREG/TM-109 (August 1977).

38. *Quarterly Progress Report on Blowdown Heat Transfer Separate-Effects Program for April–June 1977*, ORNL/NUREG/TM-134 (November 1977).

39. C. D. Pears, Southern Research Inst., USAF ASD-TDR-62-765, 1-402 [AD 298 061].

40. V. Casal et al., KFK-2368, für Kernforschung M.B.H. (September 1976).

41. W. G. Craddick et al., *PWR Blowdown Heat Transfer Separate-Effects Program Data Evaluation Report — Heat Transfer for Thermal-Hydraulic Test Facility Test Series 100*, ORNL/NUREG-45 (1978).

42. H. W. Russell, "Principles of Heat Flow in Porous Insulators," *J. Am. Ceram. Soc.* 18, 1—5 (1935).

43. M. J. Laubitz, "Thermal Conductivity of Powders," *Can. J. Phys.* 37, 798—808 (1959).

Appendix A

PHYSICAL PROPERTIES DATA

Table A.1. Physical property data for Inconel 600[a]

1 Btu/hr ft °F = 1.73 W/m °C
1 Btu/lb-°F = 1 cal/g °C
1 lb/ft^3 = 0.01602 g/cm^3
°C = 5/9 (°F − 32)
Density = 526 lb/ft^3
Melting point = 2500–2600°F

Temperature (°F)	Specific heat, C_p (Btu/lb °F)	Thermal conductivity, k (Btu/hr ft °F)
0	0.0977	8.4
50	0.1011	8.6
100	0.1041	8.7
150	0.1068	8.9
200	0.1092	9.1
250	0.1113	9.3
300	0.1132	9.5
350	0.1148	9.7
400	0.1163	9.9
450	0.1176	10.2
500	0.1188	10.4
550	0.1199	10.6
600	0.1209	10.9
650	0.1218	11.2
700	0.1228	11.4
750	0.1237	11.7
800	0.1247	12.0
850	0.1254	12.2
900	0.1262	12.5
950	0.1270	12.8
1000	0.1278	13.1
1050	0.1287	13.4
1100	0.1297	13.7
1150	0.1307	14.0
1200	0.1317	14.3
1250	0.1328	14.6
1300	0.1340	14.9
1350	0.1352	15.2
1400	0.1364	15.5
1450	0.1377	15.8
1500	0.1391	16.1
1550	0.1405	16.4
1600	0.1419	16.7
1650	0.1434	17.0
1700	0.1450	17.3
1750	0.1466	17.6
1800	0.1482	17.8

[a]Best polynomial fit to data for C_p and k:

$0 \leqslant T \leqslant 800$

$$C_p = 9.77430344 \times 10^{-2} + 7.11642206 \times 10^{-5}T - 7.72415660 \times 10^{-8}T^2 + 3.80815379 \times 10^{-11}T^3$$

$800 \leqslant T \leqslant 2500$

$$C_p = 12.04458 \times 10^{-2} - 2.680032 \times 10^{-6}T + 1.005603 \times 10^{-8}T^2$$

$0 \leqslant T \leqslant 2500$

$$k = 8.42944336 + 2.88105011 \times 10^{-3}T + 2.42143869 \times 10^{-6}T^2 - 6.19365892 \times 10^{-10}T^3,$$

where k is given in Btu/hr ft °F, C_p given in Btu/lb °F, and T in °F.

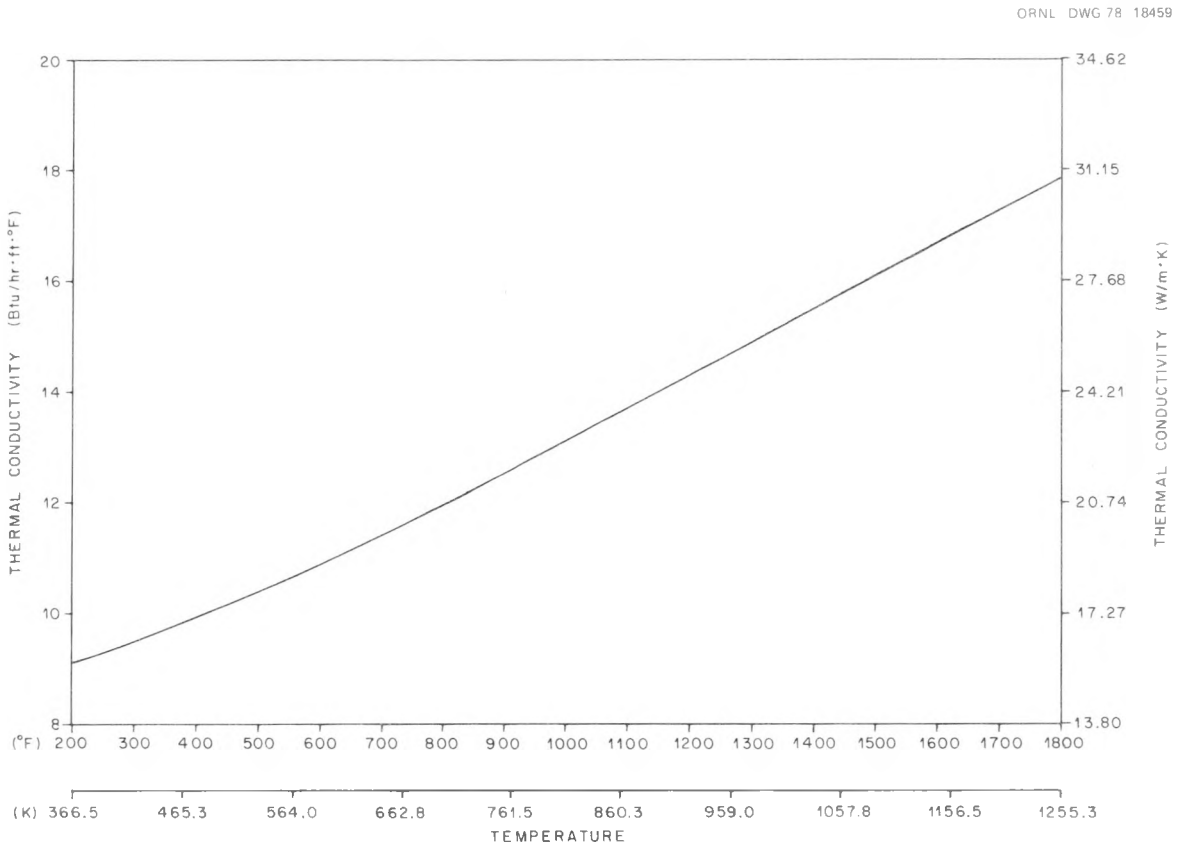

Fig. A.1. Thermal conductivity of Inconel 600.

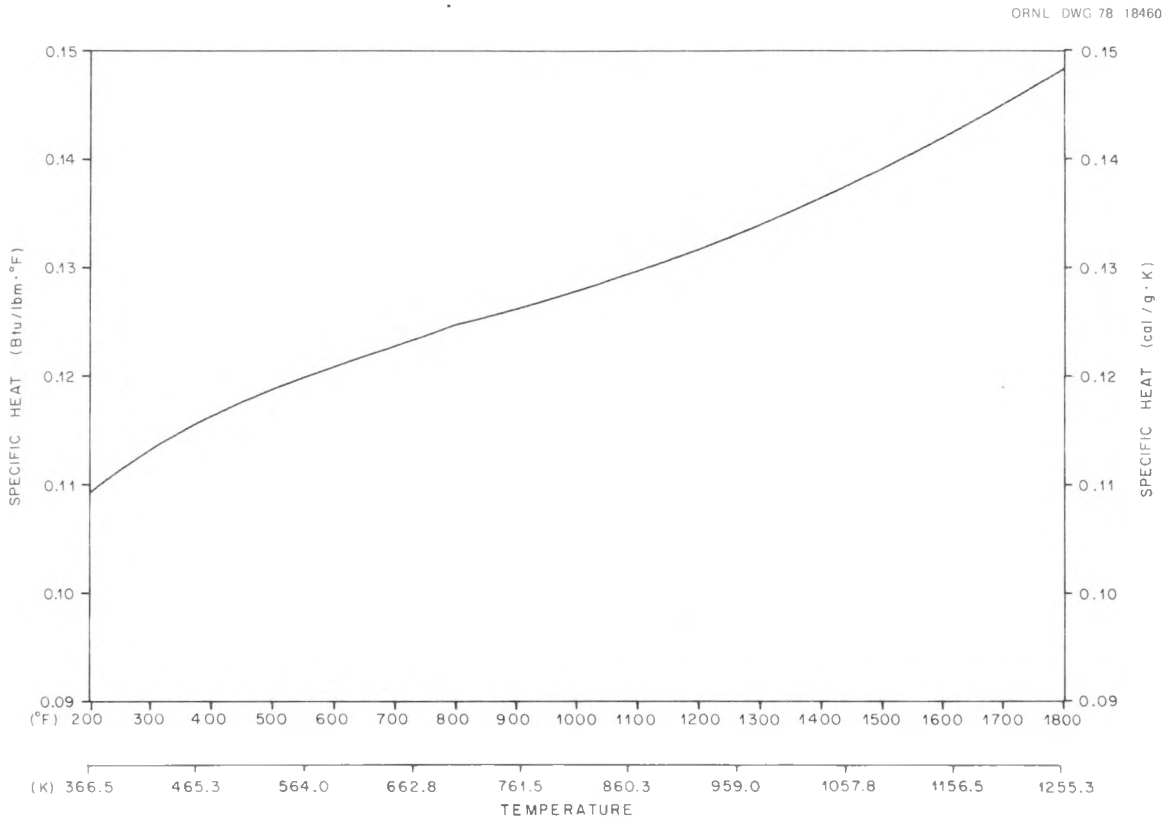

Fig. A.2. Specific heat of Inconel 600.

Table A.2. Physical property data for Cupronickel[a]

1 Btu/hr ft °F = 1.73 W/m °C
1 Btu/lb °F = 1 cal/g °C
1 lb/ft^3 = 0.01602 g/cm^3
°C = 5/9 (°F − 32)
Density = 553 lb/ft^3
Melting point = 2140–2280°F

Temperature (°F)	Specific heat, C_p (Btu/lb °F)	Thermal conductivity, k (Btu/hr ft °F)
0	0.0950	16.8
50	0.0965	16.8
100	0.0978	17.1
150	0.0991	17.5
200	0.1004	18.0
250	0.1016	18.6
300	0.1027	19.3
350	0.1039	20.1
400	0.1049	21.0
450	0.1060	21.9
500	0.1070	22.8
550	0.1080	23.8
600	0.1090	24.9
650	0.1100	26.1
700	0.1110	27.3
750	0.1119	28.6
800	0.1129	30.0
850	0.1139	31.5
900	0.1149	33.2
950	0.1159	35.1
1000	0.1169	37.2
1050	0.1180	39.5
1100	0.1191	42.2
1150	0.1203	45.2
1200	0.1215	48.6
1250	0.1227	52.4
1300	0.1240	56.8
1350	0.1253	61.7
1400	0.1268	67.2
1450	0.1282	73.4
1500	0.1298	80.4
1550	0.1314	88.3
1600	0.1332	97.0
1650	0.1350	106.8
1700	0.1369	117.6
1750	0.1389	129.6
1800	0.1410	142.9

[a]Best polynomial fit to data for C_p and k:

$0 \leq T \leq 2100$

$$C_p = 9.50193405 \times 10^{-2} + 2.93776393 \times 10^{-5}T - 1.41008059 \times 10^{-8}T^2 + 6.65068001 \times 10^{-12}T^3,$$

$$k = 1.68024902 \times 10^{1} - 1.31225586 \times 10^{-3}T + 4.43458557 \times 10^{-5}T^2 - 4.77302819 \times 10^{-8}T^3 + 2.50679477 \times 10^{-11}T^4,$$

where k is in Btu/hr ft °F, C_p in Btu/lb °F, and T in °F.

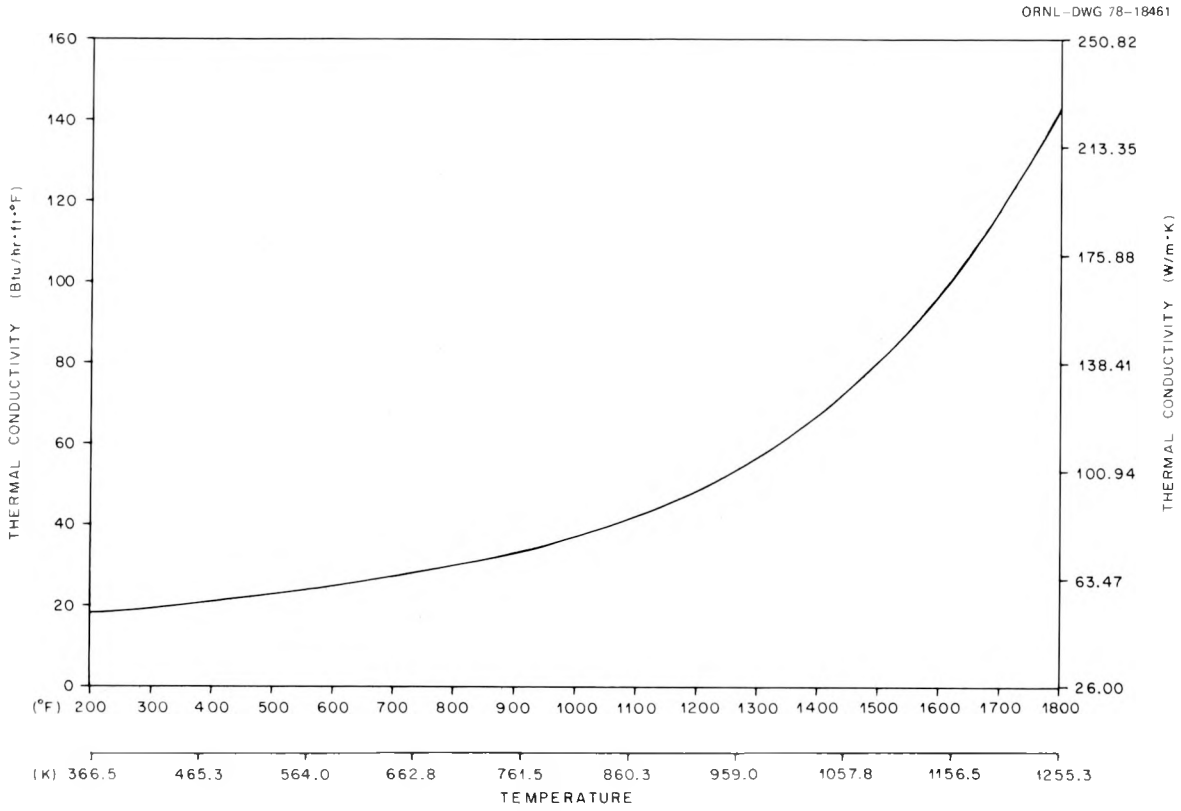

Fig. A.3. Thermal conductivity of Cupronickel.

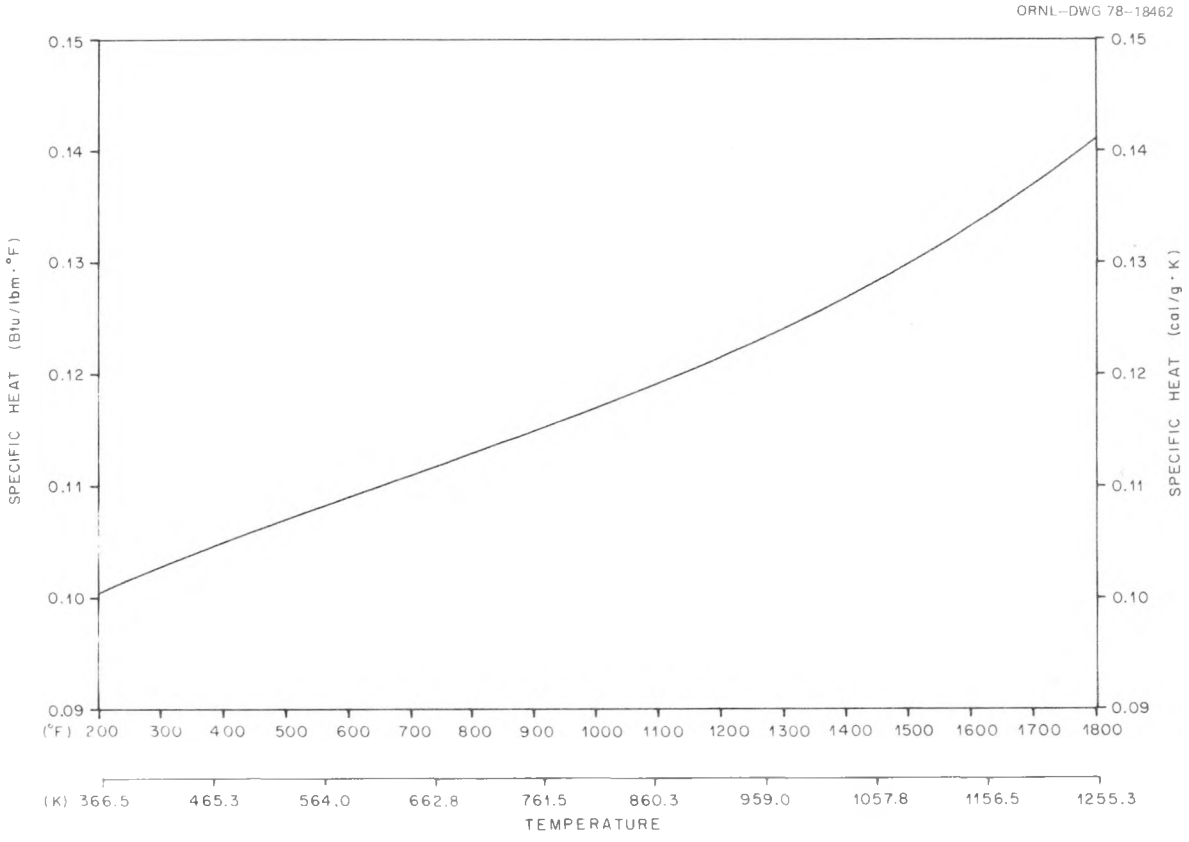

Fig. A.4. Specific heat of Cupronickel.

Table A.3. Physical property data for 316 stainless steel[a]

1 Btu/hr ft °F = 1.73 W/m °C
1 Btu/lb °F = 1 cal/g °C
1 lb/ft^3 = 0.01602 g/cm^3
°C = 5/9 (°F − 32)
Density = 496 lb/ft^3
Melting point = 2500–2550°F

Temperature (°F)	Specific heat, C_p (Btu/lb °F)	Thermal conductivity, k (Btu/hr ft °F)
0	0.1042	7.2
50	0.1072	7.5
100	0.1099	7.7
150	0.1124	8.0
200	0.1148	8.2
250	0.1170	8.5
300	0.1190	8.7
350	0.1209	8.9
400	0.1227	9.1
450	0.1243	9.4
500	0.1259	9.6
550	0.1274	9.8
600	0.1288	10.0
650	0.1301	10.2
700	0.1313	10.4
750	0.1325	10.7
800	0.1337	10.9
850	0.1348	11.1
900	0.1359	11.3
950	0.1369	11.5
1000	0.1380	11.7
1050	0.1390	11.9
1100	0.1400	12.1
1150	0.1411	12.4
1200	0.1421	12.6
1250	0.1431	12.8
1300	0.1442	13.0
1350	0.1452	13.2
1400	0.1463	13.5
1450	0.1474	13.7
1500	0.1485	13.9
1550	0.1496	14.2
1600	0.1508	14.4
1650	0.1519	14.7
1700	0.1531	14.9
1750	0.1543	15.2
1800	0.1556	15.4

[a]Best polynomial fit to data for C_p and k:

$0 \leq T \leq 2500$

$$C_p = 1.04247093 \times 10^{-1} + 6.05583191 \times 10^{-5}T - 4.37721610 \times 10^{-8}T^2 + 2.01225703 \times 10^{-11}T^3 - 3.16413562 \times 10^{-15}T^4,$$

$0 \leq T \leq 2050$

$$k = 7.24584961 + 5.07926941 \times 10^{-3}T - 9.89995897 \times 10^{-7}T^2 + 3.82840426 \times 10^{-10}T^3,$$

where k is in Btu/hr ft °F, C_p in Btu/lb °F, and T in °F.

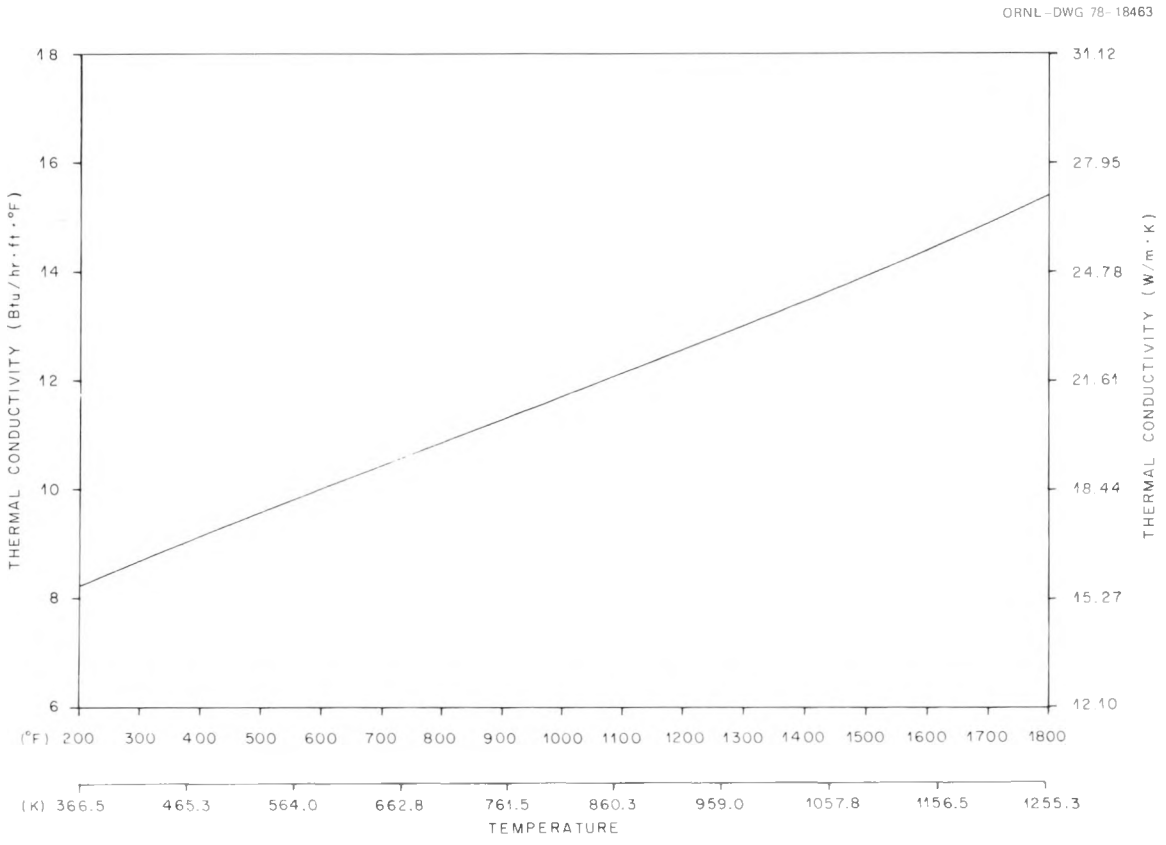

Fig. A.5. Thermal conductivity of 316 stainless steel.

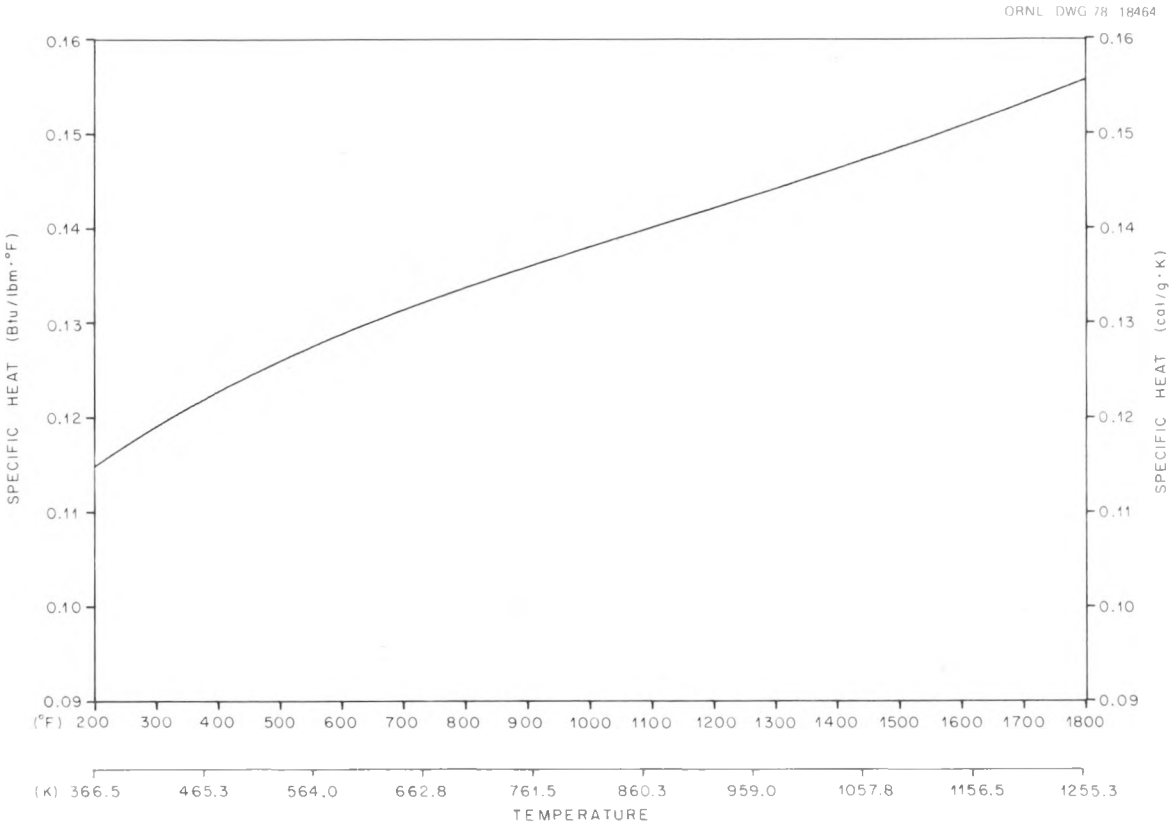

Fig. A.6. Specific heat of 316 stainless steel.

Table A.4. Physical property data for magnesium oxide[a]

1 Btu/hr ft °F = 1.73 W/m °C
1 Btu/lb °F = 1 cal/g °C
1 lb/ft^3 = 0.01602 g/cm^3
°C = 5/9 (°F − 32)
Density = 212 lb/ft^3

Temperature (°F)	Specific heat, C_p (Btu/lb °F)
0	0.2243
50	0.2302
100	0.2359
150	0.2413
200	0.2463
250	0.2511
300	0.2557
350	0.2599
400	0.2639
450	0.2677
500	0.2712
550	0.2745
600	0.2776
650	0.2805
700	0.2832
750	0.2856
800	0.2879
850	0.2901
900	0.2920
950	0.2938
1000	0.2955
1050	0.2970
1100	0.2984
1150	0.2997
1200	0.3009
1250	0.3020
1300	0.3030
1350	0.3039
1400	0.3047
1450	0.3055
1500	0.3062
1550	0.3069
1600	0.3075
1650	0.3081
1700	0.3087
1750	0.3093
1800	0.3098

[a]Best polynomial fit to data for C_p:

$$0 \leq T \leq 2400$$

$$C_p = 2.24258423 \times 10^{-1} + 1.22666359 \times 10^{-4}T - 6.35191100 \times 10^{-8}T^2 + 1.21040955 \times 10^{-11}T^3,$$

where C_p is in Btu/lb °F and T in °F.

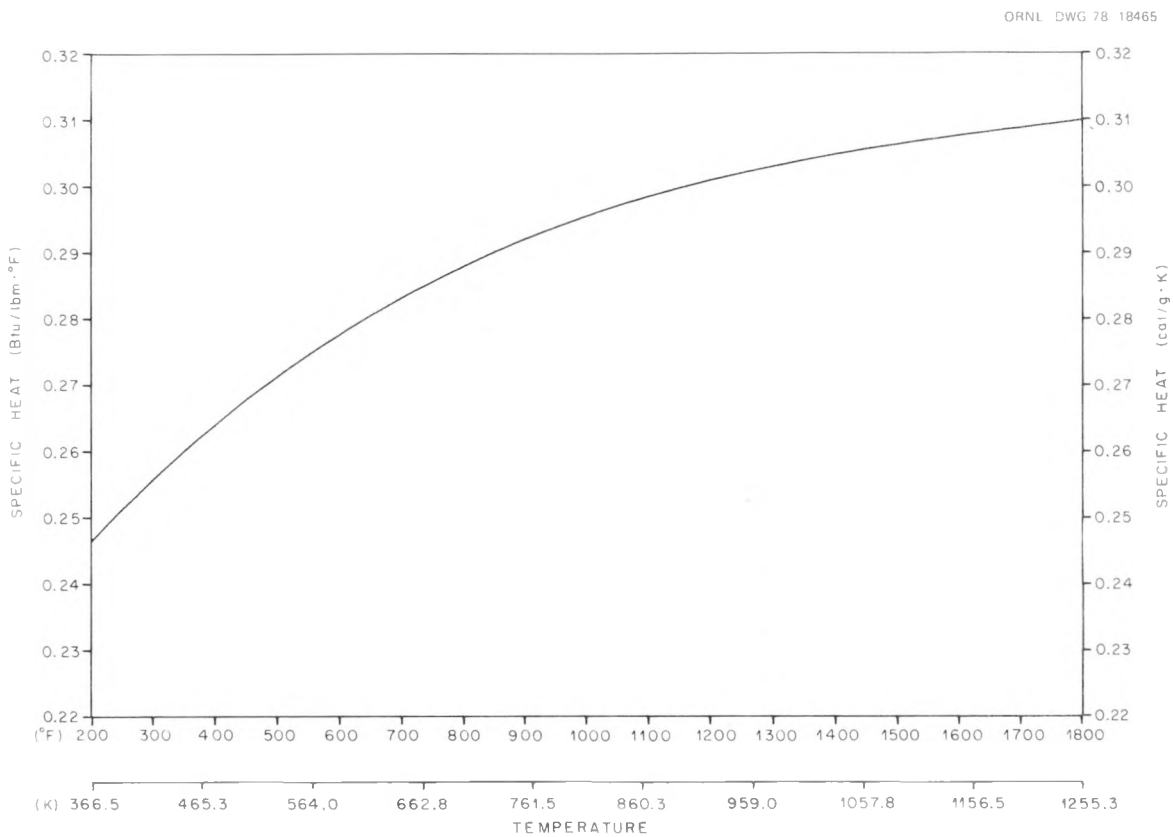

Fig. A.7. Specific heat of magnesium oxide.

Table A.5. Physical property data for boron nitride[a]

1 Btu/hr ft °F = 1.73 W/m °C
1 Btu/lb °F = 1 cal/g °C
1 lb/ft^3 = 0.01602 g/cm^3
°C = 5/9 (°F − 32)
Density = 125 lb/ft^3

Temperature (°F)	Specific heat, C_p (Btu/lb °F)
0	0.1678
50	0.1859
100	0.2031
150	0.2195
200	0.2352
250	0.2500
300	0.2641
350	0.2775
400	0.2901
450	0.3021
500	0.3134
550	0.3241
600	0.3342
650	0.3437
700	0.3526
750	0.3610
800	0.3689
850	0.3763
900	0.3832
950	0.3897
1000	0.3957
1050	0.4014
1100	0.4067
1150	0.4116
1200	0.4162
1250	0.4205
1300	0.4245
1350	0.4283
1400	0.4318
1450	0.4352
1500	0.4383
1550	0.4413
1600	0.4441
1650	0.4469
1700	0.4495
1750	0.4521
1800	0.4546

[a] Best polynomial fit to data for C_p:

$0 \leq T \leq 2000$

$$C_p = 1.67812347 \times 10^{-1} + 3.70264053 \times 10^{-4}T - 1.73793524 \times 10^{-7}T^2 + 3.14486215 \times 10^{-11}T^3,$$

$2000 \leq T \leq 2600$

$$C_p = 0.4306064 + 1.70744517 \times 10^{-5}T,$$

where C_p has units of Btu/lb °F and T has units of °F.

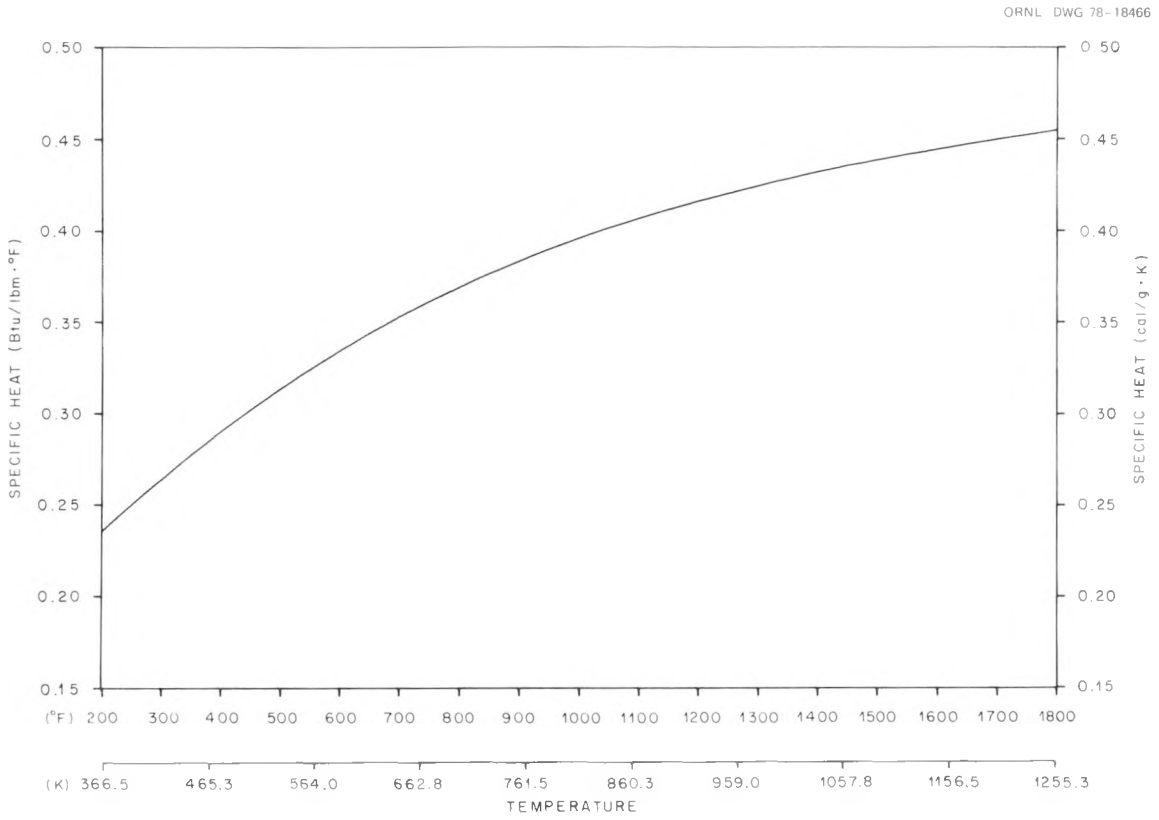

Fig. A.8. Specific heat of boron nitride.

Appendix B

OPERATING CHECKLIST FOR APPROACH TO POWER

Subject: APPROACH TO POWER	TEST NO.	DATE OF TEST:

Initial/Time

NOTE

This section applies to the type and number of computer scans to be taken during a normal approach to test power. If any of the following power levels are to be eliminated for a given test, the entry must be crossed out and initialed by the Analysis Group representative.

NOTE

All scans listed for a specific power level must be reviewed and approved by the Analysis Group representative prior to a change in loop conditions or power level.

1.0 Power level = 0 kW

_1.1 Operator's log

_1.2 Long power verification

_1.3 T/C scan (takes ∿15 minutes)

_1.4 Analog scan (100 ft) _____

2.0 Power level = 10 volts (rod resistance check)

_2.1 Long power verification _____

3.0 Power level = 20 volts (rod resistance check)

_3.1 Long power verification _____

4.0 Power level = 45 volts ∿5 kW/rod) (rod resistance check)

_4.1 Long power verification _____

5.0 Power level = 30 kW/rod

_5.1 Short power verification (repeat as necessary to verify 30 ± 0.5 kW/rod on all generators)

_5.2 Long power verification

_5.3 Operator's log

_5.4 T/C scan (takes ∿15 minutes)

_5.5 Analog scan (100 feet) _____

NOTE

The 30 kW/rod must be taken. The core inlet temperature should be ∿400°F for section 5.0 but will be allowed to drift upward for the remaining power levels.

6.0 Power level = 50 kW/rod

_6.1 Short power verification (repeat as necessary to verify 50 ± 0.5 kW/rod on all generators).

_6.2 Long power verification

_6.3 Operator's log

_6.4 T/C scan (takes ∿15 minutes)

_6.5 Analog scan (100 feet) _____

Subject: APPROACH TO POWER	TEST NO.	DATE OF TEST:

Initial/Time

7.0 Power level = 70 kW/rod

_7.1 Short power verification (repeat as necessary to verify 70 ± 0.5 kW/rod on all generators).

_7.2 Long power verification

_7.3 Operator's log

_7.4 T/C scan (takes ∿15 minutes)

_7.5 Analog scan (100 feet) _____

NOTE

I&C should be allowed to take scans required for calibration of densitometers.

8.0 Power level = 100 kW/rod

_8.1 Short power verification (repeat as necessary to verify 100 ± 0.5 kW/rod on all generators).

_8.2 Long power verification

_8.3 Operator's log

_8.4 T/C scan (takes ∿15 minutes)

_8.5 Analog scan (100 feet) _____

9.0 Power level = ____ kW/rod (test power level)

_9.1 Short power verification (repeat as necessary to verify ____ ± 0.1 kW/rod on all generators).

_9.2 Long power verification

_9.3 Operator's log (repeat as necessary to verify desired test conditions). _____

NOTE

Make sure I&C personnel and PDP-8 operator are ready for blowdown (i.e., turbine meter range set, fast-scan program loaded and ready, etc.).

10.0 At t = −15 seconds initiate

_10.1 Digital fast scan for 5 minutes

_10.2 Analog scan (800 feet)

FCTF CALIBRATION PROCEDURE

Run No. 1: Steady-state scans starting at 30 kW up to 122 kW in 10-kW increments; power drop from 122 kW at the following conditions

Pressure, ∿2250 psig
Core flow, ∿20-25 gpm
Core inlet temperature, minimum

Run No. 2: Repeat No. 1, except system pressure ∿1500 psi.

Run No. 3: Repeat No. 1, except core inlet temperature ∿550°F.

Succeeding Runs: Steady-state scans at 30, 60, 90, and 122 kW, pressure 2250 psig, core flow ∿20-25 gpm.

Run No. 4 Hold inlet temperature ∿400°F until 122 kW data point is taken.

Run No. 5 Hold inlet temperature ∿450°F until 122 kW data point is taken.

Run No. 6 Hold inlet temperature ∿500°F until 122 kW data point is taken.

Run No. 7 Hold inlet temperature ∿550°F until 122 kW data point is taken.

Runs 8 through 10 let inlet temperature float with power.

Appendix C

EXAMPLES OF ORTCAL — PART I OUTPUT

Table C.1. THTF thermocouple calibration runs

Run No.	Date	Approach to BD No.
1.1	May 4, 1976	Calibration only
1.2	May 5, 1976	Calibration only
1.3	May 5, 1976	Calibration only
1.4	May 6, 1976	Calibration only
2.1	May 19, 1976	Calibration only
2.2	May 20, 1976	Calibration only
3.1	May 26–27, 1976	101
4.1	June 17, 1976	Aborted
4.2	June 18, 1976	102
5.1	July 8, 1976	104
6.1	August 4, 1976	103
7.1	August 19, 1976	105
8.1	September 9, 1976	Aborted
8.2	October 9, 1976	Aborted
8.3	November 5, 1976	151
9.1	November 18, 1976	152
10.1	December 8, 1976	153
11.1	January 13, 1977	154
12.1	January 27, 1977	154R
13.1	February 10, 1977	155
14.1	March 10, 1977	156
15.1	March 24, 1977	157
16.1	April 28, 1977	158
17.1	May 27, 1977	160
18.1	June 16, 1977	161
19.1	June 30, 1977	162
20.1	August 23, 1977	163
21.1	September 22, 1977	164R
22.1	October 13, 1977	165
23.1	December 1, 1977	166
23.2	December 16, 1977	166R
23.3	January 19, 1978	166S
24.1	February 16, 1978	167

Table C.2. Example of ORTCAL — Part I output for thermocouple TE-318BG

TIME	NOMINAL POWER (kW)	BUNDLE INLET TEMP. (F)	BUNDLE EXIT TEMP. (F)	UPPER PLENUM PRESS. (PSIA)	LOCAL BULK PRESS. (PSIA)	LOCAL BULK TEMP. (F)	LOCAL SAT. TEMP. (F)	CORE FLOW RATE (LB/SEC)	CORE FLOW RATE (GPM)	SHEATH T/C READING (F)	MIDDLE T/C READING (F)	SURFACE H.T. COEFF.	SURFACE HEAT FLUX	H.T. MODE	DEL-T GAP (F)	GAP (MILS)
CALIBRATION RUN NUMBER 1.1 MAY 4																
23:36:56	30.3	405.4	429.8	2223.7	2239.8	419.0	652.0	53.36	442.7	477.4	566.2	6410.	130162.	F.C.	20.5	0.0414
23:44:18	40.1	403.1	434.7	2218.2	2234.4	420.8	651.7	54.49	451.3	495.4	613.1	6529.	171816.	F.C.	25.3	0.0391
23:53:20	40.5	401.9	433.3	2216.7	2232.7	419.4	651.5	55.39	458.4	494.8	613.7	6607.	173735.	F.C.	25.7	0.0395
0:29: 6	50.7	406.6	445.2	2212.9	2228.9	428.2	651.3	55.83	463.6	520.1	669.8	6700.	217618.	F.C.	30.5	0.0379
CALIBRATION RUN NUMBER 1.2 MAY 5																
14:31:56	40.7	306.2	336.9	2234.9	2254.1	323.3	652.9	59.50	463.4	402.5	522.9	6269.	174455.	F.C.	26.8	0.0374
14:50:53	50.7	350.6	389.9	2209.3	2227.7	372.5	651.2	56.80	454.0	467.3	616.7	6430.	217389.	F.C.	31.3	0.0372
15:39:21	50.6	401.7	439.8	2293.9	2311.9	423.0	656.6	56.63	468.3	516.1	663.5	6745.	216901.	F.C.	32.0	0.0399
15:56:45	60.9	405.0	451.1	2288.9	2307.2	430.7	656.3	56.24	466.3	540.3	719.2	6754.	261115.	F.C.	36.3	0.0383
16:18: 7	71.2	400.4	452.0	2286.4	2305.1	429.2	656.2	58.54	483.7	557.2	765.3	6964.	305271.	F.C.	44.0	0.0401
16:50:43	81.2	401.5	464.0	2222.4	2238.3	436.4	651.9	54.73	452.7	584.5	820.9	6640.	348228.	F.C.	50.2	0.0408
17:13:10	91.6	402.6	473.8	2192.2	2208.1	442.3	650.0	53.92	446.5	606.7	875.7	6594.	392785.	F.C.	53.9	0.0395
CALIBRATION RUN NUMBER 1.3 MAY 5																
19:21:26	102.2	404.2	480.4	2210.0	2226.4	446.7	651.1	55.88	463.3	627.9	927.7	6810.	438562.	F.C.	60.3	0.0403
19:53:59	112.1	400.7	483.6	2251.1	2267.7	447.0	653.8	56.23	464.8	644.7	970.4	6844.	480673.	F.C.	65.9	0.0405
20:22:51	124.5	401.2	498.8	2217.3	2231.7	455.7	651.5	52.66	435.6	675.6	1037.6	6540.	534211.	F.C.	70.5	0.0399
21: 4:19	124.6	440.3	536.8	2216.2	2229.6	494.2	651.4	51.32	437.6	715.7	1075.0	6582.	534540.	F.C.	73.7	0.0430
CALIBRATION RUN NUMBER 1.4 MAY 6																
12:35:24	91.6	291.6	356.2	2239.8	2259.7	327.7	653.3	63.00	486.8	494.5	757.1	6603.	392913.	F.C.	53.7	0.0356
12:57:41	91.5	293.3	357.0	2225.6	2245.6	328.8	652.4	63.83	493.6	496.6	757.6	6683.	392560.	F.C.	55.5	0.0368
13:35:46	91.4	306.2	370.6	2275.5	2295.0	342.2	655.6	62.81	489.0	507.2	769.1	6716.	391958.	F.C.	53.5	0.0358
13:48:44	91.3	322.2	386.5	2258.1	2277.6	358.1	654.4	62.59	491.7	522.3	783.4	6833.	391688.	F.C.	54.1	0.0370
CALIBRATION RUN NUMBER 2.1 MAY 19																
4: 6: 2	30.6	400.7	426.1	2259.4	2271.0	414.9	654.0	49.97	413.1	474.7	560.9	6059.	131236.	F.C.	20.4	0.0408
4:28:22	41.0	400.8	434.0	2302.9	2314.6	419.3	656.8	51.36	424.5	496.9	613.4	6218.	175676.	F.C.	25.7	0.0389
5: 8:30	51.1	400.1	441.1	2250.5	2262.2	423.0	653.5	51.56	426.0	518.3	663.2	6258.	219187.	F.C.	31.1	0.0383
5:37:54	61.4	400.7	450.0	2303.4	2315.1	428.2	656.8	51.41	424.8	540.3	714.0	6271.	263206.	F.C.	35.3	0.0368
6: 0: 0	71.5	400.7	457.4	2231.6	2242.7	432.3	652.2	51.90	429.1	559.1	763.8	6343.	306560.	F.C.	38.2	0.0347
6:45:11	81.9	400.2	464.5	2219.3	2230.0	436.1	651.4	52.14	431.0	580.5	814.9	6387.	351304.	F.C.	43.5	0.0351
7: 5:50	91.8	400.8	473.0	2234.6	2245.9	441.1	652.4	51.95	429.5	600.6	864.9	6394.	393694.	F.C.	46.9	0.0343
7:35:54	102.0	401.0	480.2	2201.9	2212.6	445.2	650.3	52.40	433.4	623.3	918.3	6461.	437530.	F.C.	54.1	0.0360
8:37: 4	112.1	401.4	488.1	2220.4	2231.0	449.8	651.4	52.49	434.2	644.9	971.0	6492.	480711.	F.C.	59.6	0.0368
CALIBRATION RUN NUMBER 2.2 MAY 19																
22:42:55	30.7	400.0	425.6	2231.1	2243.0	414.3	652.2	49.82	411.7	474.6	562.9	6041.	131859.	F.C.	20.6	0.0408
23:10:47	40.9	400.3	433.3	2218.3	2230.2	418.8	651.4	51.48	425.5	497.3	614.1	6228.	175610.	F.C.	26.8	0.0406
23:32:51	51.1	400.7	441.6	2206.6	2217.9	423.5	650.6	51.73	427.7	519.8	665.7	6278.	219333.	F.C.	32.1	0.0397
23:57:45	61.3	400.2	449.1	2198.9	2210.1	427.5	650.1	51.81	428.3	540.6	716.0	6309.	263081.	F.C.	36.6	0.0383
0:31: 6	71.5	399.8	457.1	2220.8	2232.3	431.8	651.5	51.39	424.6	562.2	766.1	6290.	306696.	F.C.	41.4	0.0378
0:55:49	81.8	400.6	465.6	2250.4	2261.9	436.9	653.4	51.56	426.2	582.8	817.6	6334.	350685.	F.C.	44.8	0.0362
1:23: 3	91.9	400.4	472.5	2236.2	2247.3	440.7	652.5	52.10	430.6	603.3	867.7	6406.	394175.	F.C.	50.1	0.0366
2:30:44	102.2	400.6	480.6	2293.1	2305.3	445.2	656.2	51.97	429.5	624.0	920.7	6416.	438512.	F.C.	53.9	0.0358
2:55:20	112.3	400.9	488.4	2256.6	2268.1	449.7	653.8	52.09	430.7	643.6	970.4	6452.	481816.	F.C.	57.6	0.0354
3:18:32	124.3	400.3	496.0	2247.9	2259.5	453.7	653.3	52.60	434.7	665.4	1027.1	6523.	533154.	F.C.	62.2	0.0351
4:35:52	124.2	449.5	545.2	2275.0	2285.5	503.0	655.0	50.06	430.0	712.2	1072.6	6488.	532716.	F.C.	60.8	0.0356
7: 5:39	124.4	499.2	591.8	2280.9	2290.3	550.9	655.3	48.15	433.7	755.9	1117.5	6474.	533511.	F.C.	57.4	0.0349
7:51:40	124.6	545.7	633.3	2281.0	2288.3	594.6	655.1	45.15	429.6	789.4	1149.0	62413.	534287.	N.B.	61.3	0.0379
8:15:29	112.2	544.7	625.5	2301.4	2308.5	589.8	656.4	44.97	427.2	773.8	1099.0	60184.	481123.	N.B.	51.3	0.0351
8:41: 8	102.3	544.1	618.9	2324.3	2331.7	585.9	657.8	44.92	426.4	759.1	1054.4	6258.	438625.	F.C.	49.9	0.0372
9:19:59	92.0	544.5	612.7	2321.5	2329.0	582.5	657.7	44.81	425.5	743.4	1006.1	6231.	394713.	F.C.	49.4	0.0405
9:43:39	81.9	544.9	606.3	2306.8	2313.9	579.2	656.7	44.58	423.6	724.4	958.7	6193.	351302.	F.C.	45.4	0.0412
10: 7:36	71.5	544.5	599.0	2297.7	2305.4	574.9	656.2	44.49	422.6	703.5	907.6	6166.	306781.	F.C.	40.9	0.0420
10:31:29	61.3	544.1	591.5	2311.1	2318.2	570.6	657.0	44.35	421.0	683.3	856.9	6133.	262928.	F.C.	37.2	0.0439
10:55:49	50.5	543.1	583.1	2302.7	2310.1	565.4	656.5	43.91	416.3	660.1	802.5	6065.	216693.	F.C.	31.9	0.0451
11:19:26	40.7	542.7	576.2	2319.4	2327.6	561.4	657.6	42.62	403.8	639.0	753.5	5908.	174644.	F.C.	26.0	0.0449
11:44:10	30.3	542.4	567.6	2307.5	2315.3	556.5	656.8	42.42	401.8	615.1	699.8	5869.	129951.	F.C.	20.0	0.0457
CALIBRATION RUN NUMBER 3.1 MAY 27																
1:14:13	30.7	401.6	426.6	2221.7	2234.6	415.6	651.7	52.14	431.4	478.6	565.5	6273.	131900.	F.C.	24.1	0.0482
1:36: 0	40.9	398.8	432.3	2235.6	2248.4	417.5	652.6	51.73	427.0	498.5	615.3	6244.	175505.	F.C.	29.4	0.0445
2: 2:32	51.1	402.3	443.2	2258.9	2271.9	425.1	654.1	52.72	436.3	524.1	669.6	6383.	219355.	F.C.	35.4	0.0439
2:23:56	61.4	402.2	450.9	2258.6	2271.6	429.4	654.1	53.02	438.8	545.5	720.7	6435.	263409.	F.C.	40.4	0.0424
2:45:31	71.6	401.9	458.9	2269.3	2282.4	433.7	654.8	52.69	435.9	567.9	771.9	6426.	306975.	F.C.	46.1	0.0422
3:11:21	81.8	403.9	468.5	2271.1	2284.2	440.0	654.9	52.78	437.3	589.8	824.2	6469.	350952.	F.C.	49.9	0.0405
3:32:41	92.0	403.8	475.8	2255.7	2268.9	444.0	653.9	53.17	440.5	609.3	874.7	6529.	394542.	F.C.	53.8	0.0393
4: 1:10	102.0	403.6	483.3	2269.5	2282.7	448.1	654.8	53.13	440.1	629.6	925.1	6546.	437431.	F.C.	58.5	0.0391
4:25:28	112.3	403.0	491.1	2268.9	2282.2	452.2	654.7	52.73	436.6	651.5	976.8	6527.	481708.	F.C.	64.0	0.0395
4:48:45	124.5	404.5	501.6	2249.4	2262.6	458.7	653.5	52.71	437.0	678.9	1038.9	6559.	534182.	F.C.	71.1	0.0403
5:17: 8	124.4	450.6	545.6	2258.5	2271.3	503.7	654.0	51.46	442.6	724.5	1082.7	6636.	533584.	F.C.	74.1	0.0435
6:22:58	124.4	547.0	633.6	2253.4	2265.1	595.4	653.6	46.29	441.4	797.9	1156.7	61245.	533724.	N.B.	71.2	0.0443
6:49:48	111.9	545.8	625.5	2271.5	2283.1	590.3	654.8	46.33	440.9	782.5	1106.0	58926.	480158.	N.B.	61.6	0.0424
7:31:58	101.9	545.7	618.9	2282.0	2293.4	586.6	655.5	46.52	442.6	766.9	1061.1	6441.	436957.	F.C.	59.5	0.0445
8: 0:56	91.8	546.2	614.0	2259.9	2271.2	584.0	654.0	45.61	434.4	750.1	1013.2	6330.	393701.	F.C.	55.8	0.0458
8:23:50	81.7	546.4	607.5	2256.7	2267.7	580.5	653.8	45.44	433.0	730.6	962.9	6296.	350335.	F.C.	51.5	0.0470
8:46:21	71.4	546.6	600.7	2248.3	2259.3	576.8	653.3	45.29	431.6	711.4	913.7	6264.	306350.	F.C.	47.9	0.0495
9: 9:52	61.4	546.1	593.2	2253.9	2264.7	572.4	653.6	45.18	430.3	689.9	863.2	6234.	263167.	F.C.	42.7	0.0505
9:42: 8	51.0	546.4	586.3	2262.3	2273.0	568.7	654.2	44.76	426.4	668.7	811.2	6173.	218890.	F.C.	37.2	0.0522
10: 4:17	40.8	546.2	579.3	2266.2	2276.9	564.7	654.4	43.68	416.0	645.8	759.7	6038.	174969.	F.C.	30.2	0.0522
10:26:10	30.7	546.4	571.3	2248.7	2259.4	560.3	653.3	43.83	417.6	623.8	707.9	6040.	131848.	F.C.	24.9	0.0564

Table C.2. (continued)

TIME	NOMINAL POWER (KW)	BUNDLE INLET TEMP. (F)	BUNDLE EXIT TEMP. (F)	UPPER PLENUM PRESS. (PSIA)	LOCAL BULK PRESS. (PSIA)	LOCAL BULK TEMP. (F)	LOCAL SAT. TEMP. (F)	CORE FLOW RATE (LB/SEC)	CORE FLOW RATE (GPM)	SHEATH T/C READING (F)	MIDDLE T/C READING (F)	SURFACE H.T. COEFF.	SURFACE HEAT FLUX	H.T. MODE	DEL-T GAP (F)	GAP (MILS)
CALIBRATION RUN NUMBER 4.1 JUNE 17																
13:41: 8	30.7	401.8	424.9	2235.9	2249.3	414.7	652.6	56.51	467.6	478.4	566.7	6685.	131844.	F.C.	26.2	0.0520
14:36:24	61.3	504.6	550.5	2292.5	2304.7	530.2	656.2	50.88	460.9	646.8	825.6	6684.	262905.	F.C.	44.0	0.0503
15: 7:57	92.0	531.3	599.0	2297.1	2309.1	569.1	656.4	47.90	447.4	735.8	1006.5	6517.	394848.	F.C.	57.7	0.0468
CALIBRATION RUN NUMBER 4.2 JUNE 18																
9:12:26	30.7	400.2	424.1	2283.4	2296.1	413.5	655.6	54.58	450.9	476.5	563.4	6493.	131554.	F.C.	24.9	0.0497
9:53:33	61.4	457.0	504.8	2266.7	2278.8	483.7	654.5	51.48	445.2	598.6	775.4	6551.	263530.	F.C.	40.6	0.0445
10:27:42	92.1	500.5	569.2	2214.3	2226.1	538.8	651.1	49.95	450.8	705.0	973.4	6622.	395092.	F.C.	57.4	0.0455
11: 5:15	112.3	547.2	625.4	2240.4	2252.1	590.9	652.8	47.10	449.3	773.7	1100.7	57577.	481602.	N.B.	54.3	0.0372
11:40:33	124.3	547.4	632.8	2274.9	2286.2	595.1	655.0	47.06	448.8	793.7	1155.2	62251.	533240.	N.B.	65.8	0.0410
CALIBRATION RUN NUMBER 5.1 JULY 8																
9:51:54	30.8	405.4	431.3	2265.8	2279.1	419.9	654.5	50.36	417.8	491.2	580.0	6125.	132075.	F.C.	31.9	0.0641
10:41:25	61.3	422.4	472.1	2280.3	2293.2	450.1	655.5	51.26	430.7	580.5	756.5	6371.	263003.	F.C.	54.7	0.0588
11:35:17	92.0	455.4	527.2	2232.1	2244.9	495.5	652.3	50.86	439.3	677.0	947.9	6540.	394430.	F.C.	71.4	0.0549
11:41: 1	91.9	456.6	528.4	2256.5	2269.3	496.7	653.9	50.71	438.4	679.4	948.5	6529.	394057.	F.C.	72.7	0.0561
13:10: 5	124.3	548.8	635.6	2302.8	2314.4	597.2	656.8	45.92	438.6	817.2	1180.0	63654.	533146.	N.B.	88.0	0.0553
CALIBRATION RUN NUMBER 6.1 AUG. 4																
9:59:10	30.8	398.8	425.1	2284.4	2297.5	413.5	655.7	49.63	409.6	482.0	572.9	6017.	131948.	F.C.	28.8	0.0574
11: 5: 4	62.0	499.1	547.6	2281.6	2293.7	526.2	655.5	48.82	439.7	653.0	833.3	6451.	266125.	F.C.	51.9	0.0588
11:39:36	91.9	497.8	568.0	2284.2	2296.6	537.0	655.7	49.14	441.9	717.9	990.8	6526.	394015.	F.C.	71.6	0.0570
12:13:36	124.2	545.5	632.0	2237.1	2249.1	593.8	652.6	46.56	443.1	814.6	1179.9	60418.	532758.	N.B.	89.1	0.0559
13:19: 7	124.1	546.9	634.0	2291.7	2303.2	595.5	656.1	46.04	438.7	815.4	1178.7	63045.	532344.	N.B.	86.9	0.0547
CALIBRATION RUN NUMBER 7.1 AUG. 19																
16:44:27	30.6	401.1	426.6	2211.3	2224.3	415.4	651.0	51.12	422.8	484.5	574.5	6174.	131399.	F.C.	30.1	0.0603
17:55:35	51.0	481.6	522.4	2263.7	2275.4	504.4	654.3	48.91	432.8	610.2	760.3	6375.	218870.	F.C.	43.4	0.0576
14:53:30	81.5	466.3	524.9	2265.4	2274.1	499.0	654.2	52.65	459.2	666.8	907.3	6739.	349525.	F.C.	71.6	0.0618
15:17: 6	81.1	510.8	568.2	2308.9	2316.9	542.8	656.9	50.44	460.0	708.5	949.0	6686.	347818.	F.C.	70.4	0.0632
15:27:52	81.0	530.4	586.9	2304.7	2311.8	561.9	656.6	49.21	459.1	726.8	966.6	6630.	347375.	F.C.	69.6	0.0636
15:36:42	80.9	545.3	601.2	2225.4	2231.9	576.5	651.5	47.71	454.1	741.1	980.7	6531.	347080.	F.C.	68.9	0.0636
CALIBRATION RUN NUMBER 12.1 JAN. 27																
11:20:34	30.7	400.2	425.2	2206.5	2217.3	414.2	650.6	50.08	414.0	489.9	580.7	6067.	131837.	F.C.	36.2	0.0726
11:44:22	51.0	409.2	449.0	2193.8	2204.3	431.4	649.7	51.80	431.1	549.2	699.4	6329.	218751.	F.C.	54.2	0.0684
12: 8:16	81.6	404.3	467.4	2231.4	2241.9	439.5	652.1	51.93	430.5	614.9	856.2	6384.	350065.	F.C.	75.1	0.0618
12:33: 5	81.6	460.5	523.9	2282.5	2291.6	495.9	655.3	49.08	425.7	669.0	911.0	6357.	349881.	F.C.	73.8	0.0636
12:59:52	81.2	525.2	585.0	2308.9	2317.2	558.6	656.9	47.22	437.8	727.2	969.3	6402.	348271.	F.C.	71.2	0.0647
13: 9:19	81.8	543.5	600.8	2274.2	2282.5	575.5	654.8	47.33	449.1	743.5	987.4	6483.	350892.	F.C.	70.8	0.0647
19: 2:42	101.4	538.6	611.4	2219.5	2229.5	579.3	651.3	47.67	449.9	772.5	1075.7	6539.	434848.	F.C.	73.9	0.0555
20: 6:22	124.5	546.7	633.0	2257.1	2266.6	594.9	653.7	46.55	443.7	811.0	1178.6	61336.	534042.	N.B.	84.3	0.0528
CALIBRATION RUN NUMBER 8.3 NOV. 5																
13:41:33	31.5	416.8	441.9	2247.9	2257.8	430.8	653.2	47.37	396.3	499.6	592.8	5888.	135008.	F.C.	27.8	0.0551
14: 9: 0	52.5	410.1	450.7	2253.8	2263.9	432.8	653.6	49.03	408.1	541.8	697.6	6062.	225220.	F.C.	42.1	0.0514
14:29:59	73.9	412.4	468.3	2257.8	2268.1	443.6	653.8	49.54	413.1	590.9	811.3	6168.	317058.	F.C.	54.6	0.0491
14:49:41	84.0	413.2	476.6	2246.3	2257.1	448.6	653.1	49.67	414.5	613.2	864.6	6206.	360533.	F.C.	59.8	0.0480
14:53:35	95.0	413.6	484.7	2246.8	2257.4	453.3	653.1	49.94	416.9	636.6	922.1	6256.	407510.	F.C.	65.8	0.0474
15: 9:45	105.4	411.2	489.5	2248.4	2259.1	454.9	653.3	50.38	419.8	656.3	973.5	6307.	452095.	F.C.	72.0	0.0474
15:44:12	104.6	534.2	605.6	2251.7	2260.1	574.1	653.3	46.15	432.9	766.3	1080.3	6348.	448761.	F.C.	67.0	0.0487
16: 5: 0	109.1	541.6	614.8	2300.4	2308.7	582.5	656.4	45.95	434.8	780.0	1108.0	6359.	468055.	F.C.	67.2	0.0472
16:18:35	113.8	539.8	615.7	2278.8	2286.7	582.2	655.0	46.16	435.9	786.9	1127.8	6381.	488046.	F.C.	69.3	0.0470
17: 5: 4	124.3	546.8	635.1	2293.5	2299.8	596.1	655.9	41.71	397.5	810.1	1178.3	62918.	533163.	N.B.	81.6	0.0512
CALIBRATION RUN NUMBER 9.1 NOV. 18																
12:51:18	30.6	412.2	437.0	2254.1	2265.2	426.0	653.6	48.27	402.5	497.0	585.0	5953.	131390.	F.C.	31.2	0.0634
13:29:59	31.1	408.4	433.1	2245.1	2256.2	422.2	653.1	48.57	403.9	494.6	584.6	5962.	133578.	F.C.	32.0	0.0638
13:52:35	51.5	413.3	453.1	2226.7	2238.2	435.5	651.9	49.43	412.6	548.1	697.1	6117.	221107.	F.C.	47.2	0.0589
14:16:33	71.4	412.3	467.1	2286.6	2298.1	442.9	655.8	50.06	417.4	591.3	798.6	6216.	306211.	F.C.	59.3	0.0551
14:38:36	81.5	413.0	475.1	2276.2	2287.2	447.7	655.1	50.16	418.4	614.1	852.5	6249.	349656.	F.C.	65.2	0.0539
14:47:36	91.6	416.9	486.1	2253.6	2264.4	455.6	653.6	50.25	420.5	638.4	908.8	6298.	393126.	F.C.	70.0	0.0524
15: 2:29	102.0	412.3	491.9	2283.4	2293.5	456.7	655.5	48.52	404.5	660.0	963.1	6128.	437585.	F.C.	76.0	0.0518
15:21:34	101.6	464.5	542.0	2315.8	2324.9	507.8	657.4	47.22	411.0	708.5	1010.4	6210.	435817.	F.C.	76.2	0.0543
15:38:27	101.4	509.8	584.3	2315.0	2324.0	551.4	657.4	45.81	417.3	749.5	1049.9	6222.	434769.	F.C.	74.8	0.0553
15:53:39	101.2	547.4	619.0	2331.8	2340.0	587.3	658.3	43.46	414.1	782.8	1082.0	6100.	434264.	F.C.	71.8	0.0545
CALIBRATION RUN NUMBER 10.1 DEC. 8																
11:25:18	31.3	406.3	437.8	2297.2	2301.5	423.9	656.0	37.82	313.9	502.3	592.2	4887.	134445.	F.C.	32.9	0.0655
11:47:24	41.5	415.9	457.2	2298.3	2302.4	438.9	656.0	38.27	320.0	538.7	659.5	4998.	178047.	F.C.	40.6	0.0626
12: 9:36	61.6	405.0	464.8	2286.3	2291.0	438.4	655.3	39.44	327.1	579.1	758.8	5118.	264380.	F.C.	54.5	0.0582
12:39: 8	82.1	406.5	486.4	2294.1	2298.9	451.1	655.8	38.86	322.8	631.4	873.0	5111.	352067.	F.C.	66.2	0.0551
13:27: 2	81.7	523.5	595.0	2267.6	2270.9	563.4	654.0	37.46	346.8	738.4	981.2	5336.	350439.	F.C.	66.3	0.0605
13:32:52	81.6	534.1	604.6	2259.5	2262.2	573.5	653.5	36.97	346.8	747.7	990.3	5314.	350105.	F.C.	65.5	0.0603
13:43:16	81.5	537.7	611.5	2314.0	2316.2	578.9	656.9	34.84	328.1	755.2	997.2	5084.	349788.	F.C.	64.9	0.0603
13:46: 3	81.5	541.2	615.0	2318.4	2320.3	582.4	657.1	34.53	326.6	758.6	1000.8	5059.	349788.	F.C.	64.5	0.0599
13:52:47	81.5	546.0	619.9	2304.9	2306.6	587.3	656.3	33.83	322.0	763.4	1004.8	4994.	349650.	F.C.	63.7	0.0595
CALIBRATION RUN NUMBER 11.1 JAN. 13																
13:49:36	30.8	428.6	451.9	2258.0	2266.6	441.6	653.7	52.92	446.9	515.1	603.7	6492.	132196.	F.C.	35.5	0.0726
14:12:27	51.3	425.0	463.2	2307.4	2316.4	446.3	656.9	53.48	450.2	560.2	709.6	6570.	220040.	F.C.	51.5	0.0653
14:34:40	81.7	426.3	485.9	2291.7	2301.4	459.6	656.0	54.05	455.6	629.6	870.2	6696.	350560.	F.C.	72.5	0.0605

Table C.2. (continued)

TIME	NOMINAL POWER (KW)	BUNDLE INLET TEMP. (F)	BUNDLE EXIT TEMP. (F)	UPPER PLENUM PRESS. (PSIA)	LOCAL BULK PRESS. (PSIA)	LOCAL BULK TEMP. (F)	LOCAL SAT. TEMP. (F)	CORE FLOW RATE (LB/SEC)	CORE FLOW RATE (GPM)	SHEATH T/C READING (F)	MIDDLE T/C READING (F)	SURFACE H.T. COEFF.	SURFACE HEAT FLUX	H.T. MODE	DEL-T GAP (F)	GAP (MILS)
CALIBRATION RUN NUMBER 13.1 FEB. 10																
10:33:25	30.8	410.8	435.8	2282.0	2294.1	424.8	655.5	47.99	399.7	498.2	589.7	5918.	132192.	F.C.	33.3	0.0672
10:54: 5	51.4	419.9	460.5	2266.3	2278.3	442.6	654.5	48.42	406.1	556.4	709.9	6051.	220294.	F.C.	48.4	0.0611
11:14: 1	61.0	426.6	474.1	2254.2	2266.2	453.1	653.7	48.93	412.5	584.5	766.6	6152.	261705.	F.C.	54.7	0.0593
11:25:44	71.3	436.9	491.8	2249.6	2261.6	467.5	653.4	48.81	415.0	617.8	831.3	6208.	305972.	F.C.	61.5	0.0586
11:40:22	81.7	446.7	509.2	2238.6	2250.3	481.6	652.7	48.34	414.4	649.9	895.2	6221.	350466.	F.C.	67.3	0.0572
12:15:12	81.3	501.5	564.1	2227.7	2238.0	536.4	651.9	44.76	404.4	703.5	948.6	6056.	348557.	F.C.	66.1	0.0591
13:47: 8	81.6	550.8	633.1	2265.6	2270.1	596.7	654.0	29.31	281.0	769.7	1012.4	49782.	349838.	N.B.	66.4	0.0622
CALIBRATION RUN NUMBER 14.1 MAR. 9																
11:17:50	30.9	422.6	451.2	2269.0	2273.4	438.6	654.2	41.21	346.4	519.2	607.5	5302.	132615.	F.C.	38.0	0.0776
11:40: 0	51.2	420.1	468.0	2265.7	2270.2	446.9	654.0	40.79	342.2	569.7	718.9	5294.	219438.	F.C.	52.6	0.0674
12: 2:29	81.7	423.5	499.7	2261.3	2265.7	466.1	653.7	40.25	338.5	648.2	891.0	5314.	350279.	F.C.	71.4	0.0605
12:25: 4	81.4	460.4	532.7	2251.6	2255.7	500.7	653.0	40.78	353.8	679.4	921.9	5500.	349212.	F.C.	71.2	0.0620
12:49:10	81.1	500.6	571.8	2306.2	2310.4	540.3	656.5	39.13	353.0	717.6	959.6	5450.	348015.	F.C.	70.2	0.0634
13:18:51	81.0	548.0	616.2	2314.3	2317.4	586.1	657.0	36.73	350.5	761.2	1004.1	5328.	347386.	F.C.	67.7	0.0634
13:34:23	81.5	546.1	619.0	2320.9	2322.4	586.8	657.3	34.46	328.0	765.8	1007.3	5066.	349549.	F.C.	67.6	0.0632
CALIBRATION RUN NUMBER 15.1 MAR. 23																
10:32: 1	30.6	402.2	423.5	2307.0	2324.4	414.1	657.4	56.43	466.9	485.2	574.5	6673.	131433.	F.C.	33.6	0.0674
10:55:54	51.2	403.6	437.1	2306.3	2324.0	422.3	657.4	59.51	492.8	533.6	683.3	7014.	219729.	F.C.	50.7	0.0628
11:40: 2	81.5	479.7	531.2	2306.4	2322.2	508.4	657.3	57.05	503.7	670.8	911.1	7228.	349536.	F.C.	69.8	0.0606
12:21:39	101.9	534.0	595.8	2277.8	2291.5	568.5	655.3	53.51	501.5	762.2	1064.9	7120.	437291.	F.C.	78.8	0.0584
13: 8:45	101.9	544.2	602.8	2346.1	2361.4	576.9	659.6	55.30	524.6	767.9	1069.4	7345.	437264.	F.C.	78.1	0.0580
CALIBRATION RUN NUMBER 16.1 APR. 27																
12:28:55	30.7	420.0	442.7	2199.9	2211.7	432.7	650.2	52.25	438.4	508.0	595.6	6379.	131703.	F.C.	37.0	0.0755
12:55:12	51.2	418.6	456.4	2215.8	2227.4	439.7	651.2	52.00	435.8	554.8	703.8	6392.	219723.	F.C.	51.7	0.0653
13:21:11	87.8	420.8	481.3	2177.8	2189.4	454.6	648.7	52.22	438.5	635.1	896.4	6491.	376463.	F.C.	74.0	0.0576
14: 0:52	102.0	484.3	556.7	2194.4	2204.5	524.7	649.7	49.60	440.4	725.0	1031.7	6529.	437417.	F.C.	78.9	0.0566
14:42:58	101.8	544.5	603.6	2333.6	2347.5	577.5	658.8	54.66	518.9	768.0	1071.9	7280.	436537.	F.C.	77.3	0.0576
CALIBRATION RUN NUMBER 17.1 MAY 26																
11:23: 5	30.7	423.5	448.8	2196.3	2205.9	437.6	649.8	46.56	391.7	515.6	603.7	5841.	131802.	F.C.	37.9	0.0776
11:45:13	51.1	422.8	464.1	2311.7	2321.8	445.8	657.2	47.37	398.0	564.2	711.1	5960.	219082.	F.C.	52.8	0.0674
12: 9:15	89.4	449.2	519.1	2202.8	2212.1	488.2	650.2	47.04	404.2	674.3	939.2	6116.	383424.	F.C.	74.8	0.0591
12:35:46	101.8	497.9	589.6	2235.6	2240.5	549.1	652.1	37.49	337.4	762.7	1069.5	5295.	436862.	F.C.	77.7	0.0576
12:52:17	101.8	528.8	620.2	2267.7	2271.4	579.8	654.0	34.88	324.9	791.4	1095.8	55673.	436668.	N.B.	76.9	0.0584
13:10:40	101.7	545.8	639.6	2295.0	2297.7	598.1	655.7	31.89	303.5	802.9	1101.2	56827.	436304.	N.B.	86.9	0.0663
13:13:25	101.8	545.7	639.2	2282.5	2285.3	597.9	654.9	32.01	304.7	802.5	1100.8	56280.	436471.	N.B.	87.2	0.0665
CALIBRATION RUN NUMBER 18.1 JUNE 15																
16:53:51	30.6	424.2	450.3	2271.3	2281.6	438.8	654.7	45.20	380.4	515.6	604.7	5709.	131138.	F.C.	36.4	0.0751
17:17:18	51.0	474.7	515.7	2262.7	2272.0	497.6	654.1	45.24	397.7	613.9	763.7	5964.	218718.	F.C.	51.5	0.0688
17:36:32	81.7	517.7	579.6	2258.1	2266.5	552.3	653.7	44.31	407.4	723.7	969.1	6063.	350579.	F.C.	70.3	0.0634
17:54:39	81.5	544.9	606.4	2221.2	2228.0	579.3	651.2	41.58	395.6	751.0	996.1	5861.	349470.	F.C.	69.4	0.0641
18: 7:50	81.5	545.3	606.8	2231.8	2238.2	579.6	651.9	41.55	395.5	750.9	996.1	5859.	349404.	F.C.	68.9	0.0638
CALIBRATION RUN NUMBER 19.1 JUNE 29																
12: 8:50	30.6	418.4	445.7	2218.4	2225.4	433.6	651.1	43.50	364.5	511.0	601.2	5513.	131172.	F.C.	36.0	0.0740
12:31:59	51.0	467.3	511.0	2245.3	2251.6	491.7	652.8	42.79	373.6	610.4	760.5	5682.	218783.	F.C.	52.1	0.0693
13: 6:26	81.7	489.2	555.1	2281.1	2287.8	526.0	655.1	43.58	388.5	699.0	944.3	5890.	350318.	F.C.	69.8	0.0616
13:31:46	101.8	542.1	617.9	2299.4	2305.1	584.4	656.2	41.70	394.9	786.1	1092.5	5891.	436505.	F.C.	74.9	0.0566
13:40:39	101.8	546.0	622.1	2322.6	2328.6	588.5	657.6	41.02	390.3	790.4	1095.9	5830.	436780.	F.C.	74.3	0.0563
CALIBRATION RUN NUMBER 20.1 AUG. 22																
11:41:52	30.5	449.1	470.8	2246.1	2256.8	461.3	653.1	53.17	456.8	538.3	624.6	6617.	130825.	F.C.	40.0	0.0844
12: 5:46	51.9	474.6	503.0	2308.9	2326.6	490.5	657.5	65.81	578.1	606.7	753.6	8009.	222753.	F.C.	59.7	0.0774
12:35:35	81.6	523.0	568.9	2268.9	2284.4	548.6	654.9	60.03	555.3	715.7	954.4	7713.	349818.	F.C.	78.2	0.0699
13: 1:53	101.8	543.7	602.1	2369.7	2383.1	576.3	661.0	55.71	528.0	776.1	1075.1	7384.	436668.	F.C.	87.5	0.0653
13:21:45	101.8	544.4	603.1	2346.2	2359.3	577.2	659.5	55.20	523.9	776.8	1075.4	7336.	436671.	F.C.	86.9	0.0649
CALIBRATION RUN NUMBER 21.1 SEP. 21																
11:49:40	30.9	438.5	465.2	2213.3	2224.1	453.4	651.0	43.83	373.3	536.0	627.7	5637.	132524.	F.C.	41.5	0.0861
12:10:45	51.4	469.0	511.3	2237.5	2247.5	492.6	652.5	43.93	384.2	617.0	769.8	5807.	220634.	F.C.	58.0	0.0769
12:43:59	71.9	526.5	580.7	2310.1	2319.9	556.7	657.1	43.66	405.3	716.6	933.1	6006.	308631.	F.C.	70.3	0.0717
15:20:14	91.8	544.7	615.3	2287.1	2295.7	584.1	655.6	40.33	383.3	778.4	1054.0	5736.	393938.	F.C.	77.8	0.0649
15:22: 6	91.8	545.3	615.6	2269.6	2277.8	584.5	654.5	40.47	385.0	778.6	1054.2	5754.	393702.	F.C.	77.9	0.0649
CALIBRATION RUN NUMBER 22.1 OCT. 12																
11:48:40	31.1	438.5	463.5	2216.7	2224.9	452.5	651.0	45.95	391.3	531.1	625.6	5849.	133244.	F.C.	38.2	0.0786
12:17:55	80.7	483.3	542.2	2235.5	2243.2	516.2	652.2	47.88	424.5	690.0	933.1	6313.	345976.	F.C.	75.6	0.0670
12:29:23	101.9	509.3	584.0	2237.7	2243.8	551.0	652.3	45.98	418.9	758.9	1066.0	6241.	437269.	F.C.	84.2	0.0620
12:50:23	102.0	546.3	621.9	2308.1	2313.1	588.5	656.7	41.31	393.3	795.6	1103.8	5864.	437492.	F.C.	79.7	0.0605
13: 0:25	102.0	548.1	623.2	2307.4	2312.5	590.1	656.7	41.44	395.5	797.5	1104.9	57580.	437588.	N.B.	80.5	0.0611
CALIBRATION RUN NUMBER 23.1 NOV. 30																
11:22: 7	31.1	425.9	450.1	2267.7	2276.4	439.4	654.4	48.27	406.7	517.1	608.7	6020.	133572.	F.C.	37.7	0.0765
11:41:15	51.8	441.1	480.9	2298.0	2306.4	463.3	656.3	48.23	411.4	582.6	735.4	6129.	222288.	F.C.	54.0	0.0690
11:58:35	72.4	478.1	531.9	2256.1	2263.5	508.1	653.5	47.73	421.0	664.6	879.1	6266.	310757.	F.C.	67.5	0.0655
12:19:17	101.9	521.0	594.5	2235.0	2240.9	562.0	652.1	45.62	421.3	767.9	1072.3	6244.	436953.	F.C.	82.5	0.0613
12:38:44	101.7	548.9	623.6	2267.2	2271.1	590.6	654.0	41.39	395.7	796.2	1100.8	55642.	436358.	N.B.	81.7	0.0622
12:44:28	101.7	549.2	624.1	2262.6	2266.2	591.0	653.7	41.22	394.3	797.0	1101.3	55426.	436354.	N.B.	82.8	0.0630

Table C.2. (continued)

TIME	NOMINAL POWER (KW)	BUNDLE INLET TEMP. (F)	BUNDLE EXIT TEMP. (F)	UPPER PLENUM PRESS. (PSIA)	LOCAL BULK PRESS. (PSIA)	LOCAL BULK TEMP. (F)	LOCAL SAT. TEMP. (F)	CORE FLOW RATE (LB/SEC)	CORE FLOW RATE (GPM)	SHEATH T/C READING (F)	MIDDLE T/C READING (F)	SURFACE H.T. COEFF.	SURFACE HEAT FLUX	H.T. MODE	DEL-T GAP (F)	GAP (MILS)
CALIBRATION RUN NUMBER 23.2 DEC. 15																
10: 5:18	31.0	429.5	454.8	2210.7	2218.4	443.6	650.6	46.02	389.1	520.4	615.5	5816.	132900.	F.C.	36.2	0.0742
10:27:17	61.5	471.1	518.8	2211.7	2218.8	497.7	650.7	46.86	410.7	634.2	819.3	6135.	263909.	F.C.	59.7	0.0670
10:39: 4	61.6	484.3	530.4	2225.9	2233.7	510.1	651.6	47.73	423.7	645.1	830.4	6275.	264070.	F.C.	59.3	0.0670
11: 9:20	102.1	542.0	614.6	2278.5	2284.0	582.5	654.9	43.85	415.3	788.0	1095.9	6127.	438096.	F.C.	81.0	0.0611
11:16:15	102.2	550.2	623.1	2290.3	2295.5	590.9	655.6	42.50	406.9	795.2	1103.4	56851.	438222.	N.B.	79.1	0.0599
11:23:26	102.1	549.5	622.7	2271.4	2276.4	590.4	654.4	42.29	404.6	795.8	1103.6	55990.	438145.	N.B.	80.8	0.0613
CALIBRATION RUN NUMBER 23.3 JAN. 19																
15: 7: 0	31.0	476.6	499.9	2113.6	2119.4	489.6	644.1	47.53	419.2	565.6	656.9	6174.	132852.	F.C.	37.2	0.0792
15:28:51	51.9	513.9	551.3	2209.0	2215.0	534.8	650.4	47.20	432.4	650.5	804.7	6313.	222708.	F.C.	52.2	0.0707
15:48:34	82.4	531.4	589.9	2178.0	2182.7	564.1	648.3	45.42	425.0	736.5	983.4	6231.	353548.	F.C.	72.1	0.0651
16:13:41	101.8	551.0	622.6	2246.2	2250.2	591.0	652.7	43.10	413.4	794.8	1100.0	54749.	436747.	N.B.	81.4	0.0618
16:17:13	101.9	549.8	621.9	2276.5	2280.8	590.1	654.7	43.06	412.1	794.8	1100.1	6075.	437206.	F.C.	80.1	0.0607
CALIBRATION RUN NUMBER 24.1 FEB. 16																
10:42: 1	30.5	441.3	467.1	2255.8	2261.7	455.7	653.4	44.45	379.3	529.9	621.3	5709.	130739.	F.C.	33.9	0.0713
11: 8:40	51.2	492.2	533.5	2252.7	2257.7	515.3	653.2	43.97	393.3	629.9	782.0	5895.	219567.	F.C.	49.4	0.0667
11:28:20	72.1	512.4	568.4	2276.5	2280.7	543.7	654.7	43.55	397.9	697.2	913.2	5949.	309283.	F.C.	63.0	0.0634
12:29: 8	102.0	544.4	618.8	2192.3	2195.2	585.9	649.1	42.04	400.0	789.0	1097.6	52466.	437687.	N.B.	78.7	0.0593
12:50:11	102.0	545.9	619.7	2186.8	2190.0	587.1	648.8	42.13	401.6	790.2	1098.6	52247.	437597.	N.B.	80.2	0.0605

Table C.3. Example of ORTCAL — Part I output for thermocouple TE-301DJ

TIME	NOMINAL POWER (KW)	BUNDLE INLET TEMP. (F)	BUNDLE EXIT TEMP. (F)	UPPER PLENUM PRESS. (PSIA)	LOCAL BULK PRESS. (PSIA)	LOCAL BULK TEMP. (F)	LOCAL SAT. TEMP. (F)	CORE FLOW RATE (LB/SEC)	CORE FLOW RATE (GPM)	SHEATH T/C READING (F)	MIDDLE T/C READING (F)	SURFACE H.T. COEFF.	SURFACE HEAT FLUX	H.T. MODE	DEL-T GAP (F)	GAP (MILS)
CALIBRATION RUN NUMBER 1.1 MAY 4																
23:36:56	30.0	405.4	429.8	2223.7	2235.5	425.1	651.7	53.36	442.7	465.3	538.0	6445.	100764.	F.C.	11.0	0.0285
23:44:18	39.7	403.1	434.7	2218.2	2230.0	428.6	651.4	54.49	451.3	481.0	577.0	6574.	133079.	F.C.	14.2	0.0281
23:53:20	40.2	401.9	433.3	2216.7	2228.3	427.2	651.3	55.39	458.4	480.4	577.4	6653.	134708.	F.C.	14.8	0.0291
0:29: 6	50.1	406.6	445.2	2212.9	2224.5	437.8	651.0	55.83	463.6	503.4	623.4	6755.	168028.	F.C.	18.3	0.0293
CALIBRATION RUN NUMBER 1.2 MAY 5																
14:31:56	40.3	306.2	336.9	2234.9	2248.9	331.0	652.6	59.50	463.4	390.5	486.1	6336.	135238.	F.C.	19.1	0.0341
14:50:53	50.2	350.6	389.9	2209.3	2222.7	382.3	650.9	56.80	454.0	450.8	571.5	6500.	168439.	F.C.	19.5	0.0297
15:39:21	50.0	401.7	439.8	2293.9	2307.0	432.5	656.3	56.63	468.3	501.2	622.2	6801.	167862.	F.C.	21.6	0.0345
15:56:45	60.3	405.0	451.1	2288.9	2302.3	442.2	656.0	56.24	466.3	524.2	670.7	6819.	202097.	F.C.	25.5	0.0345
16:18: 7	70.2	400.4	452.0	2286.4	2300.0	442.0	655.9	58.54	483.7	540.0	710.0	7040.	235351.	F.C.	33.4	0.0391
16:50:43	80.0	401.5	464.0	2222.4	2234.0	451.9	651.6	54.73	452.7	571.7	765.5	6724.	268465.	F.C.	44.7	0.0470
17:13:10	90.3	402.6	473.8	2192.2	2203.8	460.1	649.7	53.92	446.5	598.7	820.2	6686.	302718.	F.C.	54.1	0.0512
CALIBRATION RUN NUMBER 1.3 MAY 5																
19:21:26	100.6	404.2	480.4	2210.0	2221.9	465.7	650.9	55.88	463.3	635.5	882.1	6909.	337585.	F.C.	77.5	0.0672
19:53:59	110.2	400.7	483.6	2251.1	2263.2	467.6	653.5	56.23	464.8	666.2	933.2	6952.	369598.	F.C.	98.2	0.0792
20:22:51	122.3	401.2	498.8	2217.3	2227.8	480.0	651.2	52.66	435.6	716.9	1007.1	6656.	410057.	F.C.	123.5	0.0927
21: 4:19	122.4	440.3	536.8	2216.2	2226.0	518.2	651.1	51.32	437.6	752.1	1042.5	6683.	410410.	F.C.	121.5	0.0936
CALIBRATION RUN NUMBER 1.4 MAY 6																
12:35:24	90.4	291.6	356.2	2239.8	2254.3	343.8	652.9	63.00	486.8	498.1	712.8	6747.	303290.	F.C.	67.9	0.0584
12:57:41	90.3	293.3	357.0	2225.6	2240.2	344.7	652.0	63.83	493.6	498.3	712.9	6827.	303002.	F.C.	67.8	0.0584
13:35:46	90.3	306.2	370.6	2275.5	2289.8	358.2	655.2	62.81	489.0	509.3	724.8	6853.	302752.	F.C.	65.8	0.0572
13:48:44	90.1	322.2	386.5	2258.1	2272.3	374.1	654.1	62.59	491.7	522.8	739.1	6961.	302373.	F.C.	64.5	0.0568
CALIBRATION RUN NUMBER 2.1 MAY 19																
4: 6: 2	30.0	400.7	426.1	2259.4	2267.9	421.2	653.8	49.97	413.1	464.5	536.5	6094.	100638.	F.C.	13.1	0.0339
4:28:22	40.1	400.8	434.0	2302.9	2311.5	427.6	656.6	51.36	424.5	485.2	580.9	6263.	134590.	F.C.	18.1	0.0356
5: 8:30	50.2	400.1	441.1	2250.5	2259.0	433.2	653.3	51.56	426.0	504.6	624.1	6314.	168456.	F.C.	22.2	0.0354
5:37:54	60.4	400.7	450.0	2303.4	2312.0	440.5	656.6	51.41	424.8	525.3	668.3	6336.	202569.	F.C.	25.9	0.0351
6: 0: 0	70.4	400.7	457.4	2231.6	2239.7	446.5	652.0	51.90	429.1	545.0	711.2	6417.	236087.	F.C.	30.7	0.0360
6:45:11	80.5	400.2	464.5	2219.3	2227.1	452.1	651.2	52.14	431.0	564.4	753.5	6470.	270079.	F.C.	35.1	0.0366
7: 5:50	90.4	400.8	473.0	2234.6	2242.8	459.1	652.2	51.95	429.5	587.3	800.2	6484.	303195.	F.C.	42.1	0.0397
7:35:54	100.2	401.0	480.2	2201.9	2209.7	465.0	650.1	52.40	433.4	616.9	855.9	6559.	335973.	F.C.	57.4	0.0497
8:37: 4	110.2	401.4	488.1	2220.4	2228.2	471.4	651.3	52.49	434.2	660.0	924.8	6598.	369724.	F.C.	85.4	0.0688
CALIBRATION RUN NUMBER 2.2 MAY 19																
22:42:55	30.1	400.0	425.6	2231.1	2239.8	420.7	652.0	49.82	411.7	465.9	539.2	6076.	101090.	F.C.	14.9	0.0385
23:10:47	40.1	400.3	433.3	2218.3	2227.0	427.0	651.2	51.48	425.5	486.9	583.4	6273.	134612.	F.C.	20.4	0.0401
23:32:51	50.3	400.7	441.6	2206.6	2214.8	433.7	650.4	51.73	427.7	507.7	628.2	6334.	168579.	F.C.	24.9	0.0397
23:57:45	60.3	400.2	449.1	2198.9	2207.1	439.7	649.9	51.81	428.3	527.6	672.5	6374.	202310.	F.C.	29.4	0.0397
0:31: 6	70.2	399.8	457.1	2220.8	2229.2	446.0	651.3	51.39	424.6	548.2	715.3	6365.	235432.	F.C.	34.2	0.0403
0:55:49	80.4	400.6	465.6	2250.4	2258.8	453.1	653.2	51.56	426.2	569.6	761.1	6417.	269792.	F.C.	39.2	0.0410
1:23: 3	90.2	400.4	472.5	2236.2	2244.3	458.6	652.3	52.10	430.6	590.6	805.1	6497.	302644.	F.C.	46.1	0.0435
2:30:44	100.3	400.6	480.6	2293.1	2302.0	465.2	656.0	51.97	429.5	613.8	852.6	6515.	336575.	F.C.	53.6	0.0462
2:55:20	110.3	400.9	488.4	2256.6	2265.0	471.5	653.6	52.09	430.7	637.2	900.5	6558.	370108.	F.C.	61.8	0.0493
3:19:32	122.3	400.3	496.0	2247.9	2256.4	477.6	653.1	52.60	434.7	666.4	959.3	6638.	410060.	F.C.	74.9	0.0549
4:35:52	122.2	449.5	545.2	2275.0	2282.6	526.8	654.8	50.06	430.0	713.2	1009.6	6584.	409759.	F.C.	73.2	0.0559
7: 5:39	122.5	499.2	591.8	2280.9	2287.8	574.0	655.1	48.15	433.7	743.5	1027.1	6565.	410918.	F.C.	56.6	0.0443
8:41: 8	100.3	544.1	618.9	2324.3	2329.7	604.5	657.7	44.92	426.4	738.4	968.8	6373.	336466.	F.C.	40.2	0.0385
9:19:59	90.0	544.5	612.7	2321.5	2327.0	599.5	657.5	44.81	425.5	725.2	934.5	6327.	301970.	F.C.	41.0	0.0435
9:43:39	80.1	544.9	606.3	2306.8	2312.0	594.5	656.6	44.58	423.6	711.8	901.1	6271.	268840.	F.C.	41.4	0.0487
10: 7:36	70.2	544.5	599.0	2297.7	2303.3	588.5	656.1	44.49	422.6	697.0	867.6	6222.	235512.	F.C.	41.5	0.0553
10:31:29	60.2	544.1	591.5	2311.1	2316.3	582.4	656.9	44.35	421.0	681.2	831.4	6180.	201946.	F.C.	41.0	0.0630
10:55:49	49.7	543.1	583.1	2302.7	2308.1	575.4	656.4	43.91	416.3	660.8	785.4	6103.	166619.	F.C.	37.3	0.0686
11:19:26	40.1	542.7	576.2	2319.4	2325.4	569.8	657.4	42.62	403.8	639.7	740.0	5938.	134499.	F.C.	30.3	0.0682
11:44:10	29.8	542.4	567.6	2307.5	2313.2	562.8	656.7	42.42	401.8	614.9	689.0	5891.	99864.	F.C.	22.5	0.0668
CALIBRATION RUN NUMBER 3.1 MAY 27																
1:14:13	30.2	401.6	426.6	2221.7	2231.1	421.8	651.5	52.14	431.4	467.3	540.8	6309.	101403.	F.C.	15.7	0.0405
1:36: 0	40.2	398.8	432.3	2235.6	2245.0	425.8	652.3	51.73	427.0	485.5	582.7	6291.	134756.	F.C.	20.1	0.0395
2: 2:32	50.3	402.3	443.2	2258.9	2268.4	435.3	653.9	52.72	436.3	509.3	629.6	6439.	168552.	F.C.	25.3	0.0405
2:23:56	60.3	402.2	450.9	2258.6	2268.1	441.5	653.8	53.02	438.8	529.8	673.2	6501.	202372.	F.C.	30.3	0.0410
2:45:31	70.5	401.9	458.9	2269.3	2278.8	447.9	654.5	52.69	435.9	550.4	717.6	6501.	236479.	F.C.	35.0	0.0410
3:11:21	80.4	403.9	468.5	2271.1	2280.7	456.1	654.6	52.78	437.3	572.0	763.0	6552.	269727.	F.C.	39.5	0.0414
3:32:41	90.4	403.8	475.8	2255.7	2265.4	462.0	653.7	53.17	440.5	594.8	810.1	6620.	303134.	F.C.	47.8	0.0453
4: 1:10	100.2	403.6	483.3	2269.5	2279.1	468.0	654.5	53.13	440.1	623.8	864.7	6646.	336137.	F.C.	62.0	0.0539
4:25:28	110.5	403.0	491.1	2268.9	2278.6	474.1	654.5	52.73	436.6	656.3	922.9	6635.	370663.	F.C.	79.0	0.0634
4:48:45	122.3	404.5	501.6	2249.4	2259.0	482.9	653.3	52.71	437.0	694.7	994.1	6674.	410250.	F.C.	98.4	0.0730
5:17: 8	122.2	450.6	545.6	2258.5	2267.8	527.4	653.8	51.46	442.6	747.1	1043.6	6734.	409938.	F.C.	108.1	0.0836
6:22:58	122.3	547.0	633.6	2253.4	2261.9	616.9	653.4	46.29	441.4	815.9	1118.9	53552.	410110.	N.B.	105.4	0.0859
6:49:48	110.2	545.8	625.5	2271.5	2280.0	610.1	654.6	46.33	440.9	802.2	1075.4	51561.	369489.	N.B.	95.9	0.0863
7:31:58	100.1	545.7	618.9	2282.0	2290.3	604.8	655.3	46.52	442.6	789.3	1038.1	6560.	335634.	F.C.	92.7	0.0911
8: 0:56	90.2	546.2	614.0	2259.9	2268.1	600.9	653.8	45.61	434.4	774.5	999.2	6432.	302558.	F.C.	89.7	0.0971
8:23:50	80.2	546.4	607.5	2256.7	2264.7	595.7	653.6	45.44	433.0	753.1	953.2	6380.	269122.	F.C.	82.2	0.0986
8:46:21	70.1	546.6	600.7	2248.3	2256.3	590.3	653.1	45.29	431.6	716.3	887.6	6329.	235237.	F.C.	59.9	0.0807
9: 9:52	60.4	546.1	593.2	2253.9	2261.8	584.1	653.4	45.18	430.3	690.4	837.3	6283.	202559.	F.C.	48.9	0.0753
9:42: 8	50.1	546.4	586.3	2262.3	2270.1	578.6	654.0	44.76	426.4	670.6	796.2	6213.	168157.	F.C.	43.9	0.0803
10: 4:17	40.2	546.2	579.3	2266.2	2274.0	572.9	654.2	43.68	416.0	648.2	747.7	6070.	134698.	F.C.	36.1	0.0815
10:26:10	30.2	546.4	571.3	2248.7	2256.5	566.5	653.1	43.83	417.6	623.1	698.2	6063.	101452.	F.C.	27.0	0.0796

Table C.3. (continued)

TIME	NOMINAL POWER (KW)	BUNDLE INLET TEMP. (F)	BUNDLE EXIT TEMP. (F)	UPPER PLENUM PRESS. (PSIA)	LOCAL BULK PRESS. (PSIA)	LOCAL BULK TEMP. (F)	LOCAL SAT. TEMP. (F)	CORE FLOW RATE (LB/SEC)	CORE FLOW RATE (GPM)	SHEATH T/C READING (F)	MIDDLE T/C READING (F)	SURFACE H.T. COEFF.	SURFACE HEAT FLUX	H.T. MODE	GEL-T GAP (F)	GAP (MILS)
CALIBRATION RUN NUMBER 4.1 JUNE 17																
13:41: 8	30.2	401.8	424.9	2235.9	2245.7	420.4	652.4	56.51	467.6	469.5	544.0	6720.	101253.	F.C.	20.3	0.0524
14:36:24	60.5	504.6	550.5	2292.5	2301.4	541.7	656.0	50.88	460.9	640.0	789.2	6729.	202997.	F.C.	42.5	0.0628
15: 7:57	90.6	531.3	599.0	2297.1	2305.8	585.9	656.2	47.90	447.4	720.7	937.3	6589.	304008.	F.C.	51.2	0.0536
CALIBRATION RUN NUMBER 4.2 JUNE 18																
9:12:26	30.3	400.2	424.1	2283.4	2292.7	419.5	655.4	54.58	450.9	469.7	544.1	6529.	101607.	F.C.	20.9	0.0537
9:53:33	60.3	457.0	504.8	2266.7	2275.5	495.6	654.3	51.48	445.2	591.9	738.0	6604.	202112.	F.C.	39.6	0.0564
10:27:42	90.3	500.5	569.2	2214.3	2222.9	555.9	650.9	49.95	450.8	698.7	920.4	6689.	302948.	F.C.	59.8	0.0615
11: 5:15	109.9	547.2	625.4	2240.4	2248.9	610.3	652.6	47.10	449.3	742.0	996.0	50251.	368662.	N.B.	37.2	0.0327
CALIBRATION RUN NUMBER 5.1 JULY 8																
9:51:54	30.2	405.4	431.3	2265.8	2275.5	426.3	654.3	50.36	417.8	474.5	549.8	6160.	101149.	F.C.	18.1	0.0470
10:41:25	60.3	422.4	472.1	2280.3	2289.7	462.5	655.2	51.26	430.7	558.0	703.6	6432.	202359.	F.C.	37.5	0.0518
11:35:17	90.4	455.4	527.2	2232.1	2241.4	513.3	652.1	50.86	439.3	651.1	867.0	6614.	303133.	F.C.	53.5	0.0530
11:41: 1	90.3	456.6	528.4	2256.5	2265.8	514.6	653.7	50.71	438.4	652.0	868.1	6604.	302873.	F.C.	53.2	0.0528
13:10: 5	122.1	548.8	635.6	2302.8	2311.3	618.9	656.6	45.92	438.6	769.5	1055.6	55655.	409626.	N.B.	56.0	0.0449
CALIBRATION RUN NUMBER 6.1 AUG. 4																
9:59:10	30.2	398.8	425.1	2284.4	2293.9	420.0	655.5	49.63	409.6	468.0	543.1	6053.	101253.	F.C.	17.6	0.0453
11: 5: 4	60.9	499.1	547.6	2281.6	2290.4	538.3	655.3	48.82	439.7	632.2	779.7	6497.	204196.	F.C.	36.6	0.0536
11:39:36	90.3	497.8	568.0	2284.2	2293.2	554.5	655.5	49.14	441.9	693.0	912.6	6594.	302763.	F.C.	54.9	0.0563
12:13:36	122.3	545.5	632.0	2237.1	2245.9	615.3	652.4	46.56	443.1	777.0	1080.3	52887.	410338.	N.B.	67.2	0.0539
13:19: 7	122.0	546.9	634.0	2291.7	2300.1	617.3	655.9	46.04	438.7	780.7	1083.3	55148.	409357.	N.B.	67.9	0.0547
CALIBRATION RUN NUMBER 7.1 AUG. 19																
16:44:27	30.5	401.1	426.6	2211.3	2220.8	421.7	650.8	51.12	422.8	470.5	546.5	6209.	102229.	F.C.	18.5	0.0474
17:55:35	50.1	481.6	522.4	2263.7	2272.2	514.6	654.1	48.91	432.8	591.5	714.3	6415.	168079.	F.C.	29.0	0.0501
19: 2:42	100.5	538.6	611.4	2219.5	2226.8	597.4	651.2	47.67	449.9	735.0	973.5	6644.	337092.	F.C.	45.7	0.0435
20: 6:22	122.4	546.7	633.0	2257.1	2264.0	616.4	653.6	46.55	443.7	762.0	1048.4	53674.	410613.	N.B.	51.0	0.0406
CALIBRATION RUN NUMBER 8.2 OCT. 9																
2:33:52	30.3	401.5	424.3	2286.9	2294.9	419.9	655.6	51.32	424.4	468.3	544.9	6217.	101744.	F.C.	18.2	0.0468
2:57:41	50.5	456.5	493.0	2310.4	2317.9	486.0	657.0	50.77	438.7	564.0	688.4	6489.	169390.	F.C.	29.9	0.0499
3:21:26	70.7	503.7	554.4	2313.4	2320.0	544.6	657.1	48.06	434.8	650.4	823.5	6439.	237066.	F.C.	39.1	0.0499
CALIBRATION RUN NUMBER 8.3 NOV. 5																
13:41:33	30.3	416.8	441.9	2247.9	2255.1	437.1	653.0	47.37	396.3	485.4	562.0	5919.	101495.	F.C.	17.6	0.0458
14: 9: 0	50.5	410.1	450.7	2253.8	2261.2	442.9	653.4	49.03	408.1	523.4	647.7	6113.	169375.	F.C.	30.3	0.0487
14:29:59	71.3	412.4	468.3	2257.8	2265.3	457.6	653.7	49.54	413.1	569.2	743.5	6236.	239151.	F.C.	42.0	0.0495
14:49:41	81.2	413.2	476.6	2246.3	2254.2	464.4	652.9	49.67	414.5	591.1	787.5	6281.	272246.	F.C.	48.0	0.0505
14:53:35	91.7	413.6	484.7	2246.8	2254.5	471.0	653.0	49.94	416.9	612.5	834.1	6339.	307600.	F.C.	53.3	0.0503
15: 9:45	101.7	411.2	489.5	2248.4	2256.2	474.4	653.1	50.38	419.8	630.0	875.3	6398.	341029.	F.C.	58.6	0.0505
15:44:12	101.0	534.2	605.6	2251.7	2257.9	591.8	653.2	46.15	432.9	733.8	977.7	6435.	338924.	F.C.	47.9	0.0455
16: 5: 0	105.3	541.6	614.8	2300.4	2306.4	600.7	656.3	45.95	434.8	743.2	996.2	6466.	353336.	F.C.	44.9	0.0410
16:18:35	109.9	539.8	615.7	2278.8	2284.6	601.1	654.9	46.16	435.9	747.2	1009.3	6493.	368470.	F.C.	44.6	0.0393
17: 5: 4	122.8	546.8	635.1	2293.5	2298.1	618.1	655.8	41.71	397.5	763.6	1053.0	55226.	411861.	N.B.	50.5	0.0401
CALIBRATION RUN NUMBER 9.1 NOV. 18																
12:51:18	30.5	412.2	437.0	2254.1	2262.2	432.2	653.5	48.27	402.5	482.8	561.2	5984.	102225.	F.C.	19.8	0.0512
13:29:59	30.4	408.4	433.1	2245.1	2253.2	428.4	652.9	48.57	403.9	478.1	557.2	5995.	102087.	F.C.	18.9	0.0489
13:52:35	50.4	413.3	453.1	2226.7	2235.1	445.4	651.7	49.43	412.6	526.5	653.9	6167.	169069.	F.C.	31.3	0.0505
14:16:33	71.3	412.3	467.1	2286.6	2295.0	456.5	655.6	50.06	417.4	569.7	746.9	6283.	239186.	F.C.	43.8	0.0516
14:38:36	81.1	413.0	475.1	2276.2	2284.2	463.2	654.9	50.16	418.4	590.9	791.1	6324.	272034.	F.C.	49.4	0.0520
14:47:36	90.7	416.9	486.1	2253.6	2261.5	472.8	653.4	50.25	420.5	614.4	837.4	6378.	304363.	F.C.	54.6	0.0522
15: 2:29	100.4	412.3	491.9	2283.4	2290.8	476.6	655.3	48.52	404.5	634.0	879.5	6217.	336854.	F.C.	60.2	0.0526
15:21:34	100.1	464.5	542.0	2315.8	2322.4	527.0	657.3	47.22	411.0	680.9	926.1	6284.	335662.	F.C.	58.3	0.0534
15:38:27	99.8	509.8	584.3	2315.0	2321.6	570.0	657.2	45.81	417.3	722.3	971.1	6292.	334804.	F.C.	57.9	0.0549
15:53:39	99.6	547.4	619.0	2331.8	2337.8	605.2	658.2	43.46	414.1	743.5	986.9	6211.	334220.	F.C.	43.9	0.0426
CALIBRATION RUN NUMBER 10.1 DEC. 8																
11:25:18	30.2	406.3	437.8	2297.2	2300.3	431.7	655.9	37.82	313.9	493.0	567.3	4920.	101131.	F.C.	27.1	0.0715
11:47:24	40.6	415.9	457.2	2298.3	2301.3	449.2	656.0	38.27	320.0	530.6	629.8	5040.	136149.	F.C.	36.3	0.0732
12: 9:36	60.6	405.0	464.8	2286.3	2289.8	453.3	655.2	39.44	327.1	570.8	717.9	5179.	203247.	F.C.	51.7	0.0717
12:39: 8	80.6	406.5	486.4	2294.1	2297.6	471.0	655.7	38.88	322.8	622.9	817.7	5188.	270368.	F.C.	64.9	0.0701
13:27: 2	80.6	523.5	595.0	2267.6	2270.0	581.2	654.0	37.46	346.8	722.6	919.4	5397.	270319.	F.C.	58.1	0.0684
13:32:52	80.6	534.1	604.6	2259.5	2261.5	591.0	653.4	36.97	346.8	729.0	925.2	5385.	270342.	F.C.	54.6	0.0645
13:43:16	80.5	537.7	611.5	2314.0	2315.6	597.3	656.8	34.84	328.1	734.9	930.7	5163.	270037.	F.C.	52.3	0.0622
13:46: 3	80.5	541.2	615.0	2318.4	2319.8	600.8	657.1	34.53	326.6	736.5	931.9	5144.	270100.	F.C.	50.3	0.0601
13:52:47	80.5	546.0	619.9	2304.9	2306.2	605.7	656.3	33.83	322.0	737.0	931.9	5089.	270115.	F.C.	45.3	0.0541
CALIBRATION RUN NUMBER 11.1 JAN. 13																
13:49:36	30.4	428.6	451.9	2258.0	2264.2	447.4	653.6	52.92	446.9	504.0	577.2	6522.	101814.	F.C.	27.4	0.0726
14:12:27	50.6	425.0	463.2	2307.4	2314.0	455.8	656.7	53.48	450.2	546.9	668.0	6619.	169821.	F.C.	43.0	0.0703
14:34:40	80.8	426.3	485.9	2291.7	2298.8	474.5	655.8	54.05	455.6	613.4	806.0	6768.	271008.	F.C.	63.8	0.0684
14:53:30	80.4	466.3	524.9	2265.4	2271.7	513.6	654.1	52.65	459.2	650.4	841.9	6801.	269781.	F.C.	62.8	0.0697
15:17: 6	80.1	510.8	568.2	2308.9	2314.8	557.1	656.8	50.44	460.0	691.3	882.5	6743.	268560.	F.C.	60.9	0.0703
15:27:52	79.9	530.4	586.9	2304.7	2309.9	576.0	656.5	49.21	459.1	709.3	900.4	6688.	268120.	F.C.	60.0	0.0703
15:36:42	79.9	545.3	601.2	2225.4	2230.1	590.5	651.4	47.71	454.1	722.8	914.3	6602.	267971.	F.C.	58.8	0.0697

Table C.3. (continued)

TIME	NOMINAL POWER (KW)	BUNDLE INLET TEMP. (F)	BUNDLE EXIT TEMP. (F)	UPPER PLENUM PRESS. (PSIA)	LOCAL BULK PRESS. (PSIA)	LOCAL BULK TEMP. (F)	LOCAL SAT. TEMP. (F)	CORE FLOW RATE (LB/SEC)	CORE FLOW RATE (GPM)	SHEATH T/C READING (F)	MIDDLE T/C READING (F)	SURFACE H.T. COEFF.	SURFACE HEAT FLUX	H.T. MODE	DEL-T GAP (F)	GAP (MILS)
CALIBRATION RUN NUMBER 12.1 JAN. 27																
11:20:34	30.1	400.2	425.2	2206.5	2214.3	420.4	650.4	50.08	414.0	473.9	552.0	6101.	101125.	F.C.	23.3	0.0603
11:44:22	50.5	409.2	449.0	2193.8	2201.4	441.3	649.5	51.80	431.1	527.8	655.8	6382.	169282.	F.C.	37.4	0.0603
12: 8:16	81.6	404.3	467.4	2231.4	2239.0	455.3	652.0	51.93	430.5	591.1	793.6	6464.	273573.	F.C.	57.8	0.0603
12:33: 5	81.6	460.5	523.9	2282.5	2289.1	511.7	655.2	49.08	425.7	646.1	848.2	6421.	273716.	F.C.	57.0	0.0622
12:59:52	81.4	525.2	585.0	2308.9	2314.9	573.5	656.8	47.22	437.8	704.9	906.2	6461.	272929.	F.C.	55.4	0.0638
13: 9:19	80.5	543.5	600.8	2274.2	2280.3	589.7	654.6	47.33	449.1	718.0	917.9	6546.	270081.	F.C.	53.8	0.0632
CALIBRATION RUN NUMBER 13.1 FEB. 10																
10:33:25	30.4	410.8	435.8	2282.0	2290.8	431.0	655.3	47.99	399.7	486.4	564.1	5950.	102025.	F.C.	24.6	0.0640
10:54: 5	50.7	419.9	460.5	2266.3	2275.0	452.7	654.3	48.42	406.1	541.9	670.0	6100.	170011.	F.C.	38.9	0.0632
11:14: 1	60.4	426.6	474.1	2254.2	2262.9	464.9	653.5	48.93	412.5	569.6	721.0	6208.	202471.	F.C.	45.6	0.0636
11:25:44	70.4	436.9	491.8	2249.6	2258.4	481.2	653.2	48.81	415.0	601.8	777.8	6268.	236245.	F.C.	52.3	0.0640
11:40:22	80.8	446.7	509.2	2238.6	2247.2	497.1	652.5	48.34	414.4	633.3	834.0	6286.	271083.	F.C.	58.3	0.0636
12:15:12	80.4	501.5	564.1	2227.7	2235.2	552.0	651.7	44.76	404.4	687.1	887.0	6113.	269825.	F.C.	57.3	0.0657
13:47: 8	80.7	550.8	633.1	2265.6	2268.9	617.2	653.9	29.31	281.0	739.0	935.1	43735.	270537.	N.B.	46.0	0.0549
CALIBRATION RUN NUMBER 14.1 MAR. 9																
11:17:50	30.4	422.6	451.2	2269.0	2272.2	445.7	654.1	41.21	346.4	505.6	580.0	5332.	101803.	F.C.	27.2	0.0720
11:40: 0	50.7	420.1	468.0	2265.7	2269.0	458.8	653.9	40.79	342.2	554.1	678.5	5343.	169965.	F.C.	41.2	0.0676
12: 2:29	80.8	423.5	499.7	2261.3	2264.5	485.1	653.6	40.25	338.5	631.4	828.0	5386.	270988.	F.C.	61.4	0.0667
12:25: 4	80.6	460.4	532.7	2251.6	2254.6	518.7	653.0	40.78	353.8	662.0	857.6	5562.	270234.	F.C.	60.5	0.0678
12:49:10	80.3	500.6	571.8	2306.2	2309.2	558.1	656.5	39.13	353.0	699.2	894.6	5507.	269432.	F.C.	58.7	0.0680
13:19:51	80.2	548.0	616.2	2314.3	2316.6	603.1	656.9	36.73	350.5	735.7	930.7	5418.	268939.	F.C.	50.2	0.0601
13:34:23	80.6	546.1	619.0	2320.9	2322.0	604.9	657.2	34.46	328.0	738.2	933.4	5159.	270491.	F.C.	47.9	0.0572
CALIBRATION RUN NUMBER 15.1 MAR. 23																
10:32: 1	30.4	402.2	423.5	2307.0	2319.7	419.4	657.1	56.43	466.9	468.7	547.0	6705.	101979.	F.C.	20.2	0.0518
10:55:54	50.6	403.6	437.1	2306.3	2319.2	430.7	657.1	59.51	492.8	510.9	638.5	7065.	169660.	F.C.	33.5	0.0532
11:40: 2	80.9	479.7	531.2	2306.4	2317.9	521.3	657.0	57.05	503.7	642.4	842.9	7285.	271306.	F.C.	49.5	0.0545
12:21:39	100.9	534.0	595.8	2277.8	2287.8	583.9	655.1	53.51	501.5	729.8	980.1	7191.	338596.	F.C.	57.2	0.0539
13: 8:45	100.8	544.2	602.8	2346.1	2357.2	591.5	659.4	55.30	524.6	734.9	983.4	7425.	338162.	F.C.	56.4	0.0536
CALIBRATION RUN NUMBER 16.1 APR. 27																
12:28:55	30.6	420.0	442.7	2199.9	2208.5	438.3	650.0	52.25	438.4	496.5	569.8	6409.	102146.	F.C.	28.6	0.0747
12:55:12	50.7	418.6	456.4	2215.8	2224.3	449.1	651.0	52.00	435.8	540.5	663.2	6441.	170145.	F.C.	42.5	0.0688
13:21:11	81.0	420.8	481.3	2177.8	2186.3	469.7	648.5	52.22	438.5	605.3	802.6	6564.	271717.	F.C.	59.1	0.0628
14: 0:52	101.1	484.3	556.7	2194.4	2201.7	542.8	649.6	49.60	440.4	704.3	950.5	6600.	339174.	F.C.	67.9	0.0624
14:42:58	101.0	544.5	603.6	2333.6	2343.8	592.2	658.6	54.66	518.9	742.1	987.8	7362.	338611.	F.C.	62.4	0.0593
CALIBRATION RUN NUMBER 17.1 MAY 26																
11:23: 5	30.3	423.5	448.8	2196.3	2203.3	444.0	649.7	46.56	391.7	502.6	575.7	5872.	101586.	F.C.	27.7	0.0734
11:45:13	50.7	422.8	464.1	2311.7	2319.1	456.1	657.1	47.37	398.0	548.7	669.8	6008.	170054.	F.C.	41.9	0.0684
12: 9:15	88.5	449.2	519.1	2202.8	2209.6	505.6	650.1	47.04	404.2	653.4	865.1	6185.	297007.	F.C.	62.1	0.0626
12:35:46	100.9	497.9	589.6	2235.6	2239.1	571.9	652.0	37.49	337.4	742.1	984.7	5369.	338484.	F.C.	65.7	0.0624
12:52:17	100.8	528.8	620.2	2267.7	2270.4	602.6	654.0	34.88	324.9	763.1	1001.3	48950.	338108.	N.B.	61.2	0.0591
13:10:40	100.8	545.8	639.6	2295.0	2297.0	621.5	655.7	31.89	303.5	769.0	1003.4	49996.	338108.	N.B.	65.5	0.0636
13:13:25	100.8	545.7	639.2	2282.5	2284.6	621.2	654.9	32.01	304.7	768.2	1002.7	49505.	338108.	N.B.	65.5	0.0636
CALIBRATION RUN NUMBER 18.1 JUNE 15																
16:53:51	30.4	424.2	450.3	2271.3	2278.8	445.3	654.5	45.20	380.4	498.4	574.7	5740.	101984.	F.C.	21.7	0.0570
17:17:18	50.6	474.7	515.7	2262.7	2269.5	507.8	653.9	45.24	397.7	592.3	716.5	6003.	169881.	F.C.	34.3	0.0584
17:36:32	80.9	517.7	579.6	2258.1	2264.2	567.7	653.6	44.31	407.4	694.6	891.0	6120.	271299.	F.C.	48.9	0.0563
17:54:39	80.9	544.9	606.4	2221.2	2226.1	594.6	651.1	41.58	395.6	720.5	917.0	5938.	271452.	F.C.	46.9	0.0551
18: 7:50	80.9	545.3	606.8	2231.8	2236.5	595.0	651.8	41.55	395.5	720.7	917.5	5937.	271309.	F.C.	46.7	0.0549
CALIBRATION RUN NUMBER 19.1 JUNE 29																
12: 9:50	30.5	418.4	445.7	2218.4	2223.5	440.5	651.0	43.50	364.5	494.6	570.9	5545.	102371.	F.C.	22.0	0.0574
12:31:59	50.7	467.3	511.0	2245.3	2249.9	502.6	652.7	42.79	373.6	587.7	712.3	5722.	169943.	F.C.	33.5	0.0568
13: 6:26	80.8	489.2	555.1	2281.1	2286.0	542.4	655.0	43.58	388.5	671.3	867.7	5947.	271029.	F.C.	49.3	0.0557
13:31:46	100.9	542.1	617.9	2299.4	2303.5	603.3	656.1	41.70	394.9	753.4	998.8	5999.	338384.	F.C.	52.6	0.0507
13:40:39	100.9	546.0	622.1	2322.6	2327.0	607.5	657.5	41.02	390.3	756.2	1000.6	51218.	338355.	N.B.	51.1	0.0493
CALIBRATION RUN NUMBER 20.1 AUG. 22																
11:41:52	30.4	449.1	470.8	2246.1	2253.9	466.7	652.9	53.17	456.8	526.0	596.1	6644.	101968.	F.C.	30.4	0.0819
12: 5:46	50.4	474.6	503.0	2308.9	2321.8	497.6	657.2	65.81	578.1	586.5	701.7	8046.	168952.	F.C.	46.0	0.0780
12:35:35	80.5	523.0	568.9	2268.9	2280.2	560.1	654.6	60.03	555.3	691.1	876.6	7766.	269943.	F.C.	62.6	0.0719
13: 1:53	100.9	543.7	602.1	2369.7	2379.5	590.8	660.7	55.71	528.0	748.3	983.3	7462.	338596.	F.C.	70.7	0.0672
13:21:45	100.8	544.4	603.1	2346.2	2355.7	591.8	659.3	55.20	523.9	748.9	983.4	7416.	338139.	F.C.	70.1	0.0668
CALIBRATION RUN NUMBER 21.1 SEP. 21																
11:49:40	30.5	438.5	465.2	2213.3	2221.1	460.1	650.8	43.83	373.3	521.7	595.0	5665.	102152.	F.C.	30.1	0.0803
12:10:45	50.0	469.0	511.3	2237.5	2244.8	503.2	652.3	43.93	384.2	598.4	716.8	5846.	167705.	F.C.	44.9	0.0776
12:43:55	69.9	526.5	580.7	2310.1	2317.3	570.2	656.9	43.66	405.3	694.5	859.5	6055.	234463.	F.C.	56.4	0.0749
13:20:14	90.9	544.7	615.3	2287.1	2293.3	601.7	655.5	40.33	383.3	756.1	971.4	5833.	304733.	F.C.	65.1	0.0693
13:22: 6	90.8	545.3	615.6	2269.6	2275.6	602.0	654.3	40.47	385.0	756.4	971.3	5852.	304678.	F.C.	65.2	0.0695
CALIBRATION RUN NUMBER 22.1 OCT. 12																
11:48:40	30.1	438.5	463.6	2216.7	2222.7	458.7	650.9	45.95	391.3	516.0	591.9	5877.	100827.	F.C.	26.7	0.0720
12:17:55	77.6	483.3	542.2	2235.5	2241.1	530.8	652.1	47.88	424.5	664.8	851.3	6370.	260147.	F.C.	60.3	0.0703
12:29:23	101.2	509.3	584.0	2237.7	2242.2	569.6	652.2	45.98	418.9	738.5	980.6	6312.	339400.	F.C.	73.4	0.0692
12:50:23	101.1	546.3	621.9	2308.1	2311.7	607.3	656.6	41.31	393.3	771.0	1011.7	50664.	339183.	N.B.	66.6	0.0645
13: 0:25	101.1	548.1	623.2	2307.4	2311.1	608.7	656.6	41.44	395.5	771.4	1011.5	50643.	339231.	N.B.	67.1	0.0649

Table C.3. (continued)

TIME	NOMINAL POWER (KW)	BUNDLE INLET TEMP. (F)	BUNDLE EXIT TEMP. (F)	UPPER PLENUM PRESS. (PSIA)	LOCAL BULK PRESS. (PSIA)	LOCAL BULK TEMP. (F)	LOCAL SAT. TEMP. (F)	CORE FLOW RATE (LB/SEC)	CORE FLOW RATE (GPM)	SHEATH T/C READING (F)	MIDDLE T/C READING (F)	SURFACE H.T. COEFF.	SURFACE HEAT FLUX	H.T. MODE	DEL-T GAP (F)	GAP (MILS)
CALIBRATION RUN NUMBER 23.1 NOV. 30																
11:22: 7	29.9	425.9	450.1	2267.7	2274.1	445.5	654.2	48.27	406.7	502.0	575.7	6050.	100458.	F.C.	26.5	0.0709
11:41:15	50.2	441.1	480.9	2298.0	2304.1	473.2	656.1	48.23	411.4	564.0	684.5	6173.	168226.	F.C.	41.5	0.0693
11:58:35	70.4	478.1	531.9	2256.1	2261.5	521.5	653.4	47.73	421.0	643.7	811.8	6318.	236142.	F.C.	54.8	0.0693
12:19:17	101.0	521.0	594.5	2235.0	2239.3	580.3	652.0	45.62	421.3	747.2	987.8	6317.	338891.	F.C.	71.7	0.0682
12:38:44	100.9	548.9	623.6	2267.2	2270.1	609.2	654.0	41.39	395.7	770.4	1009.3	48959.	338387.	N.B.	68.5	0.0665
12:44:28	100.9	549.2	624.1	2262.6	2265.2	609.6	653.7	41.22	394.3	770.5	1009.3	48774.	338414.	N.B.	68.9	0.0668
CALIBRATION RUN NUMBER 23.2 DEC. 15																
10: 5:18	29.9	429.5	454.8	2210.7	2216.3	449.9	650.5	46.02	389.1	505.9	581.2	5845.	100406.	F.C.	25.5	0.0684
10:27:17	60.8	471.1	518.8	2211.7	2216.9	509.6	650.5	46.86	410.7	617.2	763.7	6181.	203931.	F.C.	48.5	0.0699
10:39: 4	60.8	484.3	530.4	2225.9	2231.6	521.6	651.5	47.73	423.7	627.5	774.1	6319.	203775.	F.C.	47.7	0.0693
11: 9:20	101.1	542.0	614.6	2278.5	2282.5	600.6	654.8	43.85	415.3	764.6	1005.9	6230.	338983.	F.C.	68.4	0.0659
11:16:15	101.0	550.2	623.1	2290.3	2294.1	609.1	655.5	42.50	406.9	769.8	1010.1	49940.	338912.	N.B.	66.5	0.0643
11:23:26	101.0	549.5	622.7	2271.4	2275.0	608.6	654.3	42.29	404.6	768.9	1008.5	49174.	338696.	N.B.	66.6	0.0648
CALIBRATION RUN NUMBER 23.3 JAN. 19																
15: 7: 0	29.8	476.6	499.9	2113.6	2117.8	495.4	643.9	47.53	419.2	550.3	623.1	6198.	100015.	F.C.	25.7	0.0720
15:28:51	49.9	513.9	551.3	2209.0	2213.3	544.1	650.3	47.20	432.4	631.0	751.0	6348.	167444.	F.C.	39.3	0.0701
15:48:34	79.9	531.4	589.9	2178.0	2181.4	578.7	648.2	45.42	425.0	711.6	901.4	6290.	268045.	F.C.	57.2	0.0674
16:13:41	101.0	551.0	622.6	2246.2	2249.1	608.8	652.6	43.10	413.4	768.0	1006.0	48181.	338831.	N.B.	67.3	0.0651
16:17:13	101.0	549.8	621.9	2276.5	2279.7	608.0	654.6	43.06	412.1	768.4	1007.7	49367.	338855.	N.B.	65.9	0.0638
CALIBRATION RUN NUMBER 24.1 FEB. 16																
10:42: 1	30.1	441.3	467.1	2255.8	2260.1	462.1	653.3	44.45	379.3	522.1	593.7	5737.	100928.	F.C.	29.0	0.0786
11: 8:40	50.7	492.2	533.5	2252.7	2256.3	525.5	653.1	43.97	393.3	619.5	738.8	5931.	170145.	F.C.	43.6	0.0755
11:28:20	70.8	512.4	568.4	2276.5	2279.6	557.6	654.6	43.55	397.9	682.6	849.7	5998.	237371.	F.C.	55.8	0.0724
12:29: 8	101.0	544.4	618.8	2192.3	2194.4	604.5	649.1	42.04	400.0	766.7	1003.3	46135.	338835.	N.B.	69.1	0.0667
12:50:11	101.0	545.9	619.7	2186.8	2189.2	605.5	648.7	42.13	401.6	767.0	1003.1	45933.	338691.	N.B.	69.8	0.0674

Appendix D

EXAMPLES OF ORTCAL — PART II OUTPUT

Table D.1. Example of ORTCAL — Part II output
for thermocouple TE-318BG

****
*** THERMOCOUPLE NUMBER: TE-318BG ***
****

NOMENCLATURE:
Q(KW)/ROD = NOMINAL POWER INPUT PER ROD IN KW
TCS = OBSERVED SHEATH T/C READING (DEG F)
TCSM = OBSERVED MIDDLE T/C READING (DEG F)
TCSMC = CALCULATED MIDDLE T/C READING, USING THE BEST FIT PARAMETERS (DEG F)
DIFFERENCE= TCSM - TCSMC

TOTAL RUNS = 31
IF THERE IS A DISCREPANCY BETWEEN THE TOTAL RUNS AND THE NUMBER OF RUNS SHOWN BELOW, IT IS BECAUSE TE-318MG HAS ONLY BEEN ON THE CCDAS DURING THE FOLLOWING RUNS.

RUN NO. DATE TIME	Q(KW)/ROD	TCS	TCSM	TCSMC	DIFFERENCE
* 1.1 ******MAY	4*				
23:36:56	30.3	477.4	566.2	565.7	0.51
23:44:18	40.1	495.4	613.1	612.0	1.08
23:53:20	40.5	494.8	613.7	612.7	1.03
0:29: 6	50.7	520.1	669.8	667.8	1.95
* 1.2 ******MAY	5*				
14:31:56	40.7	402.5	522.9	521.4	1.48
14:50:53	50.7	467.3	616.7	615.2	1.53
15:39:21	50.6	516.1	663.5	663.4	0.07
15:56:45	60.9	540.3	719.2	717.7	1.46
16:18: 7	71.2	557.2	765.3	764.9	0.44
16:50:43	81.2	584.5	820.9	821.7	-0.71
17:13:10	91.6	606.7	875.7	874.8	0.93
* 1.3 ******MAY	5*				
19:21:26	102.2	627.9	927.7	927.9	-0.21
19:53:59	112.1	644.7	970.4	974.2	-3.76
20:22:51	124.5	675.6	1037.6	1043.1	-5.51
21: 4:19	124.6	715.7	1075.0	1084.1	-9.06
* 1.4 ******MAY	6*				
12:35:24	91.6	494.5	757.1	762.7	-5.62
12:57:41	91.5	496.6	757.6	764.5	-6.96
13:35:46	91.4	507.2	769.1	774.6	-5.52
13:48:44	91.3	522.3	783.4	789.5	-6.10
* 2.1 ******MAY	19*				
4: 6: 2	30.6	474.7	560.9	563.8	-2.88
4:28:22	41.0	496.9	613.4	616.1	-2.65
5: 8:30	51.1	518.3	663.2	667.1	-3.88
5:37:54	61.4	540.3	714.0	719.1	-5.09
6: 0: 0	71.5	559.1	763.8	767.7	-3.85
6:45:11	81.9	580.5	814.9	819.8	-4.91
7: 5:50	91.8	600.6	864.9	869.2	-4.33
7:35:54	102.0	623.3	918.3	922.6	-4.25
8:37: 4	112.1	644.9	971.0	974.5	-3.50
* 2.2 ******MAY	19*				
22:42:55	30.7	474.6	562.9	564.0	-1.13
23:10:47	40.9	497.3	614.1	616.5	-2.43
23:32:51	51.1	519.8	665.7	668.7	-3.03
23:57:45	61.3	540.6	716.0	719.3	-3.37
0:31: 6	71.5	562.2	766.1	770.8	-4.67
0:55:49	81.8	582.8	817.6	821.7	-4.05
1:23: 3	91.9	603.3	867.7	872.3	-4.60
2:30:44	102.2	624.0	920.7	923.9	-3.14
2:55:20	112.3	643.6	970.4	973.9	-3.48
3:18:32	124.3	665.4	1027.1	1032.0	-4.83
4:35:52	124.2	712.2	1072.6	1079.2	-6.58
7: 5:39	124.4	755.9	1117.5	1124.2	-6.72

Table D.1. (continued)

RUN NO. DATE TIME	Q(KW)/ROD	TCS	TCSM	TCSMC	DIFFERENCE
7:51:40	124.6	789.4	1149.0	1159.0	-10.05
8:15:29	112.2	773.8	1099.0	1105.4	-6.40
8:41: 8	102.3	759.1	1054.4	1060.6	-6.16
9:19:59	92.0	743.4	1006.1	1013.9	-7.79
9:43:39	81.9	724.4	958.7	964.5	-5.74
10: 7:36	71.5	703.5	907.6	912.6	-4.94
10:31:29	61.3	683.3	856.9	862.1	-5.14
10:55:49	50.5	660.1	802.5	807.1	-4.66
11:19:26	40.7	639.0	753.5	757.3	-3.73
11:44:10	30.3	615.1	699.8	703.0	-3.21
* 3.1 ******MAY	27*				
1:14:13	30.7	478.6	565.5	568.0	-2.51
1:36: 0	40.9	498.5	615.3	617.6	-2.29
2: 2:32	51.1	524.1	669.6	673.0	-3.40
2:24:56	61.4	545.5	720.7	724.5	-3.78
2:45:31	71.6	567.9	771.9	776.7	-4.86
3:11:21	81.8	589.8	824.2	828.9	-4.76
3:32:41	92.0	609.3	874.7	878.6	-3.90
4: 1:10	102.0	629.6	925.1	928.8	-3.70
4:25:28	112.3	651.5	976.8	981.8	-4.93
4:48:45	124.5	678.9	1038.9	1046.4	-7.57
5:17: 8	124.4	724.5	1082.7	1092.4	-9.68
6:22:58	124.4	797.9	1156.7	1167.3	-10.60
6:49:48	111.9	782.5	1106.0	1113.6	-7.58
7:31:58	101.9	766.9	1061.1	1067.3	-6.24
8: 0:56	91.8	750.1	1013.2	1019.9	-6.74
8:23:50	81.7	730.6	962.9	970.1	-7.15
8:46:21	71.4	711.4	913.7	920.3	-6.62
9: 9:52	61.4	689.9	863.2	868.9	-5.69
9:42: 8	51.0	668.7	811.2	817.2	-6.04
10: 4:17	40.8	645.8	759.7	764.4	-4.65
10:26:10	30.7	623.8	707.9	713.0	-5.11
* 4.1 ******JUNE	17*				
13:41: 8	30.7	478.4	566.7	567.9	-1.18
14:36:24	61.3	646.8	825.6	825.5	0.07
15: 7:57	92.0	735.8	1006.5	1006.3	0.22
* 4.2 ******JUNE	18*				
9:12:26	30.7	476.5	563.4	565.8	-2.41
9:53:33	61.4	598.6	775.4	777.6	-2.22
10:27:42	92.1	705.0	973.4	975.4	-1.93
11: 5:15	112.3	773.7	1100.7	1105.7	-4.99
11:40:33	124.3	793.7	1155.2	1162.6	-7.47
* 5.1 ******JULY	8*				
9:51:54	30.8	491.2	580.0	580.7	-0.72
10:41:25	61.3	580.5	756.5	759.1	-2.60
11:35:17	92.0	677.0	947.9	946.6	1.30
11:41: 1	91.9	679.4	948.5	948.8	-0.30
13:10: 5	124.3	817.2	1180.0	1186.6	-6.60
* 6.1 ******AUG.	4*				
9:59:10	30.8	482.0	572.9	571.5	1.39
11: 5: 4	62.0	653.0	833.3	833.9	-0.64
11:39:36	91.9	717.9	990.8	987.6	3.19
12:13:36	124.2	814.6	1179.9	1183.7	-3.81
13:19: 7	124.1	815.4	1178.7	1184.2	-5.52
* 7.1 ******AUG.	19*				
16:44:27	30.6	484.5	574.5	573.6	0.94
17:55:35	51.0	610.2	760.3	758.6	1.64
19: 2:42	101.4	772.5	1075.7	1071.5	4.22
20: 6:22	124.5	811.0	1178.6	1180.9	-2.38
* 8.3 ******NOV.	5*				
13:41:33	31.5	499.6	592.8	591.1	1.69
14: 9: 0	52.5	541.8	697.6	694.7	2.90
14:29:59	73.9	590.9	811.3	806.7	4.65
14:49:41	84.0	613.2	864.6	858.9	5.72

Table D.1. (continued)

RUN NO. DATE TIME	Q(KW)/ROD	TCS	TCSM	TCSMC	DIFFERENCE
14:53:35	95.0	636.6	922.1	915.0	7.11
15: 9:45	105.4	656.3	973.5	965.9	7.59
15:44:12	104.6	766.3	1080.3	1075.0	5.26
16: 5: 0	109.1	780.0	1108.0	1102.5	5.48
16:18:35	113.8	796.9	1127.8	1123.7	4.06
17: 5: 4	124.3	810.1	1178.3	1179.3	-1.08
* 9.1 ******NOV.	18*				
12:51:18	30.6	497.0	585.0	586.0	-1.02
13:29:59	31.1	494.6	584.6	585.2	-0.54
13:52:35	51.5	548.1	697.1	698.1	-1.03
14:16:33	71.4	591.3	798.6	799.6	-1.04
14:38:36	81.5	614.1	852.5	852.3	0.17
14:47:36	91.6	638.4	908.8	906.9	1.93
15: 2:29	102.0	660.0	963.1	959.5	3.64
15:21:34	101.6	708.5	1010.4	1007.3	3.06
15:38:27	101.4	749.5	1049.9	1048.1	1.84
15:53:39	101.2	782.8	1082.0	1081.6	0.46
*10.1 ******DEC.	8*				
11:25:18	31.3	502.3	592.2	593.4	-1.26
11:47:24	41.5	538.7	659.5	659.4	0.14
12: 9:36	61.6	579.1	758.8	758.6	0.12
12:39: 8	82.1	631.4	873.0	871.4	1.58
13:27: 2	81.7	738.4	981.2	978.0	3.15
13:32:52	81.6	747.7	990.3	987.2	3.15
13:43:16	81.5	755.2	997.2	994.6	2.60
13:46: 3	81.5	758.6	1000.8	998.0	2.98
13:52:47	81.5	763.4	1004.8	1002.7	2.07
*11.1 ******JAN.	13*				
13:49:36	30.8	515.1	603.7	604.6	-0.93
14:12:27	51.3	560.2	709.6	709.5	0.08
14:34:40	81.7	629.6	870.2	868.6	1.63
14:53:30	81.5	666.8	907.3	905.2	2.13
15:17: 6	81.1	708.5	949.0	946.0	3.01
15:27:52	81.0	726.8	966.6	964.2	2.40
15:36:42	80.9	741.1	980.7	978.5	2.29
*12.1 ******JAN.	27*				
11:20:34	30.7	489.9	580.7	579.3	1.42
11:44:22	51.0	549.2	699.4	697.6	1.84
12: 8:16	81.6	614.9	856.2	853.5	2.78
12:33: 5	81.6	669.0	911.0	907.7	3.34
12:59:52	81.2	727.2	969.3	965.2	4.14
13: 9:19	81.8	743.5	987.4	983.4	3.95
*13.1 ******FEB.	10*				
10:33:25	30.8	498.2	589.7	587.8	1.92
10:54: 5	51.4	556.4	709.9	705.9	4.02
11:14: 1	61.0	584.5	766.6	762.2	4.44
11:25:44	71.3	617.8	851.3	826.0	5.35
11:40:22	81.7	649.9	895.2	888.9	6.34
12:15:12	81.3	703.5	948.6	941.5	7.07
13:47: 8	81.6	769.7	1012.4	1009.3	3.14
*14.1 ******MAR.	9*				
11:17:50	30.9	519.2	607.5	609.1	-1.59
11:40: 0	51.2	569.7	718.9	718.5	0.43
12: 2:29	81.7	648.2	891.0	887.0	4.01
12:25: 4	81.4	679.4	921.9	917.7	4.25
12:49:10	81.1	717.6	959.6	955.3	4.24
13:18:51	81.0	761.2	1004.1	998.9	5.19
13:34:23	81.5	765.8	1007.3	1005.1	2.24
*15.1 ******MAR.	23*				
10:32: 1	30.6	485.2	574.5	574.4	0.14
10:55:54	51.2	533.6	683.3	682.7	0.54
11:40: 2	81.5	670.8	911.1	909.2	1.96
12:21:39	101.9	762.2	1064.9	1062.7	2.23
13: 8:45	101.9	767.9	1069.4	1068.5	0.85

Table D.1. (continued)

RUN NO, DATE TIME	Q(KW)/ROD	TCS	TCSM	TCSMC	DIFFERENCE
*16.1 ******APR.	27*				
12:28:55	30.7	508.0	595.6	597.2	-1.65
12:55:12	51.2	554.8	703.8	703.8	-0.05
13:21:11	87.8	635.1	896.4	891.9	4.45
14: 0:52	102.0	725.0	1031.7	1025.1	6.64
14:42:58	101.8	768.0	1071.9	1068.1	3.79
*17.1 ******MAY	26*				
11:23: 5	30.7	515.6	603.7	604.9	-1.27
11:45:13	51.1	564.2	711.1	712.8	-1.77
12: 9:15	89.4	674.3	939.2	936.2	2.95
12:35:46	101.8	762.7	1069.5	1063.0	6.48
12:52:17	101.8	791.4	1095.8	1092.0	3.74
13:10:40	101.7	802.9	1101.2	1103.5	-2.25
13:13:25	101.8	802.5	1100.8	1103.1	-2.26
*18.1 ******JUNE	15*				
15:53:51	30.6	515.6	604.7	604.5	0.18
17:17:18	51.0	613.9	763.7	762.3	1.43
17:36:32	81.7	723.7	969.1	963.3	5.84
17:54:39	81.5	751.0	996.1	990.1	6.00
18: 7:50	81.5	750.9	996.1	989.9	6.18
*19.1 ******JUNE	29*				
12: 8:50	30.6	511.0	601.2	599.9	1.33
12:31:59	51.0	610.4	760.5	758.8	1.66
13: 6:26	81.7	699.0	944.3	938.2	6.10
13:31:46	101.8	786.1	1092.5	1086.5	6.04
13:40:39	101.8	790.4	1095.9	1091.0	4.90
*20.1 ******AUG.	22*				
11:41:52	30.5	538.3	624.6	626.9	-2.28
12: 5:46	51.9	606.7	753.6	757.8	-4.19
12:35:35	81.6	715.7	954.4	954.7	-0.30
13: 1:53	101.8	776.1	1075.1	1076.5	-1.37
13:21:45	101.8	776.8	1075.4	1077.1	-1.74
*21.1 ******SEP.	21*				
11:49:40	30.9	536.0	627.7	625.7	1.98
12:10:45	51.4	617.0	769.8	766.6	3.17
12:43:39	71.9	716.6	933.1	927.1	6.02
15:20:14	91.8	778.4	1054.0	1048.8	5.25
15:22: 6	91.8	778.6	1054.2	1048.9	5.28
*22.1 ******OCT.	12*				
11:48:40	31.1	531.1	625.6	621.3	4.33
12:17:55	80.7	690.0	933.1	926.2	6.92
12:29:23	101.9	758.9	1066.0	1059.3	6.64
12:50:23	102.0	795.6	1103.8	1096.8	7.03
13: 0:25	102.0	797.5	1104.9	1098.8	6.06
*23.1 ******NOV.	30*				
11:22: 7	31.1	517.1	608.7	607.6	1.10
11:41:15	51.8	582.6	735.4	733.4	2.00
11:58:35	72.4	664.6	879.1	876.2	2.85
12:19:17	101.9	767.9	1072.3	1068.3	4.05
12:38:44	101.7	796.2	1100.8	1096.7	4.10
12:44:28	101.7	797.0	1101.3	1097.5	3.82
*23.2 ******DEC.	15*				
10: 5:18	31.0	520.4	615.5	610.4	5.10
10:27:17	61.5	634.2	819.3	813.5	5.83
10:39: 4	61.6	645.1	830.4	824.5	5.89
11: 9:20	102.1	788.0	1095.9	1089.6	6.30
11:16:15	102.2	795.2	1103.4	1097.0	6.42
11:23:26	102.1	795.8	1103.6	1097.5	6.08
*23.3 ******JAN.	19*				
15: 7: 0	31.0	565.6	656.9	655.5	1.40
15:28:51	51.9	650.5	804.7	801.6	3.15
15:48:34	82.4	736.5	983.4	978.2	5.22
16:13:41	101.8	794.8	1100.0	1095.5	4.54
16:17:13	101.9	794.8	1100.1	1095.9	4.27

Table D.1. (continued)

RUN NO. DATE TIME	Q(KW)/ROD	TCS	TCSM	TCSMC	DIFFERENCE
*24.1 ******FEB. 16*					
10:42: 1	30.5	529.9	621.3	618.4	2.96
11: 6:40	51.2	629.9	782.0	778.8	3.23
11:28:20	72.1	697.2	913.2	908.0	5.23
12:29: 8	102.0	789.0	1097.6	1090.3	7.27
12:50:11	102.0	790.2	1098.6	1091.5	7.13

BEST FIT PARAMETERS FOR AKBN:

WHERE,

AKBN = C(1)+C(2)*T+C(3)*T**2+C(4)*T**3

C(1)= 0.21976151E 02
C(2)=-0.74225366E-02
C(3)=-0.73717558E-07
C(4)= 0.59715699E-09

TOTAL ERROR (SUM OF SQUARED DIFFERENCES)= 0.38925518E 04

VARIANCE OF FIT= 0.18624649E 02

Table D.2. Example of ORTCAL — Part II output
for thermocouple TE-301DJ

```
                    ********************************
                  *** THERMOCOUPLE NUMBER:  TE-301DJ  ***
                    ********************************

NOMENCLATURE:
     Q(KW)/ROD = NOMINAL POWER INPUT PER ROD IN KW
     TCS       = OBSERVED SHEATH T/C READING (DEG F)
     TCSM      = OBSERVED MIDDLE T/C READING (DEG F)
     TCSMC     = CALCULATED MIDDLE T/C READING, USING THE BEST FIT PARAMETERS (DEG F)
     DIFFERENCE= TCSM - TCSMC

TOTAL RUNS =  32
IF THERE IS A DISCREPANCY BETWEEN THE TOTAL RUNS AND THE NUMBER OF RUNS SHOWN
BELOW, IT  IS BECAUSE  TE-301MJ  HAS ONLY BEEN ON THE CCDAS DURING THE FOLLOWING RUNS.
```

RUN NO. DATE TIME	Q(KW)/ROD	TCS	TCSM	TCSMC	DIFFERENCE
* 1.1 ******MAY 4*					
23:36:56	30.0	465.3	538.0	538.4	-0.32
23:44:19	39.7	491.0	577.0	577.3	-0.28
23:53:20	40.2	480.4	577.4	578.0	-0.60
0:29: 6	50.1	503.4	623.4	624.8	-1.45
* 1.2 ******MAY 5*					
14:31:56	40.3	390.5	486.1	489.2	-3.06
14:50:53	50.2	450.8	571.5	573.0	-1.48
15:39:21	50.0	501.2	622.2	622.5	-0.33
15:56:45	60.3	524.2	670.7	670.1	0.68
16:18: 7	70.2	540.0	710.0	709.7	0.32
16:50:43	80.0	571.7	765.5	765.0	0.49
17:13:10	90.3	598.7	820.2	816.5	3.64
* 1.3 ******MAY 5*					
19:21:26	100.6	635.5	882.1	878.1	3.97
19:53:59	110.2	666.2	933.2	931.7	1.49
20:22:51	122.3	716.9	1007.1	1011.2	-4.11
21: 4:19	122.4	752.1	1042.5	1046.4	-3.95
* 1.4 ******MAY 6*					
12:35:24	90.4	498.1	712.8	717.4	-4.59
12:57:41	90.3	498.3	712.9	717.4	-4.46
13:35:46	90.3	509.3	724.8	728.1	-3.28
13:48:44	90.1	522.8	739.1	741.1	-2.02
* 2.1 ******MAY 19*					
4: 6: 2	30.0	464.5	536.5	537.4	-0.86
4:28:22	40.1	485.2	580.9	582.6	-1.72
5: 8:30	50.2	504.6	624.1	626.3	-2.26
5:37:54	60.4	525.3	668.3	671.5	-3.19
6: 0: 0	70.4	545.0	711.2	715.3	-4.12
6:45:11	80.5	564.4	753.5	758.9	-5.45
7: 5:50	90.4	587.3	800.2	805.5	-5.31
7:35:54	100.2	616.9	855.9	858.5	-2.59
8:37: 4	110.2	660.0	924.8	925.6	-0.83
* 2.2 ******MAY 19*					
22:42:55	30.1	465.9	539.2	539.2	0.02
23:10:47	40.1	486.9	583.4	584.3	-0.88
23:32:51	50.3	507.7	628.2	629.5	-1.31
23:57:45	60.3	527.6	672.5	673.6	-1.17
0:31: 6	70.2	548.2	715.3	717.9	-2.63
0:55:49	80.4	569.6	761.1	763.9	-2.78
1:23: 3	90.2	590.6	805.1	808.4	-3.32
2:30:44	100.3	613.8	852.6	855.9	-3.35
2:55:20	110.3	637.2	900.5	903.2	-2.76
3:18:32	122.3	666.4	959.3	961.0	-1.71
4:35:52	122.2	713.2	1009.6	1007.3	2.24
7: 5:39	122.5	743.5	1027.1	1038.2	-11.08
8:41: 8	100.3	738.4	968.8	979.5	-10.76

Table D.2. (continued)

RUN NO. DATE TIME	Q(KW)/ROD	TCS	TCSM	TCSMC	DIFFERENCE
9:19:59	90.0	725.2	934.5	941.6	-7.11
9:45:39	80.1	711.8	901.1	904.4	-3.28
10: 7:36	70.2	697.0	867.6	865.7	1.95
10:31:29	60.2	681.2	831.4	825.9	5.49
10:55:49	49.7	660.8	785.4	780.3	5.08
11:19:26	40.1	639.7	740.0	735.2	3.84
11:44:10	29.8	614.9	689.0	686.6	2.42
* 3.1 ******MAY	27*				
1:14:13	30.2	467.3	540.8	540.8	-0.04
1:36: 0	40.2	485.5	582.7	583.0	-0.29
2: 2:32	50.3	509.3	629.6	631.0	-1.42
2:23:56	60.3	529.8	673.2	675.8	-2.69
2:45:31	70.5	550.4	717.6	720.9	-3.24
3:11:21	80.4	572.0	763.0	766.3	-3.25
3:32:41	90.4	594.8	810.1	813.0	-2.89
4: 1:10	100.2	623.8	864.7	865.5	-0.82
4:25:24	110.5	656.5	922.9	922.6	0.25
4:48:45	122.3	694.7	994.1	989.2	4.86
5:17: 8	122.2	747.1	1043.6	1041.2	2.40
5:22:58	122.3	815.9	1118.9	1109.7	9.19
6:49:43	110.2	802.2	1075.4	1066.8	8.59
7:31:58	100.1	789.3	1038.1	1029.6	8.51
8: 0:59	90.2	774.5	999.2	991.0	8.15
8:23:50	80.2	753.1	953.2	945.7	7.58
8:46:21	70.1	716.3	887.6	884.8	2.84
9: 9:52	60.4	690.4	837.3	835.5	1.77
9:42: 8	50.1	670.6	796.2	791.1	5.11
10: 4:17	40.2	648.2	747.7	744.8	2.88
10:26:10	30.2	623.1	698.2	696.0	2.21
* 4.1 ******JUNE	17*				
13:41: 8	30.2	469.5	544.0	542.9	1.12
14:36:24	60.5	640.0	789.2	785.7	3.49
15: 7:57	90.6	720.7	937.3	938.5	-1.26
* 4.2 ******JUNE	18*				
9:12:26	30.3	469.7	544.1	543.3	0.72
9:53:33	50.3	591.9	738.0	737.3	0.72
10:27:42	90.3	698.7	920.4	915.9	4.51
11: 5:15	109.9	742.0	996.0	1006.3	-10.23
* 5.1 ******JULY	8*				
9:51:54	30.2	474.5	549.8	547.8	1.98
10:41:25	60.3	598.0	703.6	703.8	-0.19
11:35:17	90.4	651.1	867.0	868.8	-1.73
11:41: 1	90.3	652.0	868.1	869.5	-1.36
13:10: 5	122.1	769.5	1055.6	1063.2	-7.55
* 6.1 ******AUG.	4*				
9:59:10	30.2	468.0	543.1	541.4	1.66
11: 5: 4	60.9	632.2	779.7	778.8	0.90
11:39:36	90.3	693.0	912.6	910.1	2.49
12:13:36	122.3	777.0	1080.3	1071.2	9.08
13:19: 7	122.0	780.7	1083.3	1074.1	9.16
* 7.1 ******AUG.	19*				
16:44:27	30.5	470.5	546.5	544.6	1.91
17:55:35	50.1	591.5	714.3	712.3	1.96
19: 2:42	100.5	735.0	973.5	976.6	-3.07
20: 6:22	122.4	762.0	1048.4	1056.4	-8.02
* 8.2 ******OCT.	9*				
2:33:52	30.3	468.3	544.9	542.0	2.86
2:57:41	50.5	564.0	688.4	686.0	2.35
3:21:26	70.7	650.4	823.5	820.5	2.99
* 8.3 ******NOV.	5*				
13:41:33	30.3	485.4	562.0	558.9	3.14
14: 9: 0	50.5	623.4	647.7	645.6	2.14
14:29:59	71.3	569.2	743.5	741.4	2.11

Table D.2. (continued)

RUN NO- DATE TIME	Q(KW)/ROD	TCS	TCSM	TCSMC	DIFFERENCE
14:49:41	81.2	591.1	787.5	787.0	0.44
14:53:35	91.7	612.5	834.1	833.7	0.40
15: 9:45	101.7	630.0	875.3	875.2	0.14
15:44:12	101.0	733.8	977.7	976.7	0.96
16: 5: 0	105.3	743.2	996.2	996.5	-0.26
16:18:38	109.9	747.2	1009.3	1011.3	-2.07
17: 5: 4	122.8	763.6	1055.0	1058.9	-5.91
* 9.1 ******NOV.	18*				
12:51:16	80.5	482.8	561.2	556.8	4.38
13:29:59	80.4	478.1	587.2	582.0	5.12
13:52:35	50.4	526.5	653.9	648.5	5.39
14:16:33	71.3	569.7	746.9	741.9	4.96
14:38:36	81.1	590.9	791.1	786.7	4.45
14:47:36	90.7	614.4	837.4	833.2	4.19
15: 2:29	100.4	634.0	879.5	876.1	3.39
15:21:34	100.1	680.9	926.1	921.8	4.35
15:38:27	99.8	722.3	971.1	962.3	8.77
15:53:39	99.8	743.5	986.9	983.0	3.97
*10.1 ******DEC.	8*				
11:25:18	80.2	492.0	567.3	566.1	1.15
11:47:24	40.6	530.6	629.8	628.8	0.93
12: 9:36	60.6	570.8	717.9	717.2	0.74
12:39: 8	80.6	622.9	817.7	817.1	0.58
13:27: 2	80.6	722.6	919.4	916.2	3.17
13:52:52	80.6	729.0	925.2	922.5	2.63
13:43:15	80.5	734.9	930.7	928.3	2.46
13:46: 3	80.5	736.5	931.9	929.9	1.94
13:52:47	80.5	737.0	931.9	930.4	1.50
*11.1 ******JAN.	13*				
13:49:36	30.4	504.0	577.2	577.6	-0.44
14:12:27	50.6	546.9	668.0	669.3	-1.30
14:34:40	80.8	613.4	806.0	808.2	-2.12
14:53:30	80.4	650.4	841.9	844.0	-2.16
15:17: 6	80.1	691.3	882.5	883.8	-1.36
15:27:52	79.9	709.3	900.4	901.4	-0.98
15:36:42	79.9	722.8	914.3	914.7	-0.40
*12.1 ******JAN.	27*				
11:20:34	30.1	473.9	552.0	547.2	4.80
11:44:22	50.5	527.8	655.8	649.9	5.84
12: 8:16	81.6	591.1	793.6	787.9	5.63
12:33: 5	81.6	646.1	848.2	842.6	5.54
12:59:52	81.4	704.9	906.2	900.5	5.68
13: 9:19	80.5	718.0	917.9	911.5	6.36
*13.1 ******FEB.	10*				
10:33:25	30.4	486.4	564.1	560.3	3.81
10:54: 5	50.7	541.9	670.0	664.5	5.58
11:14: 1	60.4	569.6	721.0	715.4	5.64
11:25:44	70.4	601.8	777.8	771.6	6.14
11:40:22	80.8	633.3	834.0	828.0	6.00
12:15:12	80.4	687.1	887.0	880.6	6.43
13:47: 8	80.7	739.0	935.1	932.7	2.35
*14.1 ******MAR.	9*				
11:17:50	30.4	505.6	580.0	579.2	0.80
11:40: 0	50.7	554.1	678.5	676.6	1.92
12: 2:29	80.8	631.4	828.0	826.1	1.90
12:25: 4	80.6	662.0	857.6	855.9	1.75
12:49:10	80.3	699.2	894.6	892.3	2.29
13:18:51	80.2	735.7	930.7	928.3	2.49
13:34:23	80.6	738.2	933.4	931.9	1.49
*15.1 ******MAR.	23*				
10:32: 1	30.4	468.7	547.0	542.6	4.38
10:55:54	50.6	510.9	638.5	633.4	5.05
11:40: 2	80.9	542.4	842.9	837.2	5.69
12:21:39	100.9	729.8	980.1	972.5	7.60
13: 8:45	100.8	734.9	983.4	977.3	6.06

Table D.2. (continued)

RUN NO. DATE TIME	Q(KW)/ROD	TCS	TCSM	TCSMC	DIFFERENCE
*16.1 ******APR.	27*				
12:28:35	30.5	496.5	569.8	570.4	-0.63
12:55:12	50.7	540.5	663.2	663.2	-0.02
13:21:11	81.0	605.3	802.6	800.7	1.83
14: 0:52	101.1	704.3	950.5	947.5	3.01
14:42:58	101.0	742.1	957.8	984.7	3.11
*17.1 ******MAY	26*				
11:23: 5	30.3	502.6	575.7	576.0	-0.26
11:46:13	50.7	548.7	669.8	671.3	-1.54
12: 9:15	80.5	653.4	865.1	866.6	-1.52
12:35:46	100.9	742.1	984.7	984.7	-0.02
12:52:17	100.8	763.1	1001.3	1005.3	-3.98
13:10:40	100.8	759.0	1003.4	1011.1	-7.73
13:13:25	100.8	768.2	1002.7	1010.4	-7.69
*18.1 ******JUNE	15*				
16:53:51	30.4	498.4	574.7	572.2	2.50
17:17:18	50.6	592.3	716.5	714.5	2.01
17:36:32	80.9	694.6	891.0	889.0	1.93
17:54:39	80.9	720.5	917.0	915.0	2.07
18: 7:50	80.9	720.7	917.5	915.0	2.44
*19.1 ******JUNE	29*				
12: 8:50	30.5	494.6	570.9	568.6	2.28
12:31:59	50.7	587.7	712.3	710.0	2.30
13: 6:26	80.8	671.3	867.7	865.7	1.98
13:31:46	100.9	753.4	998.8	995.8	2.99
13:40:39	100.9	756.2	1000.6	998.6	1.98
*20.1 ******AUG.	22*				
11:41:52	30.4	526.0	596.1	599.5	-3.44
12: 5:46	50.4	586.5	701.7	708.0	-6.28
12:35:35	80.5	691.1	876.6	884.6	-8.00
13: 1:53	100.9	748.3	983.3	990.9	-7.56
13:21:45	100.8	748.9	983.4	991.1	-7.68
*21.1 ******SEP.	21*				
11:49:40	30.5	521.7	595.0	595.4	-0.47
12:10:45	50.0	598.4	716.8	713.9	-2.09
12:43:59	69.9	694.5	859.5	862.5	-2.97
15:20:14	90.9	756.1	971.4	974.3	-2.88
15:22: 6	90.8	756.4	971.3	974.5	-3.22
*22.1 ******OCT.	12*				
11:48:40	30.1	516.0	591.9	588.8	3.10
12:17:55	77.6	664.8	851.3	851.4	-0.11
12:29:23	101.2	738.5	980.6	981.7	-1.12
12:50:23	101.1	771.0	1011.7	1013.9	-2.19
13: 0:25	101.1	771.4	1011.5	1014.4	-2.89
*23.1 ******NOV.	30*				
11:22: 7	29.9	502.0	575.7	574.6	1.12
11:41:15	50.2	564.0	684.5	685.1	-0.59
11:58:35	70.4	643.7	811.8	813.2	-1.43
12:19:17	101.0	747.2	987.8	990.0	-2.18
12:38:44	100.9	770.4	1009.3	1012.7	-3.45
12:44:28	100.9	770.5	1009.3	1012.9	-3.63
*23.2 ******DEC.	15*				
10: 5:18	29.9	505.9	581.2	578.5	2.74
10:27:17	60.8	617.2	763.7	763.7	-0.03
10:39: 4	60.8	627.5	774.1	773.8	0.33
11: 9:20	101.1	764.6	1005.9	1007.4	-1.44
11:16:15	101.0	769.8	1010.1	1012.5	-2.46
11:23:26	101.0	768.9	1008.5	1011.4	-2.87
*23.3 ******JAN.	19*				
15: 7: 0	29.8	550.3	623.1	622.4	0.73
15:28:51	49.9	631.0	751.0	751.2	-0.21
15:48:34	79.9	711.6	901.4	903.7	-2.24
16:13:41	101.0	768.0	1006.0	1010.7	-4.70
16:17:13	101.0	768.4	1007.7	1011.1	-3.37

Table D.2. (continued)

RUN NO. DATE TIME	Q(KW)/ROD	TCS	TCSM	TCSMC	DIFFERENCE
*24.1 ******FEB. 16*					
10:42: 1	30.1	522.1	593.7	595.0	-1.30
11: 8:40	50.7	619.5	738.8	741.7	-2.91
11:28:20	70.8	682.6	849.7	852.8	-3.09
12:29: 8	101.0	766.7	1003.3	1009.4	-6.06
12:50:11	101.0	767.0	1003.1	1009.6	-6.55

BEST FIT PARAMETERS FOR AKBN:
WHERE,

AKBN = C(1)+C(2)*T+C(3)*T**2+C(4)*T**3

C(1)= 0.20594376E 02
C(2)=-0.71305782E-02
C(3)= 0.11995689E-05
C(4)= 0.19595138E-09

TOTAL ERROR (SUM OF SQUARED DIFFERENCES)= 0.32816289E 04

VARIANCE OF FIT= 0.15701573E 02

Table D.3. Example of ORTCAL — Part II output
for thermocouple TE-322BF

```
**********************************
*** THERMOCOUPLE NUMBER:  TE-322BF  ***
**********************************
```

NOMENCLATURE:
- Q(KW)/ROD = NOMINAL POWER INPUT PER ROD IN KW
- TCS = OBSERVED SHEATH T/C READING (DEG F)
- TCSM = OBSERVED MIDDLE T/C READING (DEG F)
- TCSMC = CALCULATED MIDDLE T/C READING, USING THE BEST FIT PARAMETERS (DEG F)
- DIFFERENCE= TCSM - TCSMC

TOTAL RUNS = 32
IF THERE IS A DISCREPANCY BETWEEN THE TOTAL RUNS AND THE NUMBER OF RUNS SHOWN BELOW, IT IS BECAUSE TE-322MF HAS ONLY BEEN ON THE CCDAS DURING THE FOLLOWING RUNS.

RUN NO. DATE TIME	Q(KW)/ROD	TCS	TCSM	TCSMC	DIFFERENCE
* 1.1 ******MAY 4*					
23:36:56	29.7	470.2	573.6	559.6	13.95
23:44:18	39.2	486.6	622.0	604.6	17.40
23:53:20	39.7	486.8	623.0	606.3	16.73
0:29: 6	49.6	509.5	678.7	658.7	19.99
* 1.2 ******MAY 5*					
14:31:56	39.9	397.0	532.0	517.4	14.61
14:50:53	49.7	457.4	626.4	607.1	19.32
15:39:21	49.5	505.8	673.0	654.9	18.09
15:56:45	59.7	527.3	728.9	706.9	21.95
16:18: 7	69.5	540.0	772.5	749.4	23.04
16:50:43	79.4	562.6	826.5	802.1	24.41
17:13:10	89.5	581.4	879.9	852.0	27.93
* 1.3 ******MAY 5*					
19:21:26	99.9	597.4	928.2	899.9	28.35
19:53:59	109.6	609.6	969.2	941.8	27.48
20:22:51	121.7	634.3	1030.9	1003.9	27.00
21: 4:19	121.9	670.8	1067.5	1041.2	26.31
* 1.4 ******MAY 6*					
12:35:24	90.1	472.8	763.9	745.5	18.37
12:57:41	90.0	473.7	764.4	746.1	18.31
13:35:46	90.0	485.1	776.2	757.2	19.00
13:48:44	89.9	499.5	790.8	771.3	19.53
* 2.1 ******MAY 19*					
4: 6: 2	29.9	468.2	568.3	558.1	10.16
4:28:22	40.0	488.5	621.1	608.7	12.39
5: 8:30	50.0	507.4	673.1	658.0	15.11
5:37:54	60.2	527.2	725.2	708.5	16.70
6: 0: 0	70.1	545.8	776.1	757.3	18.78
6:45:11	80.3	563.5	826.1	805.8	20.26
7: 5:50	90.1	581.2	875.7	853.3	22.36
7:35:54	99.8	598.0	925.0	899.9	25.12
8:37: 4	109.8	615.1	975.1	947.9	27.20
* 2.2 ******MAY 19*					
22:42:55	30.0	468.5	569.6	558.8	10.83
23:10:47	40.0	489.2	621.8	609.5	12.38
23:32:51	50.1	509.1	674.7	659.8	14.90
23:57:45	60.1	527.7	725.4	708.6	16.78
0:31: 6	69.9	546.0	775.3	756.7	18.64
0:55:49	80.1	564.7	827.1	806.4	20.65
1:23: 3	89.9	581.5	875.7	853.2	22.49
2:30:44	99.9	598.9	926.6	901.3	25.25
2:55:20	109.9	615.8	975.9	948.9	27.00
3:18:32	121.8	634.5	1031.7	1004.4	27.30
4:35:52	121.7	679.9	1076.6	1050.0	26.57
7: 5:39	122.1	725.9	1122.9	1097.6	25.27
7:51:40	122.2	767.6	1162.7	1140.0	22.63

Table D.3. (continued)

RUN NO. DATE TIME	Q(KW)/ROD	TCS	TCSM	TCSMC	DIFFERENCE
8:15:29	110.0	749.3	1105.6	1083.5	22.02
8:41: 8	100.0	732.5	1056.8	1035.7	21.06
9:19:56	89.7	716.3	1007.4	987.8	19.65
9:43:39	79.8	699.9	959.8	941.1	18.69
10: 7:36	69.9	682.1	910.3	893.0	17.27
10:31:29	60.0	664.2	860.3	844.7	15.59
10:55:49	49.8	644.5	806.3	793.1	13.15
11:19:26	39.9	626.6	758.3	746.4	11.83
11:44:10	29.6	606.4	703.9	695.3	8.59
* 3.1 ******MAY	27*				
1:14:13	30.1	472.4	573.2	563.0	10.24
1:36: 0	40.0	489.7	623.5	610.1	13.43
2: 2:32	50.1	512.9	678.5	663.6	14.86
2:23:56	60.1	532.3	730.0	713.3	16.65
2:45:31	70.3	550.8	781.9	762.6	19.24
3:11:21	80.1	570.7	833.4	812.5	20.96
3:32:41	90.1	588.2	883.2	860.4	22.86
4: 1:10	99.9	604.5	931.7	906.8	24.91
4:25:28	110.1	621.6	982.7	955.5	27.23
4:48:45	121.9	642.6	1040.3	1012.9	27.43
5:17: 8	121.8	684.1	1080.8	1054.4	26.41
5:22:58	121.9	770.7	1165.9	1142.1	23.83
6:49:48	109.8	751.7	1108.9	1085.5	23.43
7:31:58	99.8	735.2	1059.8	1037.7	22.08
8: 0:56	89.9	720.0	1013.6	992.1	21.55
8:26:50	80.0	703.9	964.8	945.4	19.38
8:46:21	69.9	686.6	915.0	897.3	17.69
9: 9:52	60.2	668.9	866.0	850.0	16.04
9:42: 9	50.0	650.5	814.3	800.7	13.67
10: 4:17	40.0	631.4	763.8	751.5	12.31
10:26:10	30.1	612.8	712.1	703.1	9.08
* 4.1 ******JUNE	17*				
13:41: 5	30.0	476.0	573.3	566.3	7.01
14:36:24	60.2	637.9	831.6	819.3	12.35
15: 7:37	90.3	716.8	1008.7	992.0	16.68
* 4.2 ******JUNE	18*				
9:12:26	30.2	473.8	570.1	564.6	5.55
9:53:33	60.1	589.8	781.6	770.6	11.08
10:27:42	90.0	687.8	976.0	959.9	16.15
11: 5:15	109.5	762.9	1113.1	1095.8	17.28
11:40:33	121.8	780.9	1169.3	1152.1	17.21
* 5.1 ******JULY	8*				
9:51:54	30.0	498.0	582.7	588.3	-5.57
10:41:25	60.1	585.4	759.1	766.3	-7.19
11:35:17	90.0	675.6	945.7	947.7	-1.99
11:41: 1	89.9	676.6	947.2	948.4	-1.28
13:10: 5	121.6	810.6	1184.0	1181.7	2.31
* 6.1 ******AUG.	4*				
9:59:10	30.0	481.6	573.6	571.8	1.76
11: 5: 4	60.6	646.0	831.7	828.3	3.42
11:39:36	89.9	703.5	985.1	975.4	9.71
12:13:36	121.6	800.8	1182.5	1172.4	10.12
13:19: 7	121.6	802.9	1183.0	1173.7	9.28
* 7.1 ******AUG.	19*				
16:44:27	30.3	482.3	577.0	573.3	3.74
17:55:35	49.8	604.3	760.0	754.1	5.96
19: 2:42	100.0	757.8	1074.6	1061.3	13.32
20: 6:22	121.9	799.9	1185.4	1171.7	13.67
* 8.2 ******OCT.	9*				
2:33:52	30.1	480.1	573.8	570.6	3.21
2:57:41	50.2	578.2	734.0	729.1	4.97
3:21:26	70.3	665.2	884.6	877.0	7.56

Table D.3. (continued)

RUN NO. DATE TIME	Q(KW)/ROD	TCS	TCSM	TCSMC	DIFFERENCE
* 8.3 ******NOV.	5*				
13:41:53	30.0	495.3	590.5	585.3	5.20
14: 9: 0	50.1	634.6	692.3	685.4	7.48
14:29:59	70.9	681.1	804.2	794.7	9.52
14:49:41	80.7	701.6	856.2	845.1	11.09
14:53:35	91.2	822.9	911.4	898.5	12.91
15: 9:45	101.1	839.7	961.1	945.9	15.23
15:44:12	100.5	750.6	1069.4	1055.6	13.77
16: 5: 0	104.6	765.2	1098.3	1083.4	14.83
16:18:35	109.3	771.9	1118.3	1104.2	14.12
17: 5: 4	122.2	804.7	1191.1	1177.4	13.67
* 9.1 ******NOV.	18*				
12:51:18	30.2	497.8	587.9	588.6	-0.71
13:29:59	30.2	493.6	584.0	584.4	-0.37
13:52:35	50.1	546.9	695.8	697.4	-1.60
14:16:33	70.8	590.6	803.7	804.1	-0.42
14:38:36	80.6	610.9	855.4	854.1	1.22
14:47:36	90.2	633.5	908.7	906.1	2.53
15: 2:29	99.8	650.8	959.3	953.1	6.19
15:21:34	99.5	697.6	1006.6	999.1	7.52
15:38:27	99.3	738.4	1046.3	1039.5	6.80
15:53:39	99.1	772.2	1079.7	1073.1	6.57
*10.1 ******DEC.	8*				
11:25:18	29.9	506.2	589.1	595.8	-6.70
11:47:24	40.3	545.0	658.4	666.0	-7.55
12: 9:36	60.2	583.8	757.5	764.9	-7.39
12:39: 8	80.1	632.1	869.1	873.9	-4.78
13:27: 2	80.1	738.4	978.9	980.5	-1.52
13:32:52	80.1	748.4	989.3	990.6	-1.21
13:43:16	80.0	755.8	996.1	997.8	-1.64
13:46: 3	80.0	758.9	1000.0	1000.9	-0.87
13:52:47	80.0	764.6	1005.2	1006.7	-1.43
*11.1 ******JAN.	13*				
13:49:36	30.0	527.7	505.4	617.9	-12.46
14:12:27	50.2	575.7	711.5	726.7	-15.19
14:34:40	80.3	642.9	869.9	885.2	-15.23
14:53:30	79.9	679.1	906.3	920.3	-13.99
15:17: 6	79.6	720.1	947.9	960.5	-12.55
15:27:52	79.4	738.2	966.3	978.2	-11.91
15:36:42	79.3	752.5	980.6	992.4	-11.80
*12.1 ******JAN.	27*				
11:20:34	29.9	503.6	581.0	593.3	-12.30
11:44:22	50.1	566.6	699.8	717.1	-17.30
12: 8:16	81.0	632.4	859.0	876.9	-17.92
12:33: 5	81.0	685.2	913.2	930.0	-16.82
12:59:52	80.8	743.6	972.6	988.0	-15.40
13: 9:19	80.0	756.9	983.9	998.9	-14.99
*13.1 ******FEB.	10*				
10:33:25	30.1	509.1	592.4	599.6	-7.20
10:54: 5	50.3	569.8	712.1	720.9	-8.77
11:14: 1	59.9	599.8	770.3	780.0	-9.76
11:25:44	69.9	632.6	833.8	843.3	-9.48
11:40:22	80.2	664.1	897.2	906.4	-9.21
12:15:12	79.9	716.3	950.1	957.6	-7.44
13:47: 8	80.1	785.7	1021.1	1028.3	-7.20
*14.1 ******MAR.	9*				
11:17:50	30.0	529.9	605.2	620.1	-14.90
11:40: 0	50.3	586.1	717.3	737.2	-19.86
12: 2:29	80.3	665.6	885.3	908.0	-22.63
12:25: 4	80.0	696.5	916.5	938.1	-21.56
12:49:10	79.7	733.3	954.2	974.4	-20.13
13:18:51	79.7	777.6	1000.5	1018.7	-18.10
13:34:23	80.1	781.5	1003.7	1024.0	-20.33

Table D.3. (continued)

RUN NO. DATE TIME	Q(KW)/ROD	TCS	TCSM	TCSMC	DIFFERENCE
*15.1 ******MAR.	23*				
10:32: 1	30.1	494.7	577.0	585.2	-8.16
10:55:54	50.2	547.2	685.0	698.2	-13.21
11:40: 2	80.4	686.7	913.4	929.5	-16.03
12:21:39	100.3	778.0	1065.7	1082.6	-16.87
13: 8:45	100.2	784.2	1071.7	1088.6	-16.93
*16.1 ******APR.	27*				
12:28:55	30.2	520.6	596.2	611.2	-15.04
12:55:12	50.4	574.0	704.5	725.4	-20.90
13:21:11	80.5	647.4	865.1	890.4	-25.24
14: 0:52	100.5	748.9	1051.3	1054.0	-22.74
14:42:58	100.4	791.8	1075.7	1095.7	-23.00
*17.1 ******MAY	26*				
11:23: 5	30.0	529.2	604.5	619.3	-14.81
11:45:13	50.4	585.2	714.4	736.6	-22.19
12: 9:15	88.0	703.5	940.5	969.7	-29.16
12:35:46	100.3	789.5	1067.8	1094.3	-26.51
12:52:17	100.3	819.1	1097.5	1123.9	-26.35
13:10:40	100.2	834.7	1111.6	1139.6	-28.03
13:13:25	100.2	834.2	1111.3	1139.1	-27.71
*18.1 ******JUNE	15*				
16:53:51	30.1	529.3	606.4	619.7	-13.31
17:17:18	50.2	533.4	765.2	784.3	-19.19
17:36:32	80.3	748.1	967.3	990.9	-23.58
17:54:39	80.4	775.4	996.9	1018.8	-21.90
18: 7:50	80.4	775.7	997.3	1018.8	-21.59
*19.1 ******JUNE	29*				
12: 8:50	30.2	527.8	605.9	618.5	-12.60
12:31:59	50.3	631.7	764.3	782.8	-18.45
13: 6:26	80.3	726.9	945.8	969.5	-23.69
13:31:46	100.3	817.2	1096.3	1122.2	-25.85
13:40:39	100.3	821.3	1100.4	1126.3	-25.88
*20.1 ******AUG.	22*				
11:41:52	30.0	552.9	625.9	643.0	-17.11
12: 5:46	49.9	626.1	749.9	775.9	-26.05
12:35:35	79.9	743.3	952.6	984.7	-32.04
13: 1:53	100.3	808.2	1077.1	1113.1	-35.98
13:21:45	100.2	809.2	1078.4	1113.9	-35.47
*21.1 ******SEP.	21*				
11:49:40	30.2	545.0	625.1	635.6	-10.50
12:10:45	49.6	629.9	762.3	778.9	-16.62
12:43:59	69.4	733.0	922.2	942.5	-20.34
15:20:14	90.3	802.2	1051.7	1076.0	-24.31
15:22: 6	90.2	803.1	1052.1	1076.8	-24.74
*22.1 ******OCT.	12*				
11:48:40	29.8	545.8	622.9	635.1	-12.14
12:17:55	77.0	716.0	921.4	948.6	-27.23
12:29:23	100.6	794.2	1068.8	1099.8	-31.03
12:50:23	100.5	830.6	1106.8	1136.2	-29.48
13: 0:25	100.5	832.4	1108.0	1138.1	-30.03
*23.1 ******NOV.	30*				
11:22: 7	29.6	527.3	605.5	616.3	-10.76
11:41:15	49.7	598.7	731.1	748.1	-16.95
11:58:35	69.9	685.3	873.6	896.1	-22.48
12:19:17	100.4	795.5	1074.1	1100.6	-26.57
12:38:44	100.3	823.7	1103.0	1128.7	-25.74
12:44:28	100.3	824.4	1104.1	1129.4	-25.38
*23.2 ******DEC.	15*				
10: 5:18	29.7	532.9	612.1	621.9	-9.85
10:27:17	60.4	657.2	819.0	838.9	-19.93
10:39: 4	60.3	667.5	830.2	849.2	-18.95
11: 9:20	100.5	815.1	1095.8	1120.6	-24.76
11:16:15	100.5	823.3	1104.0	1128.8	-24.78
11:23:26	100.4	823.2	1104.0	1128.6	-24.63

Table D.3. (continued)

RUN NO. DATE TIME	Q(KW)/ROD	TCS	TCSM	TCSMC	DIFFERENCE
#23.3 ******JAN. 19*					
15: 7: 0	29.5	577.5	654.9	666.1	-11.17
15:28:51	49.5	667.5	799.4	816.4	-16.99
15:48:34	79.3	758.4	976.1	998.3	-22.24
16:13:41	100.4	923.2	1102.5	1128.4	-25.94
16:17:13	100.4	822.6	1101.9	1127.8	-25.92
#24.1 ******FEB. 16*					
10:42: 1	29.8	543.5	624.8	632.9	-8.13
11: 8:40	50.3	649.3	786.2	800.5	-14.41
11:28:20	70.3	719.6	913.7	931.6	-17.87
12:29: 8	100.4	817.9	1100.3	1123.2	-22.91
12:50:11	100.4	819.6	1101.8	1124.8	-22.99

BEST FIT PARAMETERS FOR AKBN:
WHERE,

AKBN = C(1)+C(2)*T+C(3)*T**2+C(4)*T**3

C(1)= 0.21236206E 02
C(2)=-0.77911168E-02
C(3)= 0.81915749E-06
C(4)= 0.43654058E-09

TOTAL ERROR (SUM OF SQUARED DIFFERENCES)= 0.71583063E 05

VARIANCE OF FIT= 0.33765576E 03

Appendix E

EXAMPLE OF ORTCAL — PART III OUTPUT

```
**************************************************************************
*************************** CASE INFORMATION ***************************
**************************************************************************

THERMOCOUPLES NO. TE-301DJ  AND TE-301MJ

A.CALIBRATION RUNS NO.   1.1      DATE: MAY    5       TIME:   0:32:52
                         1.2            MAY    5              17:32:27
                         1.3            MAY    5              21:43:38
                         1.4            MAY    6              14:51:16
                         8.1            SEP.   9              19: 2:25

B.RADIAL NODING STRUCTURE FOR THIS RUN:
  TOTAL NUMBER OF NODES =  12
  NODING BREAK-DOWN.
                    MAGNESIUM OXIDE CORE NODES     1 THROUGH  4
                    INCONEL-600 HEATER NODES       5 THROUGH  6
                    BORON NITRIDE INSUL. NODES     7 THROUGH  9
                    INNER S.S.SHEATH NODES        10 THROUGH 12

C.FIT PARAMETERS FOR THE EFFECTIVE THERMAL CONDUCTIVITY OF MAGNESIUM OXIDE
  WHERE,
       KMGO(T)= C(1) +C(2)*T +C(3)*T**2 +C(4)*T**3 +C(5)*T**4

  REGRESSION RESULTS:
  (SPECIFICALLY FOR TE-301DJ AND TE-301MJ )

                    C( 1) =  0.77072439E 01
                    C( 2) = -0.99114478E-02
                    C( 3) =  0.79930423E-05
                    C( 4) = -0.28395633E-08
                    C( 5) =  0.37459565E-12

  TOTAL NUMBER OF DATA POINTS =   605
  VARIANCE OF FIT (I.E. SUM OF SQUARED ERROR) =  0.13066184E 05
  VARIANCE OF FIT DIVIDED BY TOTAL NO. OF DATA POINTS =  0.21776962E 02

D.MAGNESIUM CORE POROSITY (AS ESTIMATED BY THE MODIFIED RUSSELL EQN) = 0.16652715E 00
```

```
**************************************************************************
************************** TRANSIENT RESULTS *****************************
**************************************************************************

TE-301DJ AND TE-301MJ
CALIBRATION RUN NO.      1.1      DATE: MAY    5       TIME:   0:32:52

TIME-TEMPERATURE-NODE TABLE:
     TIME HAS UNITS OF SEC
     Q HAS UNITS OF BTU/SEC/FT (=PFA*QAVG)
     TEMPERATURE HAS UNITS OF DEG F
     INTERFACE FLUX (PHI) HAS UNITS OF BTU/HR/FT**2
     TCSM IS THE OBSERVED CENTER TC TEMPERATURE IN DEG F
     TCTR IS THE CALCULATED CENTER TC TEMPERATURE
```

TIME--	0.0	0.0500	0.1000	0.1500	0.2000	0.2500	0.3000	0.3500	0.4000	0.4500	0.5000	0.5500
NODE												
1	623.0283	622.9988	622.8105	622.3330	621.4807	620.2168	618.5403	616.4736	614.0532	611.3206	608.3179	605.0864
2	623.0283	622.8577	621.8665	619.9265	617.1836	613.8477	610.1067	606.1023	601.9368	597.6790	593.3767	589.0520
3	623.0283	622.3596	618.8931	613.8337	608.1431	602.3198	596.5789	591.0071	585.6282	580.4434	575.4441	570.8167
4	623.0283	620.9026	611.0759	601.3157	592.6899	585.3762	578.2312	571.9695	566.1689	560.7439	555.6326	550.7900
5	623.0283	618.5225	599.5608	587.6719	578.5925	570.9536	564.2029	558.0789	552.4426	547.1958	542.2761	537.6323
6	612.7756	608.6992	591.4028	580.2202	571.5342	564.1523	557.5903	551.6174	546.1160	540.9910	536.1877	531.6523
7	590.4243	588.2983	578.4587	569.5447	561.9106	555.1426	549.0007	543.3489	538.1211	533.2319	528.6418	524.3003
8	568.5586	567.5452	562.1270	555.8445	549.7593	543.9446	538.4707	533.3352	528.5448	524.0295	519.7710	515.7197
9	551.1790	550.7515	547.5515	543.1042	538.3123	533.3406	528.5037	523.8933	519.5540	515.4106	511.4949	507.7373
10	534.3118	534.3330	532.5007	529.4685	525.8196	521.6016	517.4072	513.3357	509.5210	505.7864	502.2581	498.8232
11	517.1152	517.6008	516.5322	514.5237	511.8171	508.1589	504.6116	501.1282	497.9141	494.6130	491.5403	488.4597
12	501.5422	502.5986	501.7473	500.3799	498.3154	494.8752	491.9490	489.0183	485.4321	483.4588	480.9094	478.1448
Q	5.18211	4.05010	0.0	0.0	0.0	0.0	0.0	0.0	0.0	0.0	0.0	0.0
PHI	176387.6	166261.9	170476.5	164932.1	159960.4	162097.9	153066.6	146619.9	138156.4	135048.1	128249.0	125139.0
TCSM	621.7	622.9	622.8	622.8	621.9	621.4	621.2	620.9	620.1	618.9	617.7	615.9
TCTR	623.0	623.0	623.0	623.0	623.0	623.0	623.0	622.3	622.4	621.5	620.3	618.8

TIME--	0.6000	0.6500	0.7000	0.7500	0.8000	0.8500	0.9000	0.9500	1.0000	1.0500	1.1000	1.1500
NODE												
1	601.6646	598.0876	594.3860	590.5857	586.7104	582.7805	578.8137	574.8250	570.8279	566.8345	562.8555	558.9004
2	584.7566	580.4744	576.2258	572.0161	567.8494	563.7295	559.6584	555.6414	551.6824	547.7849	543.9517	540.1845
3	565.9487	561.4272	557.0391	552.7695	548.6084	544.5491	540.5889	536.7258	532.9600	529.2905	525.7158	522.2314
4	546.1812	541.7720	537.5359	533.4448	529.4871	525.6545	521.9456	518.3579	514.8916	511.5420	508.2983	505.1545
5	533.2312	529.0271	524.9937	521.0974	517.3347	513.7026	510.2039	506.8374	503.6025	500.4900	497.4834	494.5750
6	527.3584	523.2539	519.3135	515.5005	511.8223	508.2791	504.8728	501.6043	498.4731	495.4651	492.5598	489.7522
7	520.1885	516.2446	512.4517	508.7681	505.2195	501.8105	498.5420	495.4158	492.4336	489.5691	486.8008	484.1262
8	511.8806	508.1646	504.5793	501.0701	497.7043	494.4829	491.4055	488.4731	485.6897	483.0112	480.4133	477.9045
9	504.1794	500.6829	497.3030	493.9570	490.7805	487.7507	484.8657	482.1321	479.5496	477.0500	474.6118	472.2603
10	495.5876	492.3154	489.1619	485.9788	483.0278	480.2237	477.5623	475.0583	472.7117	470.4075	468.1401	465.9643
11	485.6125	482.5491	479.6597	476.6252	473.9783	471.4429	469.0620	466.8435	464.7898	462.6982	460.6157	458.6504
12	475.7244	472.7834	470.1865	467.2419	464.9890	462.7349	460.6526	458.7429	457.0056	455.0942	453.1821	451.4429
Q	0.0	0.0	0.0	0.0	0.0	0.0	0.0	0.0	0.0	0.0	0.0	0.0
PHI	119025.1	119309.1	114701.3	114756.8	107836.8	104596.4	100574.3	96454.3	92265.8	90785.9	88821.4	85649.4
TCSM	613.7	611.5	608.8	606.1	603.4	600.5	597.3	594.4	591.0	587.3	583.6	580.2
TCTR	616.6	614.2	611.5	608.5	605.3	601.9	598.3	594.6	590.8	586.9	583.0	579.0

TIME--	1.2000	1.2500	1.3000	1.3500	1.4000	1.4500	1.5000	1.5500	1.6000	1.6500	1.7000	1.7500
NODE												
1	554.9773	551.0928	547.2527	543.4626	539.7271	536.0498	532.4355	528.8872	525.4067	521.9968	518.6594	515.3955
2	536.4863	532.8577	529.2996	525.8127	522.3992	519.0633	515.7971	512.6111	509.5037	506.4741	503.5215	500.6443
3	518.8345	515.5239	512.2959	509.1501	506.0894	503.1118	500.2183	497.4102	494.6851	492.0388	489.4670	486.9641
4	502.1074	499.1501	496.2778	493.4963	490.8044	488.2007	485.6877	483.2646	480.9229	478.6533	476.4492	474.3038
5	491.7642	489.0420	486.4021	483.8594	481.4102	479.0498	476.7847	474.6123	472.5122	470.4766	468.4976	466.5608
6	487.0432	484.4209	481.8804	479.4431	477.1011	474.8474	472.6936	470.6343	468.6392	466.7051	464.8228	462.9741
7	481.5520	479.0593	476.6458	474.3459	472.1409	470.0229	468.0105	466.0920	464.2239	462.4109	460.6418	458.8949
8	475.4980	473.1619	470.9009	468.7751	466.7368	464.7798	462.9412	461.1904	459.4614	457.7844	456.1404	454.4988
9	470.0176	467.8264	465.7085	463.7593	461.8772	460.0723	458.4045	456.8115	455.2009	453.6465	452.1113	450.5552
10	463.9104	461.8743	459.9158	458.1858	456.4753	454.8413	453.3789	451.9624	450.4636	449.0457	447.6238	446.1460
11	456.8291	454.9563	453.1868	451.7605	450.2327	448.8008	447.6394	446.3916	444.9790	443.7292	442.4221	441.0049
12	449.8770	448.1362	446.5688	445.5239	444.1299	442.9099	442.0383	440.9919	439.5957	438.5496	437.3279	435.9314
Q	0.0	0.0	0.0	0.0	0.0	0.0	0.0	0.0	0.0	0.0	0.0	0.0
PHI	82164.2	81242.3	78352.6	72302.4	71980.9	69301.5	64255.0	62935.0	63904.2	60451.6	60076.3	60410.8
TCSM	576.3	572.6	569.2	565.4	561.7	558.1	554.7	551.2	547.8	544.4	541.1	537.7
TCTR	575.1	571.1	567.1	563.1	559.1	555.2	551.3	547.5	543.7	539.9	536.3	532.6

TIME--	1.8000	1.8500	1.9000	1.9500	2.0000	2.0500	2.1000	2.1500	2.2000	2.2500	2.3000	2.3500
NODE												
1	512.2063	509.0903	506.0481	503.0791	500.1831	497.3601	494.6084	491.9282	489.3184	486.7781	484.3076	481.9053
2	497.8381	495.1028	492.4360	489.8386	487.3091	484.8472	482.4519	480.1213	477.8555	475.6538	473.5164	471.4435
3	484.5251	482.1497	479.8379	477.5891	475.4043	473.2827	471.2205	469.2161	467.2710	465.3879	463.5652	461.8022
4	472.2046	470.1660	468.1870	466.2664	464.4065	462.6052	460.8518	459.1506	457.5076	455.9255	454.4011	452.9316
5	464.6667	462.8330	461.0576	459.3376	457.6777	456.0737	454.5059	452.9893	451.5344	450.1428	448.8042	447.5166
6	461.1658	459.4229	457.7363	456.1060	454.5364	453.0210	451.5327	450.0991	448.7317	447.4292	446.1768	444.9724
7	457.1868	455.5522	453.9739	452.4492	450.9883	449.5776	448.1782	446.8433	445.5815	444.3862	443.2339	442.1257
8	452.8994	451.3960	449.9395	448.5334	447.1978	445.9036	444.5935	443.3735	442.2361	441.1636	440.1201	439.1179
9	449.0557	447.6814	446.3350	445.0381	443.8203	442.6306	441.3882	440.2844	439.2676	438.3103	437.3616	436.4551
10	444.7600	443.5479	442.3191	441.1438	440.0652	438.9875	437.7991	436.8472	435.9753	435.1504	434.2996	433.5002
11	439.7673	438.7837	437.6709	436.6406	435.7402	434.7795	433.6072	432.8965	432.2041	431.5332	430.7761	430.1067
12	434.8835	434.1853	433.1370	432.2632	431.5640	430.6902	429.4666	429.1169	428.5923	428.0676	427.3677	426.8428
Q	0.0	0.0	0.0	0.0	0.0	0.0	0.0	0.0	0.0	0.0	0.0	0.0
PHI	57101.8	52755.1	53220.1	50890.1	48067.3	47598.5	49426.5	42477.2	41232.2	39625.0	39587.5	37399.4
TCSM	534.1	530.9	527.6	524.2	520.8	518.1	515.1	512.2	509.3	506.7	503.8	501.1
TCTR	529.1	525.6	522.2	518.9	515.6	512.4	509.3	506.2	503.3	500.4	497.5	494.8

TIME--	2.4000	2.4500	2.5000	2.5500	2.6000	2.6500	2.7000	2.7500	2.8000	2.8500	2.9000	2.9500
NODE												
1	479.5715	477.3054	475.1050	472.9690	470.8960	468.8848	466.9336	465.0410	463.2056	461.4265	459.7017	458.0293
2	469.4336	467.4841	465.5935	463.7593	461.9792	460.2527	458.5784	456.9543	455.3811	453.8562	452.3779	450.9445
3	460.0967	458.4429	456.8381	455.2813	453.7700	452.3044	450.8843	449.5076	448.1746	446.8835	445.6318	444.4153
4	451.5107	450.1304	448.7874	447.4819	446.2170	444.9897	443.8035	442.6541	441.5435	440.4670	439.4209	438.3992
5	446.2703	445.0515	443.8623	442.7078	441.5698	440.5078	439.4556	438.4526	437.4785	436.5327	435.6091	434.7000
6	443.8049	442.6567	441.5354	440.4487	439.3987	438.3826	437.4070	436.4573	435.5469	434.6602	433.7917	432.9316
7	441.0476	439.9768	438.9319	437.9229	436.9495	436.0093	435.1118	434.2314	433.3955	432.5750	431.7666	430.9578
8	438.1343	437.1384	436.1738	435.2498	434.3616	433.5032	432.6931	431.8831	431.1318	430.3779	429.6296	428.8694
9	435.5510	434.6130	433.7214	432.8755	432.0642	431.2793	430.5513	429.7983	429.1296	428.4287	427.7305	427.0054
10	432.6777	431.7881	430.9827	430.2280	429.5034	428.7996	428.1697	427.4683	426.9055	426.2498	425.6028	424.9063
11	429.3611	428.4983	427.8115	427.1699	426.5474	425.9358	425.4348	424.7620	424.3599	423.7185	423.1274	422.4438
12	426.1431	425.2681	424.7432	424.2178	423.6926	423.1675	422.8171	422.1169	421.9417	421.2410	420.7156	420.0149
Q	0.0	0.0	0.0	0.0	0.0	0.0	0.0	0.0	0.0	0.0	0.0	0.0
PHI	37484.3	38205.5	35231.0	33958.3	32887.9	31936.6	29693.1	31176.3	25902.9	29340.6	28017.3	28795.7
TCSM	498.7	496.3	493.7	491.3	488.2	486.8	484.7	482.5	480.4	478.3	476.1	474.0
TCTR	492.1	489.5	486.9	484.4	482.0	479.7	477.4	475.2	473.1	471.0	469.0	467.0

TIME--	3.0000	3.0500	3.1000	3.1500	3.2000	3.2499	3.2999	3.3499	3.3999	3.4499	3.4999	3.5499
NODE												
1	456.4087	454.8364	453.3118	451.8313	450.3943	448.9985	447.6428	446.3257	445.0461	443.8035	442.5974	441.4272
2	449.5532	448.2014	446.8867	445.6064	444.3604	443.1477	441.9688	440.8220	439.7085	438.6274	437.5806	436.5685
3	443.2307	442.0750	440.9441	439.8401	438.7637	437.7163	436.6975	435.7070	434.7451	433.8157	432.9204	432.0627
4	437.3987	436.4121	435.4417	434.4905	433.5671	432.6707	431.7993	430.9519	430.1321	429.3477	428.6008	427.8979
5	433.8042	432.9119	432.0320	431.1702	430.3403	429.5378	428.7568	427.9968	427.2668	426.5793	425.9324	425.3362
6	432.0813	431.2273	430.3877	429.5664	428.7825	428.0256	427.2959	426.5669	425.8836	425.2422	424.6467	424.1064
7	430.1570	429.3418	428.5459	427.7705	427.0413	426.3362	425.6431	424.9702	424.3357	423.7583	423.2249	422.7527
8	428.1174	427.3350	426.5864	425.8606	425.1968	424.5488	423.9023	423.2793	422.7056	422.2026	421.7407	421.3521
9	426.2952	425.5310	424.8286	424.1492	423.5537	422.9551	422.3467	421.7693	421.2563	420.8313	420.4370	420.1335
10	424.2424	423.4819	422.8433	422.2161	421.7122	421.1631	420.5908	420.0681	419.6345	419.3115	418.9944	418.8020
11	421.8396	421.0488	420.5190	419.9514	419.5869	419.0745	418.5315	418.0837	417.7646	417.5881	417.3552	417.3230
12	419.4890	418.6130	418.2625	417.7368	417.5615	417.0354	416.5095	416.1589	415.9836	415.9836	415.8083	415.9836
Q	0.0	0.0	0.0	0.0	0.0	0.0	0.0	0.0	0.0	0.0	0.0	0.0
PHI	27338.6	29451.6	25706.9	25839.1	22590.4	23926.8	23734.2	22078.1	19921.0	17408.3	17374.0	13932.8
TCSM	472.3	470.5	468.6	467.1	465.2	463.4	461.5	459.6	458.0	456.8	455.3	454.1
TCTR	465.1	463.3	461.5	459.8	458.1	456.5	454.9	453.4	451.9	450.5	449.1	447.7

TIME--	3.5999	3.6499	3.6999	3.7499	3.7999	3.8499	3.8999	3.9499	3.9999	4.0499	4.0999	4.1499
NODE												
1	440.2937	439.1975	438.1367	437.1116	436.1204	435.1609	434.2307	433.3289	432.4541	431.6050	430.7803	429.9807
2	435.5933	434.6550	433.7510	432.8760	432.0281	431.2043	430.4026	429.6208	428.8596	428.1196	427.4016	426.7075
3	431.2449	430.4631	429.7073	428.9709	428.2515	427.5454	426.8533	426.1743	425.5127	424.8708	424.2524	423.6634
4	427.2395	426.6125	425.9910	425.3730	424.7634	424.1570	423.5544	422.9629	422.3916	421.8423	421.3220	420.8340
5	424.7881	424.2581	423.7080	423.1519	422.6018	422.0474	421.4910	420.9521	420.4390	419.9512	419.4993	419.0850
6	423.6160	423.1313	422.6064	422.0745	421.5503	421.0166	420.4800	419.9670	419.4834	419.0271	418.6128	418.2388
7	422.3315	421.8940	421.3845	420.8760	420.3801	419.8655	419.3477	418.8662	418.4197	418.0010	417.6335	417.3038
8	421.0115	420.6121	420.0952	419.6089	419.1426	418.6394	418.1387	417.6978	417.2966	416.9224	416.6143	416.3499
9	419.8691	419.4861	418.9333	418.4727	418.0354	417.5322	417.0454	416.6521	416.2976	415.9653	415.7217	415.5145
10	418.6260	418.2290	417.5952	417.1843	416.7822	416.2622	415.7937	415.4736	415.1770	414.8938	414.7390	414.6013
11	417.2471	416.7576	415.9553	415.6750	415.3132	414.7334	414.3022	414.1111	413.8843	413.6577	413.6418	413.5837
12	415.9836	415.2820	414.2297	414.2297	413.8792	413.1775	412.8267	412.8267	412.6511	412.4758	412.6511	412.6511
Q	0.0	0.0	0.0	0.0	0.0	0.0	0.0	0.0	0.0	0.0	0.0	0.0
PHI	13704.4	18388.9	22283.7	15664.0	16731.1	19242.2	17176.6	13913.2	13950.8	13396.0	10135.9	10100.0
TCSM	453.2	452.0	450.6	449.4	448.1	446.7	445.7	444.5	443.3	442.2	441.2	439.8
TCTR	446.4	445.1	443.9	442.7	441.5	440.4	439.3	438.2	437.2	436.2	435.2	434.3

TIME--	4.1999	4.2499	4.2999	4.3499	4.3999	4.4499	4.4999	4.5499	4.5999	4.6499	4.6999	4.7499
NODE												
1	429.2061	428.4570	427.7324	427.0320	426.3550	425.7030	425.0662	424.4531	423.8601	423.2859	422.7302	422.1917
2	426.0381	425.3943	424.7739	424.1748	423.5947	423.0322	422.4883	421.9612	421.4502	420.9556	420.4758	420.0093
3	423.0964	422.5576	422.0386	421.5334	421.0405	420.5625	420.0994	419.6501	419.2151	418.7927	418.3813	417.9793
4	420.3782	419.9438	419.5188	419.0947	418.6775	418.2761	417.8884	417.5090	417.1421	416.7874	416.4353	416.0874
5	418.7058	418.3374	417.9668	417.5845	417.2100	416.8564	416.5159	416.1775	415.8542	415.5405	415.2207	414.9021
6	417.8999	417.5623	417.2141	416.8462	416.4915	416.1636	415.8457	415.5254	415.2239	414.9299	414.6221	414.3171
7	417.0181	416.7119	416.3840	416.0261	415.6943	415.3979	415.1057	414.8022	414.5269	414.2546	413.9558	413.6553
8	416.1135	415.8308	415.5156	415.1582	414.8547	414.5994	414.3315	414.0405	413.7986	413.5474	413.2489	412.9735
9	415.3303	415.0554	414.7419	414.3738	414.1077	413.8965	413.6458	413.3586	413.1555	412.9187	412.6086	412.3516
10	414.4756	414.1853	413.8638	413.4702	413.2688	413.1169	412.8735	412.5813	412.4399	412.2092	411.8682	411.6436
11	413.5242	413.1599	412.8193	412.3730	412.3074	412.2363	411.9688	411.6533	411.6304	411.3748	410.9619	410.8123
12	412.6511	412.1248	411.7739	411.2476	411.4229	411.4229	411.0720	410.7209	410.8965	410.5454	410.0188	410.0188
Q	0.0	0.0	0.0	0.0	0.0	0.0	0.0	0.0	0.0	0.0	0.0	0.0
PHI	9458.8	12994.6	12508.4	13968.7	8980.7	8804.5	10896.3	11283.0	7350.7	10166.9	11991.1	8584.2
TCSM	438.7	437.9	436.8	435.8	434.9	434.2	433.5	432.8	431.9	431.2	430.5	429.8
TCTR	433.4	432.5	431.6	430.8	430.0	429.2	428.5	427.8	427.1	426.4	425.7	425.1

TIME--	4.7999	4.8499	4.8999	4.9499	4.9999	5.0499	5.0999	5.1499	5.1999	5.2499	5.2999	5.3499
NODE												
1	421.6699	421.1636	420.6719	420.1948	419.7314	419.2810	418.8442	418.4207	418.0107	417.6150	417.2329	416.8652
2	419.5554	419.1140	418.6846	418.2659	417.8584	417.4629	417.0811	416.7136	416.3605	416.0220	415.6970	415.3843
3	417.5850	417.2009	416.8262	416.4595	416.1028	415.7605	415.4343	415.1233	414.8279	414.5474	414.2778	414.0173
4	415.7456	415.4124	415.0876	414.7678	414.4575	414.1697	413.9014	413.6487	413.4131	413.1919	412.9739	412.7588
5	414.5911	414.2891	413.9946	413.7014	413.4216	413.1760	412.9497	412.7368	412.5435	412.3623	412.1716	411.9819
6	414.0215	413.7344	413.4548	413.1731	412.9099	412.6899	412.4861	412.2930	412.1223	411.9607	411.7800	411.6013
7	413.3862	413.1162	412.8535	412.5828	412.3403	412.1560	411.9780	411.8079	411.6641	411.5244	411.3489	411.1819
8	412.7141	412.4629	412.2180	411.9546	411.7402	411.6067	411.4543	411.3074	411.1973	411.0796	410.8979	410.7441
9	412.1111	411.8770	411.6475	411.3857	411.2058	411.1338	410.9976	410.8696	410.7961	410.6936	410.4915	410.3550
10	411.4268	411.2122	411.0000	410.7317	410.6084	410.6267	410.4905	410.3853	410.3628	410.2690	410.0195	409.9182
11	410.6235	410.4304	410.2373	409.9424	409.9299	410.0942	409.9033	409.8337	409.8938	409.7852	409.4304	409.4182
12	409.8433	409.6677	409.4922	409.1411	409.3167	409.6677	409.3167	409.3167	409.4922	409.3167	408.7900	408.9656
Q	0.0	0.0	0.0	0.0	0.0	0.0	0.0	0.0	0.0	0.0	0.0	0.0
PHI	9037.8	8843.6	8656.0	9855.3	6037.2	3424.9	7536.7	5591.7	3751.2	5663.5	8709.8	4301.1
TCSM	429.1	428.8	428.4	427.9	427.2	426.5	425.8	424.9	424.0	423.5	423.2	422.6
TCTR	424.5	423.9	423.3	422.8	422.2	421.7	421.2	420.7	420.2	419.7	419.3	418.9

TIME--	5.3999	5.4499	5.4999	5.5499	5.5999	5.6499	5.6999	5.7499	5.7999	5.8499	5.8999	5.9499
NODE												
1	416.5095	416.1663	415.8359	415.5166	415.2087	414.9121	414.6262	414.3503	414.0840	413.8267	413.5771	413.3352
2	415.0825	414.7903	414.5081	414.2358	413.9741	413.7222	413.4795	413.2458	413.0190	412.7971	412.5801	412.3672
3	413.7634	413.5181	413.2808	413.0530	412.8352	412.6252	412.4231	412.2271	412.0349	411.8420	411.6497	411.4597
4	412.5486	412.3440	412.1482	411.9626	411.7869	411.6165	411.4514	411.2883	411.1238	410.9500	410.7747	410.6033
5	411.7949	411.6155	411.4463	411.2886	411.1421	410.9946	410.8518	410.7065	410.5547	410.3840	410.2170	410.0574
6	411.4255	411.2583	411.1033	410.9597	410.8284	410.6897	410.5586	410.4204	410.2727	410.0991	409.9358	409.7834
7	411.0181	410.8650	410.7263	410.6006	410.4871	410.3557	410.2371	410.1050	409.9592	409.7764	409.6196	409.4761
8	410.5918	410.4551	410.3359	410.2312	410.1375	410.0076	409.9048	409.7732	409.6250	409.4224	409.2803	409.1492
9	410.2129	410.0933	409.9939	409.9092	409.8347	409.6963	409.6128	409.4749	409.3208	409.0889	408.9731	408.8542
10	409.7847	409.6887	409.6152	409.5549	409.5027	409.3391	409.2900	409.1313	408.9670	408.6841	408.6260	408.5190
11	409.2830	409.2249	409.1868	409.1567	409.1311	408.9026	408.9294	408.7102	408.5330	408.1545	408.2361	408.1248
12	408.7900	408.7900	408.7900	408.7900	408.7900	408.4390	408.6145	408.2634	408.0879	407.5610	407.9121	407.7365
Q	0.0	0.0	0.0	0.0	0.0	0.0	0.0	0.0	0.0	0.0	0.0	0.0
PHI	5924.6	4700.8	4288.0	3966.6	3689.2	6202.0	2814.6	6017.6	5404.1	8199.1	2315.3	4792.2
TCSM	422.1	421.9	421.4	420.9	420.4	420.2	419.5	419.1	418.8	418.4	417.7	417.4
TCTR	418.4	418.0	417.6	417.2	416.9	416.5	416.2	415.8	415.5	415.2	414.9	414.6

TIME--	5.9999	6.0499	6.0999	6.1499	6.1999	6.2499	6.2999	6.3499	6.3999	6.4499	6.4999	6.5499
NODE												
1	413.1001	412.8713	412.6484	412.4338	412.2268	412.0269	411.8340	411.6465	411.4636	411.2842	411.1067	410.9314
2	412.1592	411.9570	411.7627	411.5771	411.4006	411.2312	411.0654	410.9014	410.7371	410.5706	410.4031	410.2358
3	411.2751	411.0984	410.9326	410.7803	410.6377	410.4963	410.3530	410.2043	410.0476	409.8840	409.7180	409.5557
4	410.4419	410.2922	410.1619	410.0479	409.9397	409.8203	409.6899	409.5435	409.3809	409.2109	409.0435	408.8879
5	409.9141	409.7856	409.6846	409.6038	409.5164	409.4009	409.2683	409.1133	408.9360	408.7583	408.5920	408.4475
6	409.6516	409.5366	409.4541	409.3518	409.3120	409.1919	409.0542	408.8901	408.7019	408.5200	408.3569	408.2227
7	409.3606	409.2629	409.2061	409.1675	409.0908	408.9570	408.8105	408.6316	408.4260	408.2422	408.0869	407.9688
8	409.0566	408.9807	408.9604	408.9490	408.8638	408.6992	408.5405	408.3386	408.1086	407.9302	407.7903	407.6985
9	408.7898	408.7366	408.7583	408.7712	408.6606	408.4521	408.2849	408.0535	407.7971	407.6360	407.5176	407.4592
10	408.4980	408.4697	408.5554	408.5908	408.4226	408.1431	407.9778	407.6990	407.4099	407.2903	407.2056	407.1970
11	408.1799	408.1763	408.3691	408.4109	408.1106	407.7163	407.5933	407.2246	406.8958	406.8801	406.8435	406.9141
12	407.9121	407.9121	408.2632	408.2632	407.7366	407.2097	407.2097	406.6831	406.3318	406.5076	406.5076	406.6831
Q	0.0	0.0	0.0	0.0	0.0	0.0	0.0	0.0	0.0	0.0	0.0	0.0
PHI	2303.9	2857.0	-39.2	1600.7	5828.3	7260.9	4146.1	7632.9	7285.4	3433.0	3630.5	1904.2
TCSM	417.2	416.5	416.2	416.2	416.0	415.6	415.8	415.6	415.3	415.1	414.9	414.4
TCTR	414.4	414.1	413.8	413.6	413.3	413.1	412.9	412.6	412.4	412.2	412.0	411.8

TIME--	6.5999	6.6499	6.6999	6.7499	6.7999	6.8499	6.8999	6.9499	6.9999	7.0499	7.0999	7.1499
NODE												
1	410.7583	410.5881	410.4216	410.2588	410.1018	409.9502	409.8037	409.6626	409.5259	409.3936	409.2644	409.1394
2	410.0708	409.9124	409.7598	409.6155	409.4783	409.3484	409.2234	409.1021	408.9841	408.8684	408.7554	408.6458
3	409.4019	409.2590	409.1272	409.0071	408.8965	408.7908	408.6873	408.5840	408.4807	408.3782	408.2783	408.1826
4	408.7532	408.6367	408.5320	408.4436	408.3635	408.2808	408.1929	408.1023	408.0100	407.9172	407.8293	407.7493
5	408.3362	408.2446	408.1626	408.1011	408.0422	407.9692	407.8857	407.7998	407.7109	407.6229	407.5444	407.4775
6	408.1292	408.0527	407.9836	407.9380	407.8889	407.8167	407.7322	407.6484	407.5603	407.4741	407.4026	407.3438
7	407.9019	407.8450	407.7896	407.7649	407.7253	407.6487	407.5615	407.4790	407.3906	407.3064	407.2451	407.1973
8	407.6724	407.6357	407.5940	407.5991	407.5630	407.4705	407.3770	407.2976	407.2075	407.1265	407.0811	407.0476
9	407.4822	407.4590	407.4268	407.4670	407.4236	407.3047	407.2061	407.1323	407.0388	406.9622	406.9385	406.9194
10	407.2915	407.2708	407.2458	407.3408	407.2688	407.1030	407.0042	406.9426	406.8401	406.7727	406.7849	406.7825
11	407.1213	407.0630	407.0447	407.2393	407.0789	406.8301	406.7546	406.7190	406.5928	406.5476	406.6252	406.6355
12	407.0344	406.8586	406.8586	407.2100	406.8586	406.5076	406.5076	406.5076	406.3318	406.3318	406.5076	406.5076
Q	0.0	0.0	0.0	0.0	0.0	0.0	0.0	0.0	0.0	0.0	0.0	0.0
PHI	-246.4	2804.8	2010.2	-868.0	3570.1	4574.7	2672.7	2286.0	3416.7	2333.3	682.0	1383.7
TCSM	414.2	413.9	413.4	412.8	412.8	412.5	412.3	412.3	412.1	411.8	411.8	411.9
TCTR	411.6	411.5	411.3	411.1	410.9	410.8	410.6	410.4	410.3	410.1	409.9	409.8

TIME--	7.1999	7.2499	7.2999	7.3499	7.3999	7.4499	7.4999	7.5499	7.5999	7.6499	7.6999	7.7499
NODE												
1	409.0183	408.9011	408.7878	408.6780	408.5718	408.4692	408.3694	408.2725	408.1775	408.0840	407.9915	407.8992
2	408.5398	408.4377	408.3398	408.2451	408.1533	408.0640	407.9761	407.8896	407.8035	407.7161	407.6270	407.5364
3	408.0923	408.0068	407.9241	407.8433	407.7644	407.6858	407.6077	407.5283	407.4470	407.3613	407.2703	407.1775
4	407.6768	407.6069	407.5388	407.4695	407.4021	407.3323	407.2607	407.1848	407.1035	407.0127	406.9146	406.8171
5	407.4187	407.3596	407.2996	407.2349	407.1741	407.1082	407.0378	406.9607	406.8765	406.7766	406.6692	406.5715
6	407.2927	407.2380	407.1814	407.1179	407.0613	406.9951	406.9243	406.8455	406.7581	406.6604	406.5386	406.4417
7	407.1560	407.1047	407.0513	406.9866	406.9358	406.8672	406.7949	406.7129	406.6199	406.5017	406.3828	406.2910
8	407.0176	406.9663	406.9148	406.8464	406.8054	406.7290	406.6541	406.5664	406.4646	406.3279	406.2031	406.1240
9	406.8994	406.8428	406.7930	406.7168	406.6902	406.5991	406.5220	406.4268	406.3147	406.1545	406.0281	405.9705
10	406.7720	406.7007	406.6538	406.5635	406.5647	406.4419	406.3655	406.2581	406.1311	405.9346	405.8147	405.7969
11	406.6328	406.5239	406.4895	406.3687	406.4312	406.2312	406.1721	406.0408	405.8911	405.6313	405.5457	405.6060
12	406.5076	406.3318	406.3318	406.1563	406.3318	405.9805	405.9805	405.8049	405.6292	405.2778	405.2778	405.4536
Q	0.0	0.0	0.0	0.0	0.0	0.0	0.0	0.0	0.0	0.0	0.0	0.0
PHI	1355.9	2672.7	1705.1	2889.7	483.0	3901.3	2073.8	3144.2	3428.1	5005.9	2891.3	1050.8
TCSM	411.6	411.4	411.4	411.1	410.7	410.4	410.4	410.2	410.2	410.2	410.0	409.8
TCTR	409.7	409.5	409.4	409.3	409.1	409.0	408.9	408.8	408.7	408.6	408.5	408.4

TIME--	7.7999	7.8499	7.8999	7.9499	7.9999	8.0499	8.0999	8.1499	8.1999	8.2499	8.2999	8.3499
NODE												
1	407.8074	407.7163	407.6267	407.5393	407.4553	407.3750	407.2988	407.2258	407.1563	407.0894	407.0254	406.9644
2	407.4460	407.3582	407.2747	407.1975	407.1267	407.0631	406.9980	406.9397	406.8838	406.8306	406.7783	406.7261
3	407.0884	407.0073	406.9365	406.8765	406.8240	406.7754	406.7288	406.6833	406.6392	406.5972	406.5530	406.5053
4	406.7336	406.6682	406.6194	406.5847	406.5544	406.5227	406.4888	406.4543	406.4204	406.3879	406.3474	406.3000
5	406.4988	406.4536	406.4265	406.4148	406.3982	406.3743	406.3455	406.3171	406.2896	406.2612	406.2170	406.1548
6	406.3796	406.3496	406.3364	406.3376	406.3264	406.3040	406.2771	406.2502	406.2244	406.1997	406.1494	406.0938
7	406.2471	406.2395	406.2434	406.2610	406.2522	406.2290	406.2029	406.1780	406.1543	406.1331	406.0713	406.0100
8	406.1118	406.1362	406.1594	406.1965	406.1816	406.1536	406.1265	405.1038	406.0833	405.0654	405.9805	405.9145
9	406.0035	406.0596	406.0977	406.1536	406.1213	406.0857	406.0583	406.0381	406.0210	406.0068	405.8862	405.8215
10	405.8933	405.9954	406.0437	406.1245	406.0505	406.0066	405.9814	405.9653	405.9529	405.9426	405.7578	405.7090
11	405.8120	405.9622	406.0032	406.1211	405.9492	405.9070	405.8906	405.8818	405.8735	405.8706	405.5564	405.5713
12	405.8049	405.9805	405.9805	406.1563	405.8049	405.8049	405.8049	405.8049	405.8049	405.8049	405.2778	405.4536
Q	0.0	0.0	0.0	0.0	0.0	0.0	0.0	0.0	0.0	0.0	0.0	0.0
PHI	-1107.9	-784.8	249.6	-969.2	2751.0	1136.3	931.7	837.0	766.9	713.0	4798.7	578.8
TCSM	409.7	409.3	409.0	409.0	409.0	409.0	409.1	409.0	409.0	408.6	408.6	408.6
TCTR	408.3	408.2	408.1	408.0	407.9	407.8	407.7	407.6	407.5	407.4	407.4	407.3

TIME--	8.3999	8.4499	8.4999	8.5499	8.5999	8.6499	8.6999	8.7499	8.7999	8.8499	8.8999	8.9499
NODE												
1	406.9050	406.8472	406.7908	406.7366	406.6846	406.6348	406.5876	406.5420	406.4968	406.4524	406.4089	406.3677
2	406.6741	406.6221	406.5718	406.5254	406.4822	406.4421	406.4033	406.3638	406.3230	406.2822	406.2432	406.2083
3	406.4575	406.4092	406.3655	406.3289	406.2979	406.2690	406.2375	406.2004	406.1587	406.1187	406.0852	406.0523
4	406.2507	406.2051	406.1724	406.1526	406.1357	406.1155	406.0879	406.0435	405.9958	405.9595	405.9377	405.9360
5	406.1133	406.0720	406.0527	406.0503	406.0435	406.0276	406.9937	405.9353	405.8831	405.8555	405.8489	405.8718
6	406.0415	406.0042	405.9966	406.0051	406.0007	405.9846	405.9451	405.8750	405.8210	405.8040	405.8091	405.8485
7	405.9583	405.9282	405.9390	405.9626	405.9578	405.9387	405.8875	405.7991	405.7476	405.7488	405.7698	405.8350
8	405.8655	405.8499	405.8887	405.9312	405.9170	405.8899	405.8191	405.7024	405.6538	405.6985	405.7407	405.8423
9	405.7793	405.7925	405.8582	405.9163	405.8806	405.8445	405.7461	405.5952	405.5874	405.6667	405.7273	405.8735
10	405.6790	405.7144	405.8452	405.9158	405.8342	405.7878	405.6455	405.4458	405.5063	405.6541	405.7297	405.9436
11	405.5615	405.6536	405.8792	405.9392	405.7561	405.7112	405.4880	405.2166	405.4409	405.5917	405.7378	406.0923
12	405.4536	405.6292	405.9805	405.9805	405.6292	405.6292	405.2778	404.9265	405.4536	405.8049	405.8049	406.3318
Q	0.0	0.0	0.0	0.0	0.0	0.0	0.0	0.0	0.0	0.0	0.0	0.0
PHI	1168.3	-325.3	-2277.8	-438.9	2563.3	389.3	3460.8	4322.3	-1917.2	-2406.7	-502.6	-4359.8
TCSM	408.8	408.6	408.6	408.4	408.1	408.1	408.1	408.3	408.1	408.1	408.1	408.1
TCTR	407.2	407.1	407.1	407.0	407.0	406.9	406.8	406.8	406.7	406.7	406.6	406.6

TIME--	8.9999	9.0499	9.0999	9.1499	9.1999	9.2499	9.2999	9.3499	9.3999	9.4499	9.4999	9.5499
NODE												
1	406.3286	406.2937	406.2625	406.2351	406.2112	406.1902	406.1724	406.1572	406.1443	406.1335	406.1255	406.1208
2	406.1794	406.1577	406.1428	406.1309	406.1213	406.1135	406.1067	406.1013	406.0981	406.0974	406.0994	406.1057
3	406.0525	406.0520	406.0547	406.0583	406.0610	406.0625	406.0627	406.0654	406.0715	406.0813	406.0955	406.1145
4	405.9556	405.9824	406.0020	406.0166	406.0266	406.0322	406.0374	406.0481	406.0640	406.0859	406.1128	406.1472
5	405.9202	405.9658	405.9890	406.0061	406.0168	406.0217	406.0295	406.0471	406.0718	406.1035	406.1396	406.1877
6	405.9150	405.9692	405.9890	406.0049	406.0142	406.0176	406.0273	406.0505	406.0803	406.1187	406.1597	406.2163
7	405.9255	405.9851	405.9932	406.0078	406.0142	406.0144	406.0271	406.0591	406.0952	406.1423	406.1890	406.2578
8	405.9631	406.0178	405.9998	406.0151	406.0159	406.0120	406.0317	406.0774	406.1206	406.1782	406.2302	406.3171
9	406.0225	406.0574	405.9998	406.0239	406.0171	406.0098	406.0396	406.1025	406.1511	406.2214	406.2756	406.3860
10	406.1228	406.1074	405.9856	406.0400	406.0168	406.0037	406.0564	406.1453	406.1958	406.2842	406.3369	406.4363
11	406.2920	406.1553	405.9277	406.0762	406.0083	405.9934	406.0920	406.2214	406.2605	406.3813	406.4202	406.6448
12	406.5073	406.1560	405.8047	406.1560	405.9805	405.9805	406.1563	406.3318	406.3318	406.5076	406.5076	406.8586
Q	0.0	0.0	0.0	0.0	0.0	0.0	0.0	0.0	0.0	0.0	0.0	0.0
PHI	-2915.8	1186.2	2520.9	-2046.1	899.0	145.2	-1280.9	-1778.5	-765.3	-1953.1	-939.8	-3490.1
TCSM	407.9	407.9	407.7	407.6	407.6	407.6	407.4	407.6	407.4	407.6	407.6	407.6
TCTR	406.5	406.5	406.4	406.4	406.4	406.3	406.3	406.2	406.2	406.2	406.2	406.2

TIME--	9.5999	9.6499	9.6999	9.7499
1	406.1189	406.1201	406.1262	406.1372
2	406.1167	406.1338	406.1575	406.1877
3	406.1418	406.1787	406.2241	406.2778
4	406.1958	406.2583	406.3306	406.4109
5	406.2563	406.3423	406.4333	406.5330
6	406.2988	406.3979	406.4988	406.6089
7	406.3586	406.4761	406.5864	406.7095
8	406.4453	406.5845	406.7017	406.8403
9	406.5464	406.7053	406.8225	406.9795
10	406.6924	406.8713	406.9783	407.1641
11	406.9192	407.1101	407.1807	407.4248
12	407.2100	407.3855	407.3855	407.7368
Q	0.0	0.0	0.0	0.0
PHI	-4322.3	-3563.6	-2204.4	-4550.7
TCSM	407.6	407.6	407.4	407.2
TCTR	406.1	406.1	406.1	406.1

```
**************************************************************************
***************************** ENERGY BALANCE *****************************
**************************************************************************

TE-301DJ AND TE-301MJ
CALIBRATION RUN NO.      1.1      DATE: MAY     5       TIME:    9:32:52


CHANGE IN PIN INTERNAL ENERGY CONTENT =      7.827926 BTU/FT
      DETERMINED BY SUMMATION OF DELTA U'S OVER THE INTERVAL FROM T=0 TO TEND.
CHANGE IN PIN INTERNAL ENERGY CONTENT =      7.823809 BTU/FT
      DETERMINED BY DIFFERENCE IN PIN END POINT ENTHALPIES.
TOTAL HEAT INPUT = INTEGRAL OF QTOT*DT =      0.202502 BTU/FT

INTEGRAL OF SURFACE FLUX VERSUS TIME CURVE *2.0*PI*RO=      8.025964 BTU/FT

PERCENTAGE ERROR IN OVERALL HEAT BALANCE =      0.0556 PERCENT
ERROR IN OVERALL HEAT BALANCE (VIA METHOD 2)=      0.0043 PERCENT


VARIANCE FOR THIS RUN = 0.31567144E 04
```

Y FROM 4.00000000E 02 TO 6.50000000E 02 AS A FUNCTION OF X FROM 0.0 TO 1.10000000E 01
WITH Y INTERVAL SIZE 2.00000000E 00 AND WITH X INTERVAL SIZE 4.9999997JE-02

THE X AXIS HAS BEEN SHIFTED FROM 0.0 TO Y = 4.00000000E 02

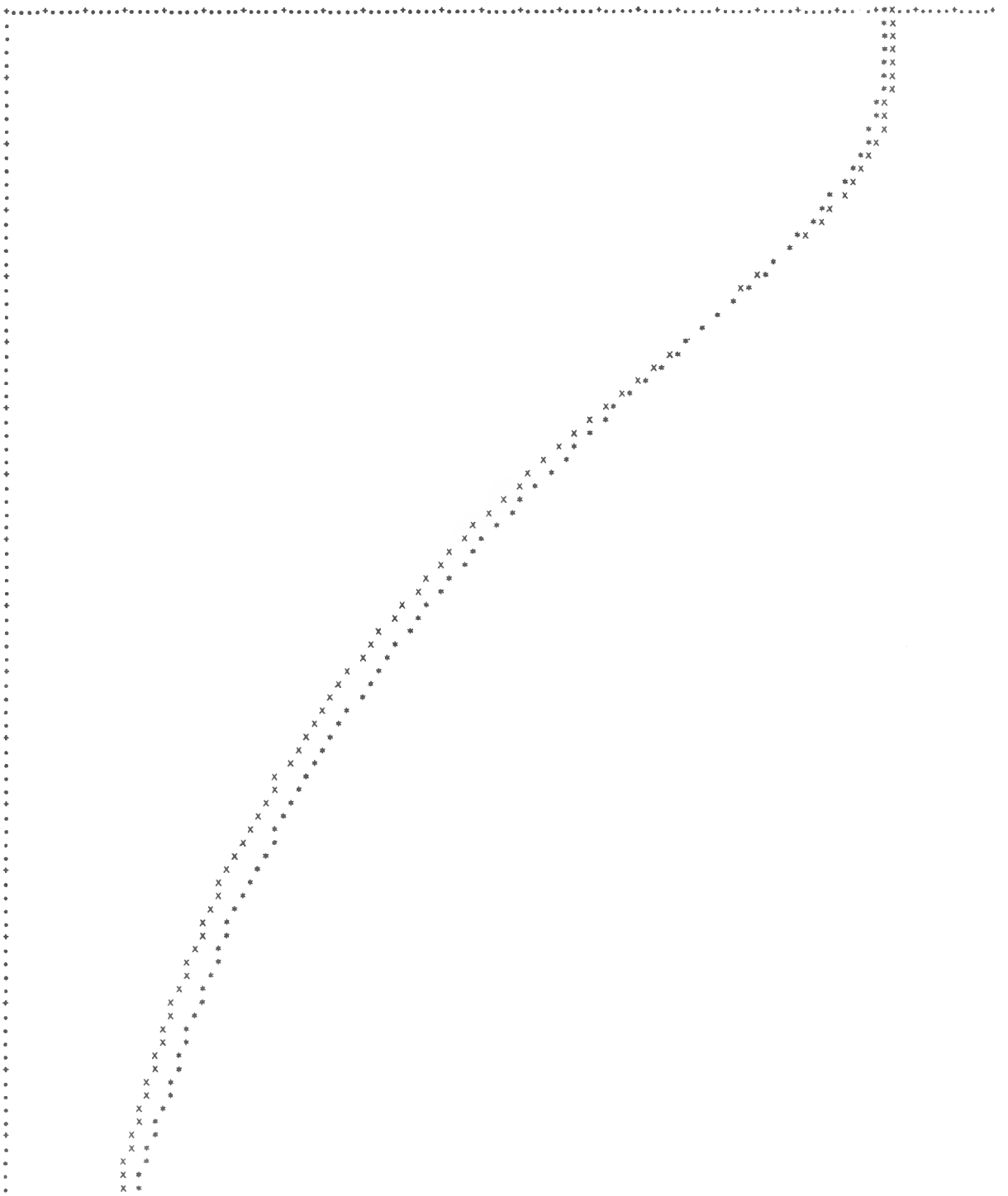

****
********** TRANSIENT RESULTS **********
****

TE-301DJ AND TE-301MJ
CALIBRATION RUN NO. 1.2 DATE: MAY 5 TIME: 17:32:27

TIME-TEMPERATURE-NODE TABLE:
TIME HAS UNITS OF SEC
Q HAS UNITS OF BTU/SEC/FT (=PFA*QAVG)
TEMPERATURE HAS UNITS OF DEG F
INTERFACE FLUX (PHI) HAS UNITS OF BTU/HR/FT**2
TCSM IS THE OBSERVED CENTER TC TEMPERATURE IN DEG F
TCTR IS THE CALCULATED CENTER TC TEMPERATURE

TIME--	0.0	0.0500	0.1000	0.1500	0.2000	0.2500	0.3000	0.3500	0.4000	0.4500	0.5000	0.5500
NODE												
1	819.6978	819.5437	819.0471	818.0574	816.4839	814.2903	811.4810	808.0879	804.1584	799.7471	794.9106	789.7051
2	819.6978	818.6436	816.1311	812.2417	807.2427	801.4265	795.0427	788.2847	781.2922	774.1641	766.9661	759.7419
3	819.6978	815.0928	807.2386	797.9360	788.0417	778.1240	768.4231	759.0342	749.9812	741.2532	732.8240	724.6643
4	819.6978	803.6841	786.1746	770.3428	756.3535	743.8760	732.5840	722.2224	712.6008	703.5674	695.0103	686.8506
5	819.6978	784.2195	761.0491	743.8569	729.7063	717.4404	706.4915	696.5159	687.2876	678.6292	670.4275	662.6094
6	802.8245	770.5281	748.6853	732.1602	718.4631	706.5491	695.8894	686.1570	677.1353	668.6465	660.5911	652.9031
7	762.5544	745.5388	728.8552	714.5476	702.1721	691.1812	681.2280	672.0593	663.4993	655.3828	647.6423	640.2314
8	721.0432	712.4395	701.4290	690.5679	680.4751	671.1006	662.3740	654.1663	646.3804	638.8728	631.6514	624.6968
9	683.2241	683.3926	676.0432	667.9634	659.9468	652.1025	644.5750	637.3123	630.2898	623.3674	616.6614	610.1643
10	658.3913	655.2627	650.4717	644.6790	638.5479	632.1265	625.7649	619.4226	613.1484	606.7703	600.5791	594.5447
11	628.6504	626.8379	623.8657	619.9373	615.4973	610.3335	605.0962	599.6265	594.0764	588.1638	582.5090	576.9507
12	601.8697	600.4368	598.7766	596.2708	593.2271	588.9998	584.7666	580.0247	575.1099	569.5129	564.4221	559.3257
Q	9.33692	0.38302	0.0	0.0	0.0	0.0	0.0	0.0	0.0	0.0	0.0	0.0
PHI	317804.8	318377.3	303408.4	289260.3	274253.8	266374.9	254619.9	247357.4	239982.3	238172.8	229229.6	223350.7
TCSM	822.9	824.1	824.2	824.3	823.3	823.0	822.5	821.8	820.5	819.0	816.8	814.4
TCTR	819.7	819.7	819.7	819.7	819.7	819.7	819.7	819.5	818.9	817.9	816.3	814.0

TIME--	0.6000	0.6500	0.7000	0.7500	0.8000	0.8500	0.9000	0.9500	1.0000	1.0500	1.1000	1.1500
NODE												
1	784.1814	778.3877	772.3665	766.1563	759.7900	753.2981	746.7068	740.0396	733.3186	726.5625	719.7881	713.0110
2	752.5210	745.3210	738.1553	731.0317	723.9558	716.9326	709.9690	703.0696	696.2400	689.4846	682.8074	676.2113
3	716.7458	709.0439	701.5364	694.2043	687.0325	680.0137	673.1423	666.4153	659.8289	653.3774	647.0585	640.8679
4	679.0254	671.4900	664.2063	657.1409	650.2778	643.6121	637.1375	630.8464	624.7307	618.7778	612.9797	607.3315
5	655.1150	647.8997	640.9282	634.1677	627.6135	621.2717	615.1345	609.1929	603.4331	597.8411	592.4048	587.1248
6	645.5271	638.4197	631.5508	624.8845	618.4285	612.1926	606.1675	600.3433	594.7012	589.2292	583.9126	578.7578
7	633.1038	626.2202	619.5579	613.0793	606.8152	600.7798	594.9587	589.3379	583.8955	578.6196	573.4939	568.5361
8	617.9741	611.4519	605.1213	598.9385	592.9832	587.2678	581.7605	576.4465	571.2961	566.3027	561.4458	556.7671
9	603.8479	597.6855	591.6880	585.7954	580.1641	574.7854	569.5986	564.5933	559.7335	555.0146	550.4180	546.0200
10	588.6353	582.8303	577.1702	571.5583	566.2864	561.2786	556.4329	551.7551	547.1902	542.7656	538.4365	534.3494
11	571.4551	566.0100	560.7051	555.3611	550.5354	545.9644	541.4929	537.1794	532.9331	528.8301	524.7847	521.0779
12	554.2256	549.1213	544.1816	539.0686	534.8044	530.7075	526.6067	522.6724	518.7351	514.9675	511.1970	507.9380
Q	0.0	0.0	0.0	0.0	0.0	0.0	0.0	0.0	0.0	0.0	0.0	0.0
PHI	218268.1	213841.3	208566.1	206058.3	196158.9	189744.8	185155.0	179891.2	176045.4	171318.4	167901.7	160750.2
TCSM	810.9	807.2	803.1	798.3	793.4	788.6	783.3	777.5	771.7	765.7	759.4	753.2
TCTR	811.1	807.7	803.7	799.2	794.4	789.1	783.6	777.7	771.7	765.5	759.1	752.6

****
********** ENERGY BALANCE **********
****

TE-301DJ AND TE-301MJ
CALIBRATION RUN NO. 1.2 DATE: MAY 5 TIME: 17:32:27

CHANGE IN PIN INTERNAL ENERGY CONTENT = 15.663449 BTU/FT
DETERMINED BY SUMMATION OF DELTA U'S OVER THE INTERVAL FROM T=0 TO TEND.
CHANGE IN PIN INTERNAL ENERGY CONTENT = 15.651159 BTU/FT
DETERMINED BY DIFFERENCE IN PIN END POINT ENTHALPIES.
TOTAL HEAT INPUT = INTEGRAL OF QTOT*DT = 0.019151 BTU/FT

INTEGRAL OF SURFACE FLUX VERSUS TIME CURVE *2.0*PI*RO= 15.677749 BTU/FT

PERCENTAGE ERROR IN OVERALL HEAT BALANCE = 0.0309 PERCENT
ERROR IN OVERALL HEAT BALANCE (VIA METHOD 2)= 0.0475 PERCENT

VARIANCE FOR THIS RUN = 0.41445703E 04

Y FROM 4.00000000E 02 TO 8.50000000E 02 AS A FUNCTION OF X FROM 0.0 TO 1.10000000E 01
WITH Y INTERVAL SIZE 3.59999943E 00 AND WITH X INTERVAL SIZE 4.99999970E-02

THE X AXIS HAS BEEN SHIFTED FROM 0.0 TO Y = 4.00000000E 02

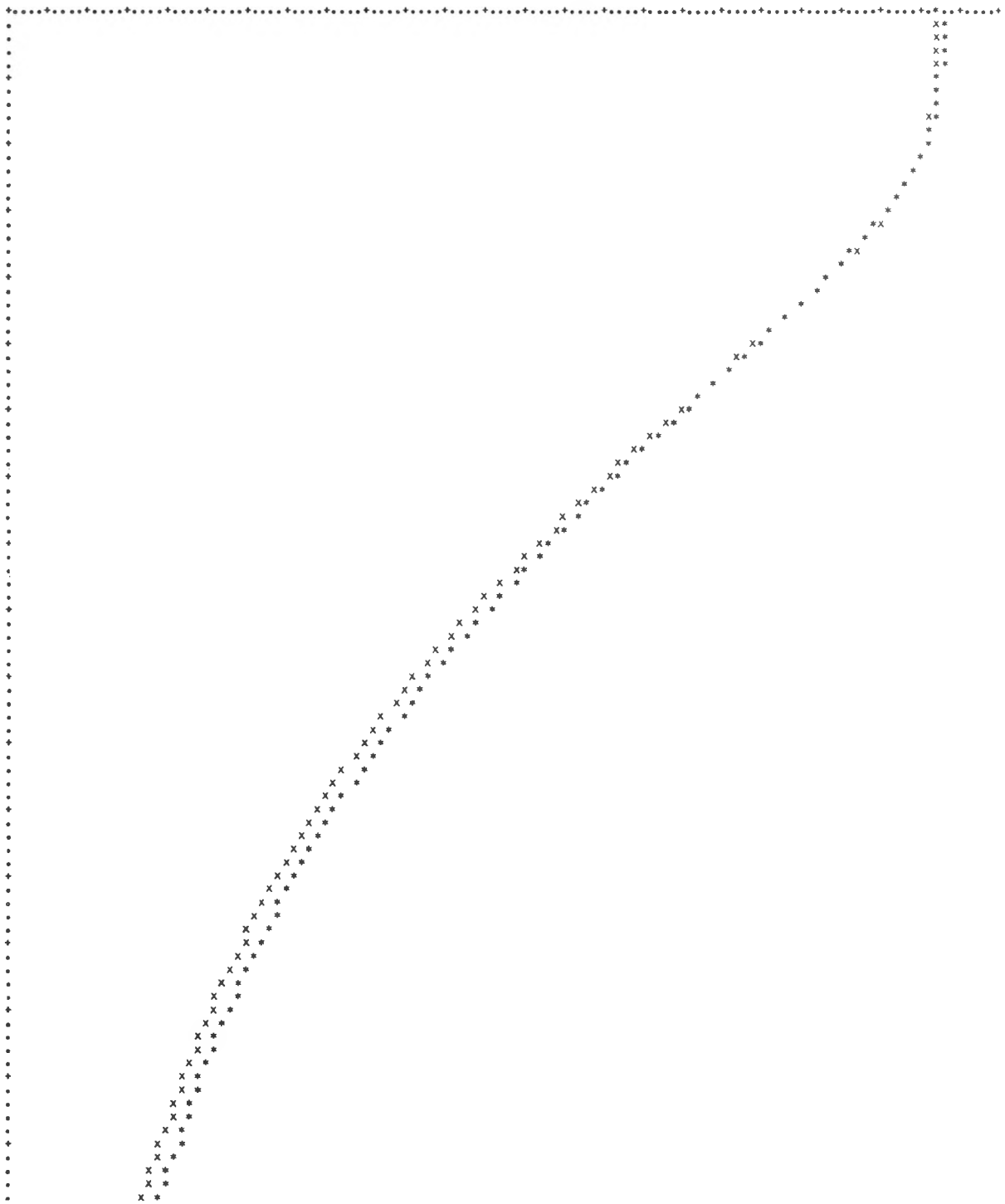

```
*****************************************************************************
**************************** TRANSIENT RESULTS ******************************
*****************************************************************************

TE-3010J AND TE-301MJ
CALIBRATION RUN NO.      1.3      DATE: MAY     5       TIME:  21:48:38


TIME-TEMPERATURE-NODE TABLE:
     TIME HAS UNITS OF SEC
     Q HAS UNITS OF BTU/SEC/FT (=PFA*QAVG)
     TEMPERATURE HAS UNITS OF DEG F
     INTERFACE FLUX (PHI) HAS UNITS OF BTU/HR/FT**2
     TCSM IS THE OBSERVED CENTER TC TEMPERATURE IN DEG F
     TCTR IS THE CALCULATED CENTER TC TEMPERATURE
```

TIME--	0.0	0.0500	0.1000	0.1500	0.2000	0.2500	0.3000	0.3500	0.4000	0.4500	0.5000	0.5500
NODE												
1	1045.4590	1045.3003	1044.7800	1043.7253	1042.0200	1039.6079	1036.4756	1032.6443	1028.1553	1023.0630	1017.4265	1011.3066
2	1045.4590	1044.2688	1041.3770	1036.8159	1030.8562	1023.8210	1016.0044	1007.6450	998.9250	989.9766	980.8938	971.7427
3	1045.4590	1039.8552	1030.2002	1018.4438	1005.8398	993.0720	980.4946	968.2344	956.3804	944.9263	933.8525	923.1292
4	1045.4590	1024.6538	1001.7239	980.7717	962.1226	945.4172	930.2739	916.3730	903.4775	891.3933	879.9717	869.1021
5	1045.4590	997.8796	967.0974	944.0762	925.0408	908.5042	893.7485	880.3320	867.9426	856.3567	845.4141	835.0022
6	1024.7991	981.2905	952.0996	929.8601	911.3472	895.2114	880.7935	867.6663	855.5195	844.1406	833.3738	823.1145
7	969.9146	947.3789	925.1611	905.9788	889.2815	874.4165	860.9912	848.6665	837.1697	826.3323	816.0200	806.1538
8	910.1670	899.3149	885.1829	871.0493	857.7053	845.2407	833.6914	822.8538	812.5332	802.6646	793.1594	783.9871
9	863.1145	857.3186	848.2593	838.1033	827.7200	817.5042	807.8015	798.4231	789.2439	780.3279	771.6125	763.1279
10	822.5750	819.2603	813.4497	806.2949	798.3235	790.0437	782.0476	773.9902	765.8198	757.7722	749.7671	741.9167
11	785.1641	783.0747	779.4192	774.5425	768.4717	761.8157	755.4268	748.5164	741.1885	733.9316	726.5486	719.2876
12	751.0601	749.4817	747.3450	744.2078	739.5405	734.2048	729.3667	723.3584	716.6790	710.1638	703.3105	696.6216
Q	12.65765	0.36439	0.0	0.0	0.0	0.0	0.0	0.0	0.0	0.0	0.0	0.0
PHI	430838.7	430157.9	412712.1	393956.1	381255.3	366315.8	344221.3	336456.2	329965.4	319260.1	313067.9	304540.8
TCSM	1043.0	1045.4	1045.4	1045.4	1043.7	1043.4	1043.1	1042.4	1041.3	1039.6	1037.0	1033.5
TCTR	1045.5	1045.5	1045.5	1045.5	1045.5	1045.5	1045.5	1045.4	1045.1	1044.3	1043.0	1041.0

TIME--	0.6000	0.6500	0.7000	0.7500	0.8000	0.8500	0.9000	0.9500	1.0000	1.0500	1.1000	1.1500
NODE												
1	1004.7603	997.8435	990.6064	983.0957	975.3525	967.4133	959.3132	951.0808	942.7422	934.3218	925.8418	917.3210
2	962.5657	953.3945	944.2498	935.1448	926.0908	917.0950	908.1619	899.2974	890.5054	881.7915	873.1599	864.6135
3	912.7245	902.6091	892.7571	883.1450	873.7532	864.5652	855.5669	846.7480	838.1021	829.6235	821.3066	813.1436
4	858.6970	848.6985	839.0557	829.7297	820.6855	811.8994	803.3499	795.0283	786.9238	779.0293	771.3284	763.8086
5	825.0361	815.4727	806.2544	797.3489	788.7188	780.3469	772.2144	764.3213	756.6538	749.2061	741.9534	734.8804
6	813.2839	803.8489	794.7500	785.9587	777.4370	769.1729	761.1479	753.3672	745.8169	738.4893	731.3547	724.3992
7	795.6687	787.5576	779.7515	770.2366	761.9692	753.9546	746.1704	738.6345	731.3259	724.2422	717.3385	710.6064
8	775.1118	766.5784	758.2788	750.2415	742.4072	734.8184	727.4377	720.3130	713.4019	706.7075	700.1621	693.7729
9	754.8599	746.9211	739.1226	731.5713	724.1650	717.0125	710.0371	703.3369	696.8254	690.5247	684.3240	678.2688
10	734.2090	726.9601	719.5107	712.4319	705.4172	698.6985	692.1082	685.8430	679.7202	673.8120	667.9275	662.1934
11	712.3999	705.3723	698.4001	691.9103	685.1436	678.8923	672.6711	666.8921	661.1528	655.6589	650.0535	644.6472
12	689.9280	685.9004	677.1992	671.1648	664.7917	659.0864	653.2100	649.0020	642.6233	637.5779	632.1934	627.1426
Q	0.0	0.0	0.0	0.0	0.0	0.0	0.0	0.0	0.0	0.0	0.0	0.0
PHI	297637.3	285828.9	284218.4	274265.3	271227.1	261447.6	257300.8	247375.3	243083.9	235950.4	234010.4	228039.4
TCSM	1029.9	1025.4	1020.7	1015.5	1009.9	1003.7	997.4	990.3	983.1	975.8	968.2	960.3
TCTR	1038.2	1034.8	1030.7	1025.9	1020.6	1014.8	1008.5	1001.8	994.7	987.3	979.7	971.9

```
*****************************************************************************
**************************** ENERGY BALANCE *********************************
*****************************************************************************

TE-3010J AND TE-301MJ
CALIBRATION RUN NO.      1.3      DATE: MAY     5       TIME:  21:49:39


CHANGE IN PIN INTERNAL ENERGY CONTENT =     23.746933 BTU/FT
     DETERMINED BY SUMMATION OF DELTA U'S OVER THE INTERVAL FROM T=0 TO TEND.
CHANGE IN PIN INTERNAL ENERGY CONTENT =     23.727570 BTU/FT
     DETERMINED BY DIFFERENCE IN PIN END POINT ENTHALPIES.
TOTAL HEAT INPUT = INTEGRAL OF QTOT*DT =      0.018219 BTU/FT

INTEGRAL OF SURFACE FLUX VERSUS TIME CURVE *2.0*PI*RO=     23.760773 BTU/FT

PERCENTAGE ERROR IN OVERALL HEAT BALANCE =      0.0184 PERCENT
ERROR IN OVERALL HEAT BALANCE (VIA METHOD 2)=      0.0631 PERCENT

VARIANCE FOR THIS RUN = 0.39392764E 04
```

Y FROM 4.50000000E 02 TO 1.05000000E 03 AS A FUNCTION OF X FROM 0.0 TO 1.10000000E 01
WITH Y INTERVAL SIZE 4.79999924E 00 AND WITH X INTERVAL SIZE 4.99999970E-02

THE X AXIS HAS BEEN SHIFTED FROM 0.0 TO Y = 4.50000000E 02

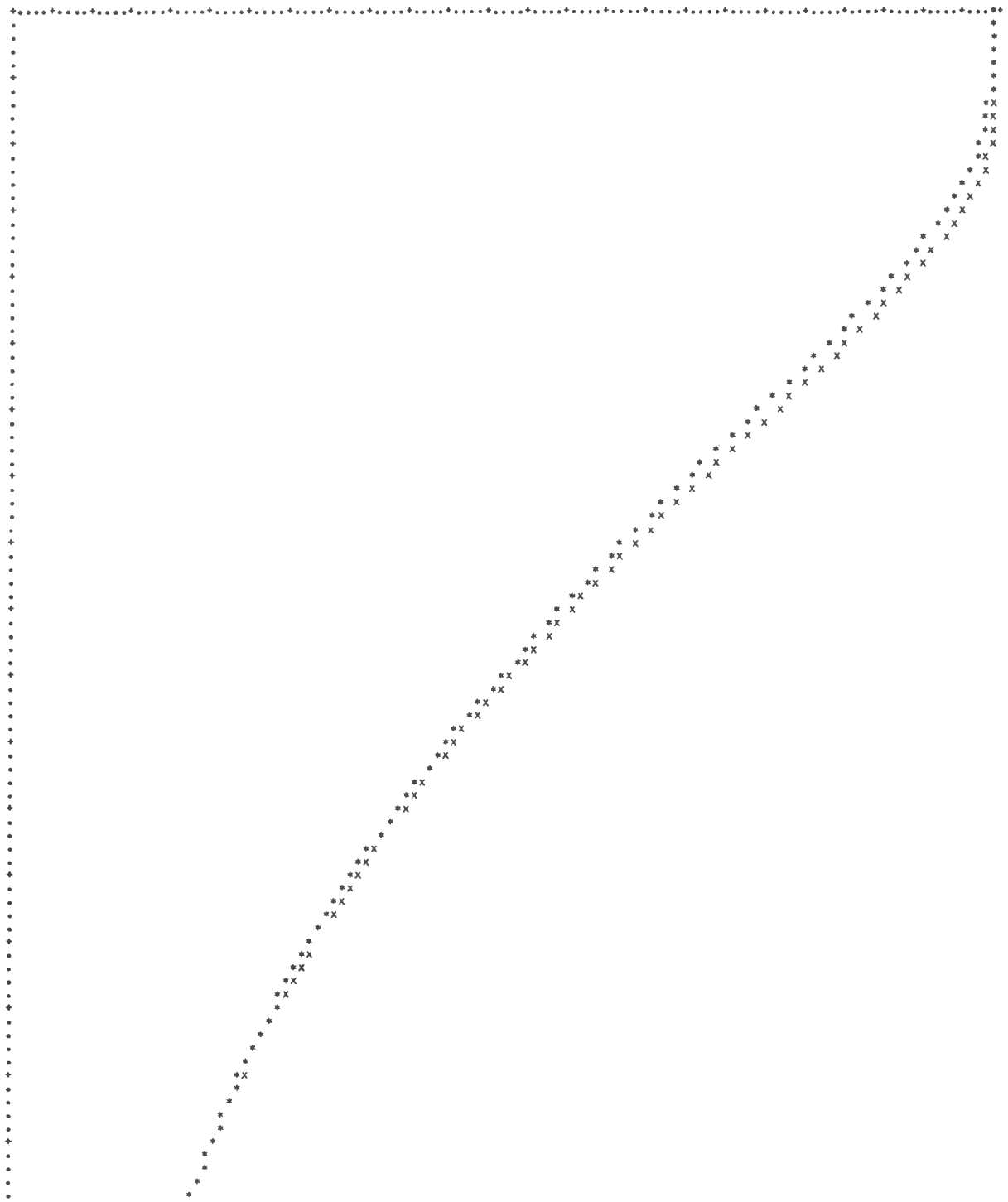

****
********** TRANSIENT RESULTS **********
****

TE-301DJ AND TE-301MJ
CALIBRATION RUN NO. 1.4 DATE: MAY 6 TIME: 14:51:16

TIME-TEMPERATURE-NODE TABLE:
TIME HAS UNITS OF SEC
Q HAS UNITS OF BTU/SEC/FT (=PFA*QAVG)
TEMPERATURE HAS UNITS OF DEG F
INTERFACE FLUX (PHI) HAS UNITS OF BTU/HR/FT**2
TCSM IS THE OBSERVED CENTER TC TEMPERATURE IN DEG F
TCTR IS THE CALCULATED CENTER TC TEMPERATURE

TIME--	0.0	0.0500	0.1000	0.1500	0.2000	0.2500	0.3000	0.3500	0.4000	0.4500	0.5000	0.5500
NODE												
1	729.9487	729.7664	729.1868	728.0476	726.2549	723.7771	720.6267	716.8457	712.4905	707.6250	702.3140	696.6194
2	729.9487	728.7646	725.9937	721.7588	716.3691	710.1433	703.3459	696.1755	688.7773	681.2510	673.6624	666.0540
3	729.9487	724.9897	716.7461	706.9739	696.7021	686.4387	676.4128	666.7134	657.3599	648.3411	639.6292	631.1912
4	729.9487	713.3250	695.5076	679.4773	665.3057	652.6279	641.1187	630.5295	620.6785	611.4238	602.6509	594.2737
5	729.9487	693.7817	670.6311	653.3379	639.0105	626.5168	615.3230	605.1030	595.6382	586.7681	578.3613	570.3311
6	712.3665	679.4612	657.6199	640.9792	627.0869	614.9229	604.0054	594.0229	584.7659	576.0747	567.8193	559.9216
7	672.2163	654.6873	637.7749	623.2532	610.6086	599.3074	589.0642	579.6282	570.8259	562.5154	554.5740	546.9492
8	631.9082	622.7778	611.2898	599.9995	589.4587	579.6355	570.5503	562.0322	553.9810	546.2856	538.8418	531.6477
9	600.0393	594.7126	586.7656	578.1030	569.4756	561.0605	553.1338	545.5303	538.2283	531.1401	524.1792	517.4133
10	569.7183	566.4641	561.0774	554.6555	547.8142	540.7605	534.0413	527.3708	520.8418	514.3674	507.8770	501.5510
11	539.1570	536.8879	533.3257	528.7676	523.5391	517.7429	512.3145	506.5657	500.8308	494.9619	488.9087	483.0513
12	511.3252	509.2583	506.9663	503.8145	499.8618	495.0457	490.9106	485.9097	480.9036	475.5466	469.8345	464.4626
Q	9.32846	0.26999	0.0	0.0	0.0	0.0	0.0	0.0	0.0	0.0	0.0	0.0
PHI	317520.4	322405.9	308398.1	294984.1	282759.6	274069.4	256440.9	250459.2	241675.9	236563.9	233382.1	226171.8
TCSM	727.9	729.6	729.9	729.9	728.7	728.2	727.7	726.2	724.7	722.2	719.2	715.7
TCTR	729.9	729.9	729.9	729.9	729.9	729.9	729.9	729.5	728.7	727.2	725.1	722.3

TIME--	0.6000	0.6500	0.7000	0.7500	0.8000	0.8500	0.9000	0.9500	1.0000	1.0500	1.1000	1.1500
NODE												
1	690.5989	684.3042	677.7820	671.0732	664.2151	657.2397	650.1760	643.0500	635.8840	628.6980	621.5095	614.3345
2	658.4548	650.8833	643.3513	635.8687	628.4443	621.0852	613.7971	606.5850	599.4534	592.4067	585.4487	578.5825
3	622.9990	615.0278	607.2559	599.6694	592.2581	585.0144	577.9282	570.9929	564.2036	557.5549	551.0420	544.6641
4	586.2336	578.4863	570.9966	563.7478	556.7288	549.9192	543.3027	536.8679	530.6084	524.5093	518.5649	512.7759
5	562.6318	555.2212	548.0635	541.1589	534.4990	528.0513	521.7988	515.7341	509.8516	504.1287	498.5649	493.1655
6	552.3462	545.0515	538.0059	531.2217	524.6887	518.3655	512.2375	506.3010	500.5515	494.9585	489.5288	484.2708
7	539.6238	532.5598	525.7297	519.1689	512.8628	506.7512	500.8303	495.1013	489.5618	484.1672	478.9395	473.8909
8	524.7244	518.0239	511.5283	505.3196	499.3591	493.5544	487.9319	482.4993	477.2556	472.1279	467.1758	462.4133
9	510.8992	504.5620	498.4009	492.5642	486.9565	481.4485	476.1216	470.9851	466.0349	461.1580	456.4790	452.0012
10	495.4758	489.5142	483.7031	478.2944	473.0745	467.8630	462.8572	458.0457	453.4197	448.7537	444.4224	440.2671
11	477.4768	471.9072	466.4761	461.6187	456.9369	451.9109	447.2830	442.8533	438.6047	434.2222	430.2395	426.4795
12	459.4312	454.2200	449.1765	444.9971	440.6392	435.9272	431.7349	427.7139	423.8652	419.6619	416.1563	412.8245
Q	0.0	0.0	0.0	0.0	0.0	0.0	0.0	0.0	0.0	0.0	0.0	0.0
PHI	219390.4	214503.8	209112.8	198159.4	193688.6	192135.3	185156.6	179718.3	174403.9	173330.3	165418.4	159878.8
TCSM	711.8	707.3	702.3	697.1	691.6	685.7	679.7	673.5	667.1	660.4	653.5	646.7
TCTR	718.9	714.8	710.2	705.2	699.7	693.8	687.7	681.3	674.7	667.9	661.0	654.0

****
********** ENERGY BALANCE **********
****

TE-301DJ AND TE-301MJ
CALIBRATION RUN NO. 1.4 DATE: MAY 6 TIME: 14:51:16

CHANGE IN PIN INTERNAL ENERGY CONTENT = 15.661705 BTU/FT
DETERMINED BY SUMMATION OF DELTA U'S OVER THE INTERVAL FROM T=0 TO TEND.
CHANGE IN PIN INTERNAL ENERGY CONTENT = 15.647122 BTU/FT
DETERMINED BY DIFFERENCE IN PIN END POINT ENTHALPIES.
TOTAL HEAT INPUT = INTEGRAL OF QTOT*DT = 0.013500 BTU/FT

INTEGRAL OF SURFACE FLUX VERSUS TIME CURVE *2.0*PI*RO= 15.671325 BTU/FT

PERCENTAGE ERROR IN OVERALL HEAT BALANCE = 0.0247 PERCENT
ERROR IN OVERALL HEAT BALANCE (VIA METHOD 2)= 0.0694 PERCENT

VARIANCE FOR THIS RUN = 0.24272646E 04

Y FROM 3.00000000E 02 TO 7.50000000E 02 AS A FUNCTION OF X FROM 0.0 TO 1.10000000E 01
WITH Y INTERVAL SIZE 3.59999943E 00 AND WITH X INTERVAL SIZE 4.99999970E-02

THE X AXIS HAS BEEN SHIFTED FROM 0.0 TO Y = 3.00000000E 02

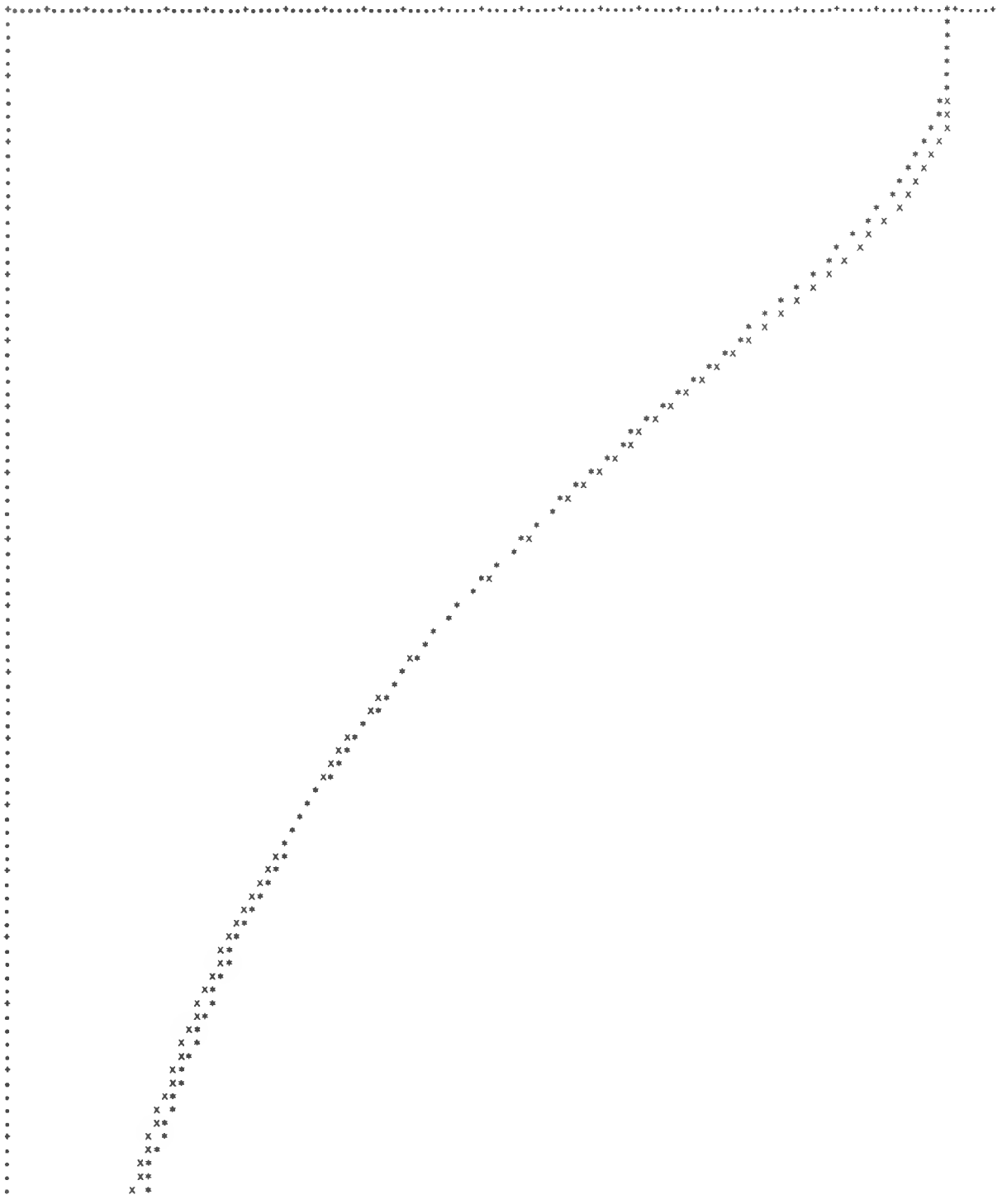

****
********** TRANSIENT RESULTS **********
****

TE-301DJ AND TE-301MJ
CALIBRATION RUN NO. 8.1 DATE: SEP. 9 TIME: 19: 2:25

TIME-TEMPERATURE-NODE TABLE:
TIME HAS UNITS OF SEC
Q HAS UNITS OF BTU/SEC/FT (=PFA*QAVG)
TEMPERATURE HAS UNITS OF DEG F
INTERFACE FLUX (PHI) HAS UNITS OF BTU/HR/FT**2
TCSM IS THE OBSERVED CENTER TC TEMPERATURE IN DEG F
TCTR IS THE CALCULATED CENTER TC TEMPERATURE

TIME--	0.0	0.0500	0.1000	0.1500	0.2000	0.2500	0.3000	0.3500	0.4000	0.4500	0.5000	0.5500
NODE												
1	658.8669	658.7466	658.3750	657.5592	656.5540	655.0498	653.1631	650.9246	648.3733	645.5469	642.4856	639.2251
2	658.8669	658.1240	656.4402	653.9307	650.7979	647.2292	643.3740	639.3374	635.1934	630.9912	626.7544	622.5349
3	658.8669	655.8760	651.0864	645.5461	639.8091	634.1250	628.5947	623.2500	618.0923	613.1130	608.2981	603.6328
4	658.8669	649.1707	639.2300	630.4487	622.7246	615.8052	609.4951	603.6609	598.2043	593.0605	588.1775	583.5144
5	658.8669	638.1182	625.5991	616.2776	608.5027	601.6580	595.4910	589.8115	584.5230	579.5486	574.8401	570.3513
6	648.7532	629.9304	618.2197	609.3435	601.8391	595.1975	589.1750	583.6270	578.4530	573.5840	568.9709	564.5598
7	626.3213	616.3970	607.3330	599.6589	592.8066	586.6057	580.9197	575.6467	570.6973	566.0349	561.5989	557.3560
8	604.1274	599.1667	593.1252	587.2195	581.3594	575.8701	570.7349	565.9075	561.3235	556.9849	552.8220	548.8198
9	586.4878	583.9651	579.9912	575.5354	570.4834	565.6780	561.0930	556.7183	552.5015	548.4978	544.6086	540.8494
10	569.6230	568.7070	566.2810	563.0588	558.5962	554.3067	550.4932	546.8006	542.7715	539.1399	535.5378	532.0398
11	552.5404	553.0320	551.6501	549.3906	545.0836	541.8140	538.4048	535.0242	531.5952	528.3953	525.0833	521.8748
12	537.2649	538.9607	537.9912	536.3386	531.5630	529.3418	526.4363	523.5293	520.4490	517.7097	514.5260	511.7117
Q	5.19886	0.0	0.0	0.0	0.0	0.0	0.0	0.0	0.0	0.0	0.0	0.0
PHI	176957.7	156016.7	160670.2	155990.6	172232.2	150883.4	147319.9	141703.7	138138.5	131494.3	129918.2	125806.4
TCSM	660.7	661.7	661.9	661.9	660.9	660.3	659.8	658.8	657.4	655.9	654.1	651.7
TCTR	658.9	658.9	658.9	658.9	658.9	658.9	658.8	658.5	657.8	656.8	655.4	653.6

TIME--	0.6000	0.6500	0.7000	0.7500	0.8000	0.8500	0.9000	0.9500	1.0000	1.0500	1.1000	1.1500
NODE												
1	635.7986	632.2366	628.5652	624.8071	620.9834	617.1123	613.2090	609.2866	605.3572	601.4302	597.5139	593.6167
2	618.3174	614.1235	609.9617	605.8359	601.7520	597.7124	593.7205	589.7771	585.8845	582.0430	578.2544	574.5198
3	599.1047	594.7053	590.4248	586.2537	582.1855	578.2170	574.3372	570.5415	566.8267	563.1893	559.6248	556.1335
4	579.0449	574.7556	570.6238	566.6309	562.7710	559.0310	555.3931	551.8516	548.4050	545.0432	541.7627	538.5698
5	566.0618	561.9648	558.0244	554.2224	550.5627	547.0212	543.5747	540.2261	536.9750	533.8113	530.7253	527.7383
6	560.3672	556.3618	552.5056	548.7959	545.2131	541.7537	538.3833	535.1121	531.9460	528.8550	525.8469	522.9468
7	553.3052	549.4575	545.7373	542.1472	538.7112	535.3750	532.1155	528.9587	525.9119	522.9275	520.0276	517.2495
8	545.0015	541.3938	537.8652	534.4595	531.2224	529.0518	524.9363	521.9358	519.0515	516.1995	513.4426	510.8330
9	537.2739	533.9219	530.5708	527.3513	524.3235	521.3069	518.3242	515.4836	512.7542	510.0281	507.4143	504.9819
10	528.7422	525.6926	522.5373	519.4980	516.7212	513.8513	511.0010	508.3503	505.8196	503.1880	500.7434	498.5298
11	513.9177	516.2510	513.1797	510.4351	507.9854	505.2271	502.5117	500.1160	497.8135	495.2483	493.0344	491.1194
12	509.1304	506.9082	503.8159	501.4114	499.3484	496.5964	494.0149	491.9480	489.8906	487.2949	485.3977	483.8450
Q	0.0	0.0	0.0	0.0	0.0	0.0	0.0	0.0	0.0	0.0	0.0	0.0
PHI	120077.6	113802.2	116895.8	110520.9	104832.9	107045.5	104816.6	99208.6	96464.1	98396.0	92350.7	87010.2
TCSM	649.2	646.5	643.8	640.6	637.6	634.0	630.5	626.6	622.9	619.1	615.3	611.5
TCTR	651.4	648.9	646.2	643.2	640.0	636.6	633.0	629.4	625.7	621.8	618.0	614.1

****
********** ENERGY BALANCE **********
****

TE-301DJ AND TE-301MJ
CALIBRATION RUN NO. 8.1 DATE: SEP. 9 TIME: 19: 2:25

CHANGE IN PIN INTERNAL ENERGY CONTENT = 8.621787 BTU/FT
DETERMINED BY SUMMATION OF DELTA U'S OVER THE INTERVAL FROM T=0 TO TEND.
CHANGE IN PIN INTERNAL ENERGY CONTENT = 8.617569 BTU/FT
DETERMINED BY DIFFERENCE IN PIN END POINT ENTHALPIES.
TOTAL HEAT INPUT = INTEGRAL OF QTOT*DT = 0.0 BTU/FT

INTEGRAL OF SURFACE FLUX VERSUS TIME CURVE *2.0*PI*RO= 8.617222 BTU/FT

PERCENTAGE ERROR IN OVERALL HEAT BALANCE = 0.0530 PERCENT
ERROR IN OVERALL HEAT BALANCE (VIA METHOD 2)= 0.0040 PERCENT

VARIANCE FOR THIS RUN = 0.27224512E 03

Y FROM 4.00000000E 02 TO 7.00000000E 02 AS A FUNCTION OF X FROM 0.0 TO 1.00000000E 01
WITH Y INTERVAL SIZE 2.39999962E 00 AND WITH X INTERVAL SIZE 4.99999970E-02

THE X AXIS HAS BEEN SHIFTED FROM 0.0 TO Y = 4.00000000E 02

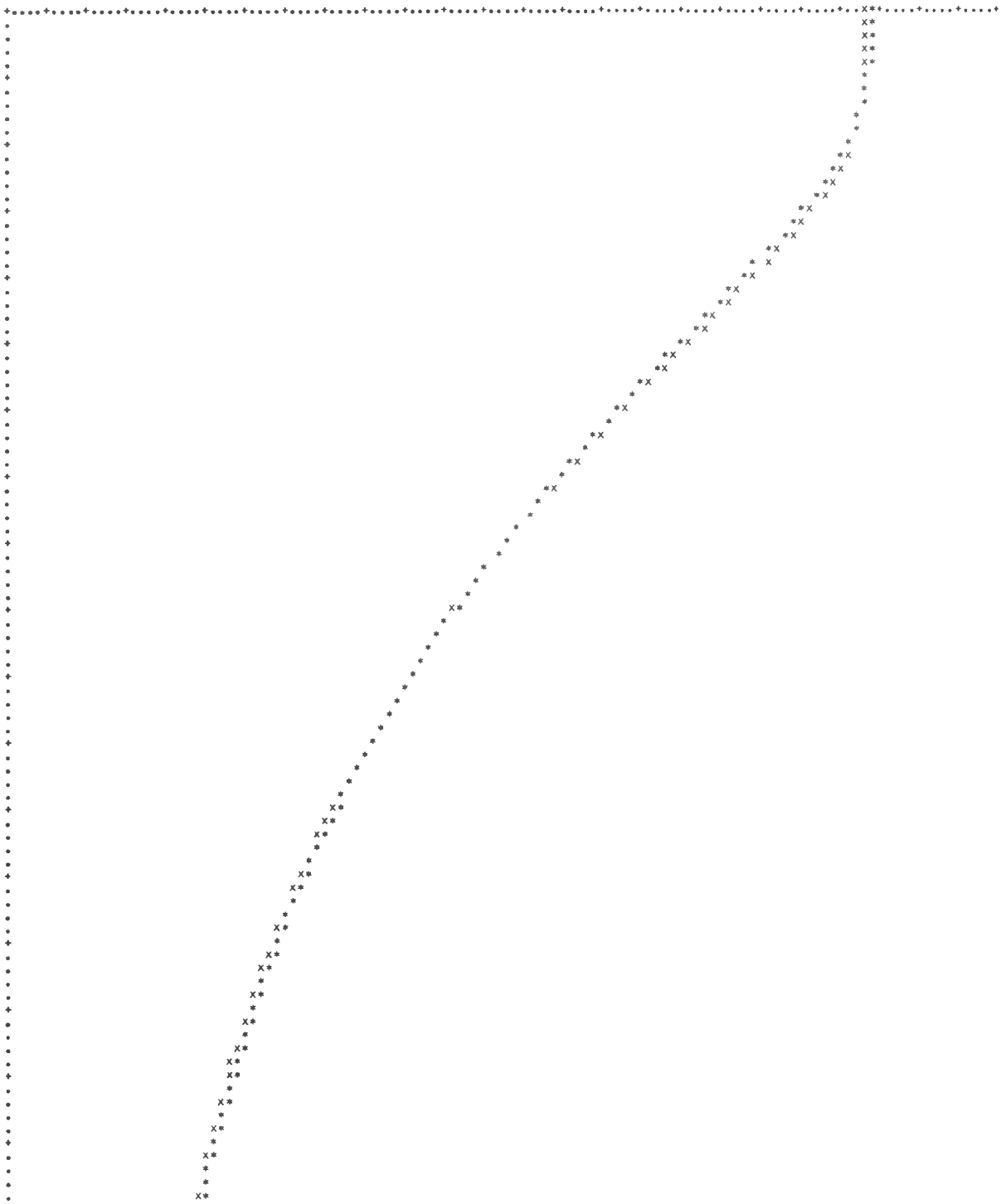

Appendix F

EXAMPLE OF ORTCAL — PART IV OUTPUT

Table F.1. ORTCAL — Part IV level regression for G level
(at thermocouple position TE-318BG)

****
*** THERMOCOUPLE NUMBER: TE-318BG ***
****

NOMENCLATURE:
Q(KW)/ROD = NOMINAL POWER INPUT PER ROD IN KW
DELTA R = GAP BETWEEN INNER AND OUTER S.S.SHEATHS (MILS OF INCHES)
TIME = WALL CLOCK TIME
NOTE:
ASTERISK DENOTES BIAS POINT

RUN NO. DATE TIME	Q(KW)/ROD	DELTA R (OBSERVED)	DELTA R (CALCULATED)	VARIANCE	WEIGHTING FACTOR
* 1.1 ******MAY	4*				
23:36:56	30.3	0.04142	0.03970	0.960803E-05	1.0000
23:44:18	40.1	0.03911	0.03891	0.217917E-05	1.0000
23:53:20	40.5	0.03949	0.03886	0.173743E-05	1.0000
* 0:29: 6	50.7	0.03795			
* 1.2 ******MAY	5*				
14:31:56	40.7	0.03737	0.04566	0.987121E-04	1.0000
14:50:53	50.7	0.03718	0.04440	0.444385E-04	1.0000
15:39:21	50.6	0.03988	0.04387	0.289226E-04	1.0000
15:56:45	60.9	0.03833	0.04293	0.174683E-04	1.0000
16:18: 7	71.2	0.04007	0.04170	0.643215E-05	1.0000
16:50:43	81.2	0.04084	0.04046	0.119112E-05	1.0000
*17:13:10	91.6	0.03949			
* 1.3 ******MAY	5*				
19:21:26	102.2	0.04026	0.04606	0.861626E-05	1.0000
19:53:59	112.1	0.04045	0.04491	0.742836E-05	1.0000
20:22:51	124.5	0.03988	0.04366	0.344360E-05	1.0000
*21: 4:19	124.6	0.04296			
* 1.4 ******MAY	6*				
12:35:24	91.6	0.03564	0.03755	0.136629E-04	1.0000
12:57:41	91.5	0.03679	0.03737	0.161433E-04	1.0000
13:35:46	91.4	0.03583	0.03732	0.324030E-05	1.0000
*13:48:44	91.3	0.03699			
* 2.1 ******MAY	19*				
4: 6: 2	30.6	0.04084	0.04471	0.954300E-04	1.0000
4:28:22	41.0	0.03891	0.04382	0.688763E-04	1.0000
5: 8:30	51.1	0.03833	0.04287	0.477013E-04	1.0000
5:37:54	61.4	0.03679	0.04199	0.330631E-04	1.0000
6: 0: 0	71.5	0.03467	0.04125	0.233608E-04	1.0000
6:45:11	81.9	0.03506	0.04017	0.124695E-04	1.0000
7: 5:50	91.8	0.03429	0.03931	0.687268E-05	1.0000
7:35:54	102.0	0.03602	0.03798	0.128860E-05	1.0000
* 8:37: 4	112.1	0.03679			
* 2.2 ******MAY	19*				
22:42:55	30.7	0.04084	0.04691	0.415466E-04	1.0000
23:10:47	40.9	0.04065	0.04594	0.338013E-04	1.0000
23:32:51	51.1	0.03968	0.04499	0.297249E-04	1.0000
23:57:45	61.3	0.03833	0.04408	0.276237E-04	1.0000
0:31: 6	71.5	0.03776	0.04310	0.269016E-04	1.0000
0:55:49	81.8	0.03622	0.04225	0.256004E-04	1.0000
1:23: 3	91.9	0.03660	0.04116	0.292236E-04	1.0000
2:30:44	102.2	0.03583	0.04021	0.310215E-04	1.0000
2:55:20	112.3	0.03545	0.03928	0.334934E-04	1.0000
3:18:32	124.3	0.03506	0.03815	0.385975E-04	1.0000
4:35:52	124.2	0.03564	0.03806	0.148006E-04	1.0000
7: 5:39	124.4	0.03487	0.03845	0.239017E-05	1.0000
* 7:51:40	124.6	0.03795			
8:15:29	112.2	0.03506	0.03975	0.375903E-05	1.0000
8:41: 8	102.3	0.03718	0.04023	0.570144E-05	1.0000

Table F.1. (continued)

RUN NO. DATE TIME	Q(KW)/ROD	DELTA R (OBSERVED)	DELTA R (CALCULATED)	VARIANCE	WEIGHTING FACTOR
9:19:59	92.0	0.04045	0.04060	0.741463E-05	1.0000
9:43:39	81.9	0.04122	0.04149	0.120243E-04	1.0000
10: 7:36	71.5	0.04200	0.04245	0.177074E-04	1.0000
10:31:29	61.3	0.04392	0.04331	0.234455E-04	1.0000
10:55:49	50.5	0.04508	0.04437	0.329178E-04	1.0000
11:19:26	40.7	0.04488	0.04548	0.467457E-04	1.0000
11:44:10	30.3	0.04566	0.04662	0.652588E-04	1.0000
* 3.1 ******MAY 27*					
1:14:13	30.7	0.04816	0.05432	0.499328E-04	1.0000
1:36: 0	40.9	0.04450	0.05344	0.407959E-04	1.0000
2: 2:32	51.1	0.04392	0.05236	0.332886E-04	1.0000
2:23:56	61.4	0.04238	0.05139	0.294067E-04	1.0000
2:45:31	71.6	0.04219	0.05027	0.280552E-04	1.0000
3:11:21	81.8	0.04045	0.04935	0.257618E-04	1.0000
3:32:41	92.0	0.03930	0.04841	0.262081E-04	1.0000
4: 1:10	102.0	0.03911	0.04736	0.287727E-04	1.0000
4:25:28	112.3	0.03949	0.04617	0.334042E-04	1.0000
4:48:45	124.5	0.04026	0.04465	0.402958E-04	1.0000
5:17: 8	124.4	0.04354	0.04396	0.217084E-04	1.0000
* 6:22:58	124.4	0.04431			
6:49:48	111.9	0.04238	0.04605	0.359745E-05	1.0000
7:31:58	101.9	0.04450	0.04664	0.633430E-05	1.0000
8: 0:56	91.8	0.04585	0.04747	0.109428E-04	1.0000
8:23:50	81.7	0.04700	0.04839	0.168949E-04	1.0000
8:46:21	71.4	0.04951	0.04923	0.224316E-04	1.0000
9: 9:52	61.4	0.05047	0.05031	0.309025E-04	1.0000
9:42: 8	51.0	0.05220	0.05139	0.417148E-04	1.0000
10: 4:17	40.8	0.05220	0.05269	0.593262E-04	1.0000
10:26:10	30.7	0.05644	0.05370	0.763916E-04	1.0000
* 4.1 ******JUNE 17*					
13:41: 8	30.7	0.05201	0.05375	0.457420E-04	1.0000
14:36:24	61.3	0.05028	0.04985	0.392647E-05	1.0000
*15: 7:57	92.0	0.04681			
* 4.2 ******JUNE 18*					
9:12:26	30.7	0.04970	0.05022	0.436890E-04	1.0000
9:53:33	61.4	0.04450	0.04688	0.146049E-04	1.0000
10:27:42	92.1	0.04546	0.04326	0.847549E-05	1.0000
11: 5:15	112.3	0.03718	0.04302	0.456798E-05	1.0000
*11:40:33	124.3	0.04103			
* 5.1 ******JULY 8*					
9:51:54	30.8	0.06415	0.06682	0.594177E-04	1.0000
10:41:25	61.3	0.05875	0.06279	0.298462E-04	1.0000
11:35:17	92.0	0.05490	0.05894	0.255009E-04	1.0000
11:41: 1	91.9	0.05606	0.05875	0.259403E-04	1.0000
*13:10: 5	124.3	0.05529			
* 6.1 ******AUG. 4*					
9:59:10	30.8	0.05741	0.06645	0.639770E-04	1.0000
11: 5: 4	62.0	0.05875	0.06176	0.333252E-04	1.0000
11:39:36	91.9	0.05702	0.05793	0.186665E-04	1.0000
12:13:36	124.2	0.05587	0.05439	0.179668E-06	1.0000
*13:19: 7	124.1	0.05471			
* 7.1 ******AUG. 19*					
16:44:27	30.6	0.06030	0.06406	0.593628E-04	1.0000
17:55:35	51.0	0.05779	0.06114	0.363830E-04	1.0000
19: 2:42	101.4	0.05548	0.05494	0.717888E-05	1.0000
*20: 6:22	124.5	0.05278			
* 8.3 ******NOV. 5*					
13:41:33	31.5	0.05509	0.06219	0.561584E-04	1.0000
14: 9: 0	52.5	0.05143	0.05987	0.334900E-04	1.0000
14:29:59	73.9	0.04912	0.05740	0.275390E-04	1.0000
14:49:41	84.0	0.04797	0.05626	0.281170E-04	1.0000
14:53:35	95.0	0.04739	0.05499	0.313488E-04	1.0000
15: 9:45	105.4	0.04739	0.05371	0.380997E-04	1.0000

Table F.1. (continued)

RUN NO. DATE TIME	Q(KW)/ROD	DELTA R (OBSERVED)	DELTA R (CALCULATED)	VARIANCE	WEIGHTING FACTOR
15:44:12	104.6	0.04874	0.05388	0.945282E-05	1.0000
16: 5: 0	109.1	0.04720	0.05370	0.776024E-05	1.0000
16:18:35	113.8	0.04700	0.05327	0.532036E-05	1.0000
*17: 5: 4	124.3	0.05124			
* 9.1 ******NOV. 18*					
12:51:18	30.6	0.06338	0.06309	0.416382E-04	1.0000
13:29:59	31.1	0.06376	0.06304	0.431213E-04	1.0000
13:52:35	51.5	0.05895	0.06048	0.360512E-04	1.0000
14:16:33	71.4	0.05509	0.05814	0.405910E-04	1.0000
14:38:36	81.5	0.05394	0.05690	0.443367E-04	1.0000
14:47:36	91.6	0.05240	0.05576	0.447510E-04	1.0000
15: 2:29	102.0	0.05182	0.05447	0.527252E-04	1.0000
15:21:34	101.6	0.05432	0.05406	0.216137E-04	1.0000
15:38:27	101.4	0.05529	0.05408	0.547528E-05	1.0000
*15:53:39	101.2	0.05452			
*10.1 ******DEC. 8*					
11:25:18	31.3	0.06550	0.06613	0.368248E-04	1.0000
11:47:24	41.5	0.06261	0.06478	0.297020E-04	1.0000
12: 9:36	61.6	0.05818	0.06233	0.434830E-04	1.0000
12:39: 8	82.1	0.05509	0.05981	0.479645E-04	1.0000
13:27: 2	81.7	0.06049	0.05916	0.257772E-05	1.0000
13:32:52	81.6	0.06030	0.05926	0.108497E-05	1.0000
13:43:16	81.5	0.06030	0.05934	0.339670E-06	1.0000
13:46: 3	81.5	0.05991	0.05941	0.130596E-06	1.0000
*13:52:47	81.5	0.05953			
*11.1 ******JAN. 13*					
13:49:36	30.8	0.07262	0.07053	0.390037E-04	1.0000
14:12:27	51.3	0.06530	0.06789	0.366852E-04	1.0000
14:34:40	81.7	0.06049	0.06385	0.489612E-04	1.0000
14:53:30	81.5	0.06184	0.06356	0.182598E-04	1.0000
15:17: 6	81.1	0.06319	0.06347	0.328581E-05	1.0000
15:27:52	81.0	0.06357	0.06349	0.646596E-06	1.0000
*15:36:42	80.9	0.06357			
*12.1 ******JAN. 27*					
11:20:34	30.7	0.07262	0.07215	0.595116E-04	1.0000
11:44:22	51.0	0.06839	0.06922	0.554169E-04	1.0000
12: 8:16	81.6	0.06184	0.06520	0.739929E-04	1.0000
12:33: 5	81.6	0.06357	0.06473	0.189223E-04	1.0000
12:59:52	81.2	0.06473	0.06474	0.669309E-06	1.0000
*13: 9:19	81.8	0.06473			
*13.1 ******FEB. 10*					
10:33:25	30.8	0.06723	0.06921	0.396606E-04	1.0000
10:54: 5	51.4	0.06107	0.06658	0.376076E-04	1.0000
11:14: 1	61.0	0.05933	0.06533	0.363945E-04	1.0000
11:25:44	71.3	0.05856	0.06389	0.350681E-04	1.0000
11:40:22	81.7	0.05721	0.06257	0.341881E-04	1.0000
12:15:12	81.3	0.05914	0.06236	0.910649E-05	1.0000
*13:47: 8	81.6	0.06222			
*14.1 ******MAR. 9*					
11:17:50	30.9	0.07763	0.06970	0.339477E-04	1.0000
11:40: 0	51.2	0.06742	0.06714	0.350464E-04	1.0000
12: 2:29	81.7	0.06049	0.06322	0.427391E-04	1.0000
12:25: 4	81.4	0.06203	0.06298	0.223444E-04	1.0000
12:49:10	81.1	0.06338	0.06289	0.743379E-05	1.0000
13:18:51	81.0	0.06338	0.06319	0.554790E-07	1.0000
*13:34:23	81.5	0.06319			
*15.1 ******MAR. 23*					
10:32: 1	30.6	0.06742	0.06737	0.632996E-04	1.0000
10:55:54	51.2	0.06280	0.06470	0.578178E-04	1.0000
11:40: 2	81.5	0.06049	0.06017	0.836105E-05	1.0000
12:21:39	101.9	0.05837	0.05790	0.193144E-06	1.0000
*13: 8:45	101.9	0.05798			

Table F.1. (continued)

RUN NO. DATE TIME	Q(KW)/ROD	DELTA R (OBSERVED)	DELTA R (CALCULATED)	VARIANCE	WEIGHTING FACTOR
*16.1 ******APR. 27*					
12:28:55	30.7	0.07551	0.06634	0.496399E-04	1.0000
12:55:12	51.2	0.06530	0.06383	0.376190E-04	1.0000
13:21:11	87.8	0.05760	0.05932	0.389671E-04	1.0000
14: 0:52	102.0	0.05664	0.05748	0.687718E-05	1.0000
*14:42:58	101.8	0.05760			
*17.1 ******MAY 26*					
11:23: 5	30.7	0.07763	0.07641	0.453552E-04	1.0000
11:45:13	51.1	0.06742	0.07382	0.308533E-04	1.0000
12: 9:15	89.4	0.05914	0.06896	0.226364E-04	1.0000
12:35:46	101.8	0.05760	0.06776	0.455475E-05	1.0000
12:52:17	101.8	0.05837	0.06790	0.254195E-05	1.0000
13:10:40	101.7	0.06627	0.06665	0.445203E-08	1.0000
*13:13:25	101.8	0.06646			
*18.1 ******JUNE 15*					
16:53:51	30.6	0.07513	0.07067	0.375023E-04	1.0000
17:17:18	51.0	0.06877	0.06760	0.857048E-05	1.0000
17:36:32	81.7	0.06338	0.06363	0.234771E-05	1.0000
17:54:39	81.5	0.06415	0.06371	0.824472E-08	1.0000
*18: 7:50	81.5	0.06376			
*19.1 ******JUNE 29*					
12: 8:50	30.6	0.07397	0.06460	0.371338E-04	1.0000
12:31:59	51.0	0.06935	0.06144	0.135704E-04	1.0000
13: 6:26	81.7	0.06164	0.05766	0.117737E-04	1.0000
13:31:46	101.8	0.05664	0.05616	0.123965E-06	1.0000
*13:40:39	101.8	0.05625			
*20.1 ******AUG. 22*					
11:41:52	30.5	0.08438	0.07445	0.479370E-04	1.0000
12: 5:46	51.9	0.07744	0.07104	0.169269E-04	1.0000
12:35:35	81.6	0.06993	0.06693	0.403976E-05	1.0000
13: 1:53	101.8	0.06530	0.06484	0.202356E-07	1.0000
*13:21:45	101.8	0.06492			
*21.1 ******SEP. 21*					
11:49:40	30.9	0.08611	0.07271	0.322082E-04	1.0000
12:10:45	51.4	0.07686	0.06955	0.125999E-04	1.0000
12:43:59	71.9	0.07166	0.06670	0.404892E-05	1.0000
15:20:14	91.8	0.06492	0.06493	0.283326E-09	1.0000
*15:22: 6	91.8	0.06492			
*22.1 ******OCT. 12*					
11:48:40	31.1	0.07860	0.06990	0.345703E-04	1.0000
12:17:55	80.7	0.06704	0.06267	0.187099E-04	1.0000
12:29:23	101.9	0.06203	0.06053	0.896044E-05	1.0000
12:50:23	102.0	0.06049	0.06117	0.177920E-07	1.0000
*13: 0:25	102.0	0.06107			
*23.1 ******NOV. 30*					
11:22: 7	31.1	0.07648	0.07230	0.412720E-04	1.0000
11:41:15	51.8	0.06896	0.06939	0.231342E-04	1.0000
11:58:35	72.4	0.06550	0.06641	0.143703E-04	1.0000
12:19:17	101.9	0.06126	0.06300	0.370245E-05	1.0000
12:38:44	101.7	0.06222	0.06310	0.275060E-07	1.0000
*12:44:28	101.7	0.06299			
*23.2 ******DEC. 15*					
10: 5:18	31.0	0.07417	0.07043	0.389465E-04	1.0000
10:27:17	61.5	0.06704	0.06595	0.142479E-04	1.0000
10:39: 4	61.6	0.06704	0.06592	0.131172E-04	1.0000
11: 9:20	102.1	0.06107	0.06122	0.325414E-06	1.0000
11:16:15	102.2	0.05991	0.06154	0.817671E-07	1.0000
*11:23:26	102.1	0.06126			
*23.3 ******JAN. 19*					
15: 7: 0	31.0	0.07917	0.06932	0.344421E-04	1.0000
15:28:51	51.9	0.07070	0.06637	0.175449E-04	1.0000
15:48:34	82.4	0.06511	0.06242	0.603905E-05	1.0000
16:13:41	101.8	0.06184	0.06049	0.587538E-07	1.0000
*16:17:13	101.9	0.06068			

Table F.1. (continued)

RUN NO. DATE TIME	Q(KW)/ROD	DELTA R (OBSERVED)	DELTA R (CALCULATED)	VARIANCE	WEIGHTING FACTOR
*24.1 ******FEB. 16**					
10:42: 1	30.5	0.07128	0.06977	0.407776E-04	1.0000
11: 8:40	51.2	0.06665	0.06671	0.178997E-04	1.0000
11:28:20	72.1	0.06338	0.06396	0.938186E-05	1.0000
12:29: 8	102.0	0.05933	0.06065	0.575870E-07	1.0000
*12:50:11	102.0	0.06049			

****
SHEATH GAP THERMAL EXPANSION MODEL REGRESSION PROGRAM
****

(AT THERMOCOUPLE POWER LEVEL G)

BEST FIT PARAMETERS FOR THERMAL EXPANSION MODEL:
WHERE,

L-LO = LO*(EXP(C(1)*(T-TO)+C(2)*(T**2-TO**2)+C(3)*(T**3-TO**3))-1.0)

C(1)=-0.75735846E 01 STD DEVIATION= 0.31148357E 01
C(2)= 0.18951051E-01 STD DEVIATION= 0.43839806E-02
C(3)=-0.81113449E-05 STD DEVIATION= 0.21456240E-05

VARIANCE OF FIT= 0.50953846E-01
VARIANCE OF FIT DIVIDED BY THE SUM OF THE WEIGHTING FACTORS= 0.16165548E-04
TOTAL NUMBER OF DATA POINTS= 3691

Table F.2. ORTCAL — Part IV individual regression for TE-318BG

****
*** THERMOCOUPLE NUMBER: TE-318BG ***
****

NOMENCLATURE:
Q(KW)/ROD = NOMINAL POWER INPUT PER ROD IN KW
DELTA R = GAP BETWEEN INNER AND OUTER S.S.SHEATHS (MILS OF INCHES)
TIME = WALL CLOCK TIME
NOTE:
ASTERISK DENOTES BIAS POINT

RUN NO. DATE TIME	Q(KW)/ROD	DELTA R (OBSERVED)	DELTA R (CALCULATED)	VARIANCE	WEIGHTING FACTOR
* 1.1 ******MAY 4*					
23:36:56	30.3	0.04142	0.04044	0.802082E-04	1.0000
23:44:18	40.1	0.03911	0.03923	0.178631E-04	1.0000
23:53:20	40.5	0.03949	0.03910	0.144493E-04	1.0000
* 0:29: 6	50.7	0.03795			
* 1.2 ******MAY 5*					
14:31:56	40.7	0.03737	0.04525	0.128405E-02	1.0000
14:50:53	50.7	0.03718	0.04432	0.517181E-03	1.0000
15:39:21	50.6	0.03988	0.04452	0.246167E-03	1.0000
15:56:45	60.9	0.03833	0.04346	0.146777E-03	1.0000
16:18: 7	71.2	0.04007	0.04174	0.628921E-04	1.0000
16:50:43	81.2	0.04084	0.04040	0.121914E-04	1.0000
*17:13:10	91.6	0.03949			
* 1.3 ******MAY 5*					
19:21:26	102.2	0.04026	0.04496	0.683349E-04	1.0000
19:53:59	112.1	0.04045	0.04374	0.614502E-04	1.0000
20:22:51	124.5	0.03988	0.04284	0.284077E-04	1.0000
*21: 4:19	124.6	0.04296			
* 1.4 ******MAY 6*					
12:35:24	91.6	0.03564	0.03683	0.188314E-03	1.0000
12:57:41	91.5	0.03679	0.03652	0.217104E-03	1.0000
13:35:46	91.4	0.03583	0.03698	0.449411E-04	1.0000
*13:48:44	91.3	0.03699			
* 2.1 ******MAY 19*					
4: 6: 2	30.6	0.04084	0.04607	0.782336E-03	1.0000
4:28:22	41.0	0.03891	0.04476	0.574933E-03	1.0000
5: 8:30	51.1	0.03833	0.04346	0.407281E-03	1.0000
5:37:54	61.4	0.03679	0.04239	0.282239E-03	1.0000
6: 0: 0	71.5	0.03467	0.04156	0.196454E-03	1.0000
6:45:11	81.9	0.03506	0.04031	0.105048E-03	1.0000
7: 5:50	91.8	0.03429	0.03946	0.557499E-04	1.0000
7:35:54	102.0	0.03602	0.03797	0.105011E-04	1.0000
* 8:37: 4	112.1	0.03679			
* 2.2 ******MAY 19*					
22:42:55	30.7	0.04084	0.04554	0.291211E-03	1.0000
23:10:47	40.9	0.04065	0.04406	0.233203E-03	1.0000
23:32:51	51.1	0.03968	0.04277	0.208484E-03	1.0000
23:57:45	61.3	0.03833	0.04165	0.200134E-03	1.0000
0:31: 6	71.5	0.03776	0.04050	0.204620E-03	1.0000
0:55:49	81.8	0.03622	0.03959	0.207294E-03	1.0000
1:23: 3	91.9	0.03660	0.03840	0.250818E-03	1.0000
2:30:44	102.2	0.03583	0.03748	0.281653E-03	1.0000
2:55:20	112.3	0.03545	0.03663	0.316406E-03	1.0000
3:18:32	124.3	0.03506	0.03558	0.368756E-03	1.0000
4:35:52	124.2	0.03564	0.03660	0.184107E-03	1.0000
7: 5:39	124.4	0.03487	0.03798	0.453838E-04	1.0000
* 7:51:40	124.6	0.03795			
8:15:29	112.2	0.03506	0.03984	0.437794E-04	1.0000
8:41: 8	102.3	0.03718	0.04019	0.791015E-04	1.0000

Table F.2. (continued)

RUN NO. DATE TIME	Q(KW)/ROD	DELTA R (OBSERVED)	DELTA R (CALCULATED)	VARIANCE	WEIGHTING FACTOR
9:19:59	92.0	0.04045	0.04043	0.115594E-03	1.0000
9:43:39	81.9	0.04122	0.04124	0.181622E-03	1.0000
10: 7:36	71.5	0.04200	0.04215	0.252631E-03	1.0000
10:31:29	61.3	0.04392	0.04299	0.313568E-03	1.0000
10:55:49	50.5	0.04508	0.04411	0.398950E-03	1.0000
11:19:26	40.7	0.04488	0.04537	0.515259E-03	1.0000
11:44:10	30.3	0.04566	0.04671	0.667382E-03	1.0000
* 3.1 ******MAY 27*					
1:14:13	30.7	0.04816	0.05277	0.353027E-03	1.0000
1:36: 0	40.9	0.04450	0.05145	0.281836E-03	1.0000
2: 2:32	51.1	0.04392	0.05004	0.231445E-03	1.0000
2:23:56	61.4	0.04238	0.04883	0.212988E-03	1.0000
2:45:31	71.6	0.04219	0.04752	0.218536E-03	1.0000
3:11:21	81.8	0.04045	0.04658	0.221924E-03	1.0000
3:32:41	92.0	0.03930	0.04564	0.247467E-03	1.0000
4: 1:10	102.0	0.03911	0.04459	0.289929E-03	1.0000
4:25:28	112.3	0.03949	0.04344	0.347113E-03	1.0000
4:48:45	124.5	0.04026	0.04203	0.416290E-03	1.0000
5:17: 8	124.4	0.04354	0.04230	0.258202E-03	1.0000
* 6:22:58	124.4	0.04431			
6:49:48	111.9	0.04238	0.04611	0.448688E-04	1.0000
7:31:58	101.9	0.04450	0.04657	0.948120E-04	1.0000
8: 0:56	91.8	0.04585	0.04729	0.168384E-03	1.0000
8:23:50	81.7	0.04700	0.04815	0.256750E-03	1.0000
8:46:21	71.4	0.04951	0.04890	0.332355E-03	1.0000
9: 9:52	61.4	0.05047	0.04995	0.425995E-03	1.0000
9:42: 8	51.0	0.05220	0.05110	0.526923E-03	1.0000
10: 4:17	40.8	0.05220	0.05255	0.678808E-03	1.0000
10:26:10	30.7	0.05644	0.05371	0.817382E-03	1.0000
* 4.1 ******JUNE 17*					
13:41: 8	30.7	0.05201	0.05247	0.418396E-03	1.0000
14:36:24	61.3	0.05028	0.04928	0.336731E-04	1.0000
*15: 7:57	92.0	0.04681			
* 4.2 ******JUNE 18*					
9:12:26	30.7	0.04970	0.04850	0.302637E-03	1.0000
9:53:33	61.4	0.04450	0.04518	0.168420E-03	1.0000
10:27:42	92.1	0.04546	0.04217	0.170636E-03	1.0000
11: 5:15	112.3	0.03718	0.04306	0.580364E-04	1.0000
*11:40:33	124.3	0.04103			
* 5.1 ******JULY 8*					
9:51:54	30.8	0.06415	0.06477	0.447656E-03	1.0000
10:41:25	61.3	0.05875	0.05990	0.308789E-03	1.0000
11:35:17	92.0	0.05490	0.05672	0.459228E-03	1.0000
11:41: 1	91.9	0.05606	0.05653	0.461865E-03	1.0000
*13:10: 5	124.3	0.05529			
* 6.1 ******AUG. 4*					
9:59:10	30.8	0.05741	0.06457	0.475781E-03	1.0000
11: 5: 4	62.0	0.05875	0.06046	0.561328E-03	1.0000
11:39:36	91.9	0.05702	0.05663	0.391681E-03	1.0000
12:13:36	124.2	0.05587	0.05432	0.145354E-05	1.0000
*13:19: 7	124.1	0.05471			
* 7.1 ******AUG. 19*					
16:44:27	30.6	0.06030	0.06211	0.426855E-03	1.0000
17:55:35	51.0	0.05779	0.05977	0.487793E-03	1.0000
19: 2:42	101.4	0.05548	0.05462	0.136780E-03	1.0000
*20: 6:22	124.5	0.05278			
* 8.3 ******NOV. 5*					
13:41:33	31.5	0.05509	0.06060	0.443554E-03	1.0000
14: 9: 0	52.5	0.05143	0.05731	0.259277E-03	1.0000
14:29:59	73.9	0.04912	0.05451	0.271582E-03	1.0000
14:49:41	84.0	0.04797	0.05334	0.311352E-03	1.0000
14:53:35	95.0	0.04739	0.05207	0.372015E-03	1.0000
15: 9:45	105.4	0.04739	0.05075	0.446100E-03	1.0000

Table F.2. (continued)

RUN NO. DATE TIME	Q(KW)/ROD	DELTA R (OBSERVED)	DELTA R (CALCULATED)	VARIANCE	WEIGHTING FACTOR
15:44:12	104.6	0.04874	0.05357	0.170746E-03	1.0000
16: 5: 0	109.1	0.04720	0.05361	0.120959E-03	1.0000
16:18:35	113.8	0.04700	0.05322	0.812439E-04	1.0000
*17: 5: 4	124.3	0.05124			
* 9.1 ******NOV. 18*					
12:51:18	30.6	0.06338	0.06131	0.293555E-03	1.0000
13:29:59	31.1	0.06376	0.06113	0.309668E-03	1.0000
13:52:35	51.5	0.05895	0.05778	0.273614E-03	1.0000
14:16:33	71.4	0.05509	0.05507	0.327447E-03	1.0000
14:38:36	81.5	0.05394	0.05381	0.369049E-03	1.0000
14:47:36	91.6	0.05240	0.05279	0.386517E-03	1.0000
15: 2:29	102.0	0.05182	0.05155	0.461792E-03	1.0000
15:21:34	101.6	0.05432	0.05233	0.221013E-03	1.0000
15:38:27	101.4	0.05529	0.05333	0.629185E-04	1.0000
*15:53:39	101.2	0.05452			
*10.1 ******DEC. 8*					
11:25:18	31.3	0.06550	0.06424	0.301208E-03	1.0000
11:47:24	41.5	0.06261	0.06261	0.238824E-03	1.0000
12: 9:36	61.6	0.05818	0.05950	0.367694E-03	1.0000
12:39: 8	82.1	0.05509	0.05703	0.402667E-03	1.0000
13:27: 2	81.7	0.06049	0.05862	0.265767E-04	1.0000
13:32:52	81.6	0.06030	0.05894	0.113682E-04	1.0000
13:43:16	81.5	0.06030	0.05917	0.349899E-05	1.0000
13:46: 3	81.5	0.05991	0.05931	0.132078E-05	1.0000
*13:52:47	81.5	0.05953			
*11.1 ******JAN. 13*					
13:49:36	30.8	0.07262	0.06918	0.327338E-03	1.0000
14:12:27	51.3	0.06530	0.06564	0.334845E-03	1.0000
14:34:40	81.7	0.06049	0.06118	0.422040E-03	1.0000
14:53:30	81.5	0.06184	0.06188	0.153775E-03	1.0000
15:17: 6	81.1	0.06319	0.06276	0.300522E-04	1.0000
15:27:52	81.0	0.06357	0.06319	0.628595E-05	1.0000
*15:36:42	80.9	0.06357			
*12.1 ******JAN. 27*					
11:20:34	30.7	0.07262	0.07037	0.564368E-03	1.0000
11:44:22	51.0	0.06839	0.06655	0.532947E-03	1.0000
12: 8:16	81.6	0.06184	0.06201	0.655462E-03	1.0000
12:33: 5	81.6	0.06357	0.06300	0.159597E-03	1.0000
12:59:52	81.2	0.06473	0.06440	0.692754E-05	1.0000
*13: 9:19	81.8	0.06473			
*13.1 ******FEB. 10*					
10:33:25	30.8	0.06723	0.06718	0.318530E-03	1.0000
10:54: 5	51.4	0.06107	0.06390	0.308972E-03	1.0000
11:14: 1	61.0	0.05933	0.06259	0.297473E-03	1.0000
11:25:44	71.3	0.05856	0.06123	0.291705E-03	1.0000
11:40:22	81.7	0.05721	0.06012	0.294818E-03	1.0000
12:15:12	81.3	0.05914	0.06115	0.100449E-03	1.0000
*13:47: 8	81.6	0.06222			
*14.1 ******MAR. 9*					
11:17:50	30.9	0.07763	0.06771	0.267004E-03	1.0000
11:40: 0	51.2	0.06742	0.06451	0.287384E-03	1.0000
12: 2:29	81.7	0.06049	0.06060	0.361560E-03	1.0000
12:25: 4	81.4	0.06203	0.06111	0.201593E-03	1.0000
12:49:10	81.1	0.06338	0.06189	0.766445E-04	1.0000
13:18:51	81.0	0.06338	0.06311	0.781734E-06	1.0000
*13:34:23	81.5	0.06319			
*15.1 ******MAR. 23*					
10:32: 1	30.6	0.06742	0.06567	0.501562E-03	1.0000
10:55:54	51.2	0.06280	0.06193	0.500354E-03	1.0000
11:40: 2	81.5	0.06049	0.05862	0.923950E-04	1.0000
12:21:39	101.9	0.05837	0.05775	0.209945E-05	1.0000
*13: 8:45	101.9	0.05798			

Table F.2. (continued)

RUN NO. DATE TIME	Q(KW)/ROD	DELTA R (OBSERVED)	DELTA R (CALCULATED)	VARIANCE	WEIGHTING FACTOR
*16.1 ******APR. 27*					
12:28:55	30.7	0.07551	0.06468	0.373535E-03	1.0000
12:55:12	51.2	0.06530	0.06139	0.295129E-03	1.0000
13:21:11	87.8	0.05760	0.05653	0.323968E-03	1.0000
14: 0:52	102.0	0.05664	0.05647	0.722832E-04	1.0000
*14:42:58	101.8	0.05760			
*17.1 ******MAY 26*					
11:23: 5	30.7	0.07763	0.07437	0.321093E-03	1.0000
11:45:13	51.1	0.06742	0.07108	0.235547E-03	1.0000
12: 9:15	89.4	0.05914	0.06668	0.312597E-03	1.0000
12:35:46	101.8	0.05760	0.06722	0.960571E-04	1.0000
12:52:17	101.8	0.05837	0.06797	0.308796E-04	1.0000
13:10:40	101.7	0.06627	0.06665	0.432931E-07	1.0000
*13:13:25	101.8	0.06646			
*18.1 ******JUNE 15*					
16:53:51	30.6	0.07513	0.06908	0.308057E-03	1.0000
17:17:18	51.0	0.06877	0.06622	0.624206E-04	1.0000
17:36:32	81.7	0.06338	0.06304	0.234145E-04	1.0000
17:54:39	81.5	0.06415	0.06370	0.695318E-07	1.0000
*18: 7:50	81.5	0.06376			
*19.1 ******JUNE 29*					
12: 8:50	30.6	0.07397	0.06254	0.256347E-03	1.0000
12:31:59	51.0	0.06935	0.05953	0.149579E-03	1.0000
13: 6:26	81.7	0.06164	0.05616	0.178693E-03	1.0000
13:31:46	101.8	0.05664	0.05606	0.152226E-05	1.0000
*13:40:39	101.8	0.05625			
*20.1 ******AUG. 22*					
11:41:52	30.5	0.08438	0.07316	0.338672E-03	1.0000
12: 5:46	51.9	0.07744	0.06920	0.131470E-03	1.0000
12:35:35	81.6	0.06993	0.06608	0.773254E-04	1.0000
13: 1:53	101.8	0.06530	0.06481	0.169650E-06	1.0000
*13:21:45	101.8	0.06492			
*21.1 ******SEP. 21*					
11:49:40	30.9	0.08611	0.07086	0.223242E-03	1.0000
12:10:45	51.4	0.07686	0.06766	0.115301E-03	1.0000
12:43:59	71.9	0.07166	0.06591	0.805847E-04	1.0000
15:20:14	91.8	0.06492	0.06494	0.525210E-08	1.0000
*15:22: 6	91.8	0.06492			
*22.1 ******OCT. 12*					
11:48:40	31.1	0.07860	0.06801	0.251074E-03	1.0000
12:17:55	80.7	0.06704	0.06075	0.261713E-03	1.0000
12:29:23	101.9	0.06203	0.05960	0.109566E-03	1.0000
12:50:23	102.0	0.06049	0.06115	0.345898E-06	1.0000
*13: 0:25	102.0	0.06107			
*23.1 ******NOV. 30*					
11:22: 7	31.1	0.07648	0.07029	0.286230E-03	1.0000
11:41:15	51.8	0.06896	0.06692	0.192059E-03	1.0000
11:58:35	72.4	0.06550	0.06451	0.227325E-03	1.0000
12:19:17	101.9	0.06126	0.06240	0.559753E-04	1.0000
12:38:44	101.7	0.06222	0.06311	0.285530E-06	1.0000
*12:44:28	101.7	0.06299			
*23.2 ******DEC. 15*					
10: 5:18	31.0	0.07417	0.06856	0.273926E-03	1.0000
10:27:17	61.5	0.06704	0.06396	0.196527E-03	1.0000
10:39: 4	61.6	0.06704	0.06417	0.207092E-03	1.0000
11: 9:20	102.1	0.06107	0.06106	0.485437E-05	1.0000
11:16:15	102.2	0.05991	0.06154	0.739574E-06	1.0000
*11:23:26	102.1	0.06126			
*23.3 ******JAN. 19*					
15: 7: 0	31.0	0.07917	0.06806	0.312597E-03	1.0000
15:28:51	51.9	0.07070	0.06522	0.269000E-03	1.0000
15:48:34	82.4	0.06511	0.06168	0.126416E-03	1.0000
16:13:41	101.8	0.06184	0.06045	0.488448E-06	1.0000
*16:17:13	101.9	0.06068			

Table F.2. (continued)

RUN NO. DATE TIME	Q(KW)/ROD	DELTA R (OBSERVED)	DELTA R (CALCULATED)	VARIANCE	WEIGHTING FACTOR
*24.1 ******FEB. 15*					
10:42: 1	30.5	0.07128	0.06833	0.299707E-03	1.0000
11: 8:40	51.2	0.06665	0.06549	0.230164E-03	1.0000
11:28:20	72.1	0.06338	0.06300	0.181000E-03	1.0000
12:29: 8	102.0	0.05933	0.06066	0.595021E-06	1.0000
*12:50:11	102.0	0.06049			

BEST FIT PARAMETERS FOR THERMAL EXPANSION MODEL:
WHERE,

L-L0 = L0*(EXP(C(1)*(T-T0)+C(2)*(T**2-T0**2)+C(3)*(T**3-T0**3))-1.0)

C(1)= 0.62502546E 01 STD DEVIATION= 0.12002551E 02
C(2)= 0.60596764E-02 STD DEVIATION= 0.17433237E-01
C(3)=-0.43716855E-05 STD DEVIATION= 0.87200751E-05

VARIANCE OF FIT= 0.14808461E-01
VARIANCE OF FIT DIVIDED BY THE SUM OF THE WEIGHTING FACTORS= 0.81365113E-04
TOTAL NUMBER OF DATA POINTS= 213

Table F.3. Summary of ORTCAL — Part IV regression
for TE position 318BG

```
   ********************************
*** THERMOCOUPLE NUMBER:  TE-318BG  ***
   ********************************


SUMMARY:
        LEVEL REGRESSION---NO ERRORS
        INDIVIDUAL T/C REGRESSION---NO ERRORS
        THE FIRST DERIVATIVES OF BOTH SOLUTIONS ARE POSITIVE AT ALL BIAS POINTS.
        SUMMATION OF VARIANCES FOR BOTH SOLUTIONS:
                BY LEVEL SOLUTION= 0.36986982E-02
                BY INDIVIDUAL T/C SOLUTION= 0.31808661E-02
```

Table F.4. Summary of ORTCAL — Part IV regressions
for THTF bundle 1 through Run 24.1

****
***LEVEL A ***
****

(THTF BUNDLE NUMBER 1 DOES NOT HAVE ROD THERMOCOUPLES ON THIS LEVEL)

****
***LEVEL B ***
****

(THTF BUNDLE NUMBER 1 DOES NOT HAVE ROD THERMOCOUPLES ON THIS LEVEL)

****
***LEVEL C ***
****

(THTF BUNDLE NUMBER 1 DOES NOT HAVE ROD THERMOCOUPLES ON THIS LEVEL)

****
***LEVEL D ***
****

INDIVIDUAL THERMOCOUPLE LISTING:

T/C NO.	TYPE OF REGRESSION	C(1)	C(2)	C(3)	TMAX
301AD	FAILED				
304AD	FAILED				
309AD	FAILED				
310AD	INDIVIDUAL	-40.145	0.10251	-0.554344E-04	753.8
312AD	FAILED				
313AD	INDIVIDUAL	-78.915	0.15663	-0.834799E-04	733.8
317AD	INDIVIDUAL	-46.153	0.09332	-0.481768E-04	702.8
318AD	FAILED				
320AD	FAILED				
322AD	INDIVIDUAL	-22.445	0.04177	-0.839944E-05	680.1
323AD	INDIVIDUAL	22.742	-0.01605	0.102341E-04	706.8
325AD	INDIVIDUAL	-73.236	0.14489	-0.751986E-04	697.7
326AD	FAILED				
331AD	FAILED				
338AD	FAILED				
339AD	FAILED				
341AD	INDIVIDUAL	-42.871	0.08579	-0.454424E-04	700.5
349AD	FAILED				
324AD	DEAD				
333AD	DEAD				
330AD	METRASCOPE				
332AD	METRASCOPE				
334AD	METRASCOPE				
319AD	METRASCOPE				

TOTAL NUMBER OF INDIVIDUAL T/C REGRESSIONS= 7
MEAN REGRESSION COEFFICIENTS: -40.146 0.08698 -0.436996E-04

**THERE WERE NO LEVEL T/C REGRESSIONS AVAILABLE IN THE CDT ARRAYS.

Table F.4. (continued)

****
***LEVEL E ***
****

INDIVIDUAL THERMOCOUPLE LISTING:

T/C NO.	TYPE OF REGRESSION	C(1)	C(2)	C(3)	TMAX
301AE	LEVEL				
304AE	INDIVIDUAL	-12.477	0.02524	-0.117173E-04	732.9
309AE	INDIVIDUAL	-15.172	0.03732	-0.188683E-04	750.0
312AE	INDIVIDUAL	1.700	0.01745	-0.118790E-04	805.3
313AE	INDIVIDUAL	-23.179	0.06178	-0.326217E-04	767.2
317AE	INDIVIDUAL	-3.336	0.03144	-0.181708E-04	760.8
318AE	INDIVIDUAL	-24.553	0.04865	-0.243825E-04	747.1
320AE	INDIVIDUAL	9.160	0.01445	-0.102358E-04	783.6
322AE	INDIVIDUAL	-33.075	0.06626	-0.283788E-04	730.3
323AE	INDIVIDUAL	44.742	-0.04066	0.223233E-04	738.1
324AE	INDIVIDUAL	-53.540	0.09497	-0.471450E-04	737.4
325AE	INDIVIDUAL	-38.113	0.08856	-0.456615E-04	738.9
326AF	INDIVIDUAL	-49.722	0.09929	-0.560044E-04	750.7
331AE	INDIVIDUAL	-27.586	0.05592	-0.265679E-04	750.6
333AE	INDIVIDUAL	-24.444	0.04972	-0.259172E-04	729.8
338AE	INDIVIDUAL	-48.352	0.08909	-0.480215E-04	723.5
339AE	LEVEL				
341AE	INDIVIDUAL	26.910	-0.01910	0.809371E-05	765.2
349AE	LEVEL				
310AE	DEAD				
330AE	METRASCOPE				
332AE	METRASCOPE				
334AE	METRASCOPE				
319AE	METRASCOPE				

TOTAL NUMBER OF INDIVIDUAL T/C REGRESSIONS= 16

MEAN REGRESSION COEFFICIENTS:	-16.940	0.04502	-0.234471E-04
LEVEL REGRESSION COEFFICIENTS:	-34.541	0.07141	-0.380442E-04

****
***LEVEL F ***
****

INDIVIDUAL THERMOCOUPLE LISTING:

T/C NO.	TYPE OF REGRESSION	C(1)	C(2)	C(3)	TMAX
301BF	INDIVIDUAL	27.830	-0.04133	0.234332E-04	839.6
304BF	INDIVIDUAL	47.101	-0.07012	0.396057E-04	789.2
309BF	INDIVIDUAL	40.691	-0.05123	0.278024E-04	815.6
310BF	INDIVIDUAL	29.594	-0.02492	0.149031E-04	867.8
312BF	INDIVIDUAL	38.644	-0.03982	0.235163E-04	844.9
313BF	INDIVIDUAL	15.654	-0.00410	0.488843E-05	832.6
317BF	INDIVIDUAL	66.609	-0.08061	0.419395E-04	829.0
320BF	INDIVIDUAL	20.451	-0.01351	0.760119E-05	848.7
322BF	INDIVIDUAL	-5.305	0.01975	-0.634452E-05	834.7
323BF	INDIVIDUAL	30.344	-0.02199	0.118078E-04	840.1
324BF	INDIVIDUAL	-26.506	0.04789	-0.174963E-04	798.1
325BF	INDIVIDUAL	4.604	0.01249	-0.932566E-06	823.7
326BF	INDIVIDUAL	24.905	-0.02847	0.139857E-04	813.3

Table F.4. (continued)

T/C NO.	TYPE OF REGRESSION	C(1)	C(2)	C(3)	TMAX
331BF	LEVEL				
333BF	INDIVIDUAL	13.323	-0.01177	0.755858E-05	799.8
338BF	INDIVIDUAL	38.478	-0.04941	0.253618E-04	814.7
341BF	INDIVIDUAL	44.908	-0.04935	0.241982E-04	865.2
349BF	LEVEL				
318BF	DEAD				
339BF	DEAD				
330BF	METRASCOPE				
332BF	METRASCOPE				
334BF	METRASCOPE				
319BF	METRASCOPE				
TOTAL NUMBER OF INDIVIDUAL T/C REGRESSIONS=		16			
MEAN REGRESSION COEFFICIENTS:		25.708	-0.02541	0.151143E-04	
LEVEL REGRESSION COEFFICIENTS:		13.754	-0.01112	0.837150E-05	

****
***LEVEL G ***
****

INDIVIDUAL THERMOCOUPLE LISTING:

T/C NO.	TYPE OF REGRESSION	C(1)	C(2)	C(3)	TMAX
301BG	LEVEL				
304BG	INDIVIDUAL	32.639	-0.04861	0.267623E-04	802.5
309BG	INDIVIDUAL	13.724	-0.01608	0.832567E-05	842.5
310BG	INDIVIDUAL	-7.174	0.02513	-0.127434E-04	915.3
312BG	INDIVIDUAL	-16.731	0.05432	-0.272220E-04	879.9
313BG	INDIVIDUAL	-18.048	0.03750	-0.165786E-04	876.3
317BG	INDIVIDUAL	10.245	0.00694	-0.518925E-05	884.7
318BG	INDIVIDUAL	6.250	0.00606	-0.437169E-05	817.2
320BG	INDIVIDUAL	-9.195	0.04095	-0.206186E-04	907.0
322BG	INDIVIDUAL	8.295	0.00275	0.186155E-05	804.4
323BG	LEVEL				
325BG	INDIVIDUAL	23.491	-0.01084	0.386484E-05	842.1
326BG	LEVEL				
331BG	INDIVIDUAL	3.865	0.01003	-0.551025E-05	847.8
333BG	INDIVIDUAL	-8.755	0.02086	-0.102926E-04	826.6
338BG	INDIVIDUAL	-8.384	0.02445	-0.142865E-04	790.1
339BG	INDIVIDUAL	101.792	-0.14269	0.676555E-04	802.9
341BG	INDIVIDUAL	9.414	0.00128	-0.457405E-05	853.4
349BG	LEVEL				
324BG	DEAD				
330BG	METRASCOPE				
332BG	METRASCOPE				
334BG	METRASCOPE				
319BG	METRASCOPE				
TOTAL NUMBER OF INDIVIDUAL T/C REGRESSIONS=		15			
MEAN REGRESSION COEFFICIENTS:		9.429	0.00080	-0.861132E-06	
LEVEL REGRESSION COEFFICIENTS:		-7.574	0.01895	-0.811134E-05	

Table F.4. (continued)

****
***LEVEL H ***
****

INDIVIDUAL THERMOCOUPLE LISTING:

T/C NO.	TYPE OF REGRESSION	C(1)	C(2)	C(3)	TMAX
301CH	FAILED				
302AH	FAILED				
303AH	FAILED				
304CH	FAILED				
305AH	FAILED				
306AH	FAILED				
307AH	FAILED				
308AH	FAILED				
309CH	FAILED				
310CH	FAILED				
311AH	FAILED				
312CH	FAILED				
313CH	FAILED				
314AH	FAILED				
315AH	FAILED				
316AH	FAILED				
317CH	FAILED				
318CH	FAILED				
320CH	FAILED				
321AH	FAILED				
322CH	FAILED				
323CH	FAILED				
324CH	FAILED				
325CH	FAILED				
326CH	FAILED				
327AH	FAILED				
328AH	FAILED				
331CH	FAILED				
333CH	FAILED				
336AH	FAILED				
337AH	FAILED				
338CH	FAILED				
339CH	FAILED				
340AH	FAILED				
341CH	FAILED				
342AH	FAILED				
343AH	FAILED				
344AH	FAILED				
345AH	FAILED				
346AH	FAILED				
348AH	FAILED				
349CH	FAILED				
329AH	METRASCOPE				
330CH	METRASCOPE				
332CH	METRASCOPE				
334CH	METRASCOPE				
335AH	METRASCOPE				
319CH	METRASCOPE				
347AH	METRASCOPE				

**THERE WERE NO INDIVIDUAL T/C REGRESSIONS FOR THIS LEVEL (IN THE CDT ARRAYS);
THERFORE, MEAN REGRESSION COEFFICIENTS COULD NOT BE DETERMINED.

**THERE WERE NO LEVEL T/C REGRESSIONS AVAILABLE IN THE CDT ARRAYS.

Table F.4. (continued)

****
***LEVEL I ***
****

INDIVIDUAL THERMOCOUPLE LISTING:

T/C NO.	TYPE OF REGRESSION	C(1)	C(2)	C(3)	TMAX
301CI	FAILED				
302AI	INDIVIDUAL	101.633	-0.10599	0.542323E-04	787.1
303AI	INDIVIDUAL	35.907	-0.04657	0.281355E-04	792.9
304CI	INDIVIDUAL	84.407	-0.13872	0.763129E-04	786.7
305AI	FAILED				
306AI	INDIVIDUAL	36.449	-0.04454	0.229843E-04	782.9
307AI	INDIVIDUAL	44.855	-0.06283	0.351923E-04	780.3
308AI	INDIVIDUAL	101.157	-0.14778	0.795754E-04	786.3
309CI	INDIVIDUAL	74.945	-0.11030	0.594786E-04	769.4
310CI	INDIVIDUAL	68.017	-0.09146	0.486445E-04	866.5
311AI	INDIVIDUAL	83.262	-0.11893	0.614463E-04	817.6
312CI	INDIVIDUAL	50.068	-0.05423	0.279295E-04	867.2
313CI	INDIVIDUAL	56.041	-0.07554	0.406202E-04	830.0
314AI	INDIVIDUAL	24.036	-0.03954	0.231110E-04	779.7
315AI	INDIVIDUAL	55.597	-0.06413	0.336418E-04	857.9
316AI	INDIVIDUAL	158.330	-0.20181	0.100393E-03	830.0
317CI	INDIVIDUAL	71.019	-0.08404	0.404205E-04	825.3
318CI	INDIVIDUAL	-60.349	0.10318	-0.513518E-04	761.5
320CI	INDIVIDUAL	87.506	-0.12072	0.607520E-04	820.1
321AI	INDIVIDUAL	30.688	-0.03887	0.208915E-04	792.9
322CI	INDIVIDUAL	65.059	-0.09992	0.554906E-04	791.8
323CI	INDIVIDUAL	61.557	-0.07802	0.411323E-04	800.9
324CI	INDIVIDUAL	134.927	-0.20256	0.105696E-03	795.0
325CI	INDIVIDUAL	28.018	-0.02401	0.138970E-04	890.5
326CI	INDIVIDUAL	72.655	-0.09801	0.487478E-04	781.2
327AI	FAILED				
328AI	FAILED				
331CI	INDIVIDUAL	49.934	-0.07167	0.364730E-04	800.8
333CI	INDIVIDUAL	20.810	-0.03336	0.197699E-04	775.8
336AI	INDIVIDUAL	123.997	-0.18210	0.974085E-04	789.2
337AI	INDIVIDUAL	52.692	-0.07007	0.364213E-04	829.0
338CI	INDIVIDUAL	84.093	-0.13427	0.744063E-04	752.0
339CI	INDIVIDUAL	199.274	-0.31182	0.162764E-03	746.6
340AI	INDIVIDUAL	122.479	-0.17397	0.883182E-04	781.5
341CI	INDIVIDUAL	43.098	-0.05395	0.252785E-04	823.8
342AI	INDIVIDUAL	75.392	-0.10435	0.543323E-04	805.7
343AI	INDIVIDUAL	78.240	-0.10785	0.547511E-04	840.8
344AI	INDIVIDUAL	135.132	-0.20422	0.112431E-03	782.2
345AI	INDIVIDUAL	96.196	-0.10819	0.549271E-04	801.2
346AI	FAILED				
348AI	INDIVIDUAL	-38.580	0.08641	-0.478837E-04	781.0
349CI	FAILED				
329AI	METRASCOPE				
330CI	METRASCOPE				
332CI	METRASCOPE				
334CI	METRASCOPE				
335AI	METRASCOPE				
319CI	METRASCOPE				
347AI	METRASCOPE				

TOTAL NUMBER OF INDIVIDUAL T/C REGRESSIONS= 36

MEAN REGRESSION COEFFICIENTS:	69.682	-0.09485	0.499102E-04	

**THERE WERE NO LEVEL T/C REGRESSIONS AVAILABLE IN THE CDT ARRAYS.

Table F.4. (continued)

****
***LEVEL J ***
****

INDIVIDUAL THERMOCOUPLE LISTING:

T/C NO.	TYPE OF REGRESSION	C(1)	C(2)	C(3)	TMAX
301DJ	FAILED				
302CJ	FAILED				
303CJ	FAILED				
304DJ	FAILED				
305CJ	INDIVIDUAL	32.613	-0.04492	0.244870E-04	790.2
306CJ	FAILED				
307CJ	FAILED				
308CJ	FAILED				
309DJ	FAILED				
310DJ	FAILED				
311CJ	INDIVIDUAL	516.864	-0.69963	0.322674E-03	800.9
312DJ	INDIVIDUAL	34.520	-0.04147	0.214911E-04	854.5
313DJ	FAILED				
314CJ	FAILED				
316CJ	FAILED				
317DJ	INDIVIDUAL	-5.229	0.00825	0.113172E-05	831.9
318DJ	FAILED				
320DJ	FAILED				
321CJ	INDIVIDUAL	28.377	-0.03674	0.176082E-04	796.8
322DJ	FAILED				
323DJ	FAILED				
324DJ	FAILED				
325DJ	FAILED				
326DJ	FAILED				
327CJ	INDIVIDUAL	-20.504	0.05405	-0.267689E-04	816.4
328CJ	INDIVIDUAL	12.777	-0.00929	0.601217E-05	796.7
331DJ	FAILED				
333DJ	FAILED				
336CJ	FAILED				
337CJ	INDIVIDUAL	9.621	-0.00318	0.232490E-05	800.6
338DJ	FAILED				
339DJ	FAILED				
340CJ	FAILED				
341DJ	FAILED				
342CJ	INDIVIDUAL	59.095	-0.08291	0.412412E-04	805.1
343CJ	FAILED				
344CJ	INDIVIDUAL	36.696	-0.06126	0.345548E-04	792.8
346CJ	FAILED				
347CJ	FAILED				
349DJ	FAILED				
315CJ	FAILED				
348CJ	DEAD				
329CJ	METRASCOPE				
330DJ	METRASCOPE				
332DJ	METRASCOPE				
334DJ	METRASCOPE				
335CJ	METRASCOPE				
319DJ	METRASCOPE				
TOTAL NUMBER OF INDIVIDUAL T/C REGRESSIONS=		10			
MEAN REGRESSION COEFFICIENTS:		70.483	-0.09171	0.444755E-04	

**THERE WERE NO LEVEL T/C REGRESSIONS AVAILABLE IN THE CDT ARRAYS.

Table F.4. (continued)

****
***LEVEL K ***
****

INDIVIDUAL THERMOCOUPLE LISTING:

T/C NO.	TYPE OF REGRESSION	C(1)	C(2)	C(3)	TMAX
345CK	LEVEL				
301DK	LEVEL				
304DK	LEVEL				
309DK	LEVEL				
310DK	INDIVIDUAL	91.646	-0.14155	0.795902E-04	810.6
312DK	INDIVIDUAL	77.787	-0.09674	0.487595E-04	830.8
313DK	INDIVIDUAL	136.906	-0.19427	0.997185E-04	816.9
317DK	INDIVIDUAL	103.397	-0.14459	0.797189E-04	797.4
318DK	INDIVIDUAL	101.476	-0.15675	0.849126E-04	757.9
320DK	INDIVIDUAL	108.178	-0.14533	0.756317E-04	794.8
322DK	LEVEL				
323DK	INDIVIDUAL	146.132	-0.21907	0.118053E-03	767.8
324DK	INDIVIDUAL	154.367	-0.24060	0.131740E-03	737.9
325DK	INDIVIDUAL	16.369	-0.00441	0.968150E-05	851.6
326DK	INDIVIDUAL	44.778	-0.06551	0.336453E-04	763.8
331DK	LEVEL				
333DK	INDIVIDUAL	103.184	-0.16032	0.846731E-04	755.8
338DK	LEVEL				
339DK	LEVEL				
341DK	INDIVIDUAL	72.986	-0.09905	0.480061E-04	803.9
349DK	LEVEL				
330DK	METRASCOPE				
332DK	METRASCOPE				
334DK	METRASCOPE				
319DK	METRASCOPE				

TOTAL NUMBER OF INDIVIDUAL T/C REGRESSIONS= 12

MEAN REGRESSION COEFFICIENTS:	96.434	-0.13901	0.745108E-04
LEVEL REGRESSION COEFFICIENTS:	81.768	-0.12620	0.703059E-04

****
***LEVEL L ***
****

INDIVIDUAL THERMOCOUPLE LISTING:

T/C NO.	TYPE OF REGRESSION	C(1)	C(2)	C(3)	TMAX
301EL	LEVEL				
302CL	LEVEL				
303CL	INDIVIDUAL	32.361	-0.04441	0.228885E-04	752.6
304EL	LEVEL				
305CL	INDIVIDUAL	53.659	-0.09059	0.537827E-04	739.1
306CL	INDIVIDUAL	0.593	0.00747	-0.274301E-05	757.9
307CL	INDIVIDUAL	128.385	-0.19780	0.103781E-03	752.6
308CL	INDIVIDUAL	103.061	-0.15800	0.832313E-04	769.2
309EL	LEVEL				
310EL	INDIVIDUAL	54.601	-0.07572	0.431188E-04	827.2
311CL	LEVEL				

Table F.4. (continued)

T/C NO.	TYPE OF REGRESSION	C(1)	C(2)	C(3)	TMAX
312EL	INDIVIDUAL	63.907	-0.08272	0.438729E-04	806.6
313EL	INDIVIDUAL	91.992	-0.13357	0.753222E-04	772.8
315CL	LEVEL				
316CL	INDIVIDUAL	48.008	-0.07060	0.352876E-04	758.6
317EL	INDIVIDUAL	68.804	-0.09035	0.477697E-04	774.1
318EL	LEVEL				
320EL	INDIVIDUAL	80.302	-0.10514	0.525661E-04	799.4
321CL	LEVEL				
322EL	LEVEL				
323EL	INDIVIDUAL	69.632	-0.08945	0.467995E-04	771.5
324EL	LEVEL				
325EL	LEVEL				
326EL	LEVEL				
327CL	INDIVIDUAL	63.355	-0.07504	0.373441E-04	797.9
328CL	INDIVIDUAL	-10.119	0.01435	-0.391968E-05	786.7
331EL	INDIVIDUAL	60.665	-0.08451	0.401095E-04	752.4
333EL	LEVEL				
336CL	INDIVIDUAL	39.215	-0.04245	0.211927E-04	764.9
337CL	INDIVIDUAL	75.069	-0.10655	0.570739E-04	773.0
338EL	INDIVIDUAL	111.697	-0.16530	0.873686E-04	767.5
339EL	LEVEL				
340CL	LEVEL				
341EL	LEVEL				
342CL	INDIVIDUAL	144.561	-0.22279	0.115207E-03	757.0
343CL	INDIVIDUAL	76.913	-0.08896	0.475425E-04	778.3
344CL	INDIVIDUAL	41.751	-0.05930	0.323666E-04	766.8
345CL	LEVEL				
346CL	LEVEL				
347CL	LEVEL				
348CL	LEVEL				
349EL	LEVEL				
314CL	DEAD				
329CL	METRASCOPE				
330EL	METRASCOPE				
332EL	METRASCOPE				
334EL	METRASCOPE				
335CL	METRASCOPE				
319EL	METRASCOPE				
TOTAL NUMBER OF INDIVIDUAL T/C REGRESSIONS=		21			
MEAN REGRESSION COEFFICIENTS:		66.591	-0.09340	0.495219E-04	
LEVEL REGRESSION COEFFICIENTS:		56.016	-0.09044	0.500993E-04	

Table F.4. (continued)

****
***LEVEL M ***
****

INDIVIDUAL THERMOCOUPLE LISTING:

T/C NO.	TYPE OF REGRESSION	C(1)	C(2)	C(3)	TMAX
301EM	FAILED				
304EM	FAILED				
309EM	FAILED				
325EM	FAILED				

**THERE WERE NO INDIVIDUAL T/C REGRESSIONS FOR THIS LEVEL (IN THE CDT ARRAYS); THERFORE, MEAN REGRESSION COEFFICIENTS COULD NOT BE DETERMINED.

**THERE WERE NO LEVEL T/C REGRESSIONS AVAILABLE IN THE CDT ARRAYS.

****
***LEVEL N ***
****

INDIVIDUAL THERMOCOUPLE LISTING:

T/C NO.	TYPE OF REGRESSION	C(1)	C(2)	C(3)	TMAX
301FN	LEVEL				
304FN	LEVEL				
325FN	INDIVIDUAL	169.070	-0.27175	0.160929E-03	732.6
309FN	DEAD				

TOTAL NUMBER OF INDIVIDUAL T/C REGRESSIONS= 1

MEAN REGRESSION COEFFICIENTS:	169.070	-0.27175	0.160929E-03
LEVEL REGRESSION COEFFICIENTS:	64.366	-0.12514	0.863555E-04

Appendix G

DEVELOPMENT OF THE MODIFIED RUSSELL EQUATION

G.1 Introduction

The thermal conductivities of porous media (solid + gas) are best correlated with Russell's[42] equation,

$$\frac{k_{comp}}{k_{cont}} = \frac{\nu p^{2/3} + 1 + p^{2/3}}{\nu(p^{2/3} - p) + 1 - p^{2/3} + p} , \tag{G.1}$$

where the subscripts comp and cont denote values for the composite mixture and the continuous phase; p is the porosity (i.e., volume fraction of voids) given for a solid-gas mixture by

$$p = \frac{\rho_{sol} - \rho_{comp}}{\rho_{sol} - \rho_{gas}} . \tag{G.2}$$

The term ν is the ratio of the thermal conductivity of the gas to that of the continuous phase; that is,

$$\nu = \frac{k_{gas}}{k_{cont}} . \tag{G.3}$$

Note, for p = 0 (i.e., solid with no gas voids), Eq. (G.1) reduces to

$$\frac{k_{comp}}{k_{cont}} = 1 . \tag{G.4}$$

For p = 1 (all gas), Eq. (G.1) reduces to

$$\frac{k_{comp}}{k_{cont}} = \nu = \frac{k_{gas}}{k_{cont}} , \tag{G.5}$$

or

$$k_{comp} = k_{gas} . \tag{G.6}$$

So, Eq. (G.1) is applicable for $0 < p < 1$.

When gas is the continuous phase of a solid-gas mixture (e.g., powders), Laubitz[43] noted that Eq. (G.1) does not give good agreement with

experimental data. However, by doubling the right-hand side of Eq. (G.1) and adding a radiative heat transfer mechanism, the accuracy of Eq. (G.1) is restored; that is,

$$k_{comp} = 2k_{cont}\ [\text{Eq. (G.1)}] + 4\sigma T^3 \varepsilon \frac{a}{p} (1 - p^{2/3} + p^{4/3}) , \qquad (G.7)$$

where

ε = emissivity,

a = linear dimension of the particles,

σ = Stefan-Boltzman constant,

T = absolute temperature.

Laubitz studied powders (MgO, Al_2O_3, and ZrO_2) with porosities ranging from 0.55 to 0.75.

G.2 Application to BDHT Heater MgO

The initial attempt to apply the Russell equation to the MgO cores of the BDHT fuel pin simulators involved a slight modification of Eq. (G.7) (this gives the best fit for Laubitz's experimental powder data). The approach taken is that the multiplier in Eq. (G.7) is an adjustable parameter; also, the emissivity and particle linear dimension product (ε*a) in the second part of Eq. (G.7) is an adjustable parameter; therefore, the modified equation appears as

$$k_{comp} = C_1 k_{cont} \left[\frac{\nu p^{2/3} + 1 - p^{2/3}}{\nu(p^{2/3} - p) + 1 - p^{2/3} + p} \right] + 4\sigma T^3 \frac{C_2}{p} (1 - p^{2/3} + p^{4/3}) , \qquad (G.8)$$

where C_1 and C_2 are adjustable parameters.

If the solid MgO is treated as the continuous phase and the porous material is air, literature data[6] is available for the thermal conductivity of MgO with porosities of 0.0, 0.050–0.100, and 0.220 (Fig. G.1).

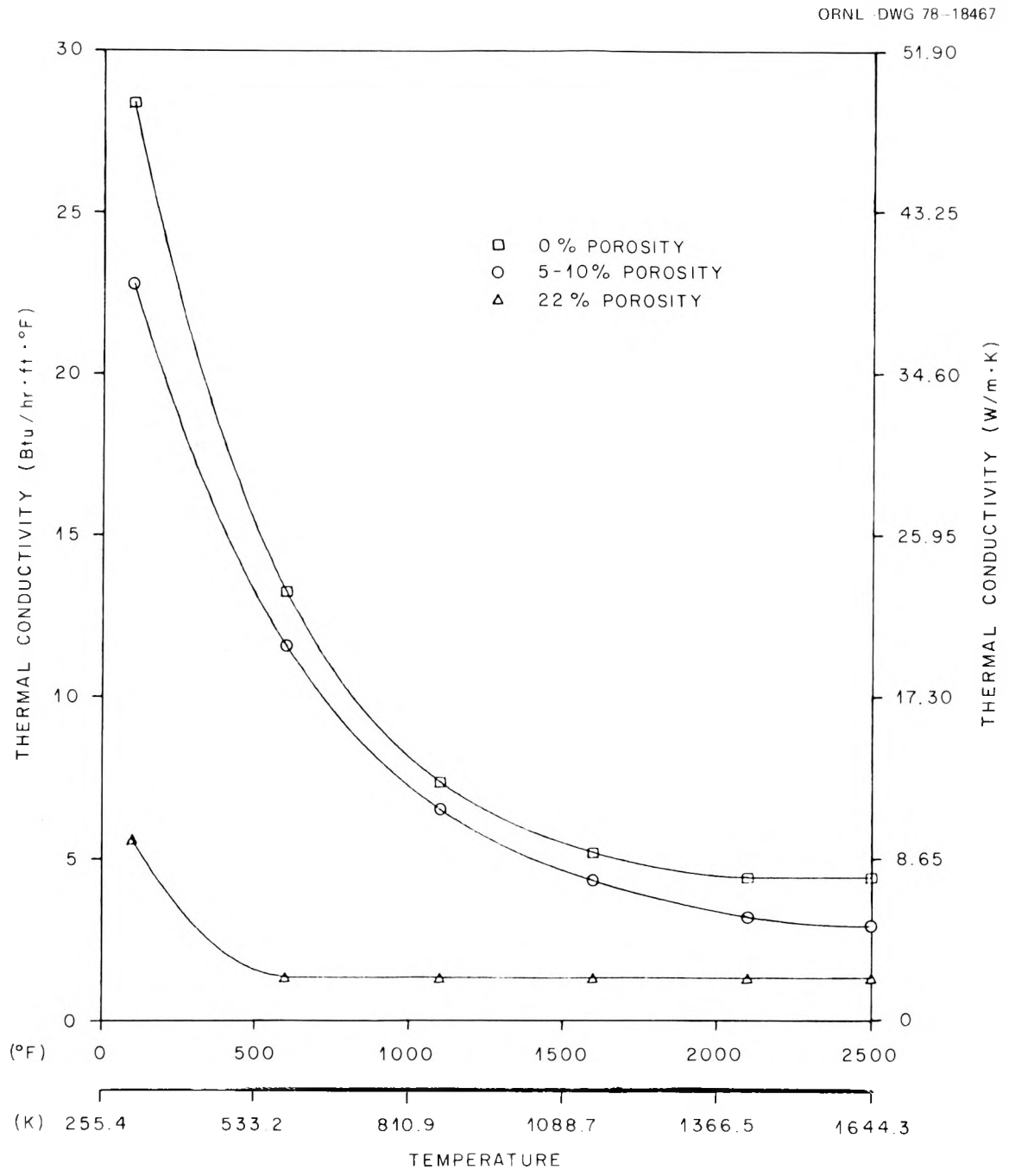

Fig. G.1. MgO thermal conductivity as a function of temperature and porosity (literature data).

Therefore, the following function could be formulated

$$F(C_1,C_2) = \sum_{j=1,2} \sum_{i=1,80} (k_{comp_i} - k_{lit_i})^2 , \qquad (G.9)$$

where

k_{comp} = MgO thermal conductivity calculated by Eq. (G.8),

k_{lit} = literature value of MgO thermal conductivity,

$\sum_{i=1,80}$ represents the discretized temperature domain (200—1800°F),

$\sum_{j=1,2}$ represents the 0.050 and 0.220 porosity curves, and

C_1 and C_2 are the adjustable parameters of Eq. (G.8).

Equation (G.9) is minimized with respect to the C_1 and C_2 parameters and essentially represents a least-squares fit of Eq. (G.8) to the literature data.

Unfortunately, the "best" fit of Eq. (G.8) to the literature data is very poor at best. The $k_{comp}(x)$ values are overlayed with k_{lit} values in Fig. G.2 and G.3 for 0.05 and 0.22 porous MgO, respectively. No further attempt to fit Eq. (G.8) to the literature data has been made.

A modified form of Eq. (G.1) was used in lieu of intermediate trial equations. First, the Russell equation [Eq. (G.1)] was rearranged in the following form:

$$\frac{k_{comp}}{k_{cont}} = \frac{1 + p^{2/3}\ (\nu - 1)}{1 + p^{2/3}\ (\nu - 1) - p\ (\nu - 1)} . \qquad (G.10)$$

The form of the equation which was fitted to the literature data,

$$\frac{k_{comp}}{k_{cont}} = \frac{1 + (C_1 p)^{C_2}(\nu - 1)}{1 + (C_1 p)^{C_2}(\nu - 1) - (C_1 p)(\nu - 1)} , \qquad (G.11)$$

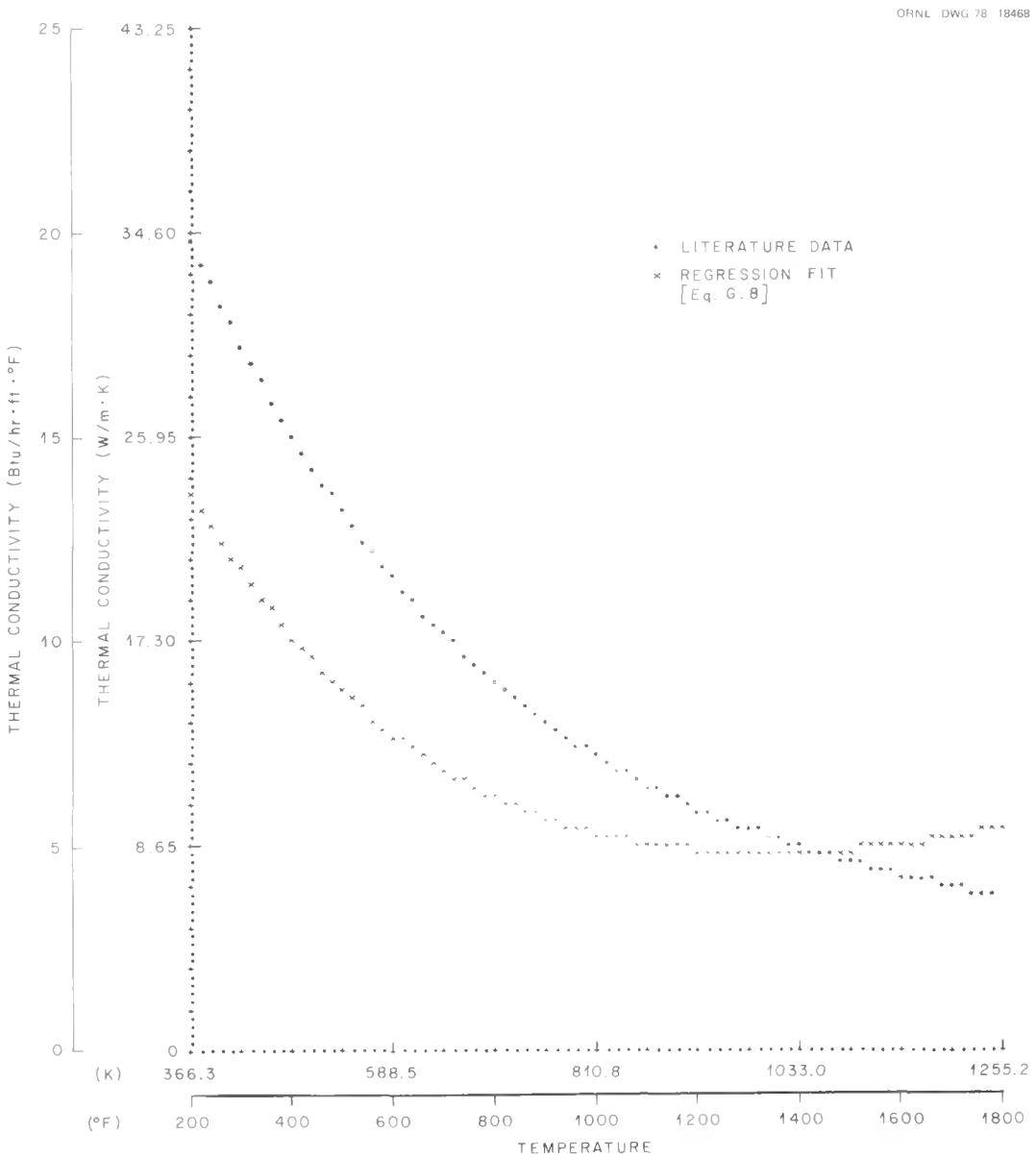

Fig. G.2. k_{MgO} vs temperature for 5% porous MgO [literature data and regression fit of Eq. (G.8)].

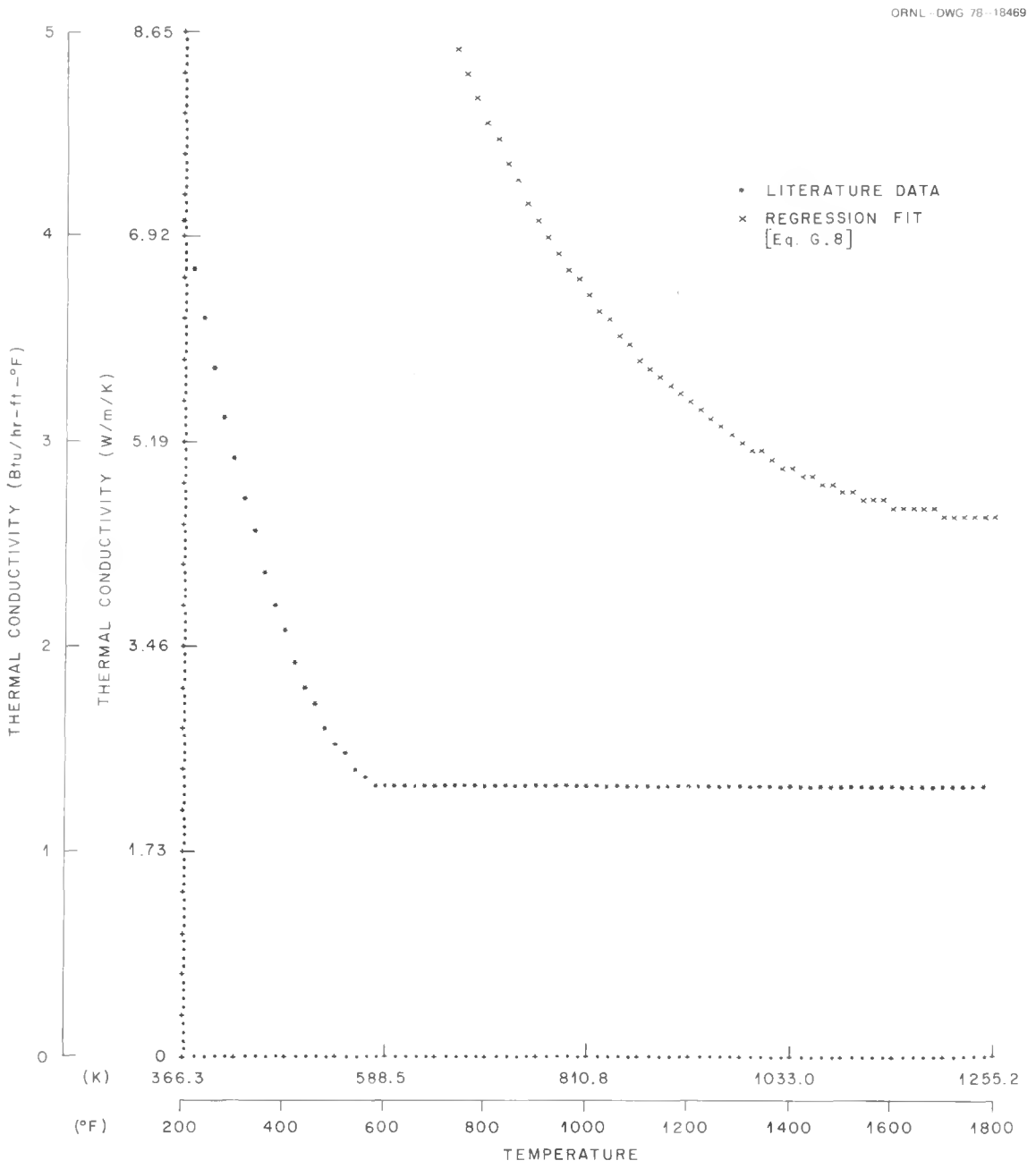

Fig. G.3. k_{MgO} vs temperature for 22% porous MgO [literature data and regression fit of Eq. (G.8)].

shows C_1 and C_2 as the parameters. Again, Eq. (G.9) was minimized with respect to C_1 and C_2. The least-squares fit resulted in $C_1 = 3.891$ and $C_2 = 0.856$. Overlays of k_{comp} vs k_{lit} are presented in Figs. G.4 and G.5 for this regression fit.

The modified form of the Russell equation which will be used to determine the MgO thermal conductivity given the temperature and porosity is

$$\frac{k_{MgO}(T)}{k_{MgO}(T) \text{ at } 0\% \text{ p}} = \frac{1 + (3.891p)^{0.856}\ (\nu - 1)}{1 + (3.891p)^{0.856}\ (\nu - 1) - (3.891p)(\nu - 1)}\ , \qquad (G.12)$$

where p = porosity, $\nu = k_{air}(T)/k_{MgO}(T)$ at 0% p, and T = temperature. A plot [using Eq. (G.12)] similar to Fig. G.1 and illustrating the family of curves for k_{MgO} (with the parameter being porosity) is presented in Fig. G.6.

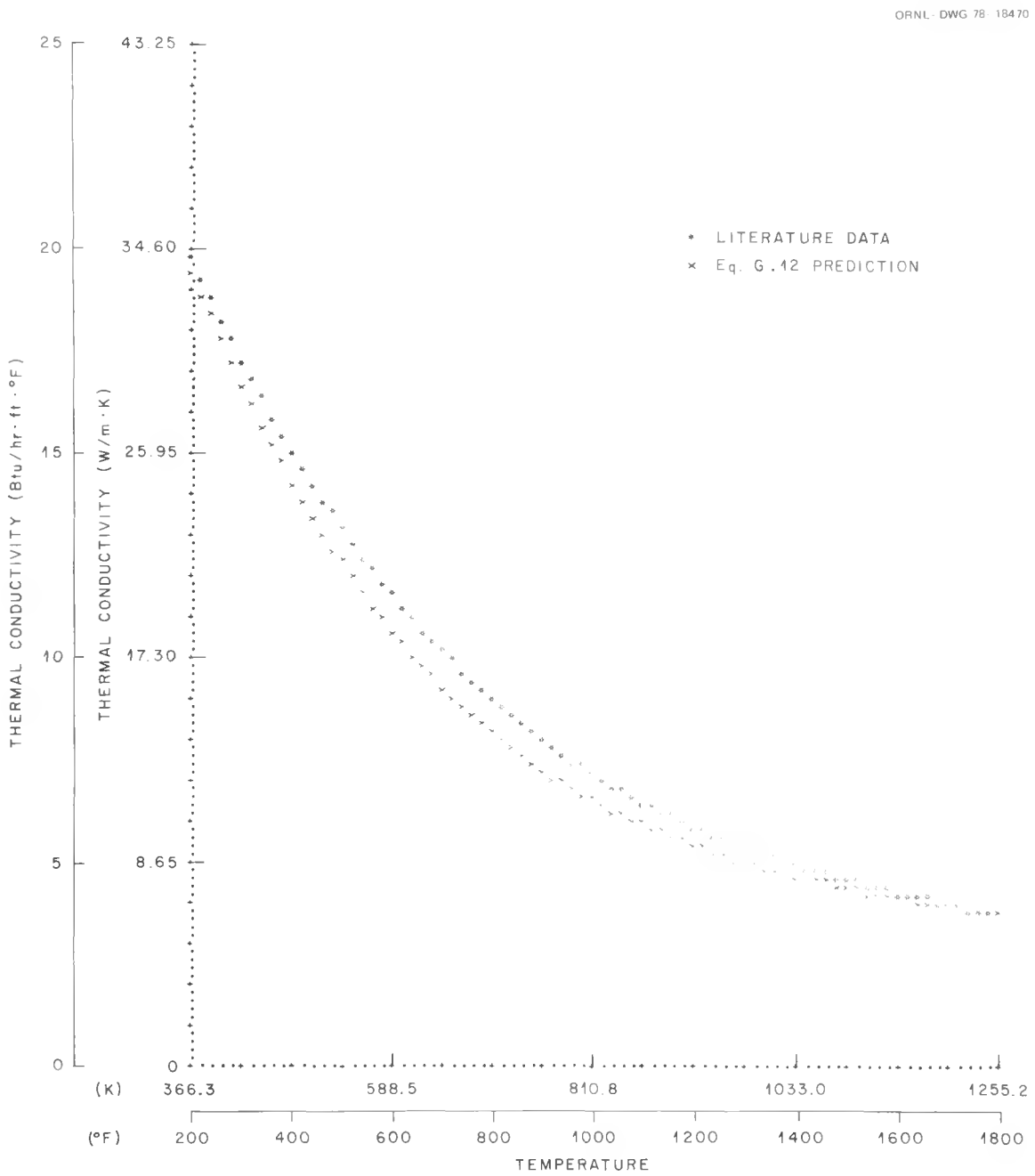

Fig. G.4. k_{MgO} vs temperature for 5% porous MgO [literature data and regression fit of Eq. (G.12)].

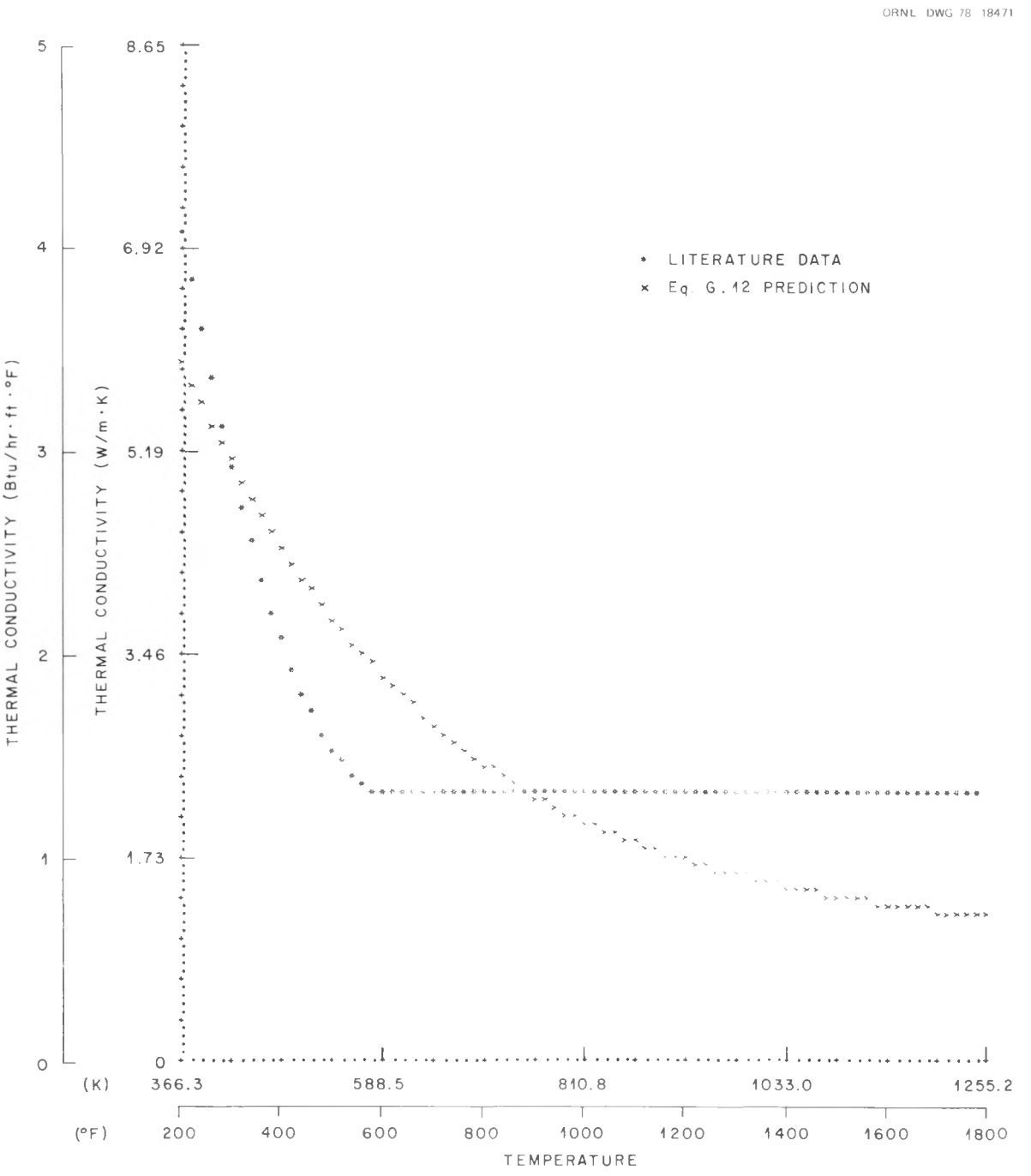

Fig. G.5. k_{MgO} vs temperature for 22% porous MgO [literature data and regression fit of Eq. (G.12)].

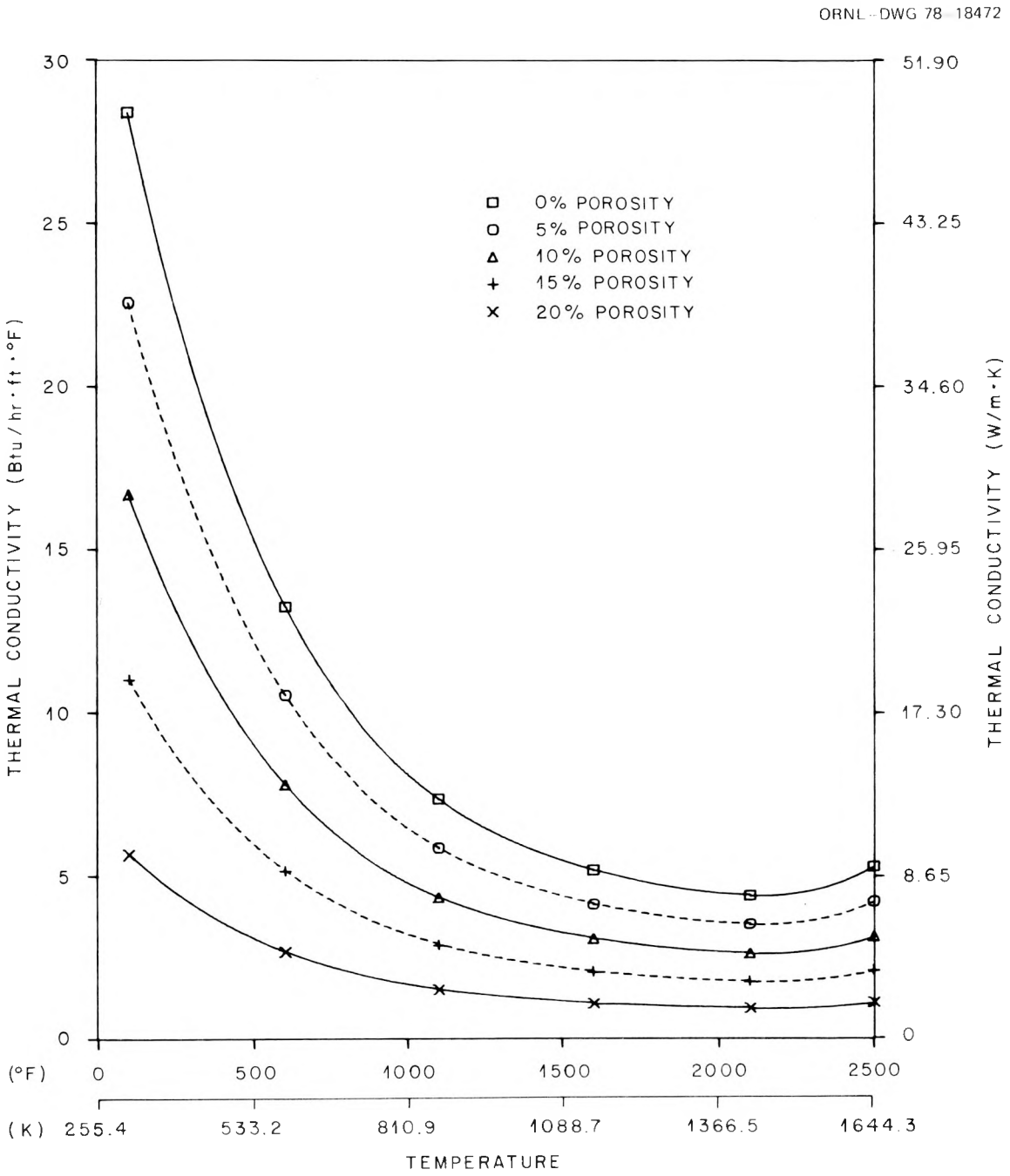

Fig. G.6. MgO thermal conductivity as a function of temperature and porosity [modified Russel equation — Eq. (G.12)].

NUREG/CR-0342
ORNL/NUREG-51
Dist. Category R2

Internal Distribution

1. M. Bender
2. R. E. Bohanan
3. K. W. Childs
4. S. B. Cliff
5. W. G. Craddick
6. R. D. Dabbs
7. H. L. Falkenberry
8. R. M. Flanders
9. M. H. Fontana
10. R. C. Hagar
11. R. F. Hibbs
12. H. W. Hoffman
13. A. F. Johnson
14. B. F. Maskewitz
15. R. W. McCulloch
16. F. R. Mynatt
17-26. L. J. Ott
27. H. Postma
28. Myrtleen Sheldon
29. J. A. Smolen
30. R. E. Textor
31. H. E. Trammell
32. D. B Trauger
33. J. D. White
34. Patent Office
35-36. Central Research Library
37. Document Reference Section
38-40. Laboratory Records Department
41. Laboratory Records (RC)

External Distribution

42-43. Director, Division of Reactor Safety Research, Nuclear Regulatory Commission, Washington, D.C. 20555
44. Office of Assistant Manager, Energy Research and Development, DOE, ORO
45-360. Given distribution as shown in category R2 (TIC-2, NTIS-25)

☆U.S. GOVERNMENT PRINTING OFFICE: 1979-748-189/401